NAVAL AEROSPACE MEDICAL RESEARCH LABORATORY
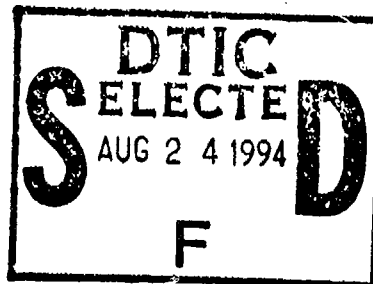## 51 HOVEY ROAD, PENSACOLA, FL 32508-1046

NAMRL Monograph 46

HUMAN VESTIBULAR RESPONSE
DURING 3 G_Z CENTRIFUGE
STIMULATION

B. J. McGrath

DTIC
SELECTED
AUG 2 4 1994
F

94-26845

94 8 23 039

Approved for public release; distribution unlimited.

Reviewed and approved _20 Apr 93_

A. J. MATECZUN, CAPT, MC USN
Commanding Officer

HUMAN VESTIBULAR RESPONSE DURING
3 Gz CENTRIFUGE STIMULATION

by

BRADEN J. MCGRATH

B.E.(Hons), University of Sydney, 1986

Submitted in partial fulfillment
of the requirements for the
degree of

MASTER OF SCIENCE

in

AERONAUTICS AND ASTRONAUTICS

at the

MASSACHUSETTS INSTITUTE OF TECHNOLOGY

Cambridge, Massachusetts

September, 1990

Signature of Author _____

Certified by _____
Dr. Charles M. Oman
Thesis Supervisor

Accepted by _____
Professor Harold Y. Wachman
Chairman, Department Graduate Committee

Human Vestibular Response During
3 G$_Z$ Centrifuge Stimulation

by

BRADEN J. McGRATH

Submitted to the
Department of Aeronautics and Astronautics in partial fulfillment
of the requirements for the Degree of
Master of Science in Aeronautics and Astronautics

ABSTRACT

·Pilots of high performance aircraft routinely experience high G forces which are rapid in onset and prolonged in duration. Centrifuges are increasingly used to train pilots to avoid G Induced Loss of Consciousness (GLOC). Vestibular research interest has recently focussed on human oculomotor and perceptual responses, both in centrifuges and maneuvering aircraft. In this experiment, the vestibulo-ocular reflex was recorded in the dark from 15 naive subjects who were repeatedly tested on the 20.5 foot radius Coriolis Acceleration Platform centrifuge at the Naval Aerospace Medical Research Laboratory, Pensacola, FL. Subjects sat head erect in a pendulous chair. As the centrifuge was accelerated from 0 to 120°/sec (1 to 3 G$_Z$) in 19 seconds, the chair rolled out through 72°, so that the resultant gravito-inertial force was continuously directed downward with respect to the body. After 5 minutes at constant velocity, the centrifuge was decelerated using a similar profile. Tests were repeated on separate days up to 3 times with clockwise rotation (subject facing motion), and 3 times with counterclockwise rotation (subject back to motion), in random order. 60 Hz. horizontal and vertical axis eye position data was obtained using a commercial infrared video eye movement monitor (ISCAN, Inc.). Nystagmus slow phase velocity (SPV) was calculated using a Macintosh computer based single axis, single pass, acceleration algorithm (Massoumnia, 1983), and an interactive manual editing system developed for this project.

Six subjects experienced one or more episodes of G-LOC, and one other withdrew due to unrelated sickness. The SPV records and sensations of the 8 subjects who completed all six runs were analyzed. Centrifuge acceleration and deceleration produced strong pitch, roll, and yaw sensations attributable to cross coupled vestibular Coriolis stimulation. Subjective pitch amplitude change was consistently greater during deceleration than acceleration, regardless of the direction of centrifuge rotation. Analysis of horizontal and vertical SPV profiles showed that responses during the first run in a given direction were significantly different than the two subsequent runs. The maximum vertical SPV magnitudes did not correspond to asymmetries in pitch sensation. In addition to the transient Coriolis vestibular reaction, a sustained upbeating nystagmus was observed (mean SPV 8°/sec after 80 secs) during constant velocity rotation. The effect was clearly present in 7 of 8 subjects (range 1 - 21°/sec after 80 secs; 1 - 12°/sec after 300 secs), although the magnitude and time course of this component was an individual characteristic. Average SPV response profiles were computed for each of the 8 subjects for the 2nd and 3rd runs in each direction, and were consistent with the view that the total VOR during centrifugation is composed of interacting angular and linear VOR responses.

Thesis Supervisor: Dr. Charles M. Oman
Title: Senior Research Engineer,
        Department of Aeronautics and Astronautics

ACKNOWLEDGEMENTS

TABLE OF CONTENTS

LIST OF FIGURES

LIST OF TABLES

1. INTRODUCTION

Humans have evolved over the last million years in the gravitational force environment of the Earth. The normal gravitational force experienced by humans is an acceleration of $9.8m/sec^2$ and for most people throughout their lives, this acceleration is approximately constant and is experienced as weight. However, in the last 50 years, as aircraft have become faster and manned space flight has become a reality, pilots and astronauts are exposed to large variations of acceleration as part of their normal working life.

Today's high performance aircraft can generate large, prolonged accelerations during dive pull outs and banked turns. Large accelerations are also present during spacecraft lift-off and re-entry profiles. These accelerations can have a detrimental effect on the performance of the pilot/astronaut up to the point where they are unable to perform their flight duties. This can result in catastrophe in some circumstances. So that the pilot/astronaut can operate the aerospace vehicle in a safe manner, we need to understand the physiological limits of the pilot/astronaut exposed to large accelerations. However, not only do we need to know the absolute physiological limits of acceleration exposure, we also need to determine the level of accelerations that can be tolerated so that performance at their flight duties is not degraded below unsatisfactory limits. By studying the effects of acceleration, we may develop a better understanding of human response, so that proper design of the work place may mitigate any degradation in performance caused by acceleration.

The human response to applied accelerations depends upon the onset, the duration, the direction, and the magnitude of the acceleration. In describing any acceleration, it has become the convention to express the acceleration in terms of the normal gravitational force

on earth (designated by G). Therefore, if a pilot says he is pulling 3G, it means he is experiencing an acceleration 3 times the magnitude of gravity.

Exposure to large accelerations affects the body in a number of ways: motor coordination skills are impaired, the cardiovascular/respiratory system is stressed, thus impairing brain function and vision, and the vestibular system is stimulated in an abnormal manner that may result in various illusions. The direct effect of large accelerations on the vestibular system is still largely unknown.

One effect of exposure to large accelerations that is of great concern to the aeromedical community is G induced loss of consciousness (GLOC) (Gillingham and Fosdick, 1988). GLOC occurs because of the effect of large accelerations on the cardiovascular/respiratory systems. As a human experiences positive G_z (where subscript z indicates head to toe direction), the acceleration generates a large abnormal hydrostatic pressure gradient between the heart and the head, causing the blood to be drawn away from the head and eyes and forced into the lower limbs. As positive G_z increases, pilots experience: increased body weight, drooping of the soft body tissue, inability to move limbs, difficulty in breathing, tingling sensations in the feet, visual greyout, tunnel vision and blackout. Finally, unconsciousness occurs (GLOC). Conversely, negative G_z forces blood into the head and eyes, causing redout and brain impairment.

For pilots of high performance aircraft, G_z exposure is a critical performance parameter, since the pilot is seated in a approximate upright position for visual/control reasons and the majority of maneuvers generate G_z accelerations. To minimize the effects of G_z and reduce the possibility of GLOC, the following countermeasures are currently implemented: protective maneuvers (straining and muscle tensing), protective devices (tilted seat backs and G-suits), and centrifuge training.

Centrifuge training is used to expose pilots and astronauts to large positive G forces to prepare them for their working environment. Human centrifuges provide the only suitable ground-based method for prolonged acceleration in a controlled environment. Centrifuge training is used to increase G tolerance and to learn and improve protective straining maneuvers. During acceleration and deceleration of the centrifuge, the pendulous chair pivots so that the resultant gravito-inertial force is always directed down with respect to the body (Figure 1.1). As the cab swings, subjects experience strong sensations of pitch, roll and yaw, and spatial disorientation and motion sickness often occur. Subjective reports also indicate that deceleration is more disturbing than acceleration. The mechanism by which the disorientation and motion sickness occur are not completely understood. Most orientation researchers attribute the sensations to be primarily due to the Coriolis vestibular reaction that is caused by the swinging cab.

centripetal force

Clockwise Motion

gravity

RESULTANT GRAVIO-INERTIAL FORCE
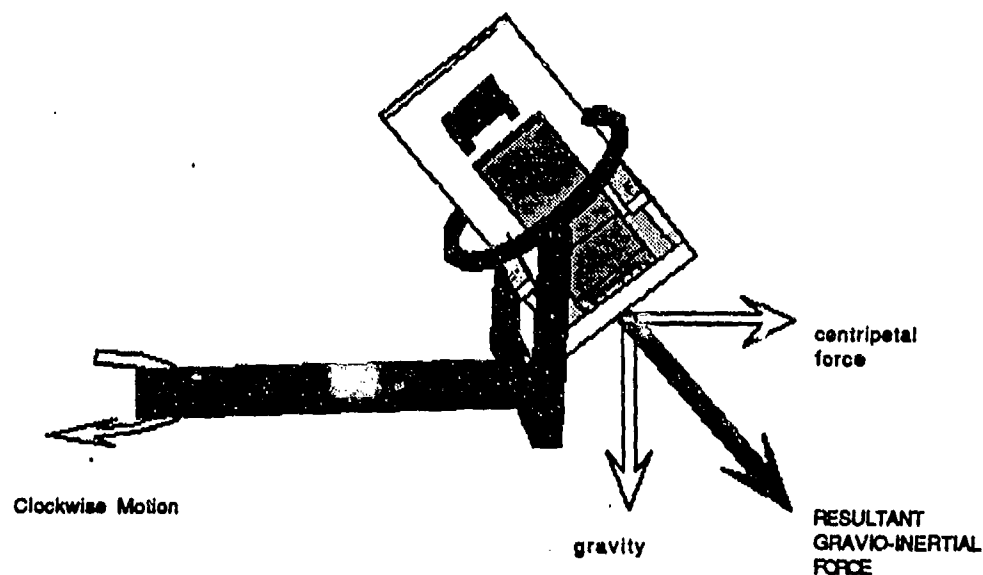
Figure 1.1. Pendulous Chair Centrifuge.

The Coriolis vestibular reaction occurs when a person rotates his head about one axis, while he is also rotating about another axis, producing a cross-coupled angular acceleration stimulus to the vestibular system. The resulting sensations are disorienting because of conflict between signals from the angular information sensors (semicircular canals) and the gravito-inertial sensors (otoliths), and the stimulus is known to be nauseogenic (Guedry and Benson, 1978). On the centrifuge a further complexity is introduced because the human is located off of the axis of rotation, and the otolith organs are stimulated by a much higher gravito-inertial force than when on axis in a simple rotating chair.

Data on subjective orientation during cross-coupled Coriolis stimulation was obtained by Clark and Stewart (1967). However, except for a study by Guedry and Montague (1961), there exist no quantitative horizontal and vertical eye movement data produced by cross-coupled Coriolis stimulation, and this data was taken with the subject on the axis of rotation. Therefore, no data is available on combined horizontal and vertical eye movements during off-axis, cross-coupled Coriolis stimulation.

To develop a better understanding of the vestibular system, and to predict the vestibular response from stimulation outside the normal physiological environment, mathematical models of the vestibular system have been developed (e.g: Young 1967, Robinson 1977, Raphan et al. 1979). Vestibular models are a simplification of the highly complex physiological system, and attempt to explain various features of the vestibular response. These models have provided insight into the functionality of the vestibular system. Engineers and physiologists use vestibular models in a wide variety of applications, including; design of aerospace vehicles with the human as a major control/decision making element, and studies on adaptation of humans to weightlessness.

The aim of this research was to obtain horizontal and vertical eye movement data during two phases of a 3 G_Z pendulous cab centrifuge run. During acceleration and deceleration of the centrifuge, horizontal and vertical eye movements were recorded to study the vestibular reaction during off-axis, cross-coupled Coriolis stimulation. Secondly, data from the constant velocity section was obtained to study the effects of sustained linear accelerations (G_Z) on the vestibular system.

This data will be used to gain insight into the causes of disorientation and motion sickness during centrifuge acceleration and deceleration, and the difference between acceleration and deceleration subjective sensation reports. Additionally, the data will be used to quantify the vestibulo-ocular response during sustained 3 G_Z. The eye movement data was obtained using state-of-the-art video based techniques that overcome many of the limitations of traditional EOG eye movement recording methods. Repeat runs in clockwise (forward facing) and counterclockwise (backward facing) directions were performed on all subjects to study repeatability of responses and the effects of direction. In a follow on study - not part of this thesis - the data will be used to develop a predictive mathematical model of the vestibular response under combined linear and angular accelerations on a centrifuge.

1.1 THESIS ORGANIZATION

Chapter 2 reviews the relevant research concerned with the effects of linear acceleration on vestibular nystagmus. Cross-coupled stimulation to the vestibular system is defined and previous research presented.

Chapter 3 describes the methods used to conduct the experiment to gather horizontal and vertical eye movement data during a 3 G_Z pendulous cab centrifuge run. The video based measurement system used to record the eye movements (ISCAN) is described along with

15

the data reduction software developed for this project. Chapter 4 describes the complicated stimulus to the vestibular system during the centrifuge run. A program evaluates the linear and angular accelerations in terms of a head fixed coordinate system.

Chapter 5 presents the results of the experiment for 15 human subjects and discusses these experimental results in light of the stimulus profiles presented in Chapter 4 and the background studies reviewed in Chapter 2. Finally, the findings and conclusions are summarized in chapter 6.

2. BACKGROUND

The vestibular system is located within the inner ear and consists of two types of sense organs; one sensing angular acceleration (semicircular canals), and the other sensing linear acceleration and gravity (otolith organs). The vestibular system provides information that is used to stabilize vision when motion of the head and body would otherwise result in blurring of the retinal image. It supplements the visual system for orientation and equilibrium and provides information for both skilled and reflexive motor activities. The vestibular system provides, in the absence of visual cues, a reasonably accurate perception of motion and position within a certain range of stimulation.

Aerospace flight often stimulates the vestibular system outside its normal physiological range causing illusions, spatial disorientation and motion sickness. In low visibility or during large acceleration stimulation, the vestibular cues dominate over other spatial orientation cues, and visual or postural illusions may occur.

2.1 VESTIBULO-OCULAR REFLEX

An important role of the vestibular system is to maintain stabilization of the visual retinal image during head movements. If one just glances over one's shoulder, the head easily achieves angular velocities of 200 - 300°/s. If the eyes did not compensate for this head movement, the resulting retinal image slip would preclude any type of useful vision during the movement. The retinal image is stabilized by means of vestibulo-ocular reflexes (VOR). Traditionally, VOR was thought to be primarily induced by angular acceleration only, and that linear acceleration induced little or no VOR (Jongkees 1967). However,

there is considerable evidence that suggests the total VOR response is composed of two components; an angular VOR whose origin is the semicircular canals, and a linear VOR whose origin is likely in the otolith organs.

When the head is subjected to an acceleration, the brain generates a compensatory eye movement. For a head rotation, the eye movement relative to the skull is in the same plane as, but in a direction opposite to, the plane of head rotation relative to space. During prolonged stimulation very rapid "saccadic" eye movements occur in the opposite direction to the compensatory eye movements. These rapid movements are necessary because the amount of angular displacement of the eye is limited and they return the eye in the opposite direction, such that compensatory eye movements can continue. These very rapid eye movements are anticompensatory, and scene motion during this phase is perceptually suppressed.

During sustained accelerations, the compensatory and anticompensatory eye movements are repeated. This rhythmic eye movement is known as vestibular nystagmus, with the compensatory phase known as the slow phase, and the anticompensatory phase known as the fast phase. The direction of the nystagmus is conventionally taken as that associated with the fast phase.

2.2.1   Nystagmus as Measure of Vestibular Function

With the present state of the art, it is not possible to make direct neural recordings without radical surgery, therefore, neural recording from the human vestibular system is out of the question until a non-destructive method is found. Therefore it is necessary to use other measures of vestibular stimulation to study the performance of man's spatial orientation system.

18

The ability of man to sense his direction of motion, and give a subjective estimate of its relative magnitude, is one such measure of vestibular stimulation. However, this technique suffers from the limitations that the subjective responses are influenced by the subject's experience and mental alertness at the time of the experiment. Unfortunately, there is no way to directly measure orientation perception.

A more quantitative measure of vestibular stimulation can be obtained by measurement of vestibular nystagmus. With a knowledge of the acceleration stimulus, the resulting nystagmus will give a measure of the combined function of the semi-circular canals, the otoliths, and the central oculomotor system. Nystagmus eye movement recordings provide a continuous quantitative measure of vestibular function that is relatively easy - as compared to neural recordings - to obtain and analyze. By recording eye velocity and detecting and removing the fast phase saccades from the eye velocity record, investigators are able to infer the net compensatory eye velocity command to the oculomotor system coming from the central vestibular system.

2.2.2 Angular and Linear VOR

When the head is subjected to angular acceleration, an angular VOR response is elicited that helps to stabilize the visual retinal image. The semicircular canals are the primary transducers of angular accelerations. The semicircular canals act as fluidic integrating angular accelerometers, and convert angular acceleration of the head into a primary afferent neural signal. This neural signal is proportional to the angular velocity of the head for ordinary head motions encountered in terrestrial activities.

However, the oculomotor response to angular rotation does not directly reflect activity in the semicircular canal primary afferents. For example, postrotational nystagmus in the

19

monkey was seen to last well beyond the activity of the primary afferents from the semicircular canals. Also, optokinetic after nystagmus (OKAN) was seen to last beyond the visual stimulation. Furthermore, it appeared that the time course of these response were related. These phenomena have been attributed to additional CNS processes termed "central velocity storage". The velocity storage hypothesis proposed that a CNS neural element was responsible for the extension of vestibular nystagmus and for OKAN. Several different models have been developed to describe this effect. One model (Robinson 1977) uses feedback, while another (Raphan et al. 1977) uses feedforward topology.

Evidence also shows that linear acceleration modifies conventional angular VOR. Benson and Bodin (1966b) showed that head tilt from the earth vertical shortens the apparent time constant of postrotational nystagmus after rotation about a vertical axis. Raphan et al. (1981) and Harris (1987) showed that on experiments with monkeys and cats respectively, there was a build up of vertical nystagmus during off-vertical axis rotation. Merfeld (1990) showed that in squirrel monkeys the linear centripetal acceleration altered the angular VOR by changing the axis of eye rotation, the peak value of slow phase eye velocity, and the time constant of per-rotary decay. The axis of eye rotation tended to align itself with the gravito-inertial force during the centrifuge simulation. The above studies suggest that linear acceleration cues from the otoliths act via the velocity storage mechanism to modify angular VOR.

When the head is subjected to linear acceleration without rotation, there is also evidence that these accelerations produce a linear VOR ("LVOR") response. The otolith organs are the primary transducers of linear accelerations and represent the most likely origin of a LVOR response. Jongkees and Phillipszoon (1962) and Niven et al. (1965) recorded nystagmic eye movements in man generated by linear horizontal acceleration. The evidence of vertical nystagmus generated by vertical linear accelerations is not so conclusive. McCabe (1964),

demonstrated occasional nystagmic eye movements in man, cats and chinchillas subjected to oscillating vertical linear accelerations. Niven et al. (1965), on the other hand, never observed vertical nystagmus when the subject was oscillated on a horizontal sled along his longitudinal axis. Lansberg et al. (1965) conducted a series of experiments where the angular velocity of the body was maintained constant and the effect of linear acceleration (centripetal) was investigated by placing the subjects in different orientations relative to the centripetal acceleration. Results showed that the centripetal linear acceleration stimulus modified the expected horizontal nystagmus generated by the body rotation. A horizontal and vertical component of nystagmus was observed that was attributed to the centripetal acceleration. In a similar experiment with cats, where the protocol eliminated any possibility of canal asymmetry accounting for any observed changes, Crampton (1966) confirmed Lansberg's results.

A number of researchers have investigated the mechanism which produces LVOR. The evidence largely supports the notion of direct action on the otolith being responsible for the observed LVOR. Crampton (1966), recording from the vestibular nucleus in canal sensitive fibers of anesthetized cats, found no change in the response for angular acceleration at various positions of the net linear acceleration vector. Correia and Money (1970), blocked all six semicircular canals of cats, and found that although the horizontal and vertical nystagmus in response to angular acceleration about a vertical axis was abolished, the bias nystagmus during constant rotation about a horizontal axis remained. Their conclusion was that the source of this bias nystagmus could not have been the semicircular canal, but some other complementary system - such as the otoliths. Janeke (1968), cut the nerves from the utricular maculae, leaving the canal system intact, and found that this completely eliminated the unidirectional bias nystagmus, but left the conventional transitory nystagmus unchanged.

21

Additional evidence for the existence of vertical nystagmus generated by vertical linear acceleration comes from recent studies by Marcus (1989), and Marcus and Van Holten (1990) at the TNO Institute for Perception in Sosterberg, Holland. In the first study, Marcus conducted 13 runs in 9 human subjects, accelerating them from 1.05 G_z to 3 G_z in the pendulous cab of a 4 metre radius centrifuge. Vertical eye movements were recorded with a photoelectric monitor. Subjects wore G suits. Four subjects were tested with head erect, 3 with head tilted back 40°, and 6 with head tilted back 90°. Principal findings were: In six of nine subjects, Marcus found an upbeating L-nystagmus during sustained 3 G_z in one or more head positions. Three of the 4 subjects tested head erect showed a sustained L_z-nystagmus. Dependence on head position was not apparent. The vertical nystagmus generated by semicircular canal stimulation during centrifuge acceleration had a longer apparent time constant than deceleration response thus providing further evidence that the linear acceleration has modified the angular VOR.

In the later TNO study, Marcus and Van Holten (1990) exposed 5 subjects on the 4 metre centrifuge to the following profile: acceleration +0.2 G_z/sec, 3 G_z sustained for 3 mins, deceleration -0.2 G_z/sec. Subjects were run facing the motion and back to the motion in randomized order. Vertical eye movements were recorded using DC electro-oculography (EOG). Subjects wore G-suits. Results showed that 3 G_z induced a subject dependent upbeating vertical nystagmus. In a 1 G baseline study with different subjects, Marcus also found that vertical nystagmus due to pitch angular acceleration about an earth vertical axis appeared up-down symmetric. Therefore, he concluded that by adding the 3 G_z centrifuge forwards and backwards data, the G_z effect can be obtained and by subtracting the forward and backward data, the angular velocity effect is obtained. This linear analysis gave an average magnitude for the G_z induced nystagmus of 27°/sec at 16 secs from G onset, and 11°/sec after 3 minutes.

2.2.3 Models for Angular and Linear VOR

Based on experimental data from Niven et al. (1965), Benson and Bodin (1966a), Correia and Guedry (1966) and Lansberg (1965), Young (1967) postulated the existence of a additive nystagmus component due to horizontal linear acceleration. This he termed "L-nystagmus". To account for L nystagmus, Young developed the model shown in Figure 2.1. One pathway represents the conventional angular VOR response pathway. Angular acceleration is input to an element that represents semicircular canal dynamics ("torsion pendulum model", Van Egmond et al. 1949). Primary afferent signals from the semicircular canal are input to a functional element entitled "cross-coupling effect of specific force". Central velocity storage mechanisms (a concept originating a decade later) were not included. Output from the "cross-coupling effect of specific force" element represents the modified angular neural signal used by the oculomotor system to generate compensatory eye movements to angular motion. The model depicts an LVOR pathway which compensates for linear acceleration. This LVOR component was assumed to represent additive L-Nystagmus. Young noted that the dynamics of L-nystagmus response to applied linear acceleration were probably nonlinear. Based on Lansberg's data, Young estimated an L-nystagmus in the head horizontal direction of 9.7°/sec/G, and in the vertical direction, a sensitivity of 4°/sec/G. He hypothesized that L-nystagmus is caused by utricular shear. During vertical stimulation with the head upright, the utricles are only partially sheared due to the 30° utricular tilt from the horizontal plane, thus the vertical sensitivity value is lower than the horizontal value.

Marcus (1989) presented the model shown in Figure 2.2. This model is apparently loosely based on the earlier model presented by Young (Figure 2.1). The addition of a Raphan et al. (1979) velocity storage element replaces the "cross-coupling effect of specific force" element. Marcus's model consist of three major components: an angular VOR component,

23

a velocity storage mechanism and a direct LVOR pathway. The angular VOR component uses torsion pendulum can il dynamics similar to Young's model. As noted earlier, the velocity storage mechanism is based on Raphan et al. (1979) model and the indirect otolith path to the velocity storage mechanism accounts for the modification of angular VOR by linear acceleration. The direct LVOR pathway uses a second order system dynamic model, apparently based on Young and Meiry (1967). The direct otolith pathway accounts for the observed upbeating L-Nystagmus due to the high G linear acceleration. Signals from all three components sum to give the total SPV command, therefore the interaction of angular VOR and LVOR is assumed to be largely a linear additive process.

Merfeld (1990) developed a model based upon optimal observer theory (Figure 2.3). The model hypothesizes that the CNS creates an internal model of the sensory systems based on its "knowledge" of the dynamics of the sensory organs. The input to the internal model is the internal estimate of gravito-inertial linear acceleration and angular velocity. The output of the internal model is the expected sensory afference. The expected sensory afference is compared to the actual sensory afference to yield sensory conflict. The sensory conflict information drives the internal estimate of linear acceleration and angular velocity towards the true values. Merfeld showed that this sensory conflict model qualitatively demonstrated the characteristics of a number of vestibular experiments which combine angular and linear acceleration stimulus.
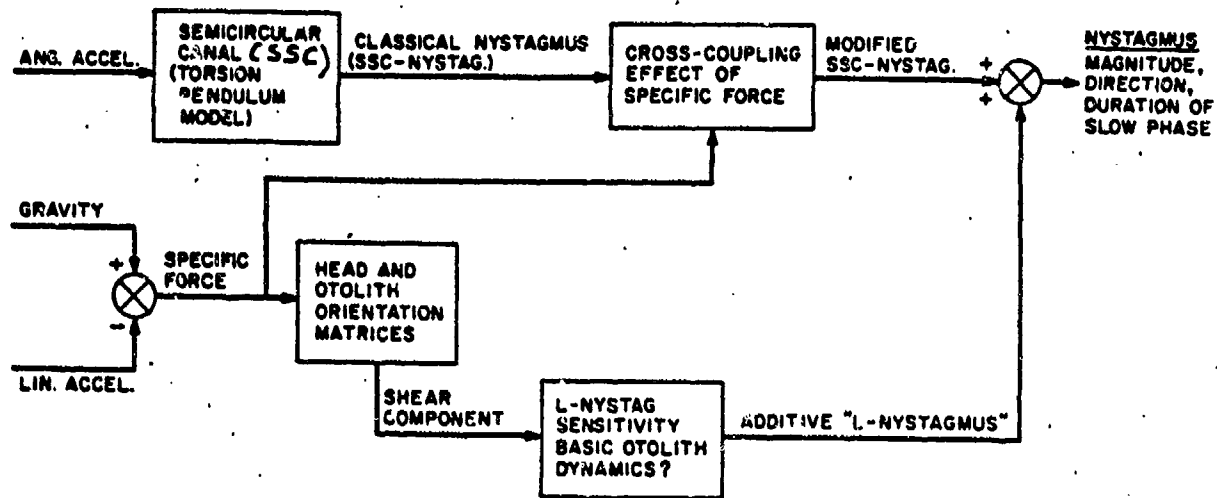
Figure 2.1. Model of Influence of Linear
Acceleration on Angular Nystagmus (Young 1967).
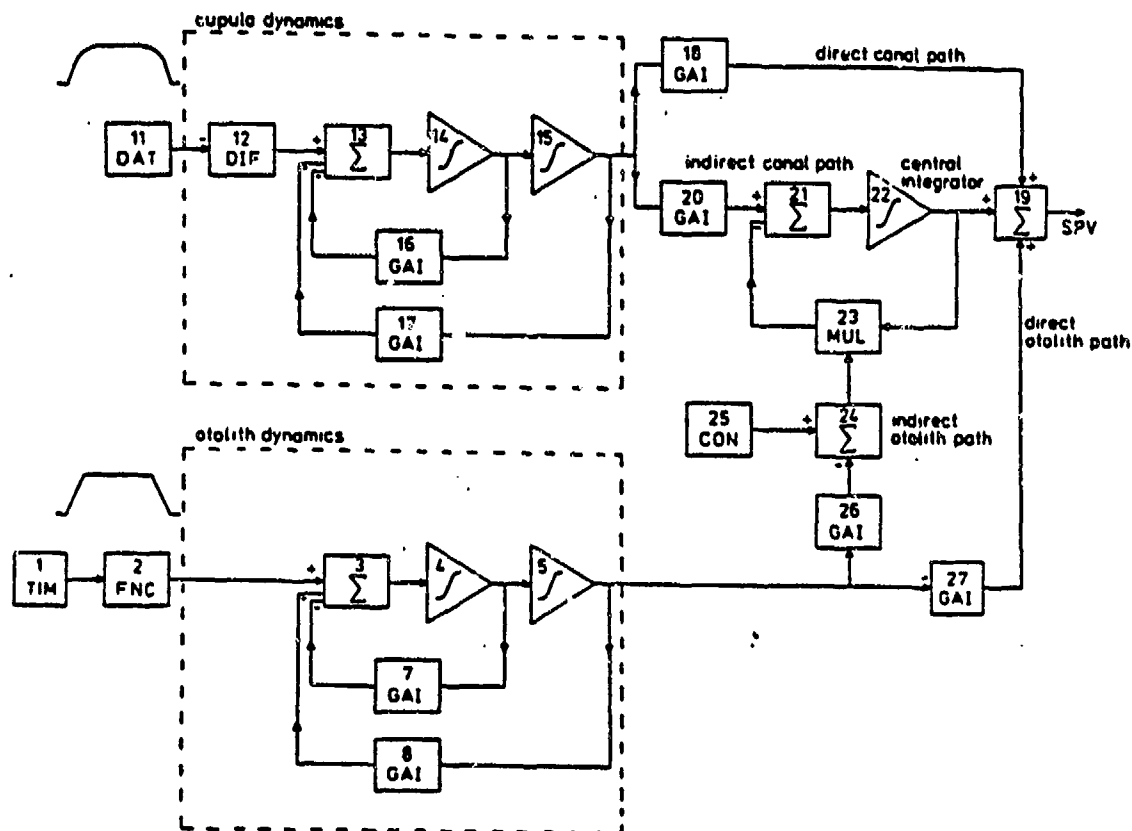
Figure 2.2. Marcus Model (Marcus 1989).

THREE DIMENSIONAL SENSORY CONFLICT MODEL
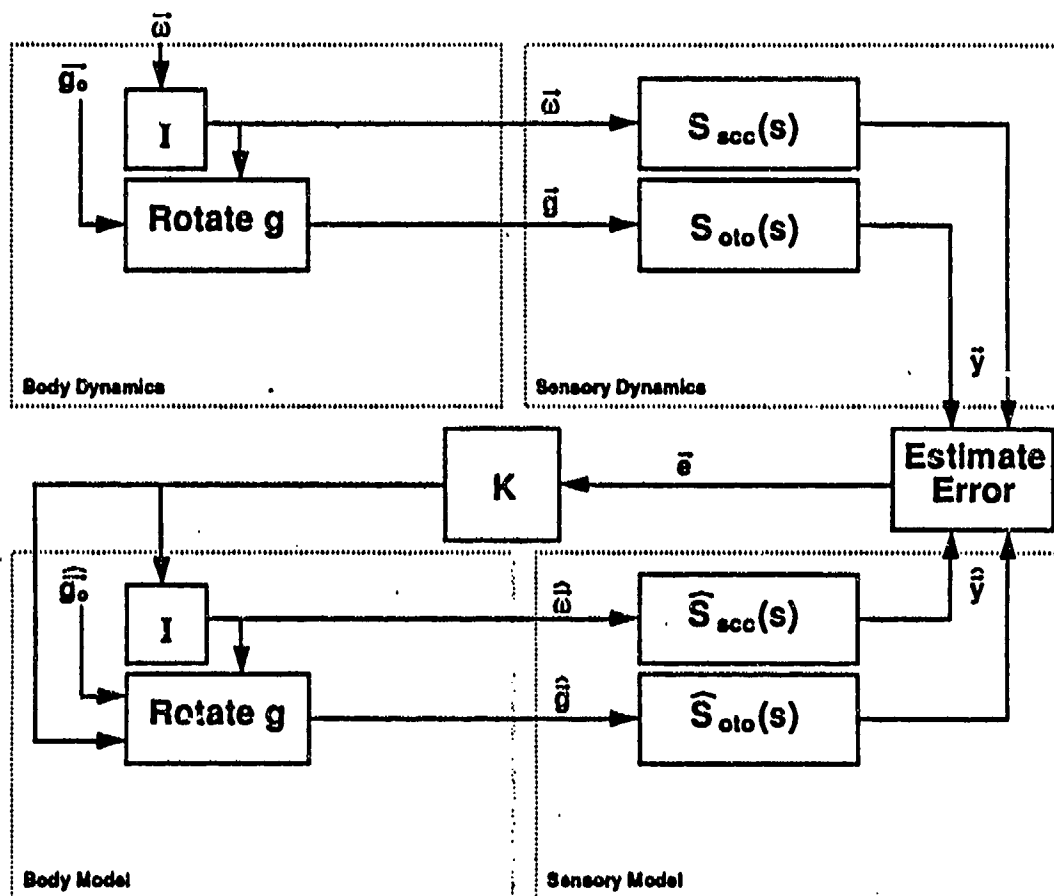
Figure 2.3. Merfeld's Sensory Conflict Model (Merfeld 1990).

2.2 CORIOLIS VESTIBULAR REACTION

The Coriolis vestibular reaction occurs when a person rotates his head about one axis, while he is also rotating about another axis, producing a cross-coupled angular acceleration stimulus to all three semicircular canals. The subject experiences an apparent rotation which can be disturbing and is one of the most provocative stimuli for causing motion sickness.

This cross-coupled stimulation was described by Schubert (1932) and refered to as a Coriolis effect. Bornschein and Schubert (1958), Valentnuzzi (1967), Peters (1969) presented mathematical analysis that showed that during cross-coupled head movements, the semicircular canals are stimulated by an inertial torque. The inertial torque is derived from the integration of the Coriolis accelerations that act parallel to the plane of the canal duct. However, other investigators Lansberg (1960), Peters (1969) showed that the stimulus to the canals can also be derived from analyses of cross-coupled effects of the angular velocity vectors. Results from both analysis were shown to be mathematically equivalent (Peters 1969).

To illustrate cross-coupled Coriolis stimulation, let us consider a subject rotating with the head z-axis aligned to the earth vertical, which is the normal position for spinning with the head erect. He then tilts his head towards the left shoulder, say 90 degrees for simplicity. In other words, he rotates his head about the x-axis (Figure 2.4). In making the rolling head movement, he removes his horizontal semicircular canal from the plane of rotation, and inserts the vertical canals into the plane of rotation. In particular, he introduces the pitch canal into the plane of rotation. In the absence of visual cues, or if the stimulus is large enough, the subject will sense a yaw (due to the change in acceleration in the horizontal canal), a roll (due to head tilt), and a pitch (due to the insertion of the pitch canal into the plane of rotation).

27
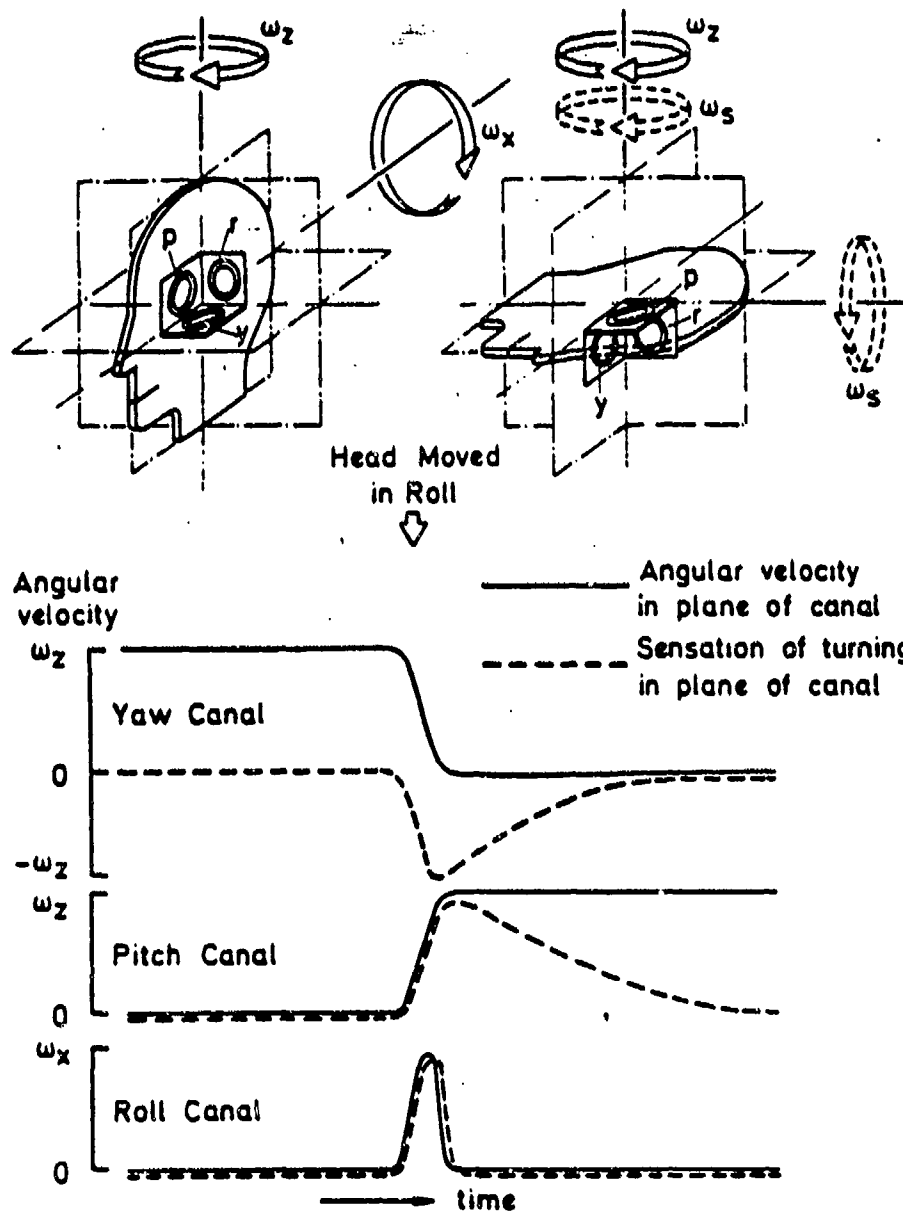
Figure 2.4. Illustration of cross-coupled stimulation.
Rolling head movement during sustained yaw rotation (Benson 1978).

28

Experimentally, the response to cross-coupled Coriolis stimulation is dependent upon the following factors: nature of the rotation and rotation rate of the device, the angle and rate of the head movement, and the gravito-inertial force level.

Guedry and Montague (1961), showed that there was a direct and approximate linear relationship between the subjective response and angular velocity of a turntable during cross-coupled head movements. They also showed that the magnitude of vestibular nystagmus was linearly related to the angular velocity of the device. The results were predictable by analysis of the kinematics of the vestibular system.

In an experiment where cross-coupled Coriolis head movements were made on-axis, Guedry and Benson (1978), demonstrated that the magnitude of the disorientating and nauseogenic effect depends upon when the cross-coupled head movements were made in relation to the time course of the stimulus. Experimental results indicated that cross-coupled head motion made during acceleration of the device produced little or no disturbance. Cross-coupled head movements made during deceleration of the device after a sustained period of rotation produced the greatest disturbance with cross-coupled stimulation during constant velocity in between the two. The absence of disturbance during acceleration was attributed to the fact that after the head movement, the resultant angular acceleration vector is aligned with gravity. Therefore, there is little or no conflict between the semicircular canal input and the otolith input.

The sensations of discomfort and frequently of motion sickness resulting from these cross-coupled Coriolis stimulus are most likely attributable to the conflict between semicircular canals and otolith cues, rather than to the unexpected cross-coupled angular acceleration semicircular canal responses themselves. As mentioned previously, it is hypothesized that the processing of the canal signal by the CNS depends upon the gravito-inertial force level

29

and is thus dependent upon otolithic input. Support for this theory comes from the result of the cross-coupled experiments performed aboard Skylab (M-131, Graybiel et al. 1977). The goal of the M-131 experiment was to determine how nausogenic cross-coupled stimulation would be during orbital flight. Although the initial tests were not carried out early during the weightlessness period, so the possibility of generalized motion sickness habituation exists, it was found that cross-coupled stimulation was less provocative inflight, as compared to preflight levels. In weightlessness, no steady-state otolith conflict exists to support or contradict the semicircular canal cues following head movements.

Furthermore, Lackner and Graybiel (1984,1986) extended the M-131 findings by showing that making head movements while rotating is less stressful in the zero-G phases of parabolic flight and more stressful in the high G periods as compared to 1G on the ground. DiZio et al. (1987) confirmed this result and showed that the magnitudes of subjective and oculomotor responses to cross-coupled Coriolis stimulation are dependent upon gravito-inertial force level.

In conclusion, these previous studies indicate that during the constant high G phase of a centrifuge run the otoliths will be stimulated generating a vertical L-nystagmus. During acceleration and deceleration of a swinging cab centrifuge, a cross-coupled Coriolis stimulus to the semicircular canals will occur. The overall response of the vestibular system will be complicated, since imposed on the semicircular canal response will be a time varying otolith response as the G builds up/down. Conflict between the semicircular canal cues and the otolith cues will most likely be the cause for the reported discomfort during the acceleration and deceleration of the centrifuge.

30

3. METHOD

3.1 EQUIPMENT

The Coriolis Acceleration Platform (CAP) located at the Naval Aerospace Medical Research Laboratory (NAMRL) was used to generate the $3G_Z$ environment required for this experiment. Hixson and Anderson (1966) provide a full description of the facility. For this experiment, the CAP was configured with a swinging pendulous chair enclosed in a darkened cabin, located 20.5 ft from the center of rotation.

The pendulous chair was oriented such that it rolled about the centrifuge tangential axis, with the roll axis located through the subject's chest. The subject was seated upright and faced the motion for a clockwise run and had his back to the motion for a counterclockwise run. The pendulous chair was fitted with an adjustable head rest, and a 5 point LED (light emitting diode) calibration fixture. The 5 LED's were arranged in a cross configuration allowing for 2 point calibration in the horizontal and vertical directions and a center target. The head rest was used to position and stabilize the head in a normal upright position. Video, audio and key press communications were maintained between the subject and control room throughout the experimental session

3.1.1 Instrumentation

Nystagmus eye movements were recorded using the following methods:

1) A video based eye movement measurement system (ISCAN, Inc.)

2) Conventional DC electro-oculography (EOG).

31

ISCAN is a real time system that tracks movement of the pupil under infrared (IR) illumination. The complete system consisted of a head mounted imaging sensor and a digital video tracking processor (Model RK-426 Pupil/Corneal Reflection Tracking Unit). The eye was illuminated with a low-level IR light source and then scanned by a IR-sensitive video camera. Since the IR source was not coaxial with the camera, the pupil of the eye appeared as a dark circle to the camera. This dark pupil video image was input to the RK-426; a real time image processing system that outputs pupil size and position coordinates relative to the horizontal and vertical scan lines of the video camera. The RK-426 used custom integrated circuitry whose function was to acquire and track the dark pupil, even in the presence of shadows, or other clutter. Automatic illumination compensation automatically adjusted the pupil tracker threshold to maintain proper image contrast during changing light conditions. A video image of the eye with crosshairs superimposed over the dark pupil image was presented to the operator who could verify that accurate pupil position was being computed. The video image of the eye was divided into a 512 by 256 pixel grid. This typically gave a resolution of 0.7 degrees / pixel over a +/- 20 degree pupil range.

The commercially available ISCAN imaging system helmet was modified and strengthened to withstand the high G_z environment encountered in this experiment. Figure 3.1 shows the ISCAN camera as worn by a test subject. As modified, the helmet consisted of the following components:

Bitebar attachment: A bitebar was used to ensure that there was no relative motion between the helmet and the head. The bitebar was fabricated from 3M Vinyl Polysiloxane impression material. This material provided a flexible bitebar that was comfortable to wear and not damage teeth, but rigid enough to provide the necessary support.

Camera: The video camera was a Pulnix TM-540 miniature CCD camera, fitted with a IR sensitive filter, with a 60Hz. frame rate.

IR light source: The IR light source consisted of 4 IR LED's mounted on a adjustable arm assembly. Two of the original four LED's supplied with the ISCAN helmet were replaced with two RTW OP133 Gallium Aluminium Arsenide (GaAs) Hermatic IR emitting diodes. These new LED's had lensed caps that provided a narrow focused beam that was used to illuminate shadows in the nasal area of the eye. The two remaining original LED's were unfocused and provided diffuse lighting to illuminate the entire eyeball area. The combination of two unfocused and two focused LED's resulted in an improved IR light source. The 4 LED's supplied 3×10^{-4} mW/cm^2 of light at 880nm wavelength. This intensity was below published safety standards (see Appendix A), but of sufficient intensity to illuminate the eye for satisfactory ISCAN operation.

Stable illumination of the eye is critical to the proper function of the ISCAN system, and the IR source could be adjusted to illuminate the eye, and then be locked in place relative to the helmet using locking screws. Therefore, the illumination source would not move under the $3G_z$ load.

Dichroic mirror: The mirror reflects IR and transmits visible light, and thus is transparent to the subject. The mirror could be adjusted to image the eye and then be locked in place such that the image of the eye was not moved during the $3G_z$ load.

Adjustable Helmet, Velcro Straps: The adjustable helmet provided a stable, but comfortable platform for the camera, light source, mirror and bitebar. The velcro straps were used to distribute the weight of the camera over the entire head.

Figure 3.1: Subject with ISCAN helmet

34

EOG was used as a backup to ISCAN for this experiment since there was initially some concern of satisfactory ISCAN performance in the high G environment of this experiment. However, only a small difference between calibration data before and after the centrifuge run confirmed that ISCAN camera remained stable throughout the run. Another concern was ISCAN vertical linearity. To this end, a pilot experiment was conducted with 4 subjects looking at +/-30° calibration targets at 5° intervals (Figure 3.2). Results (Figure 3.3) showed that ISCAN was extremely linear in the +/-10° range which was the normal range of eye movements during this experiment. Therefore EOG eye position data was not analyzed in this study.
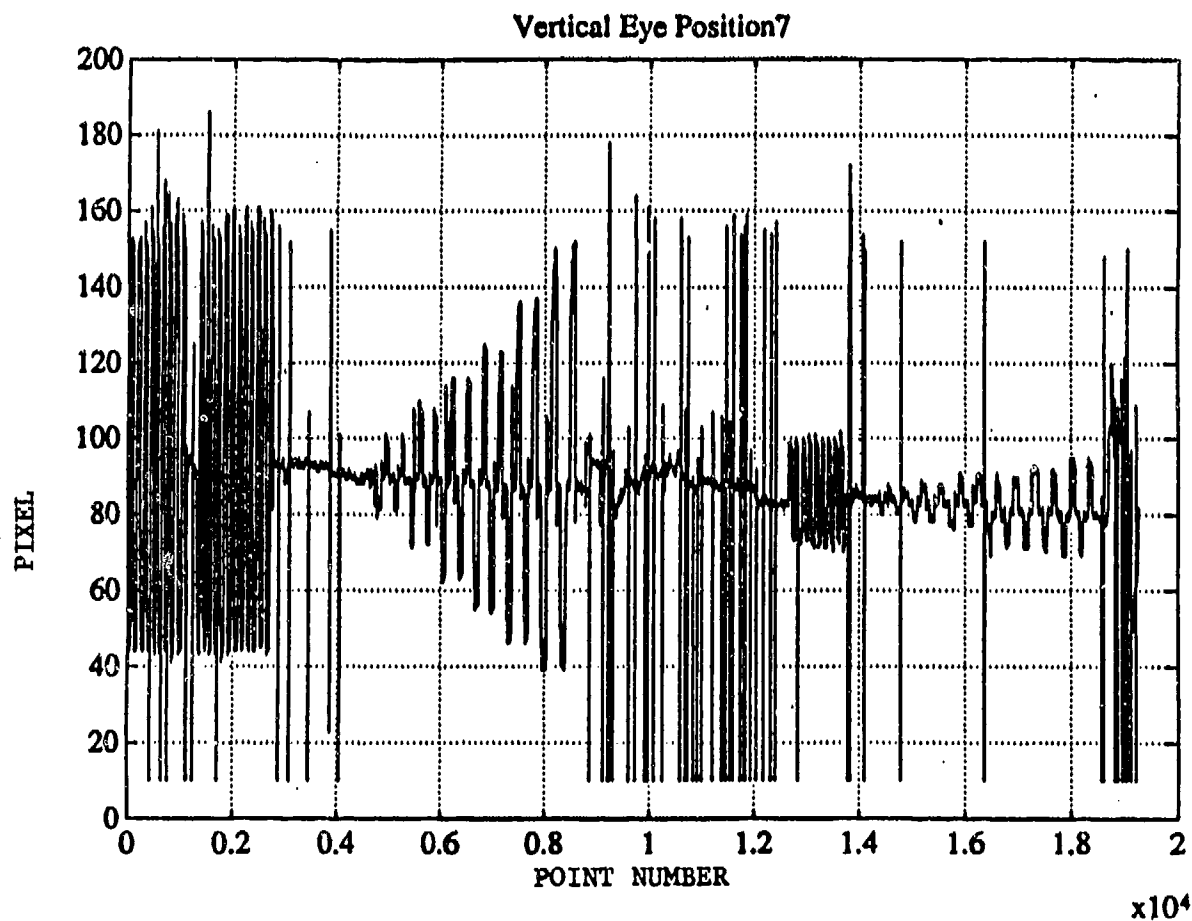
Figure 3.2: Representative Vertical Eye Position Calibration

35
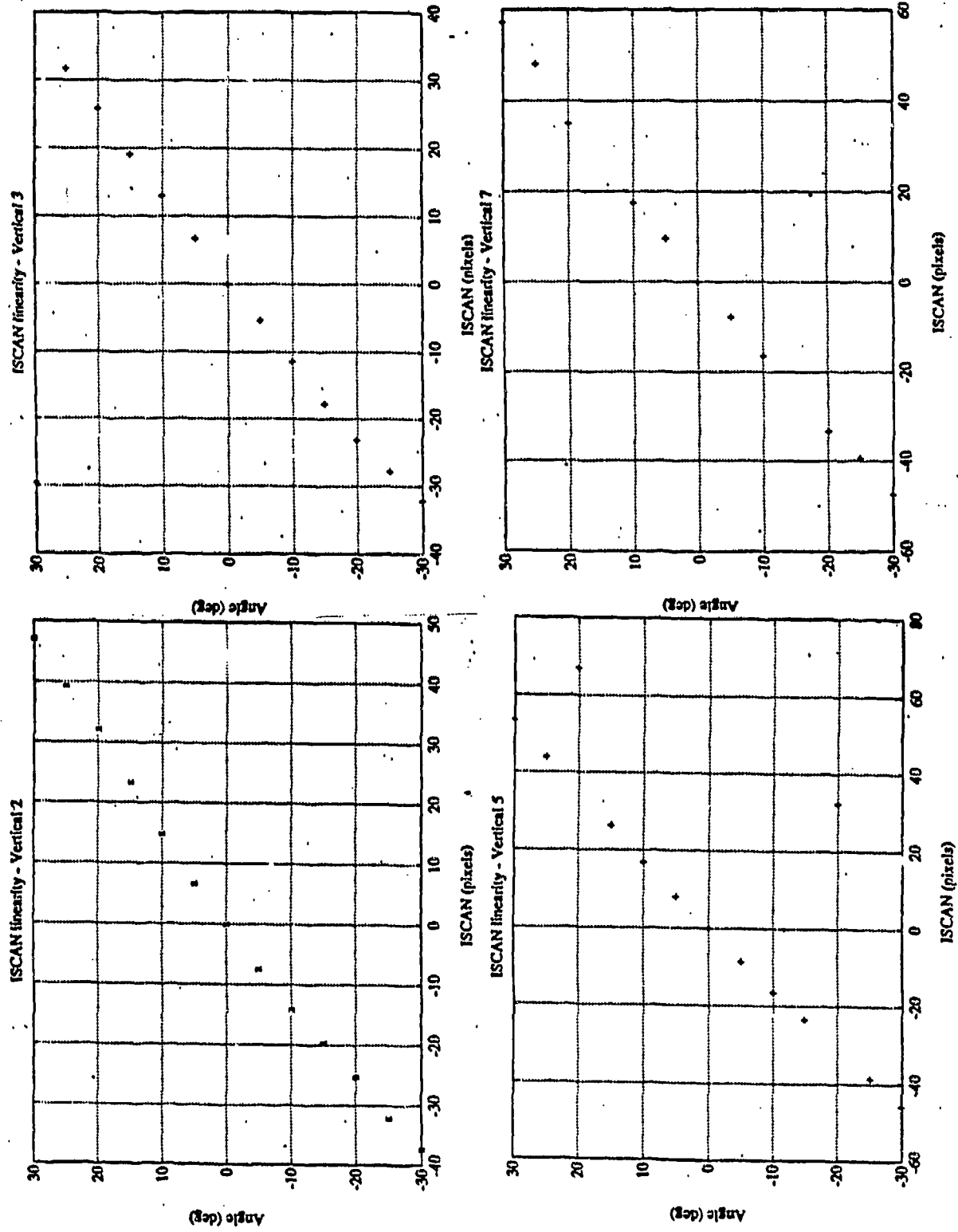
Figure 3.3: Results Vertical ISCAN Linearity
4 Subjects, Angle (deg) vs Pixel

36

3.1.2 Data Path

The ISCAN video signal from the camera was routed to a Panasonic Model AG1830 S-VHS video recorder located on the center of rotation of the CAP. A S-VHS video recorder was used due to its 400 line resolution and recorded the video signal for archival purposes. As shown in Figure 3.4 the video signal was then amplified using a Radio Shack 15-1102 Video Signal Amplifier and passed through the CAP slip rings to the control room. The signal was then deamplified using a another Video Amplifier before passing to the ISCAN RK-426 Pupil/Corneal Reflection Tracking Unit. The signal was amplified and deamplified to reduce noise interference generated by the slip rings.

Eight bit digital data of horizontal and vertical eye position from the ISCAN unit, analog data of eye position from EOG, and the CAP velocity (tachometer) were recorded "on-line" by an Apple Macintosh IIx computer equipped with a Data Translation DT2211-PGH data acquisition board and LabTech NoteBook data acquisition software. Appendix B shows the LabTech Notebook configuration used. The use of digital data avoided any loss of accuracy that may occur during digital to analog (D/A) and analog to digital (A/D) conversions. Digital data also avoided noise problems often found on poorly grounded analog signals. D/A converted ISCAN data was available from the RK426. A hard copy of the data was monitored using a stripchart recorder and saved.

Some of the on-line ISCAN eye position data was lost due to computer crashes and back-ups damaged during transportation, and therefore an "off-line" analysis was performed to recover the lost data. The off line analysis consisted of playing the original S-VHS video tapes and routing the video signal to the ISCAN unit directly. Digital data of horizontal and vertical eye position from the ISCAN unit was recorded by the Apple Macintosh IIx computer equipped with a Data Translation DT2211-PGH data acquisition board and

37

LabTech NoteBook data acquisition software. The same LabTech Notebook configuration shown in Appendix B was used.

Eye Position and Tachometer data files were converted from LabTech NoteBook format to M-File format using a C program called CONVERT. M-File format is the data format required by the ¹ata analysis program MatLab for Macintosh (© MathWorks) used for subsequent data analysis (See Section 3.4). Appendix C lists the C code of the program CONVERT.
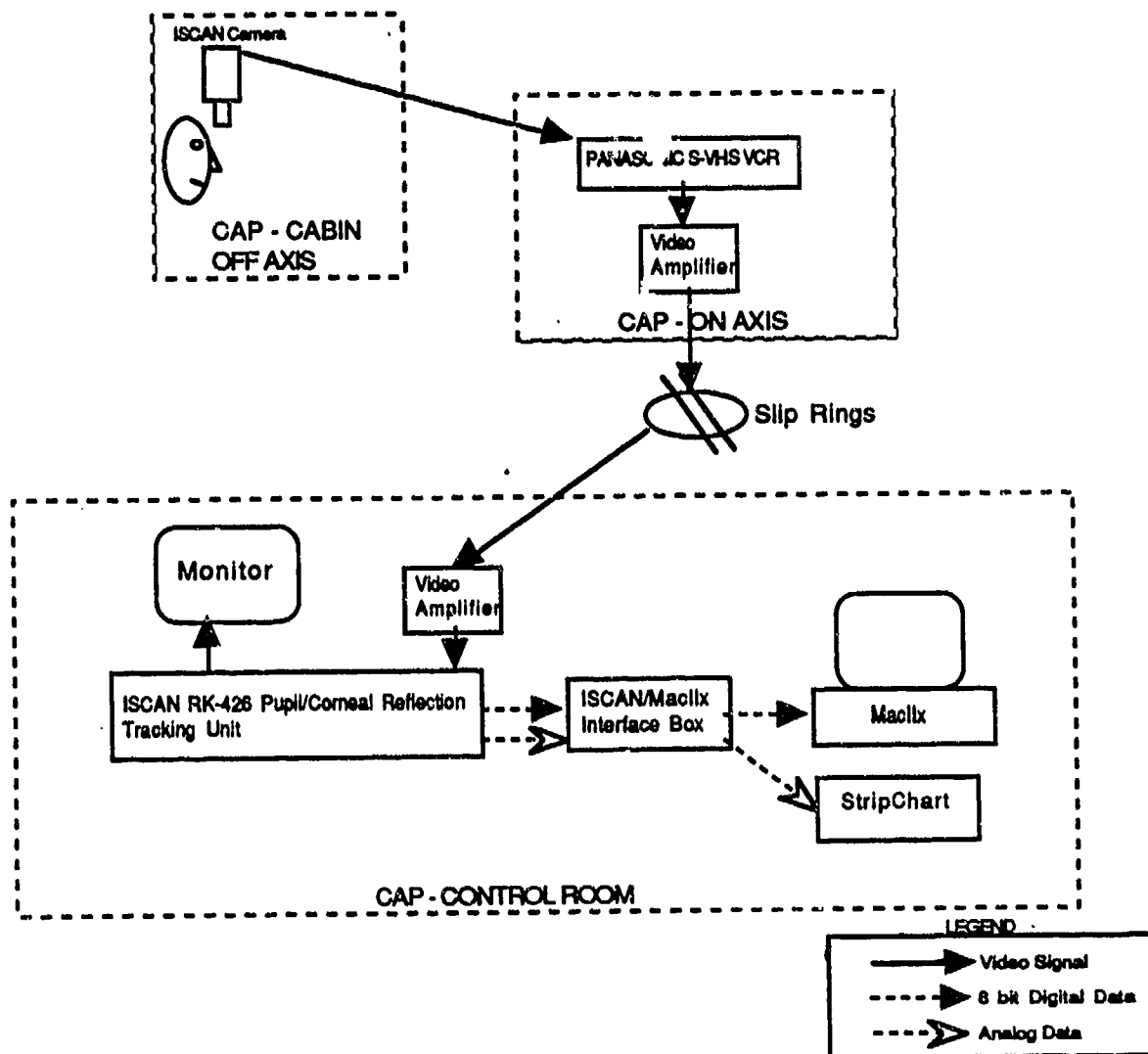
Figure 3.4: Experiment Data Path

38

3.2 SUBJECTS

Fifteen US Navy and Marine Pilot candidates awaiting flight training served as subjects. The subjects were male, ages 21-24, and all had passed Navy flight physical examinations without signs of vestibular disorders. None of the subjects had experienced sustained high G's either in a centrifuge or high performance aircraft before this experiment.

3.3 PROCEDURE

Each subject participated in six $3G_z$ runs: 3 runs were made facing the direction of motion (clockwise), and 3 runs were made with their back to the motion (counterclockwise). One run was made per day to avoid fatigue effects, and the order of the run direction was randomized to avoid habitation effects. Table 3.1 shows the run order for each subject. Mental arithmetic, general knowledge and sensation questions were asked throughout the run to maintain alertness and monitor subject safety. Subjects typically completed the required six runs in a period of eight to nine days.

Before each run, the subject's head was positioned erect in the head rest, such that the plane described by the line between the outer canthus of the eye and the top of the tragus was approximately 20 degrees above the horizontal. Due to safety considerations, the head was free to drop forward, such that in the event of GLOC, the head would drop, reducing the hydrostatic pressure difference between the heart and the head and restoring adequate blood flow to the brain. The subject was instructed not to move his head throughout the run.

Subject	Run #1	Run #2	Run #3	Run #4	Run #5	Run #6	Run #7
4	CW	CCW*					
5	CCW	CW	CCW	CW	CCW	CW	
6	CW	CW	CW	CCW	CCW	CCW	
7	CCW*						
8	CW	CCW	CW	CCW	CW	CCW	
9	CW	CCW	CW	CCW**	CCW	CW	CCW
10	CW	CCW	CW	CCW	CW	CCW	
11	CW	CCW	CW	CCW	CW	CCW	
12	CCW*						
13	CW*						
14	CW	CCW	CW	CCW	CW	CCW	
15	CW*	CW*					
16	CCW	CW	CCW	CW	CCW		
17	CW	CCW	CW	CCW	CW*	CCW	CW
18	CW	CCW	CCW	CW	CCW	CW	

* GLOC episode

** CAP Mechanical Failure, no data.

Table 3.1: Run Order

Subjects were instructed to look at the center LED of the calibration target. This position was recorded on the operator video screen. After calibration lights were turned off, the subject was instructed to maintain the same gaze direction throughout the centrifuge run. During the run any deviations from this "straight ahead" gaze direction were noted by the operator, and the subject was instructed with the appropriate eye movement to return to the "straight ahead" gaze direction. Therefore, subject was looking straight ahead for the duration of the centrifuge run.

The CAP profile for each run (see Figure 4.4) consisted of a constant angular acceleration for 19 seconds to a constant velocity of 120°/sec. This generated a $3G_Z$ force at the chair that was sustained for 5 minutes. After the 5 minute sustained G_Z, a constant deceleration for 19 seconds completed the run.

Eye movements were recorded throughout the run, and either 1 minute after the run, or until the subject indicated he felt he was seated in a normal upright position, whichever was longer. Two point (+/- 10 deg) vertical and horizontal eye position calibration was performed before and after each run. For each subject, the distance from his eyes to the calibration fixture was recorded. Subjective sensations to be used in a companion study were obtained in a debrief immediately following the run. A copy of the debrief questionnaire can be found in Appendix F.

3.4 EYE MOVEMENT ANALYSIS

3.4.1 Background

Calculation of slow phase velocity (SPV) has traditionally been one of the major steps in analysis of eye movement records in vestibular research laboratories and neuro-otology clinics for more than thirty years.

Initially, nystagmus analysis was a manual process that was time consuming, labor intensive, and therefore expensive. An experienced operator identified each saccade and measured the slope of the eye position vs. time plot, either with a ruler or an analog electronic differentiator. Shortcut methods, such as quantification of peak or average SPV, nystagmus duration, or beat count and/or frequency were often used to save time. These methods provided reasonably accurate results, however they are prone to operator dependent errors. Gentles and Barber (1973) showed that the manual analysis of nystagmus leads to large person-to-person variability due to personal biases.

With the advent of digital computers and advanced digital processing methods, semi-automated and automated methods for nystagmus analysis have become available that overcome some of the limitations of manual analysis. Merfeld (1990) provided a review of the history and current state-of-the-art nystagmus analysis methods, and concluded that an acceleration based method is the most appropriate method if the signal is relatively noise free (like the digital data from ISCAN).

42

3.4.2 Method Used

The separation of the nystagmus eye movements into slow and fast phase components and calculation of SPV was performed using an analysis package called NysA (Nystagmus Analysis Package) that was developed at MIT. NysA is a Macintosh based, semi-automated analysis that uses a single axis, single pass, acceleration based algorithm developed by Massoumnia, (1983) to calculate slow phase velocity.

Preprocessing of data (calculation of calibration scale factor, prefiltering), postprocessing (manual editing, filtering, decimation, hard copy), and statistical analysis (means, variances) were performed using the commercially available data analysis program MatLab for Macintosh (© MathWorks). Figure 3.5 shows graphically the process flowpath used to calculate SPV profiles.

3.4.2.1 MATLAB Preprocess

Preprocessing of the eye position data was required before analysis by NysA. Three functions were performed;

      i) Loading of Data,

      ii) Calculation of Calibration scale factors, and

      iii) Stripping of unwanted data.

The functions were implemented using M-Files in MatLab and are listed in Appendix D.

43
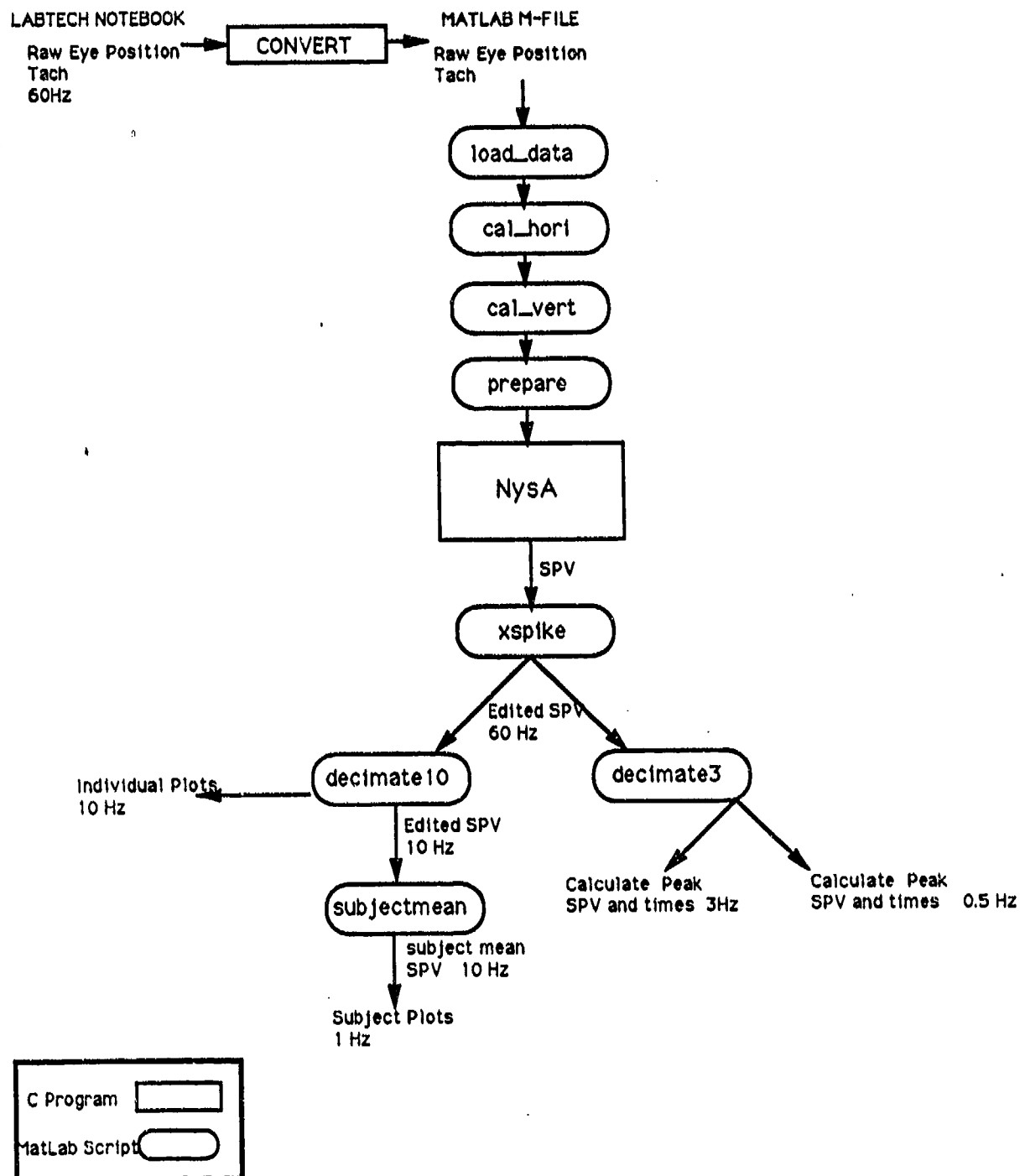
Figure 3.5: SPV Analysis Pathway

44

ISCAN eye position data, CAP tachometer and subject calibration parameters are loaded into MatLab for further analysis. The script LOAD_DATA performs this function.

Horizontal and vertical calibration scale factors (pixels/deg) were calculated using a 2 pt (+/-10 deg) calibration scheme. For each eye position axis, the region where the eye position signal is steady on the positive and negative targets is identified by the user, and the average eye position is calculated. Using this average eye position and the known calibration angle, the calibration scale factor is calculated. Calibration scale factors are calculated before and after the centrifuge run and averaged to obtain a single scale factor for use by NysA. The programs which implement this analysis for the two axes are called CAL_HORI and CAL_VERT.

Due to the nature of centrifuge operations, the data acquisition was started many minutes before the run, and ended a long time after the run. Therefore the data files contain unwanted eye position data that needs to be removed before NysA analysis. The script PREPARE creates a segment of the eye position and tachometer files starting 10secs before acceleration and finishing 90 secs after the run. The purpose of this function is to extract from the long eye movement record the segment of the data which needs to be analyzed by NysA. This gives a 438sec long data file sampled at 60 Hz to be analyzed by NysA.

3.4.2.2 NysA - Massoumnia Algorithm

NysA uses a modified acceleration/velocity trajectory based algorithm to calculate slow phase velocity. NysA detects fast eye movements and classifies them as fast phase saccades or other (blinks, artifacts etc) and calculates SPV in the following manner. For a full description see the NysA manual (Oman et al. 1990).

The beginning of a fast eye movement is when;

      i) the acceleration is increasing,

      ii) the magnitude of the acceleration is greater than a starting threshold T_S,

      iii) the eye velocity has the same sign as the acceleration.

When RMS eye acceleration calculated over the previous 250ms is low, T_S is equal to a user supplied minimum acceleration threshold T_{ma}, or when RMS eye acceleration exceeds $0.5 * T_{ma}$, then Ts = RMS acceleration + $0.5 * T_{ma}$. For ISCAN data T_{ma} was set between 200 and $700°/sec^2$.

The endpoint of the fast phase detection scheme has been modified from the original Massoumnia algorithm to accommodate the character of blink artifacts that appear in ISCAN data. The end of the fast eye movement is when:

      i) the magnitude of the acceleration is below the ending threshold T_e,

      ii) the sign of the velocity has reversed from its onset value, and

      iii) that at some time during the fast event, the acceleration signal has changed sign at least once from its value at the event onset.

or when 250 msec has elapsed. The ending threshold $T_e = 0.7 * T_S$.

Once the starting and ending points for the event have been established, the velocity spike during the event is clipped by resetting all values equal to the average of the velocity at the fourth point before and the third point after the event. The resulting "clipped" velocity is then low pass filtered to smooth out the clipping transitions, and output as SPV.

NysA uses three Finite Impulse Response (FIR) digital filters to compute the 1st and 2nd derivatives of the eye position: a 9 point acceleration filter, a 9 point velocity filter and a 7 point low pass SPV smoothing filter. The filters are calculated based on the data sampling rate F_S specified by the user.

46

3.4.2.3. MATLAB SPV Postprocess

Postprocessing of the NysA slow phase velocity data was required since NysA only detected and removed correctly approximately 80% of the fast phases/saccades. Programs that could be used to remove missed saccades were implemented using M-Files in MatLab and are listed in Appendix E.

Slow phase velocity output files from NysA contained "missed saccades". The script XSPIKE permits interactive graphical editing of slow phase velocity data to allow the user to remove the "missed saccades". XSPIKE displays the NysA SPV file and allows the user to "zoom in" to a region of interest. It then displays the original eye position, raw eye velocity and NysA calculated SPV (see Figure 3.6)

The position and raw eye velocity are plotted such that a more informed decision can be made on whether a "spike" in the SPV is in fact an artifact (e.g. a missed fast phase) or unusual data. It also allows the user to accurately identify the start and the end of the artifact. After user has identified the artifact by mouse clicks, the script linearly interpolates the velocity data across the region designated and then redisplays the edited velocity data for inspection. When all artifacts are removed XSPIKE saves the data and prompts the user to view the NysA SPV and the new edited SPV plots to compare differences.

47
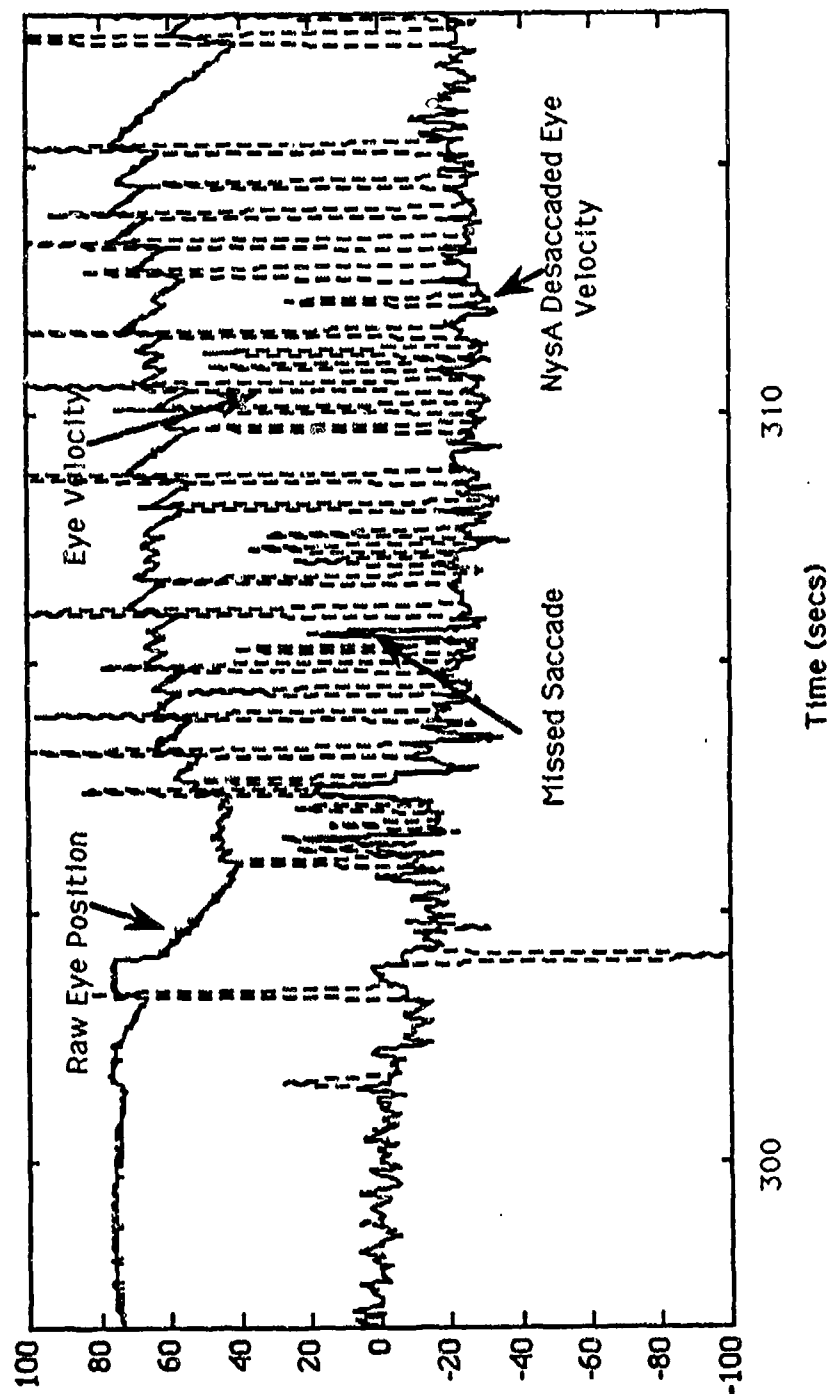
Figure 3.6: Screen shot of XSPIKE results

48

3.4.2.4. MATLAB Further Processing

Further processing of the slow phase velocity data was performed to generate hard copies of the SPV response, calculate mean responses, and to calculate the peak SPV. Program scripts are listed in Appendix E.

For presentation of individual runs (see section 5.3) and calculation of subject means (see sections 5.5), the edited SPV data file was decimated from the original 60 Hz sampling rate to 10 Hz using the script DECIMATE10. This script uses the built-in MatLab function decimate. Decimate10 resamples the data at the lower rate 10 Hz after first lowpass filtering the data with an 12th order Chebyshev type I lowpass filter with cutoff frequency 4 Hz. Given the nature of the stimulus it was expected that the SPV response would have significant dynamics with frequency content of less than 0.5 Hz. Therefore a low pass cut off frequency of 4 Hz was considered a very conservative value such that no information was expected to be lost during the filtering. For presentation of the individual runs, hard copies of the horizontal and vertical slow phase velocity plots are produced.

The subject means are then calculated using the above 10Hz SPV files. For presentation, the mean SPV response files are further low passed filtered to 1 Hz using the built-in MatLab function filtfilt. Filtfilt applies a specified filter in a non-causal manner that produces no phase distortion and minimizes startup transients. It does this by filtering the data file twice, first in the forward direction and then in reverse, to produce a sequence with exactly zero phase distortion. In this case the filter applied is a 12th order Chebyshev type I lowpass filter with cutoff frequency 1 Hz. Hard copies of the horizontal and vertical slow phase velocity plots are then produced. The mean responses were filtered to produce a cleaner plot by removing unwanted noise. MatLab script SUBJECTMEAN performs the above analysis.

49

For calculation of the estimate of peak SPV values (see section 5.4), the SPV data file was decimated from 60 Hz to 3 Hz using the MatLab script DECIMATE3. This script uses the built-in MatLab function decimate. This script resamples the data at the lower rate 3 Hz after first lowpass filtering the data with an 8th order Chebyshev type I lowpass filter with cutoff frequency 1.2 Hz. The times of peak SPV were then calculated by plotting the SPV data and locating the time at which the peak SPV occured. The peak SPVs were then obtained by taking the mean of the SPV 1/3 sec before, and 1/3 sec after, the time of peak SPV. The vertical SPVs at set times (100, 150 and 315 secs) were obtained by taking the mean of the SPV 10 secs before and 10 secs after the indicated time. The peak SPV values and the SPV's at set times were averaged over time to avoid any problem of noise spikes that may occur at the required time.

Then the SPV file was low pass filtered to 0.5 Hz using the built-in MatLab function filtfilt. Since this analysis was to find an estimate of the peak SPV and the corresponding time, a missed saccade at the time of peak SPV would give a large error. The SPV data was heavily filtered to remove all spikes and the peak SPV values are then recalculated using the above method. A comparison was then made between the SPV results from the 1.2Hz data and 0.5Hz. data, and if any large descrepancies were noted the 60 Hz data file was used to see if the discrepancy was from a spike or other artifacts, and an estimate of peak SPV was then approximated from the three SPV data sets (60Hz., 1.2Hz, and 0.5Hz.).

50

3.4.3 Conclusion

Figures 3.7 and 3.8 show the slow phase velocity during the various stages of processing. Figure 3.7 shows the horizontal response and Figure 3.8 the vertical response. This data set is typical for all the data analyzed. Some runs required more manual editing due to poor performance of NysA when ISCAN illumination levels were poorly set. This problem highlighted the sensitivity of the ISCAN data quality on illumination, and therefore reinforced the point that the operator must take the time and adjust the illumination properly.

For this experiment the ISCAN 60 Hz sampling rate and 8 bit spatial resolution produced a signal that approximated a fairly continuous signal that was adequately analysed by NysA. However, for high fast phase beat frequency eye position data the combination of 8-bits and the 60Hz. sampling rate would give a discrete time signal that consisted of a few quantized levels for the slow phase followed by the fast phase. The data would be noisy due to quantization and undersampling, and the NysA algorithm would be expected to perform poorly. Modifications to NysA or increasing spatial and temporal resolution of the ISCAN system could eventually overcome any problems associated with high frequency nystagmus.
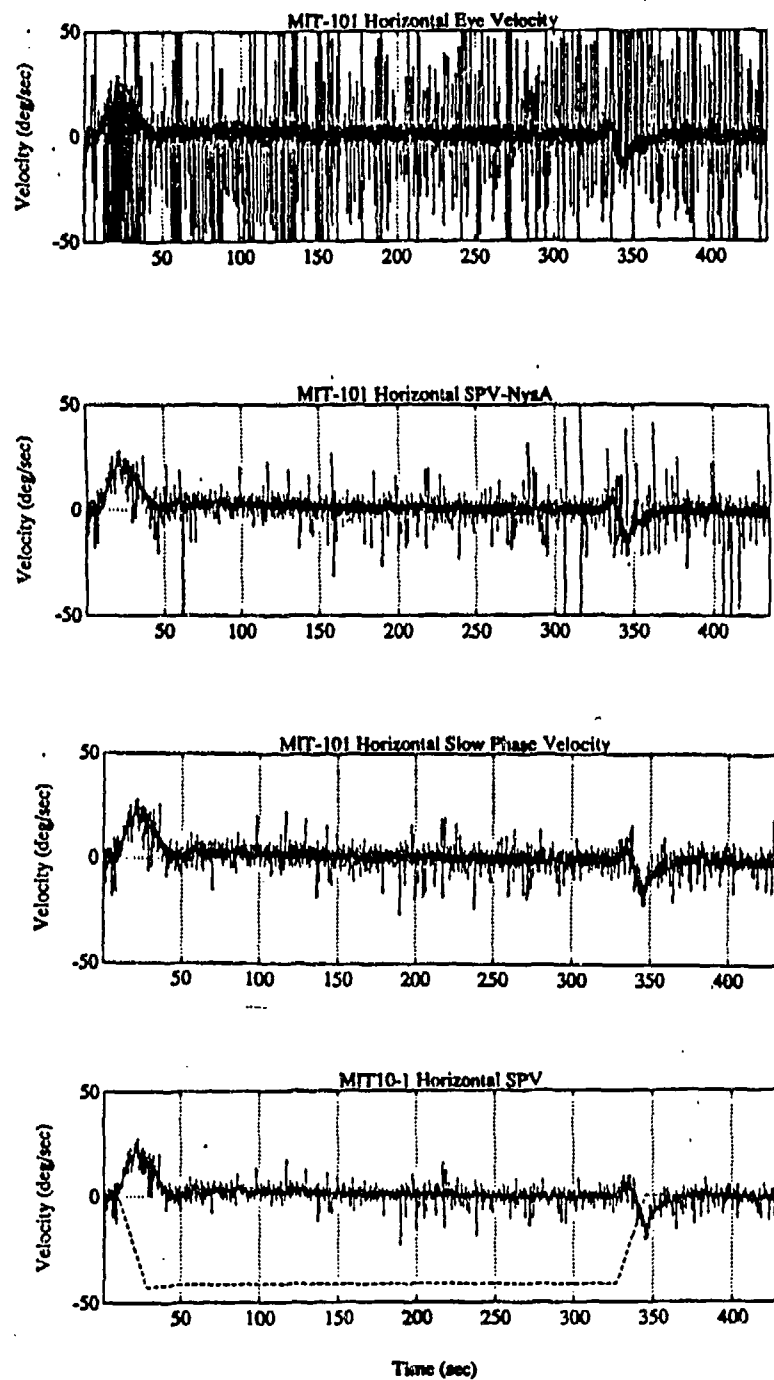
Figure 3.7: Horizontal SPV Processing
a. Raw Eye Velocity
b. NysA Desaccaded Eye Velocity
c. Manual Edited Eye Velocity - 60 Hz
d. Edited Eye Velocity - 10 Hz

52
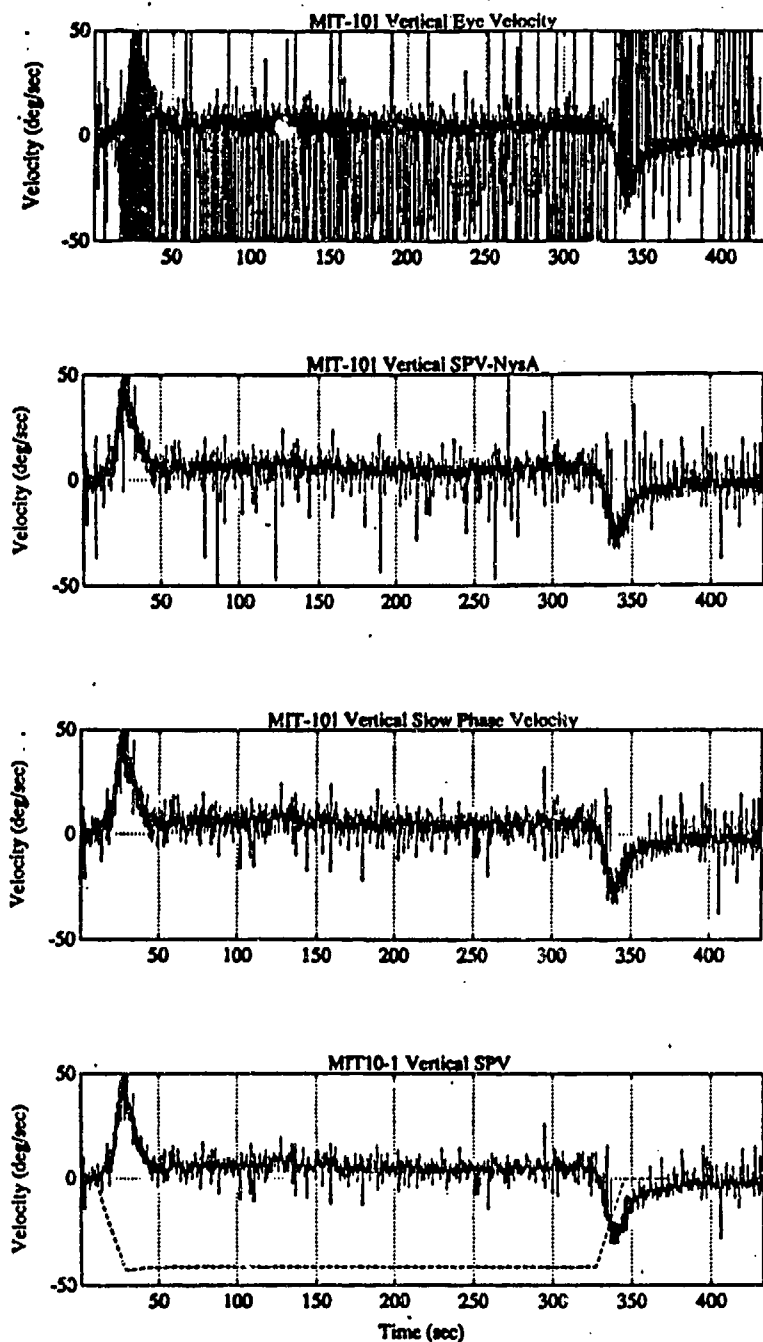
Figure 3.8: Vertical SPV Processing
a. Raw Eye Velocity
b. NysA Desaccaded Eye Velocity
c. Manual Edited Eye Velocity - 60 Hz
d. Edited Eye Velocity - 10 Hz

53

4. STIMULUS TO THE VESTIBULAR SYSTEM

4.1 INTRODUCTION

Since this experiment is of the input-output variety (acceleration in, nystagmus out) and we are using this data to infer function of the vestibular system, an accurate description of the stimulus to the vestibular system is required. However, due to the kinematics of the swinging cab centrifuge the stimulus to the vestibular system is very complicated. To address this issue, a program was developed that calculates the linear and angular accelerations and the angular velocities that are experienced by the human subject riding a pendulous centrifuge. The program was developed using the software package Extend(© Imagine That).

The program uses three dimensional Euler angle concepts to derive the body angular rates from the centrifuge angular rates, and a direction cosine matrix based on the Euler angles to transform inertial forces in a centrifuge frame to a body frame. The program uses a 3D rotational kinematics approach so that in the future the program can be expanded to include more complicated cases, for example, a 2 or 3 gimbal centrifuge. The use of Euler attitude angles overcomes the problem that 3D rotations cannot be treated as vectors since 3D rotations are not commutative, and are dependent upon the order of rotation. Therefore angular position cannot be differentiated to give angular velocity.

4.2 COORDINATE SYSTEMS

4.2.1 Head Fixed System

To describe the accelerations and forces in a head fixed coordinate system the coordinate system defined by Hixson et al (1966) for vestibular research will be used. This orthogonal right-handed coordinate is shown in Figure 4.1. Positive x direction is forward, positive y direction is out the subject's left ear, and the positive z direction is directed upwards.

Using the right hand rule to define angular quantities it can be seen that;

- positive ω_x represents a roll right ear down

- positive ω_y represents a pitch nose down

- positive ω_z represents a yaw to the left.

4.2.2 Cabin Fixed System

A convenient coordinate system is defined to describe the forces generated by the centrifuge and as an intermediate coordinate system between the inertial coordinate system and the head fixed coordinate system. This coordinate system is fixed with respect to the capsule at the end of the arm and is rotating with the angular velocity of the centrifuge ω_c (Figure 4.2).

PHYSIOLOGICAL ACCELERATION
NOMENCLATURE
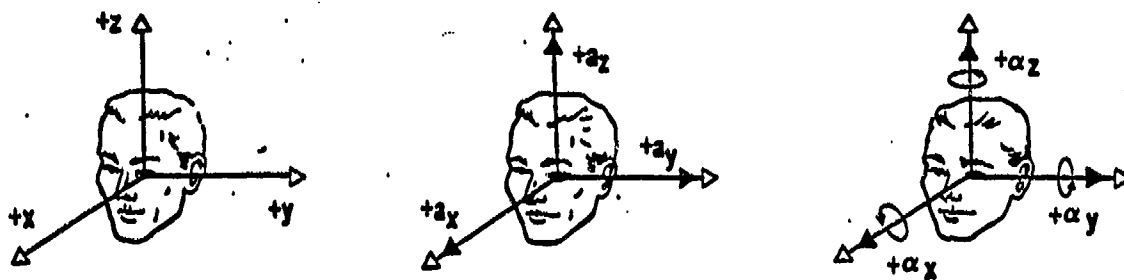
ANATOMICAL AXES x,y,z   **LINEAR ACCELERATION** a_x, a_y, a_z **ANGULAR ACCELERATION** $\alpha_x, \alpha_y, \alpha_z$

Figure 4.1. Diagram of Human co-ordinate system for vestibular research (Hixson et al. 1966)
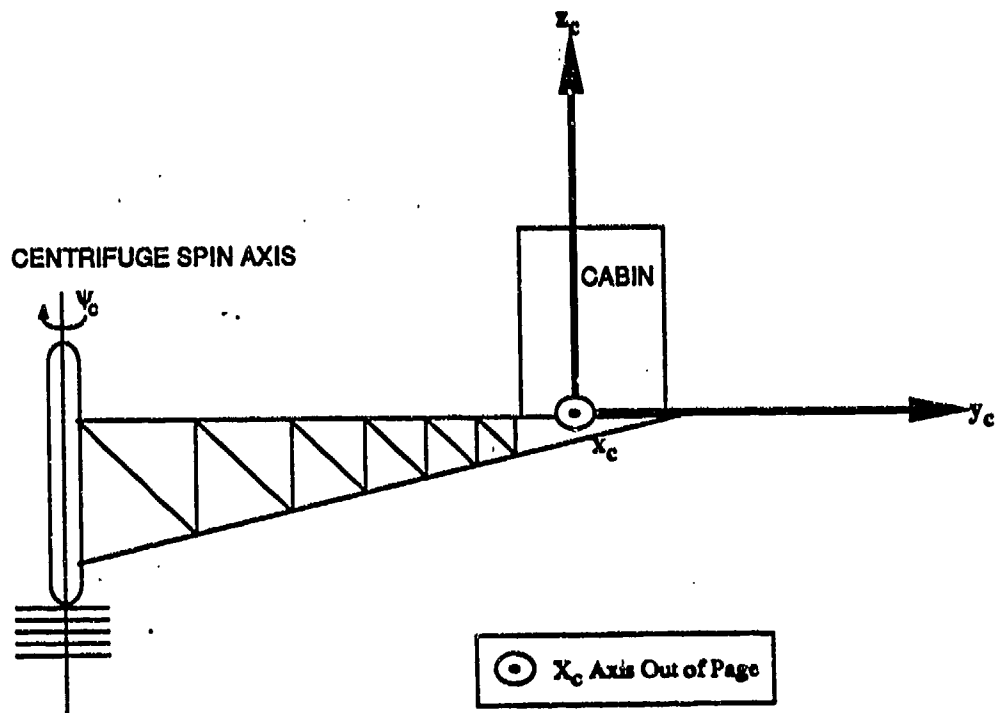
Figure 4.2: Capsule Fixed Coordinate System.

56

4.2.3 Euler Angles

The orientation of the head in space is defined by its Euler angles. The Euler angles will be defined going from the cabin to the head coordinate system by the following set of rotations (Figure 4.3):

first rotation is a yaw (ψ) about the z_c-axis,

second rotation is a pitch (θ) about the new y axis,

and the third rotation is a roll (ϕ) about the new x axis.
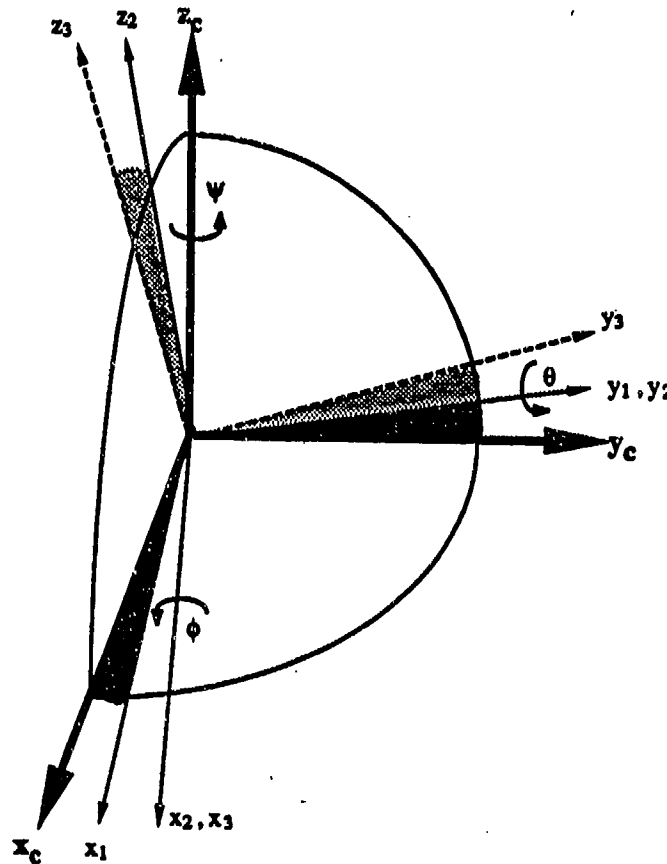
Figure 4.3:   Definition of Euler Angles.

4.3 CENTRIFUGE STIMULUS

The stimulus to the centrifuge is a ramp velocity profile and for a counter clockwise run is depicted in Figure 4.4 along with the acceleration profile. As the centrifuge accelerates the subject rolls with respect to gravity such that the resultant gravitio-inertial force is always in the negative head fixed z direction. Figure 4.5a depicts the orientation of the subject with respect to gravity and Figure 4.5b depicts the orientation of the subject with respect to the resultant GIF.
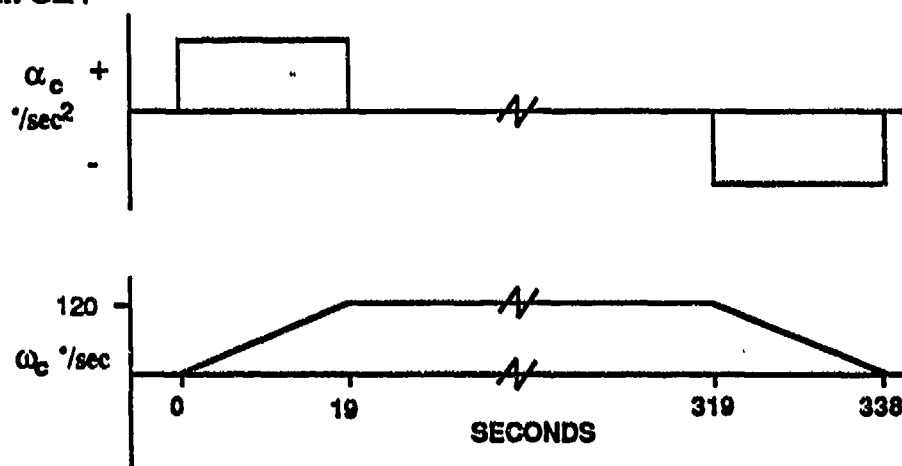
Figure 4.4: Centrifuge Velocity Profile (Counter Clockwise).
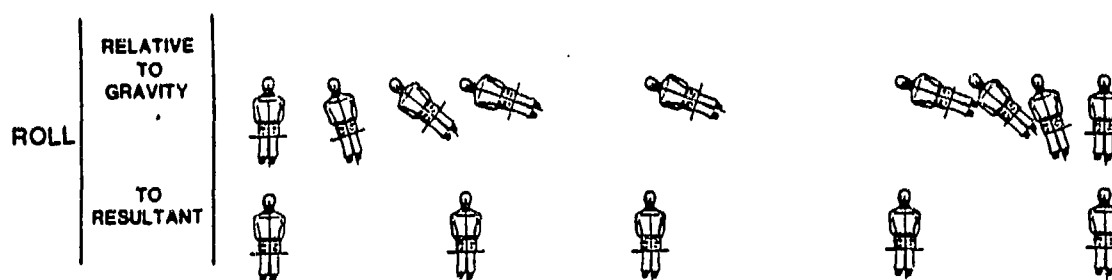
Figure 4.5: Orientation of Subject
a. w.r.t. gravity
b. w.r.t resultant GIF

58

4.4 DESCRIPTION OF THE EXTEND PROGRAM

The Extend program takes as input the velocity profile, ω_c as shown in figure 4.4.

It then calculates centrifuge angular acceleration,

$$\alpha_c = \frac{\partial \omega_c}{\partial t}$$

The centripetal and tangential forces in and the total gravitio-inertial force(GIF) in G units are then calculated in the capsule axes,

$$\text{Centripetal Force} = \frac{r\omega_c^2}{g}$$

$$\text{Tangential Force} = \frac{r\alpha_c}{g}$$

$$\text{GIF} = \sqrt{1 + \text{centripetal}^2 + \text{tangential}^2}$$

Then the Euler rates and angles are calculated for the head fixed axis with respect to the capsule axis. For this CAP experiment, the subject does not yaw or pitch relative to the capsule, thus,

$$\dot{\psi} = \psi = 0$$

$$\dot{\theta} = \theta = 0$$

and the roll angle is dependent upon the magnitude of the centripetal acceleration since the G.I.F is always in the head fixed z direction. Since the chair is gimballed, the roll angle is an Euler angle and thus can be differentiated to give roll rate, thus

$$\phi = \tan^{-1}(\text{centripetal})$$

$$\dot{\phi} = \frac{\partial \phi}{\partial t}$$

59

Transformation of inertial forces between the capsule and head axis is accomplished using a direction cosine matrix.

$$\begin{bmatrix} F_x \\ F_y \\ F_z \end{bmatrix} = \begin{bmatrix} l_1 & l_2 & l_3 \\ m_1 & m_2 & m_3 \\ n_1 & n_2 & n_3 \end{bmatrix} \begin{bmatrix} F_{x1} \\ F_{y1} \\ F_{z1} \end{bmatrix}$$

where F_x, F_y, F_z are the inertial forces in head axis, and F_{x1}, F_{y1}, F_{z1} are the inertial forces in the capsule axis. Noting that

$$F_{x1} = \text{tangential}$$

$$F_{y1} = \text{centripetal}$$

$$F_{z1} = -1$$

The direction cosines, l_1, l_2 etc are defined in terms of the Euler angles by the following equations (from Rolfe and Staples, 1986. eqn 3.10).

$$l_1 = \cos \theta \cos \psi$$

$$l_2 = \cos \theta \sin \psi$$

$$l_3 = - \sin \theta$$

$$m_1 = \sin \phi \sin \theta \cos \psi - \cos \phi \sin \psi$$

$$m_2 = \sin \phi \sin \theta \sin \psi + \cos \phi \cos \psi$$

$$m_3 = \sin \phi \cos \theta$$

$$n_1 = \cos \phi \sin \theta \cos \psi + \sin \phi \sin \psi$$

$$n_2 = \cos \phi \sin \theta \sin \psi - \sin \phi \cos \psi$$

$$n_3 = \cos \phi \cos \theta$$

The components of angular velocity about the head fixed axis are calculated from the Euler rates and angles using the following relationships (Rolfe and Staples,1986. eqn 3.6)

$$\omega_x = \dot{\phi} - \dot{\psi} \sin \theta$$

$$\omega_y = \dot{\theta} \cos \phi + \dot{\psi} \sin \phi \cos \theta$$

$$\omega_z = - \dot{\theta} \sin \phi + \dot{\psi} \cos \phi \cos \theta$$

See Appendix G for a listing of the program code.

4.5 RESULTS

4.5.1 Angular Acceleration

Figure 4.6 shows the angular acceleration experienced by the subject during a clockwise CAP centrifuge run. During CAP centrifuge acceleration (Figure 4.6a), the yaw angular acceleration stimulus (α_z) to the horizontal canals initially steps down to -6.3 °/sec². It (α_z) then increases and reverses sign at 21.3 sec. It continues to increase until it reaches a value of 1.7 °/sec². At the end of CAP centrifuge acceleration α_z steps down to zero. The pitch angular acceleration stimulus (α_y) to the vertical canal is approximately a ramp to -8.9 °/sec² at 21.4 secs. It (α_y) then increases slightly to -6.64 °/sec² and then at the end of the CAP centrifuge acceleration (29 secs) , α_y is step to zero.

During CAP centrifuge deceleration (Figure 4.6b), the yaw stimulus is a small step to -1.7 °/sec² then it increases and reverses at 336 secs until reaching 6.3 °/sec². At the end of CAP centrifuge deceleration α_z steps down to zero. The pitch angular acceleration stimulus (α_y) to the vertical canal is a step to 7.3 °/sec². It (α_y) then increases slightly to 8.9°/sec² at 337 secs followed by a approximate ramp decrease to zero.

61

The angular acceleration for counterclockwise runs would be the same as for clockwise runs except the signs would be reversed.
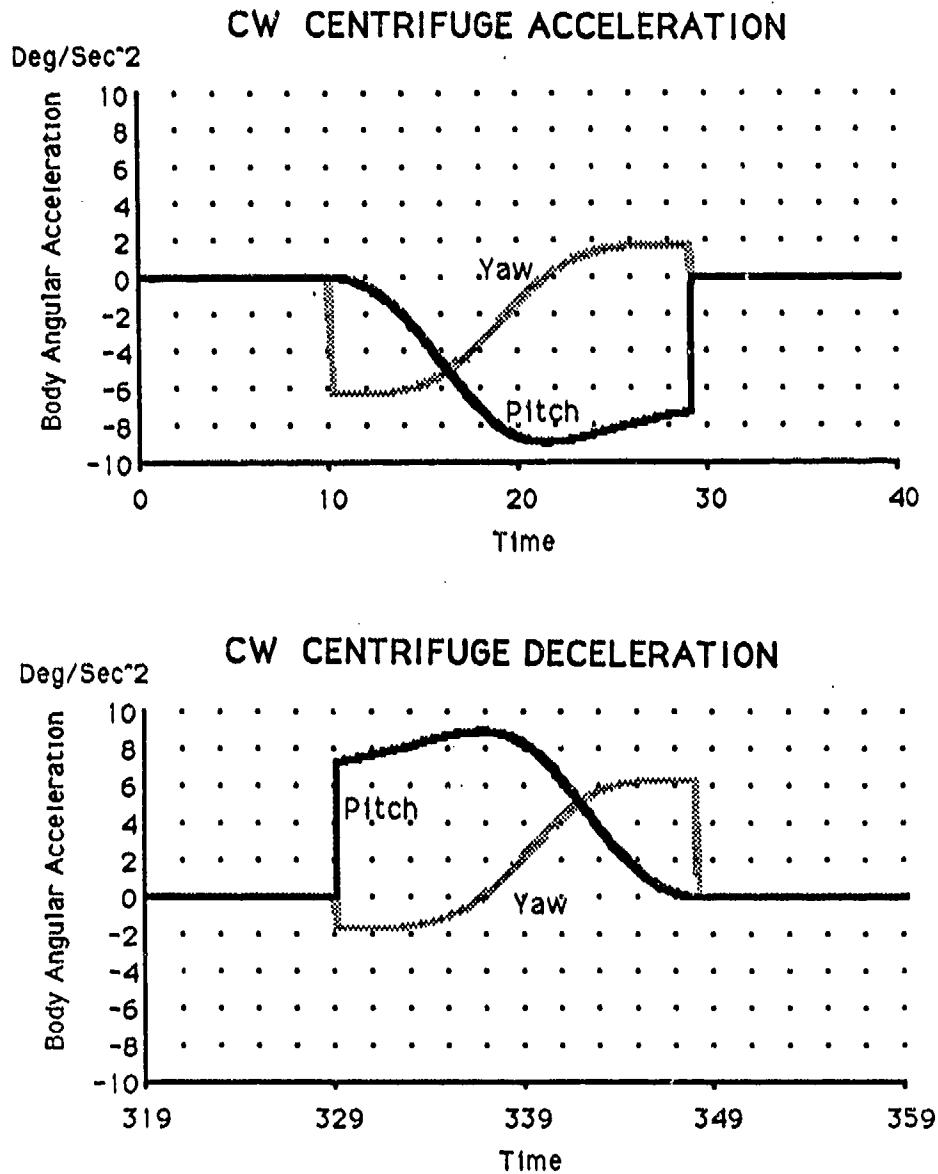

Figure 4.6: Angular Acceleration Stimulus (Clockwise).
    a. During CAP centrifuge acceleration
    b. During CAP centrifuge deceleration

62

4.5.2 Angular Velocity (Body Rates)

Figure 4.7 shows the angular velocity (body rates) experienced by the subject during a clockwise CAP centrifuge run. During CAP centrifuge acceleration (Figure 4.7a), the yaw angular velocity stimulus (ω_z) to the horizontal canals initially decreases "ramp-like" from 0 °/sec to -50.7 °/sec. It (ω_z) then increases to -40.4 °/sec at 29 secs and remains constant until CAP centrifuge deceleration. The pitch angular velocity stimulus (ω_y) to the vertical canals slowly decreases exponentially and then ramps down rapidly to -113.0 °/sec and then remains constant until CAP centrifuge deceleration. Roll angular velocity stimulus (ω_x) reaches a maximum of 5.75°/sec at 18.75 sec before returning to zero at 29.0 sec.

During CAP centrifuge deceleration (Figure 4.7b), the yaw velocity stimulus decreases from -40.4 °/sec to -50.5 °/sec at 336.5 sec, it then reverses and increases to zero at 348 sec. The pitch velocity stimulus (ω_y) initially ramps down rapidly from -113 °/sec then the slope of the ramp decreases until it reaches zero at the end of CAP centrifuge deceleration. Roll angular velocity stimulus (ω_x) during deceleration is a "mirror" image of acceleration.

The angular velocity for counterclockwise runs is the same as for clockwise runs except the sign is reversed.

63

BODY ANGULAR VELOCITY
DURING CLOCKWISE CENTRIFUGE ACCELERATION

BODY ANGULAR VELOCITY
DURING CLOCKWISE CENTRIFUGE DECELERATION
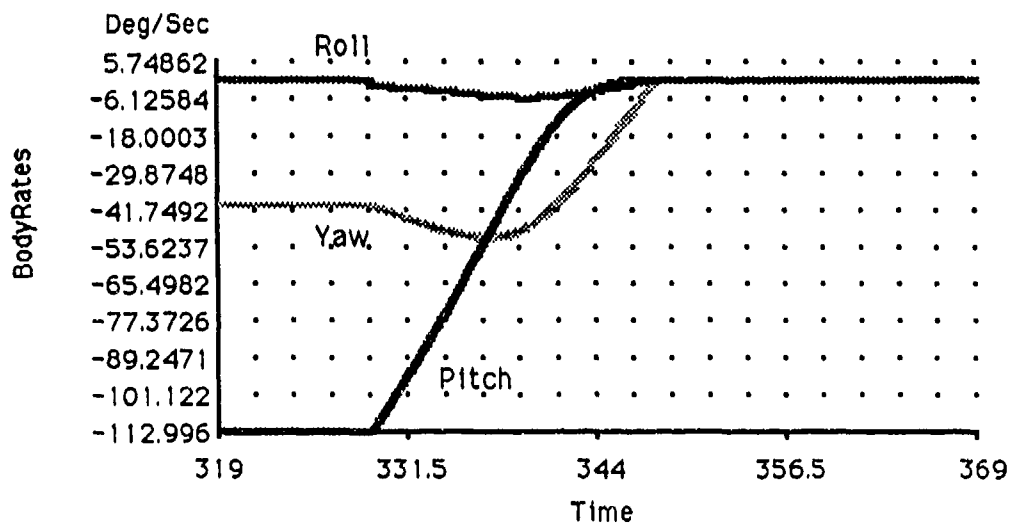
Figure 4.7: Angular Velocity Stimulus (Clockwise).
a. During CAP centrifuge acceleration
b. During CAP centrifuge deceleration

64

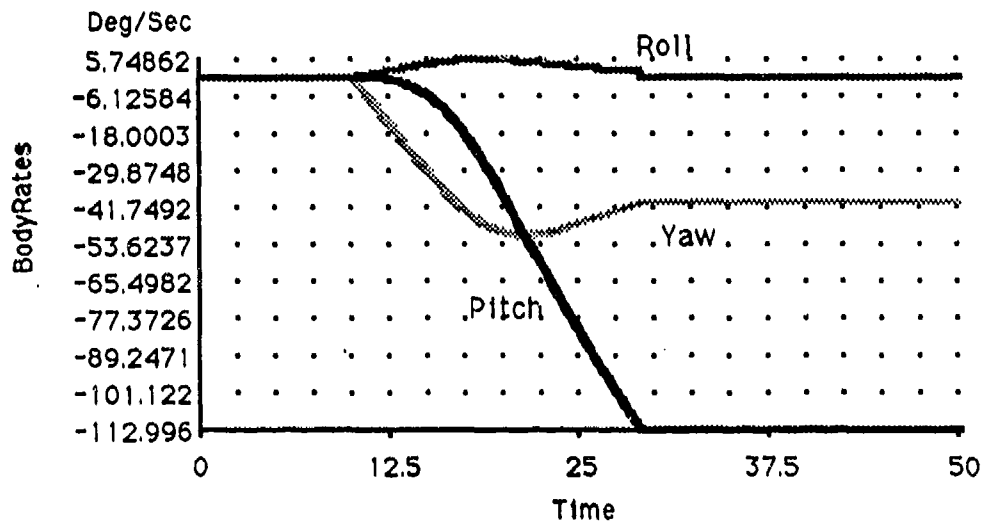## 4.5.3 Linear Acceleration Components

The inertial forces present during the CAP centrifuge run consist of a force F_x during CAP centrifuge acceleration and deceleration, and a gravitio-inertial force F_z that is constant throughout the constant velocity section of the run (Figure 4.8).

The F_x force is a step input during acceleration and deceleration and is equal to 0.07 G_x. This has the effect of swinging the gravito-inertial force F_z out of the YZ plane by an angle of 4 ° at the start of CAP centrifuge acceleration/deceleration and this angle reduces to 1.3 ° at the end of the CAP centrifuge acceleration/deceleration. The F_z force increases to 3 G_z during centrifuge acceleration and is maintained constant throughout the run, before decreasing to 1 G_z during centrifuge deceleration.

BODY INERTIAL FORCES
DURING A CLOCKWISE CENTRIFUGE RUN

Figure 4.8:   Linear Acceleration Components.

65

4.6 DISCUSSION

From Figure 4.6 one can see that angular acceleration during centrifuge acceleration is the time reversed "mirror image" of the centrifuge deceleration. During centrifuge acceleration, the vestibular system initially receives a ramp acceleration in the pitch direction, whereas during deceleration the system is initially stimulated with a step input. Therefore, during the initial phases of the stimulus the rate of onset of pitch velocity is greater dur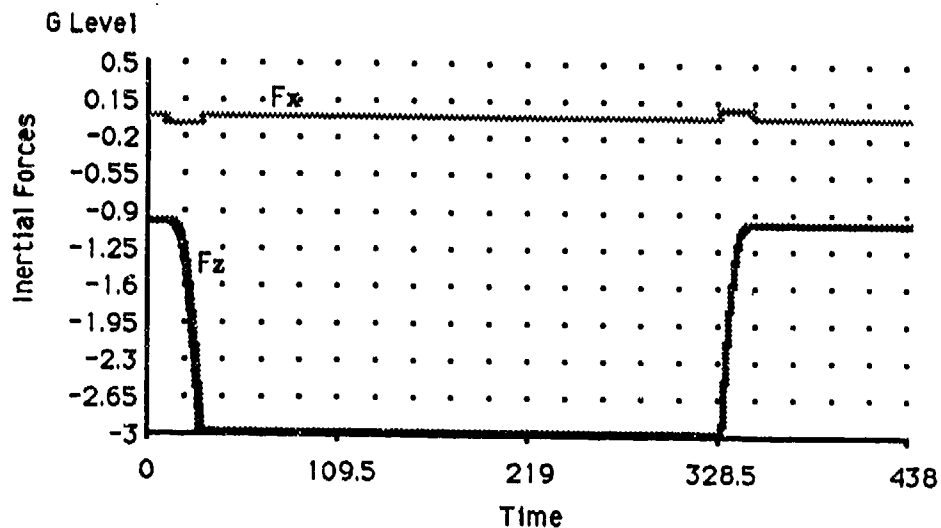ing deceleration than acceleration. By the end of the acceleration or deceleration, the time integral of the pitch cumulative angular velocity stimulus to the pitch canals is equal and opposite. However, the temporal nature is different. This difference is reflected in the angular velocity plots (Figure 4.7) where the build up of angular velocity is greater during the initial phases of the deceleration.

Secondly, the F_x inertial force swings the gravito-inertial force F_z out of the YZ plane by an angle of 4 ° at the start of CAP centrifuge acceleration/deceleration and this angle reduces to 1.3 ° at the end of the CAP centrifuge acceleration/deceleration. The F_x inertial force combines with F_z force vector to create a total resultant gravito-inertial force directed down and backwards during acceleration for a clockwise run. The subject, perceiving down to be in the direction of the total gravito-inertial force, will experience a weak pitch up sensation (Gillingham and Wolfe, 1986). During centrifuge deceleration for a clockwise run, the subject will experience a weak pitch down sensation. Conversely, during a counterclockwise run the small tangential acceleration will produce a weak pitch down sensation during centrifuge acceleration, and a weak pitch up sensation during centrifuge deceleration.

Thirdly, the rate of F_z onset is much higher during centrifuge deceleration then acceleration (Figure 4.8). The rate of change of linear force F_z is much higher during the initial phase of the centrifuge deceleration as compared to the initial phase of the centrifuge acceleration. This same effect was noticed for pitch angular velocity.

Finally, it is worth noting that at the end of centrifuge acceleration, the pitch angular acceleration stimulus and the linear acceleration stimulus are at a maximum. However, at the end of centrifuge deceleration, the pitch angular acceleration stimulus is a maximum whereas the linear acceleration stimulus is at a minimum.

5. RESULTS & DISCUSSION

5.1. GLCC EPISODES

Fifteen subjects participated in this experiment. Eight subjects (Nos 5, 6, 8, 9, 10, 11, 14, 18) completed all six runs, 6 Subjects (Nos 4, 7, 12, 13, 15, 17) experienced GLOC, and 1 Subject (No 16) became ill from other causes. For this experiment, GLOC is defined as a condition where the subject was unable to respond to simple requests from the operator. Unless stated below, the centrifuge run was operator aborted.

T. . GLOC episodes occurred during the following runs:

Subject 4: Counter Clockwise Run #1, Subject's 2nd Run.

Subject 7: Counter Clockwise Run #1, Subject's 1st Run.

Subject 12: Counter Clockwise Run #1, Subject's 1st Run.

Subject 13: Clockwise Run #1, Subject's 1st Run.

Subject 15: Clockwise Run #1, Subject's 1st Run (self abort @ 4.5mins).

Subject 15: Clockwise Run #2, Subject's 2nd Run (self abort @ 4.0mins).

Subject 17: Clockwise Run #3, Subject's 5th Run.

Only eye movement data from the 8 subjects who completed all six runs without GLOC were analyzed for this study. Subject 16 completed four runs before leaving the study, however this data was not analyzed due to its incompleteness. Subject 17 completed four runs before a GLOC episode on the first attempt at the 5th run and subsequently returned to finish all six. However, this data was not analyzed since the effects of GLOC on vestibular responses are not well understood, and to investigate these effects to allow inclusion of the

68

data set was considered to be beyond the scope of this research. Data from both subjects is available for future analysis.

The relatively high number of GLOC episodes could be attributed to the following factors:

Inexperience: None of the subjects had experienced sustained high G's before.

Fear/Apprehension: A combination of the dark cabin, ISCAN helmet with bitebar, and temperature created an environment that was troublesome to the subject.

Training/Protective Devices: No G-suit or adequate instruction on straining manoeuvres were provided.

Fatigue: Subject 17 had only 2 hrs sleep after being awake all night moving apartments.

After subjects had experienced a run in both directions, they appeared to have no problems, except Subject 17. It is felt that his GLOC was caused by fatigue. All subjects reported that a 3G centrifuge run was "getting easy" or "piece of cake" by their third or fourth runs.

5.2. SENSATIONS

Table 5.1 shows the subjective sensations for the pitch response obtained in the debrief. The symbol θ indicates the magnitude of the final pitch angle that the subject felt he had moved to. The symbol W indicates the number of complete turns or "tumbles" the subject felt before reaching the final position indicated by θ. Positive indicates pitching forward, negative indicates pitching backward. For example, θ -15 indicates a pitch back of 15° and W-(3) θ-90 indicates pitching backwards three complete turns and ending up pitched back 90° i.e lying on their back. The majority of the subjective sensation data will be used in a companion study. For the purposes of this thesis, from Table 5.1. one should note the large difference in pitch sensations between centrifuge acceleration and deceleration.

69

PITCH RESPONSE Clockwise

Run	Acceleration	Deceleration
5-2	W(0) θ-15	W+ θ+90
5-4	W(0) θ-0	W+ θ+70
5-6	W(0) θ-15	W+ θ+50
6-1	W(0) θ-30	W+
6-2	W(0) θ-40	W+ θ+120
6-3	W(0) θ-25	W+(1)
8-1	W(0) θ-20	W+(8) θ+55
8-3	W(0) θ-15	W+(2) θ+◌
8-5	W(0) θ-30	W+(1) θ+60
9-1	W(0) θ-45	W+ . θ+40
9-3	W(0) θ-15	θ+15
9-5	W(0) θ-30	*
10-1	W(0) θ-30	θ-80
10-3	W(0) θ-30	W+
10-5	W(0) θ-15	θ-70
11-1	W(0) θ-25	W+(3)
11-3	W(0) θ-45	W+(1) W-(2)
11-5	W(0) θ+45	W+(3) θ+60
14-1	W(0) θ-20	W+(3) θ+90
14-3	W(0) θ-	θ+90
14-5	W(0) θ-5	W+ θ+5
18-1	W(0) θ<<	W- θ+90
18-4	W(0) θ-15	W+(3) θ+270
18-6	W(0) θ-15	W+(4) θ+270

PITCH RESPONSE CounterClockwise

Run	Acceleration	Deceleration
5-1		W-(3) θ-135
5-3	W(0) θ-10	W- θ-70
5-5	W(0) θ0	W- θ-90
6-4	W(0) θ+50	W-(3) θ-90
6-5	W(0) θ-50	W-(3) θ-70
6-6	W(0) θ-60	W-(2) θ-70
8-2	W(0) θ+40	W-(5) θ-90
8-4	W(0) θ+15	W-(4) θ-130
8-6	W(0) θ+30	W-(4) θ-100
9-2	W(0) θ-20	**
9-5	W(0) θ-20	W- θ-90
9-7	W(0) θ0	W-(3) θ-10
10-2	W(0) θ-20	W-(5) θ-90
10-4	W(0) θ-<	W-(2) θ-20
10-6	W(0) θ+20	W-(1) θ-30
11-2	W(0) θ+45	W+(4) θ-50
11-4		W-(2)
11-6	W(0) θ+60	W-(2) θ-45
14-2	W(0) θ+30	W-(2) θ-90
14-4	W(0) θ+10	W-(2) θ-45
14-6	W(0) θ+30	θ-90
18-2	W(0) θ-15	W-(4) θ-90
18-3	W(0) θ+30	W-(2) θ-90
18-5	W(0) θ+20	W-(3) θ+20

* Subject 9-6 reported tumbling in the roll plane 3-4 turns during deceleration.

** Subject 9-2 reported a "hammerhead turn" during deceleration.

Table 5.1: Subjective Pitch Sensations.

During centrifuge acceleration the majority of subjects reported that they felt pitched up or down by a small angle less than 60°. During centrifuge deceleration, subjects reported the sensation of pitching forward or backwards head over heels from 1-8 complete turns, before ending up in a range of positions. Even though the cumulative pitch stimulus to the vestibular system is equivalent for centrifuge acceleration and deceleration, the pitch subjective sensations differ by a large amount.

5.3. INDIVIDUAL SLOW PHASE VELOCITY RESPONSES

In Figures 5.1 through 5.32 the horizontal and vertical slow phase velocity plots for individual runs are presented. Each figure contains a subjects response on one axis for all three runs in one direction. For example, Figure 5.3 shows the horizontal slow phase velocity response from subject 5's three counterclockwise runs (5-1, 5-3, 5-5), and Figure 5.2 shows the vertical slow phase velocity response from subject 5's three counterclockwise runs (5-1,5-3,5-5).

Note that there is no data for 5-6, as this data was lost due to a computer crash, and the 8-1 signal is lost during the run because the ISCAN illuminator wire worked its way loose. The centrifuge tachometer signal is plotted on some of the graphs as a dashed line. At the end of some of the plots a small step in the tachometer signal can be seen with a corresponding horizontal SPV response (For example Figures 5.13,5.14). This is the centrifuge being repositioned to the subject entry and exit location after subject has indicated that he feels seated in a normal upright position. Slow phase velocity (SPV) sign is defined using the coordinate system defined by Hixson et al. (1966) for vestibular research (Figure 4.1.). For example, up beating nystagmus which corresponds to SPV down is defined as positive, and SPV to the left (right beating nystagmus) is defined as positive.
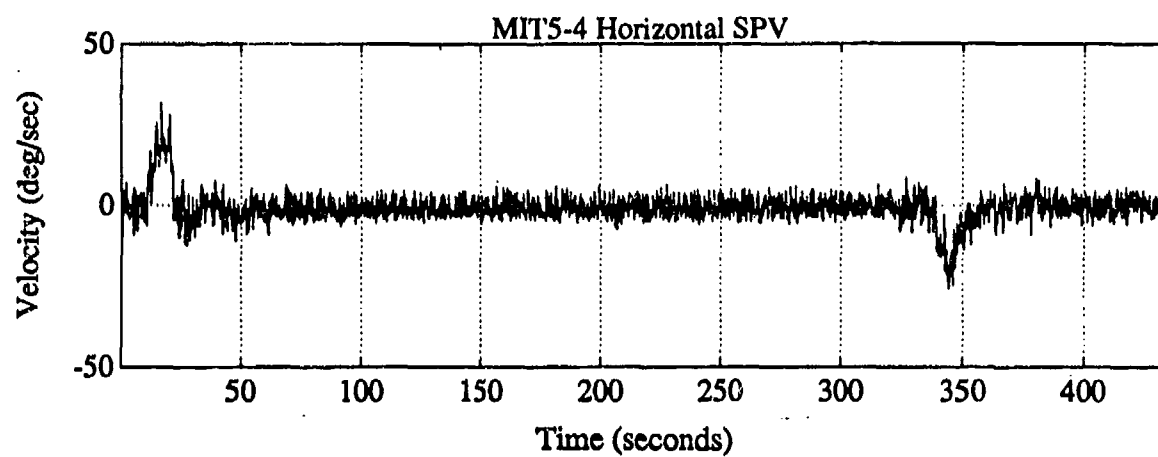
Figure 5.1: Horizontal SPV
Subject 5, Clockwise

72

Figure 5.2: Vertical SPV
Subject 5, Clockwise

73
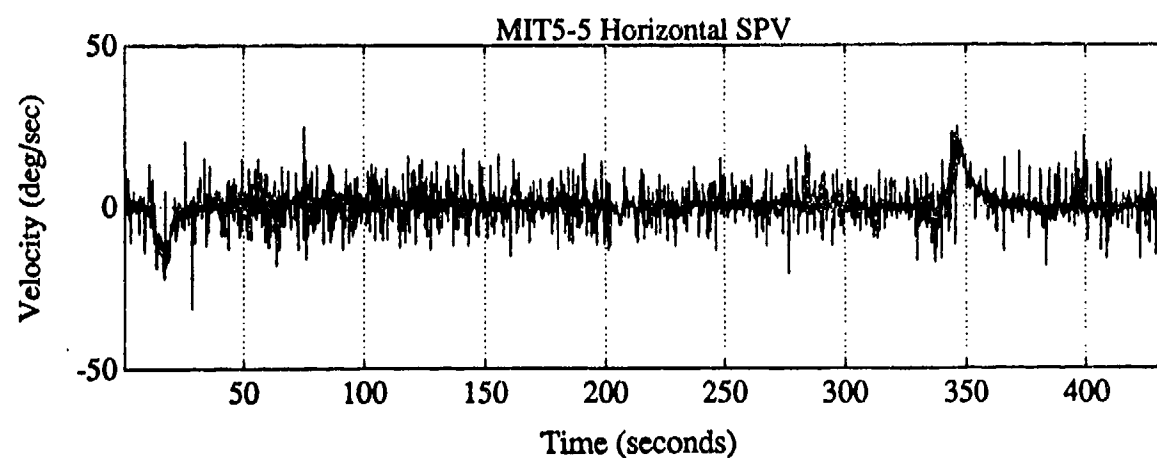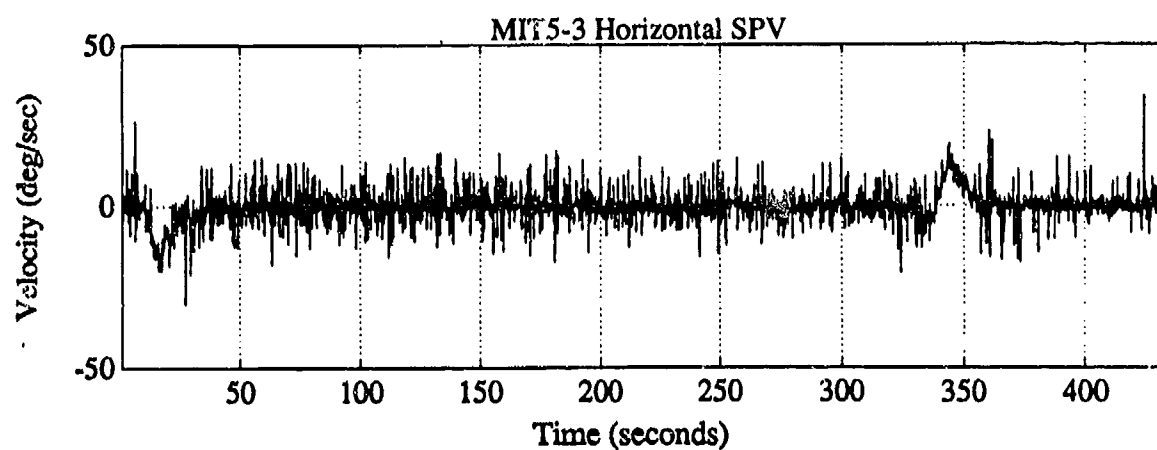
Figure 5.3: Horizontal SPV
Subject 5, CounterClockwise

74

Figure 5.4: Vertical SPV
Subject 5, CounterClockwise

75

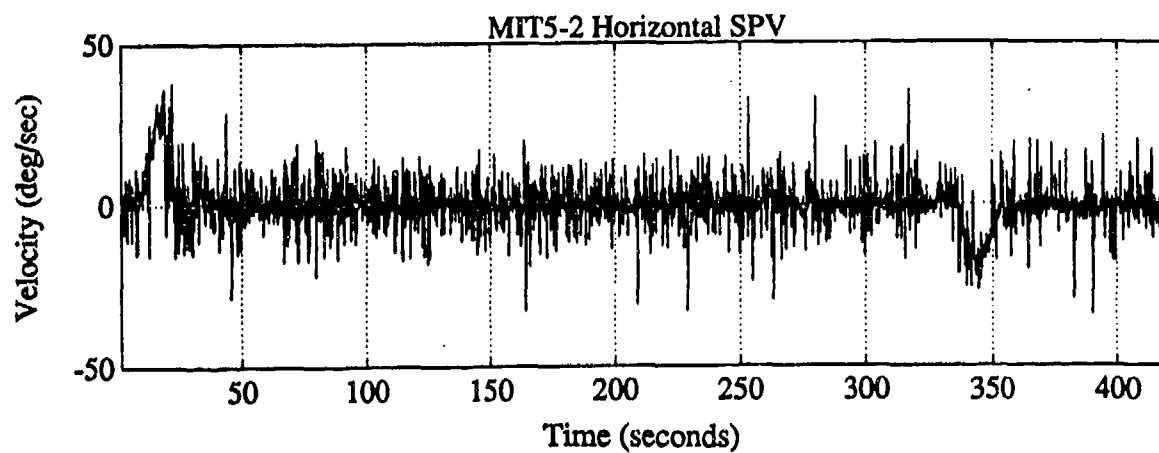Figure 5.5: Horizontal SPV
Subject 6, Clockwise

Figure 5.6: Vertical SPV
Subject 6, Clockwise

77

Figure 5.7: Horizontal SPV
Subject 6, CounterClockwise

78

Figure 5.8: Vertical SPV
Subject 6, CounterClockwise

79
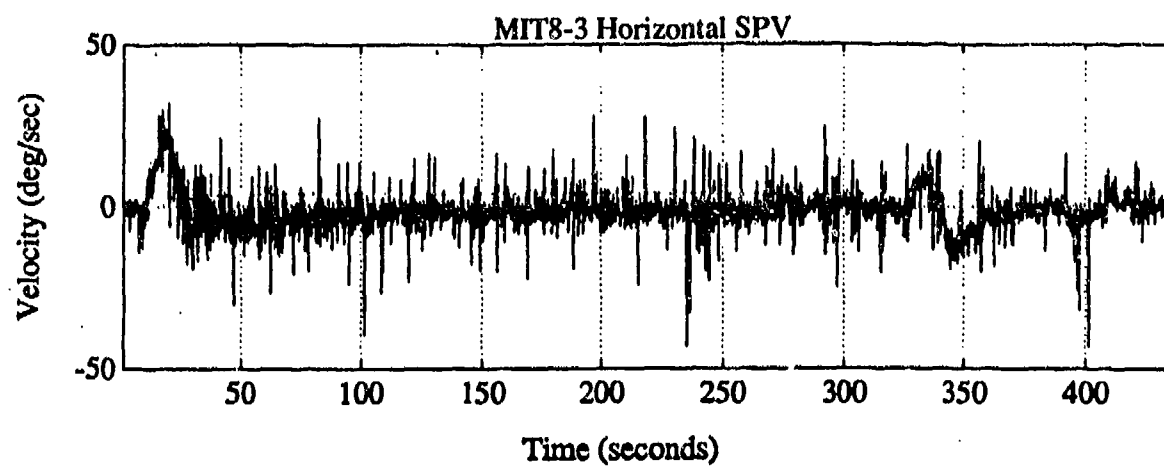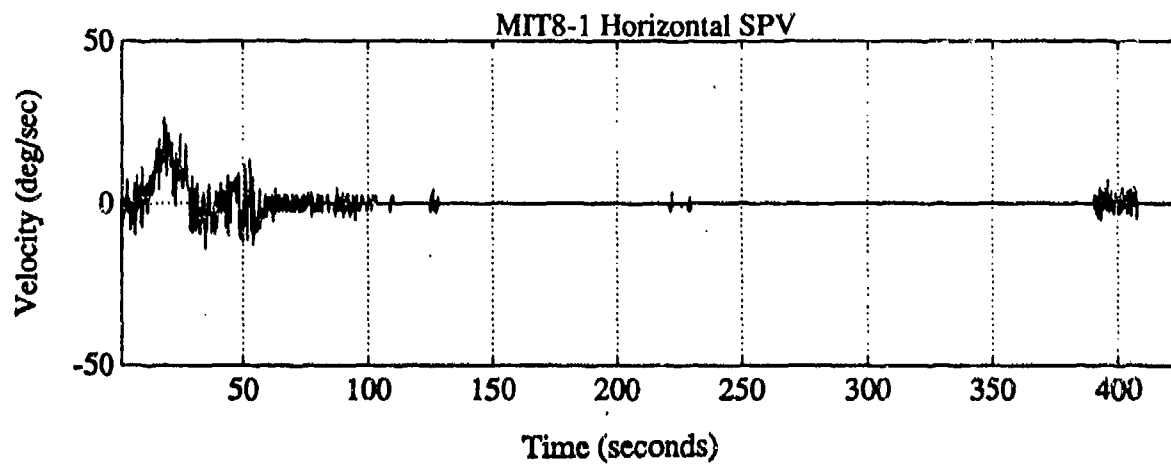
Figure 5.9: Horizontal SPV
Subject 8, Clockwise
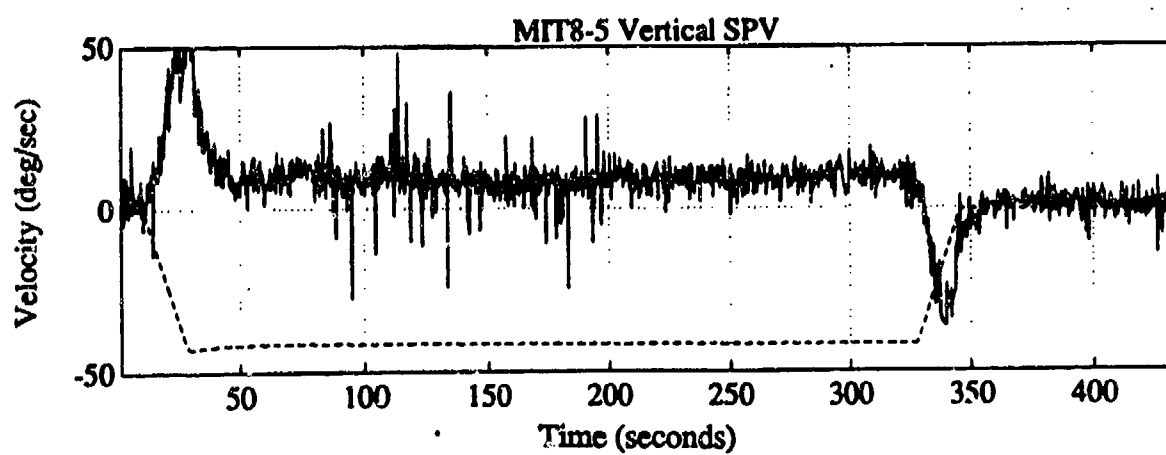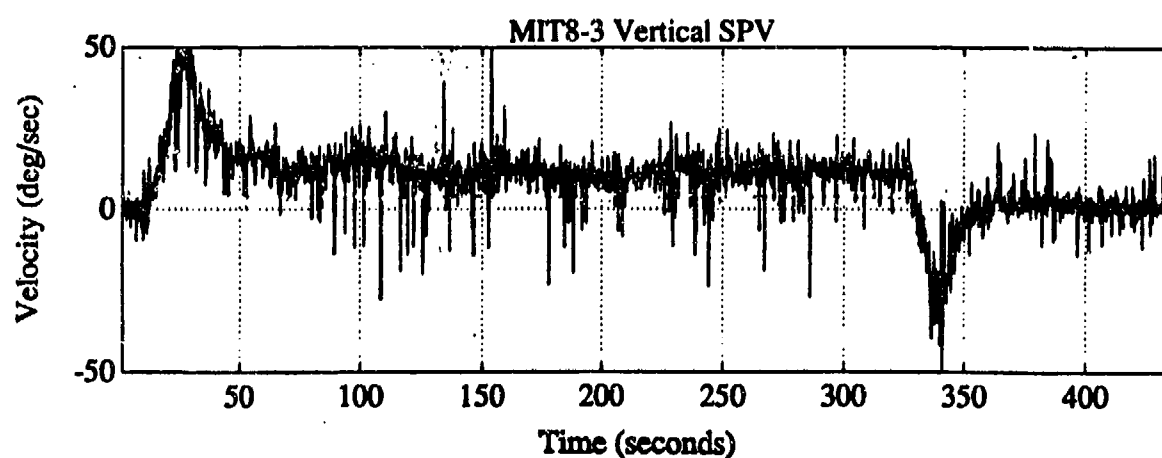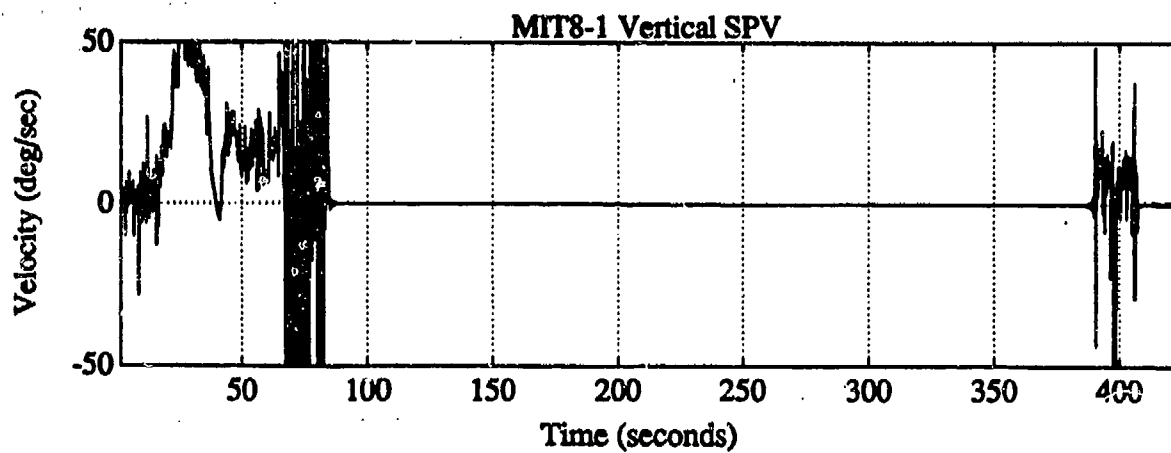
Figure 5.10: Vertical SPV
Subject 8, Clockwise

81
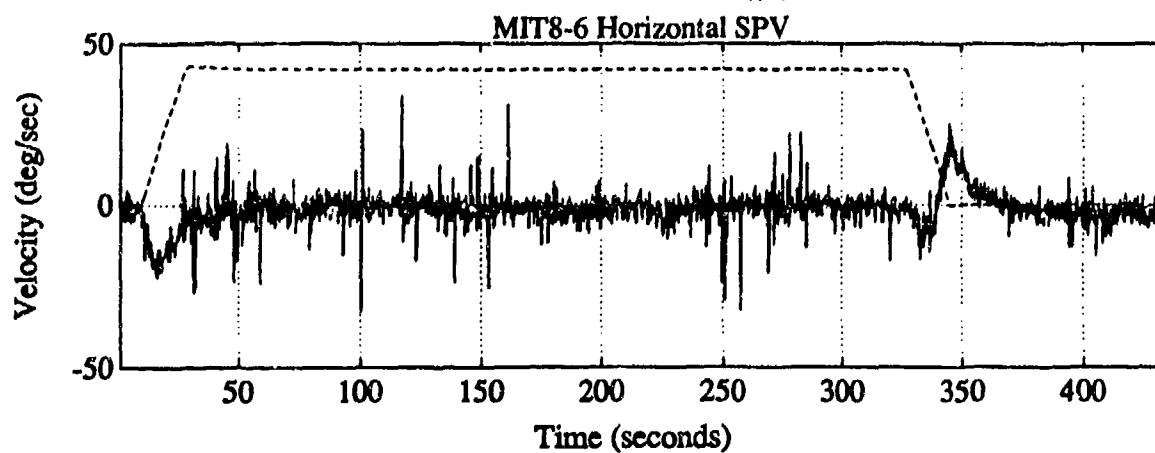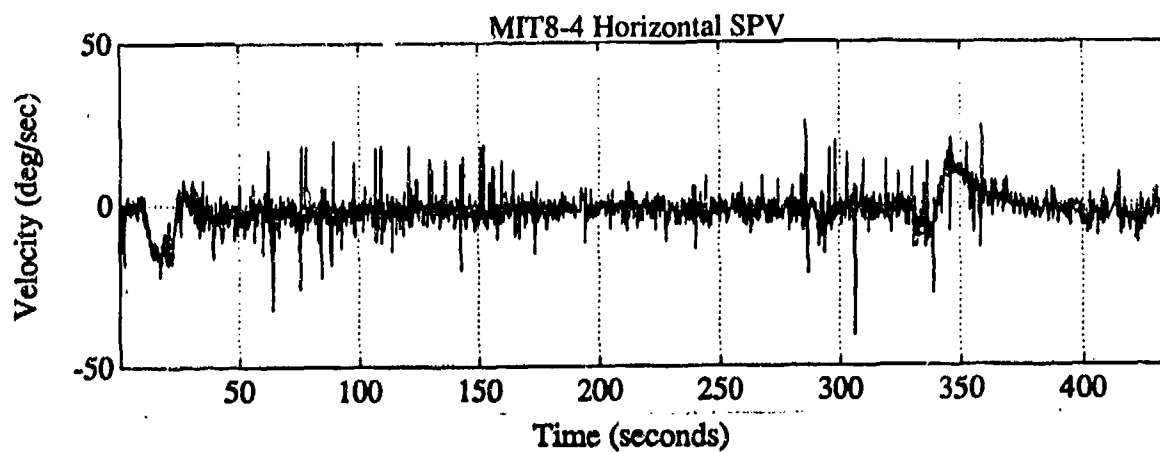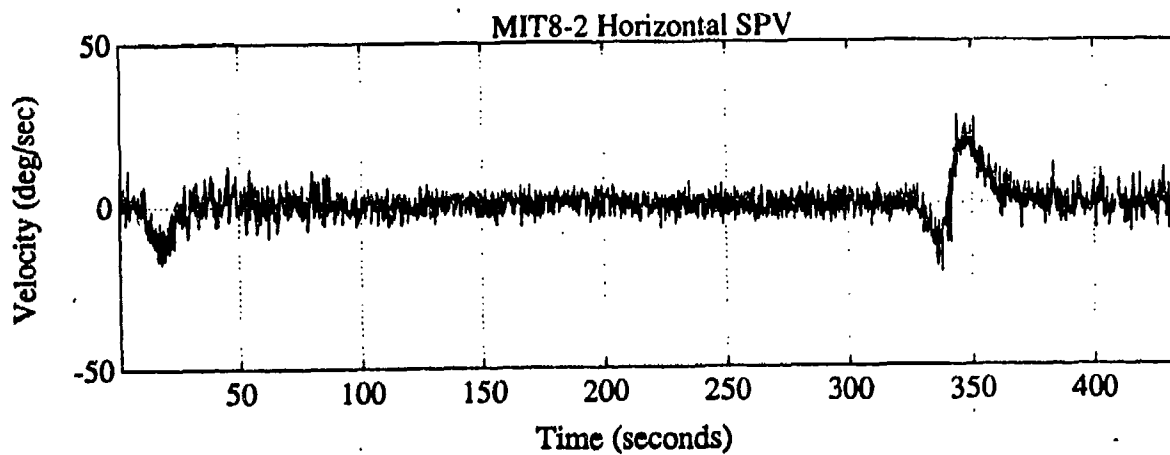
Figure 5.11: Horizontal SPV
Subject 8, CounterClockwise

82
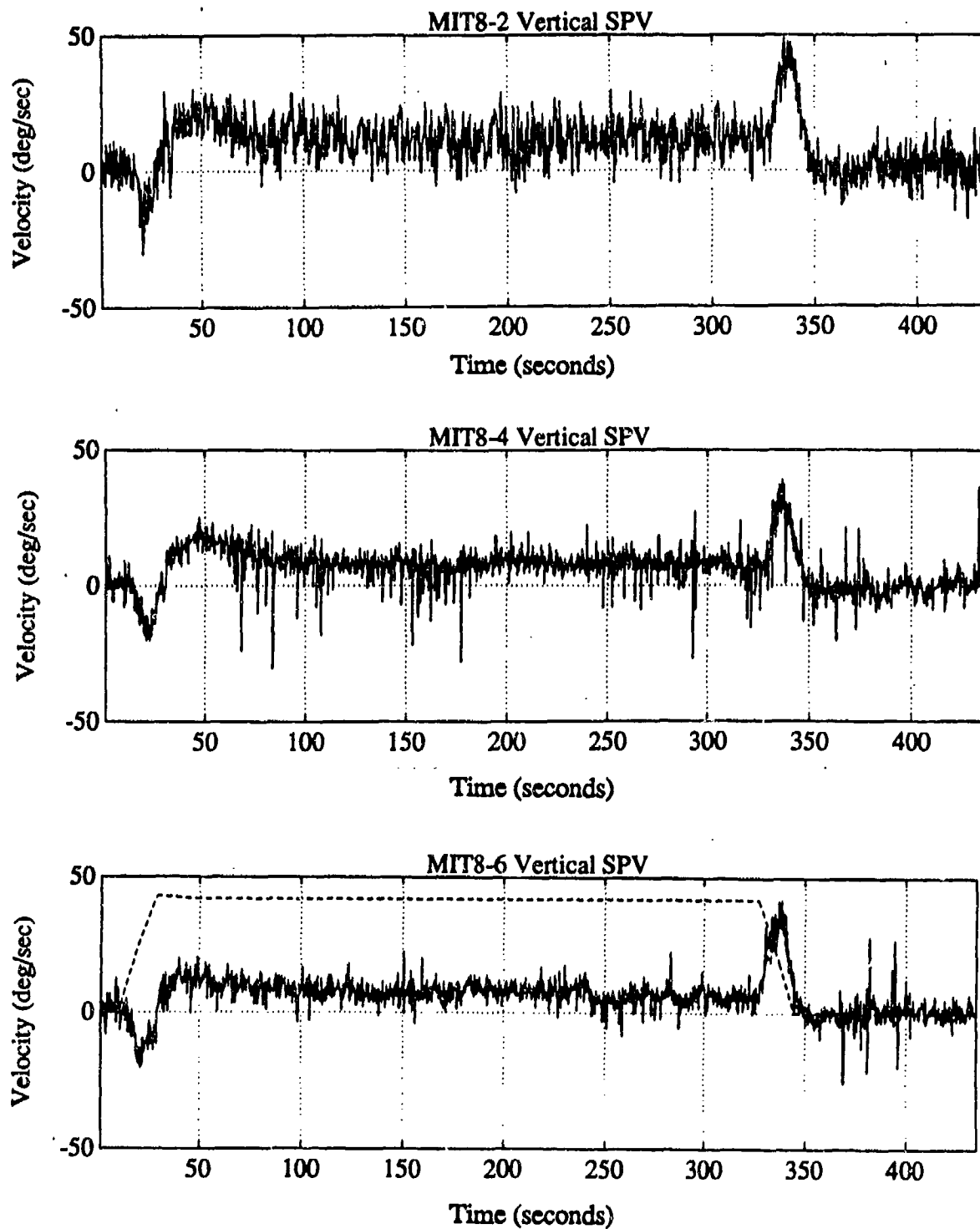
Figure 5.12: Vertical SPV
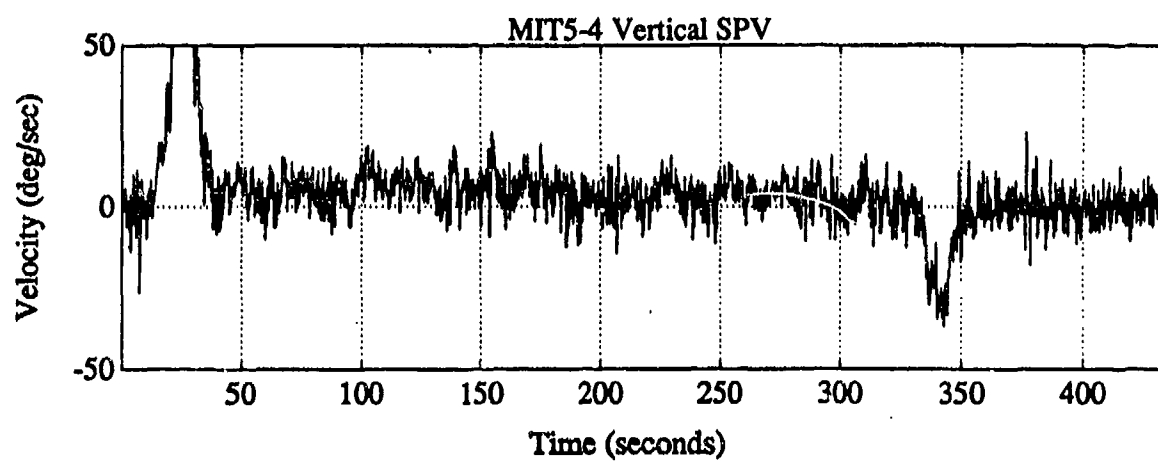Subject 8, CounterClockwise

83
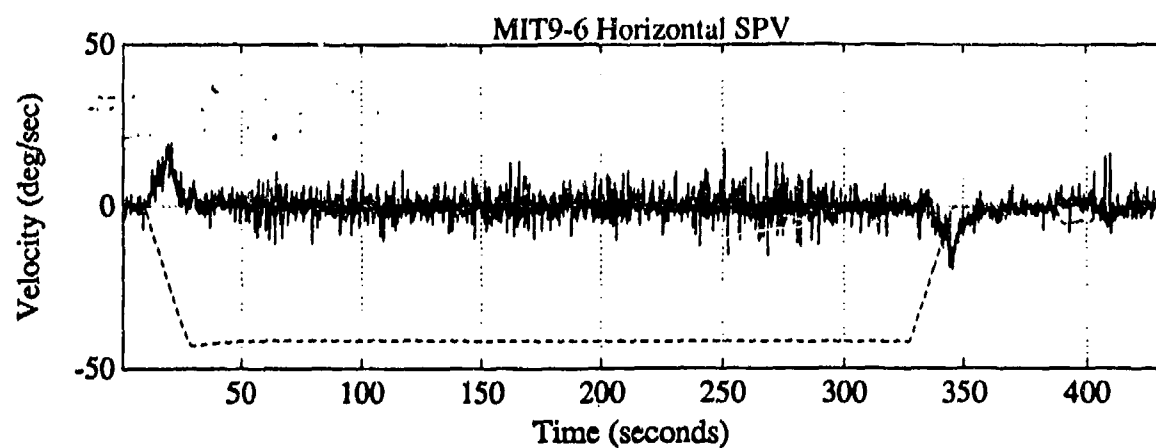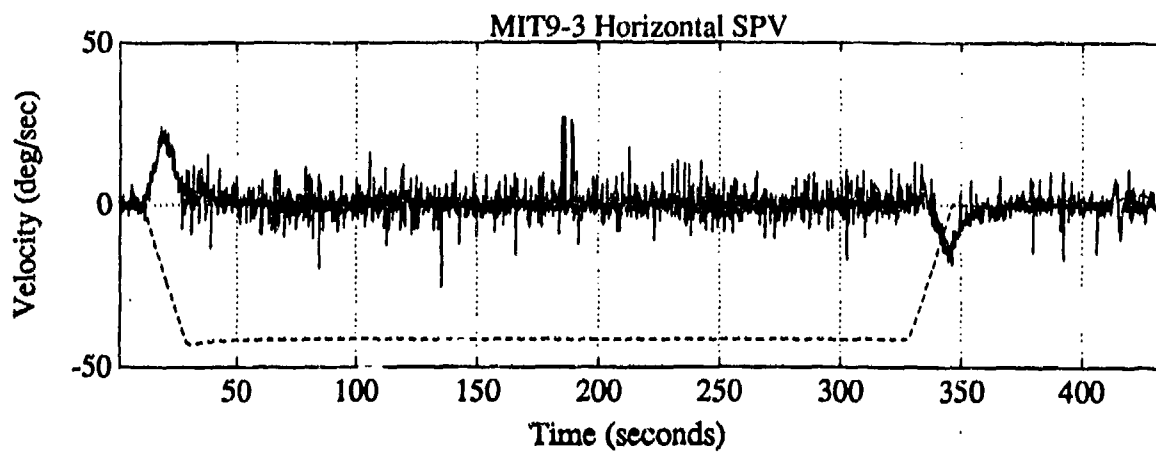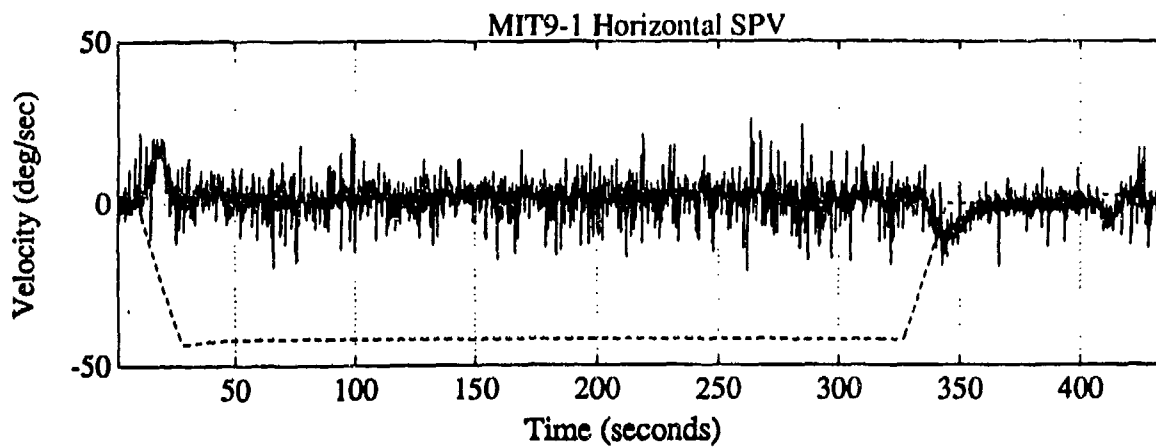
Figure 5.13: Horizontal SPV
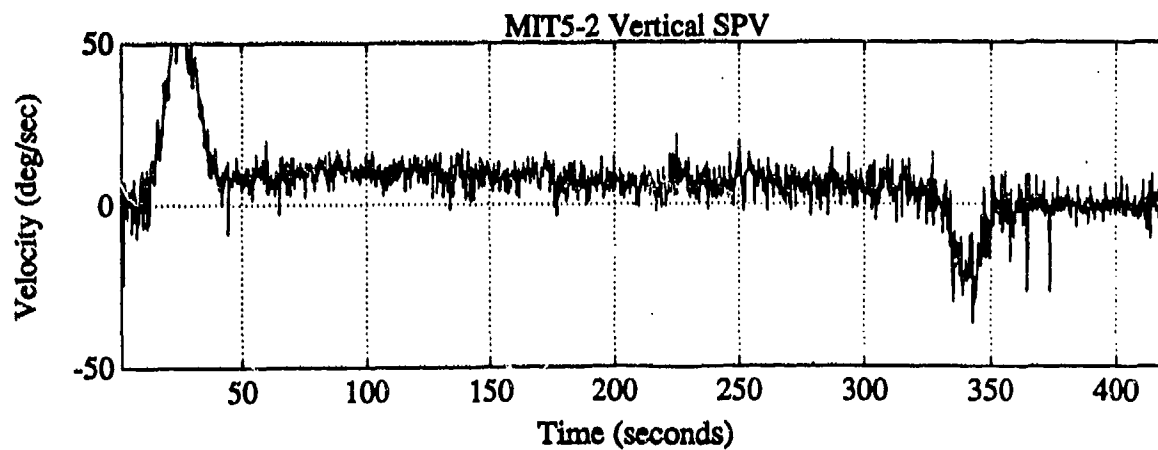Subject 9, Clockwise

84
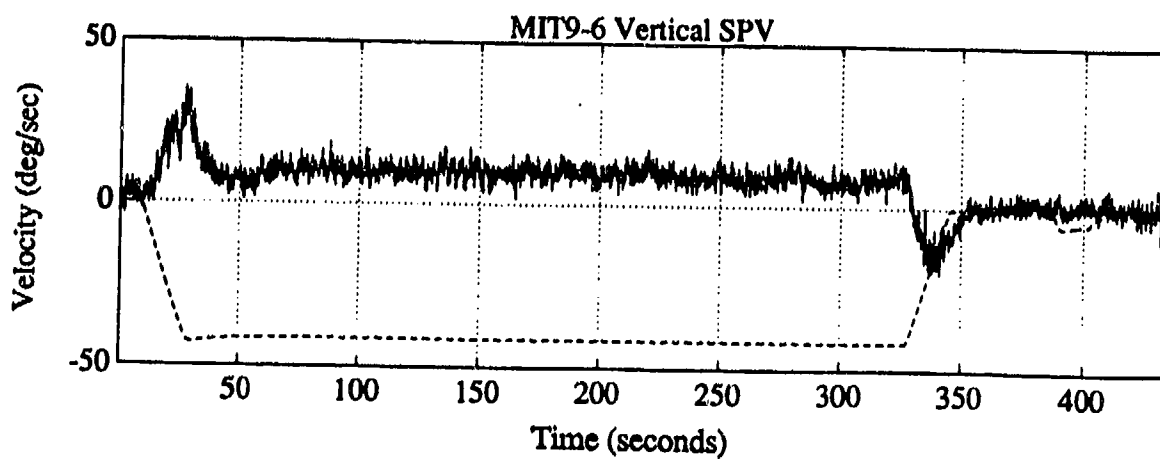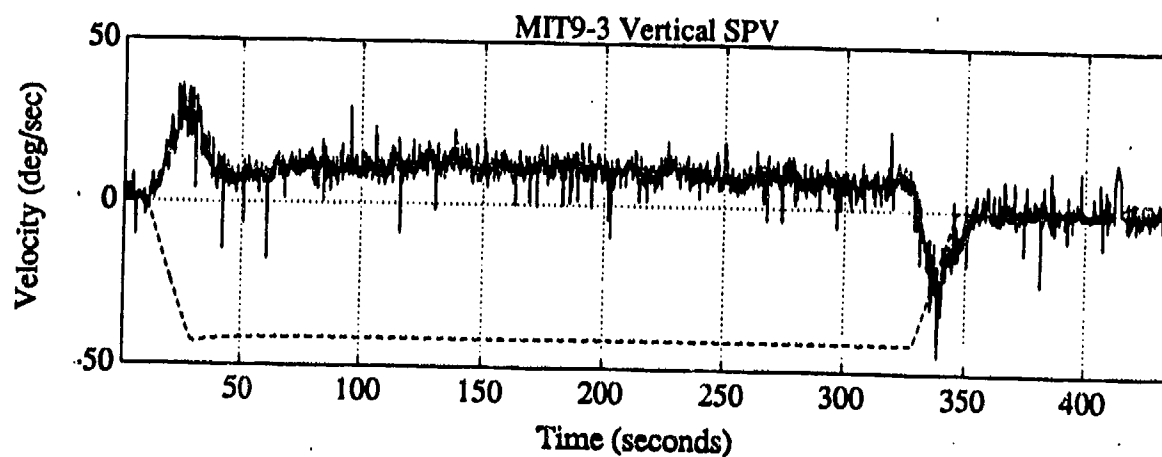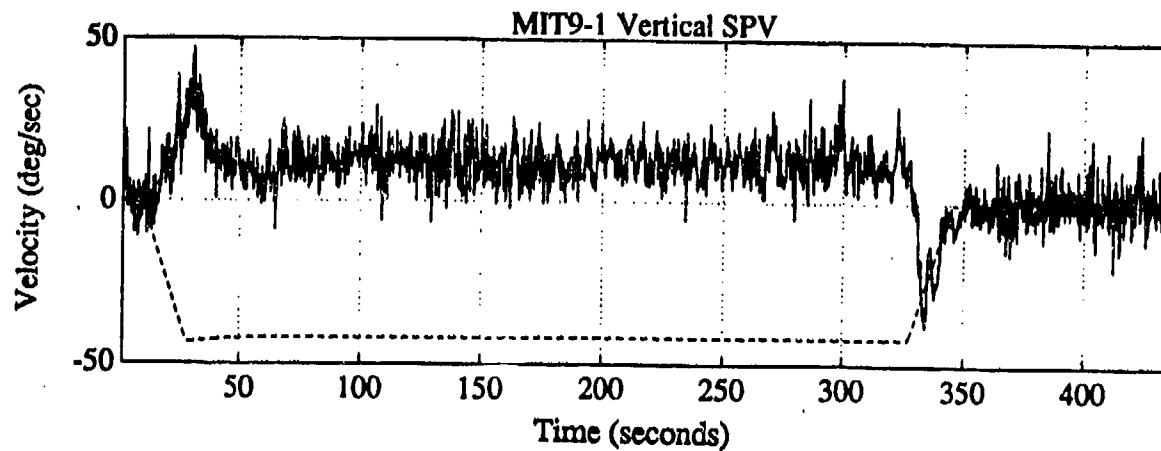
Figure 5.14: Vertical SPV
Subject 9, Clockwise

85
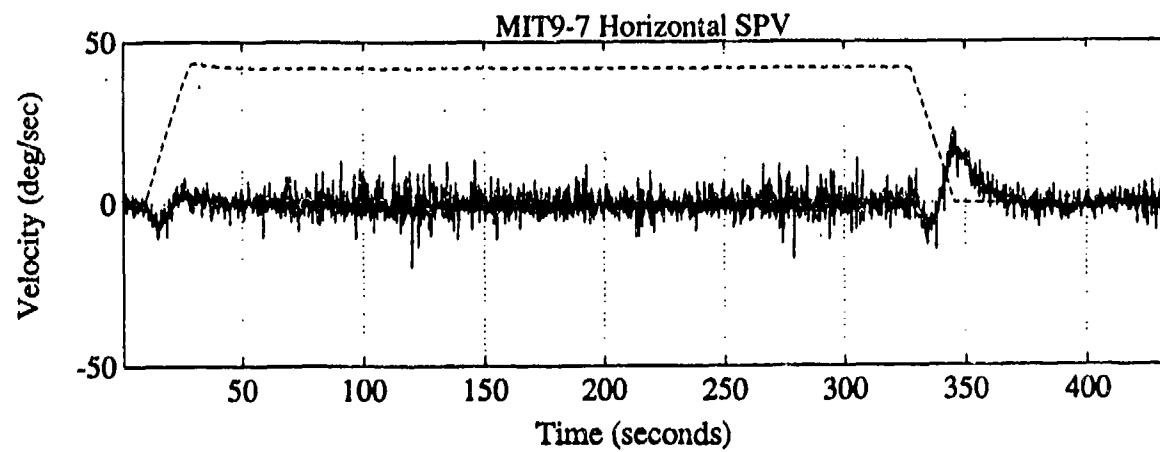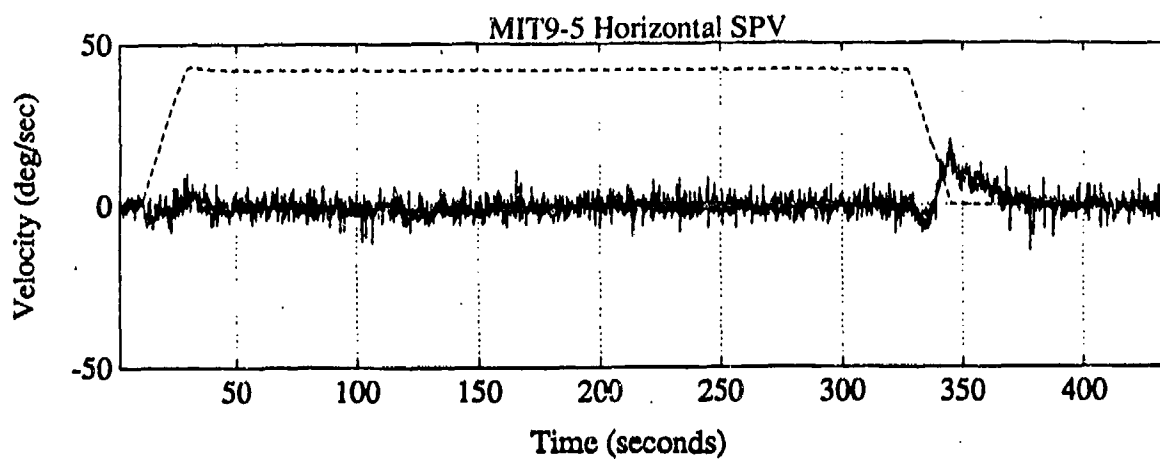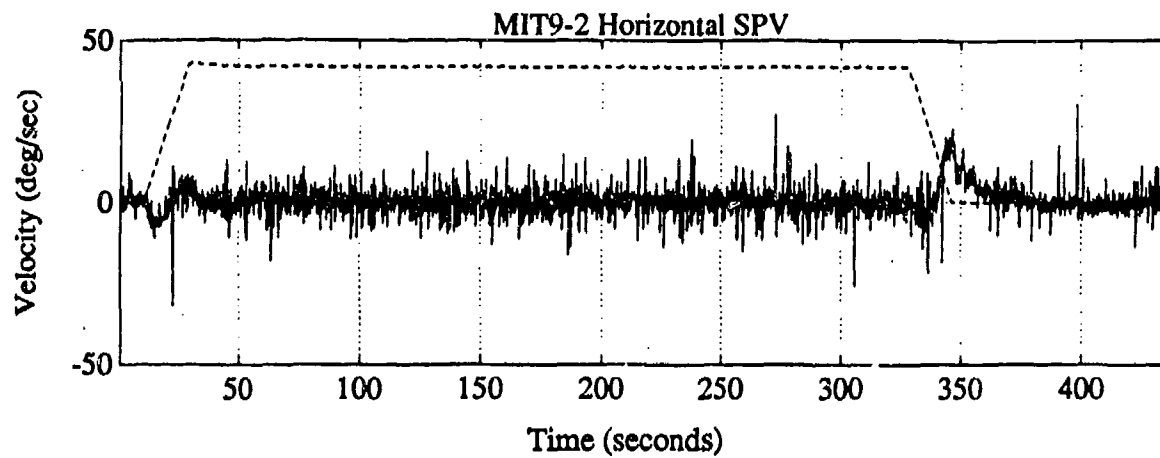
Figure 5.15: Horizontal SPV
Subject 9, CounterClockwise

86
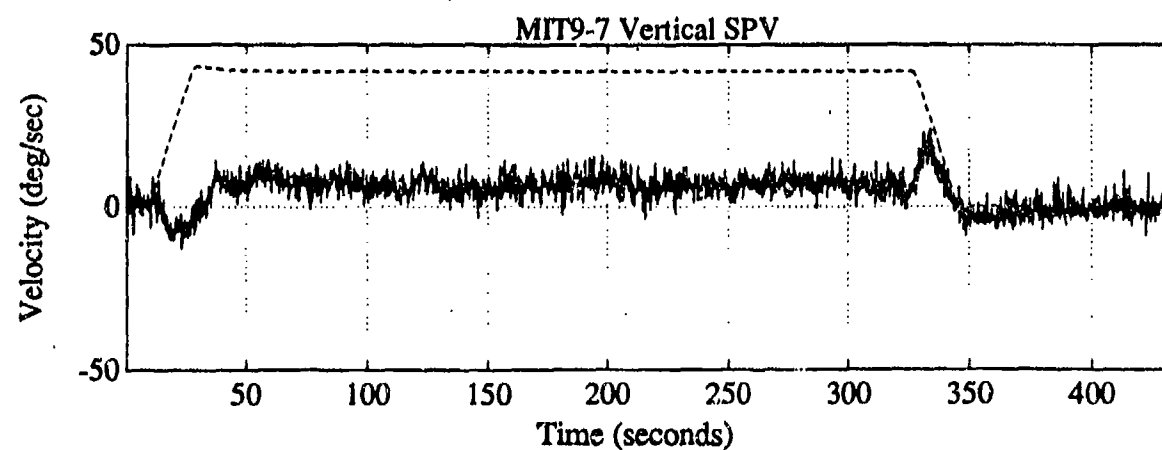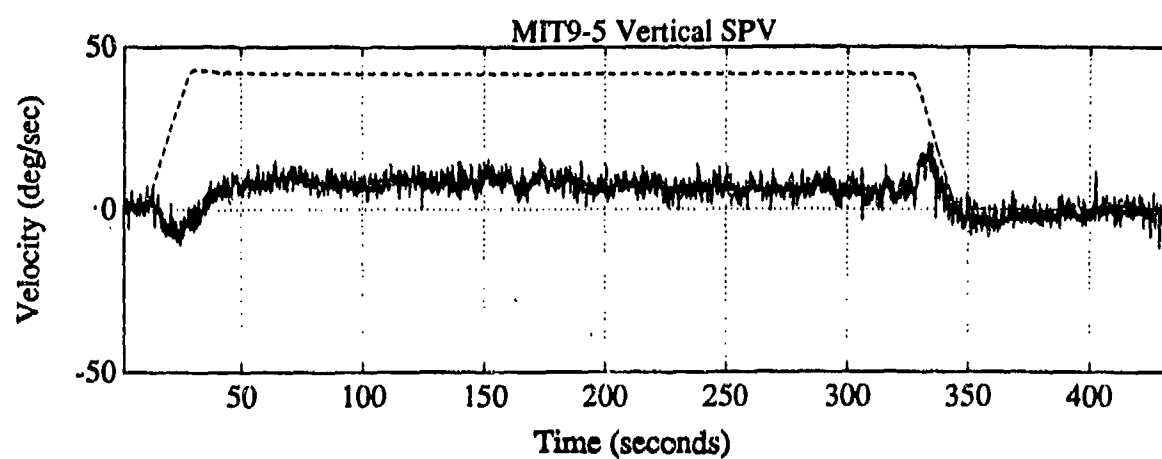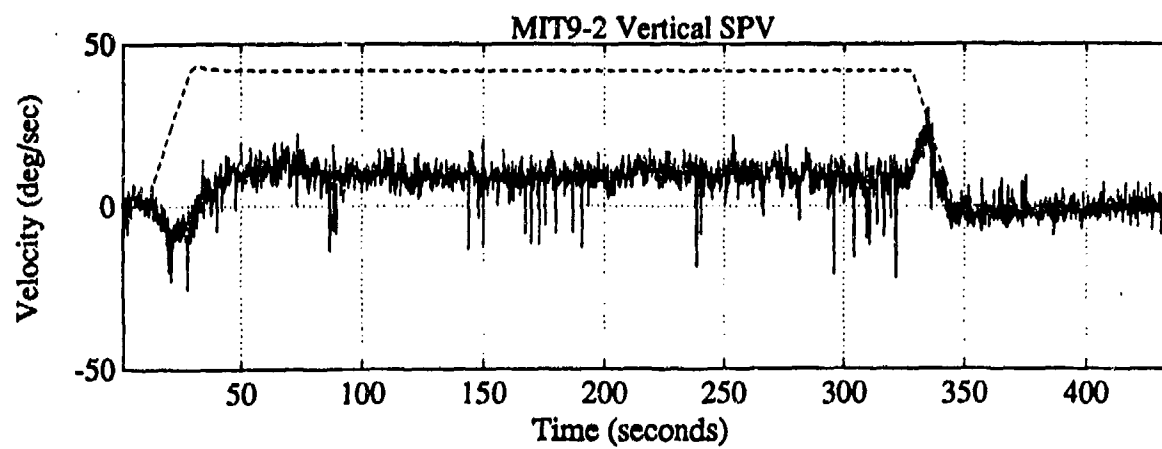
Figure 5.16: Vertical SPV
Subject 9, CounterClockwise

87
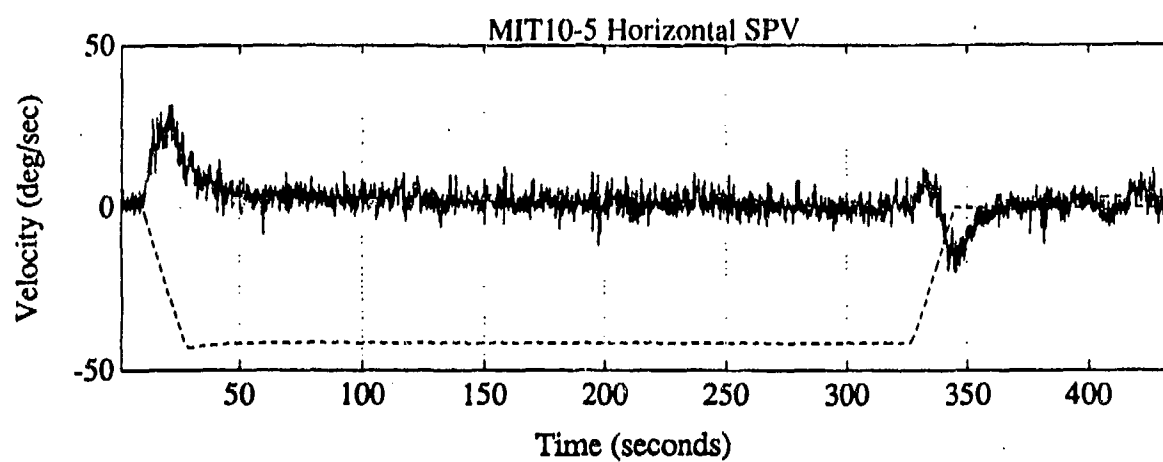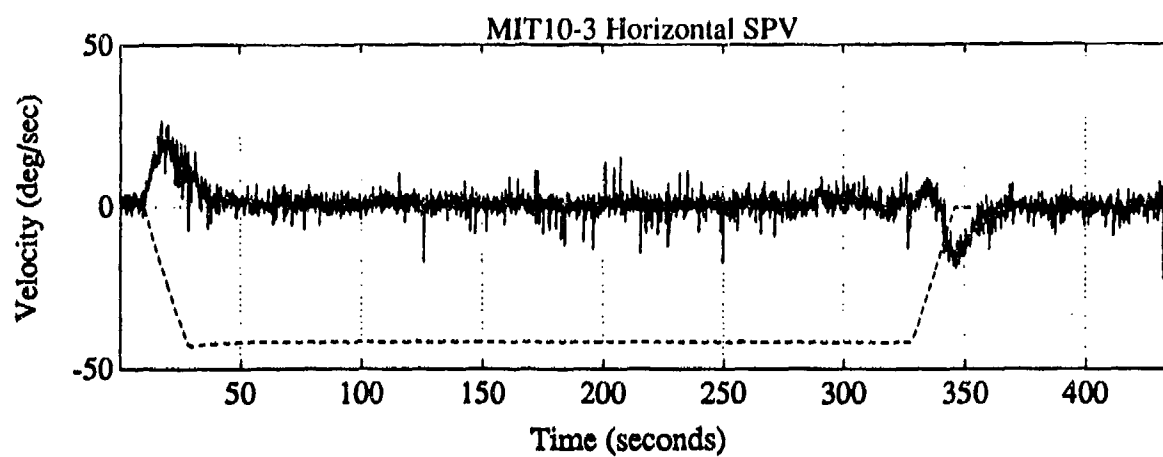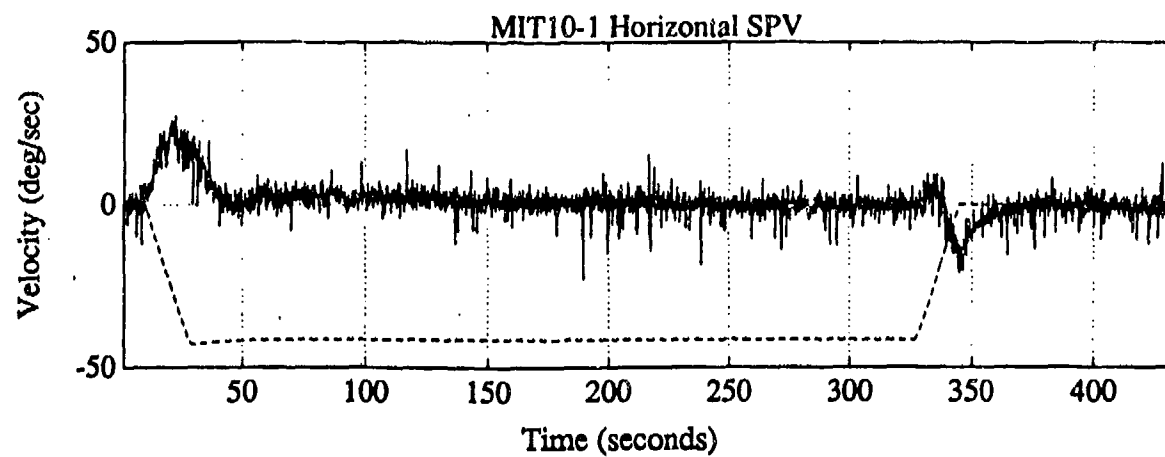
Figure 5.17: Horizontal SPV
Subject 10, Clockwise

88
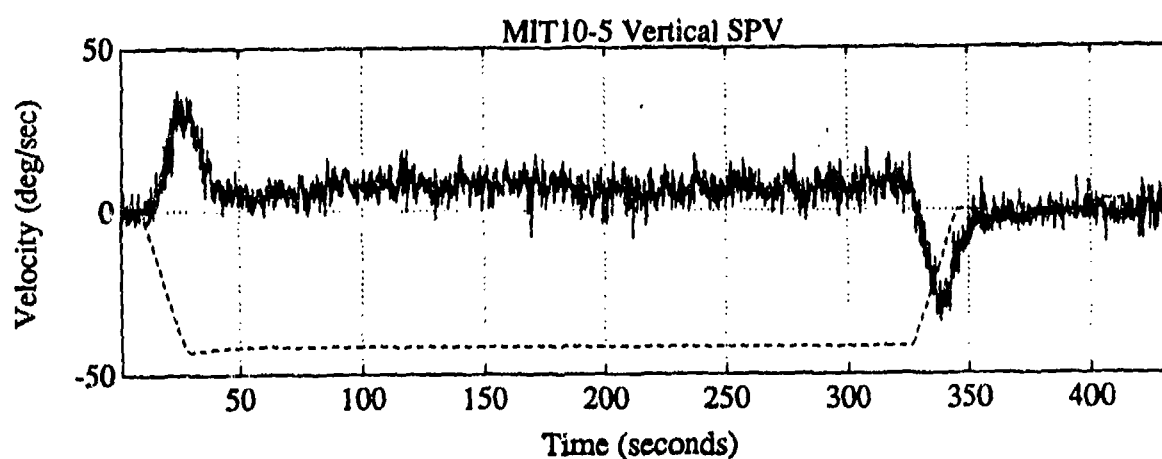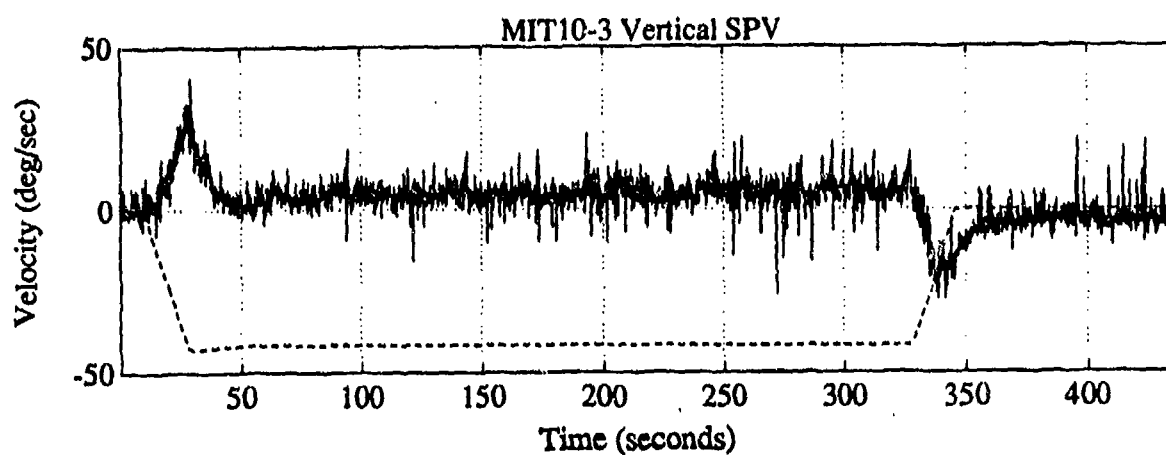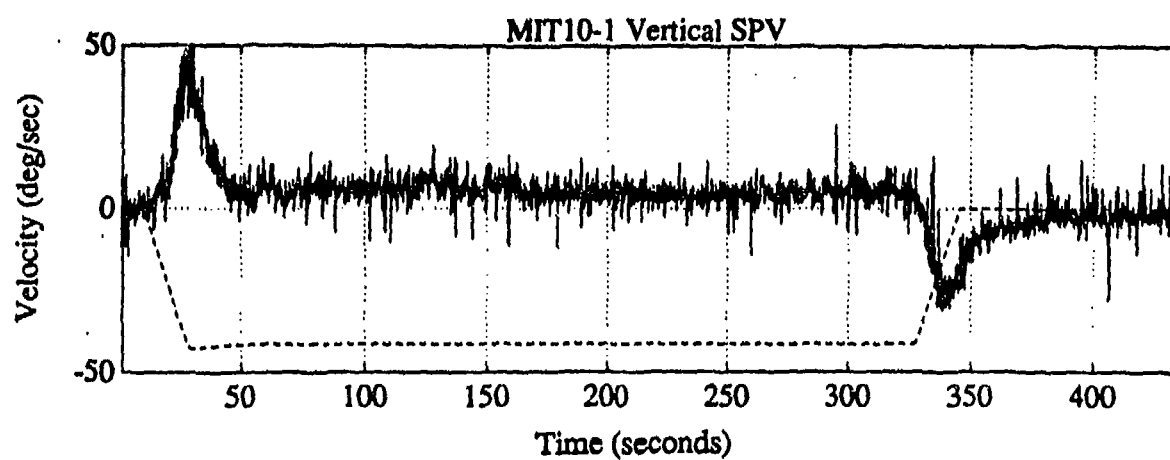
Figure 5.18: Vertical SPV
Subject 10, Clockwise

89
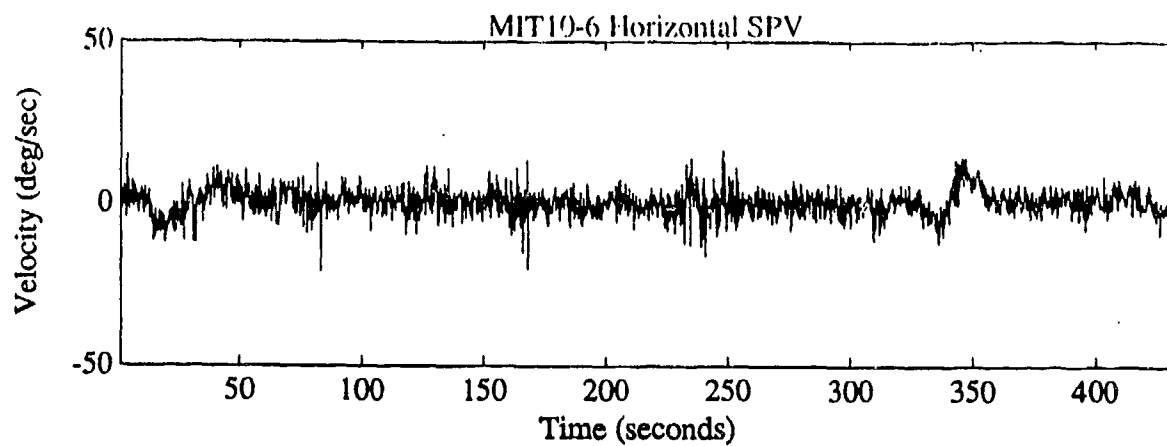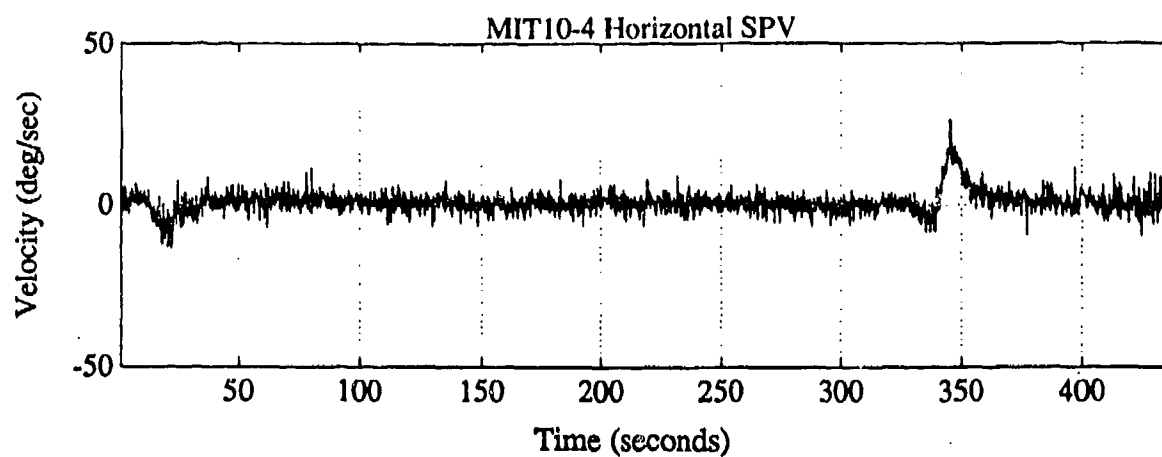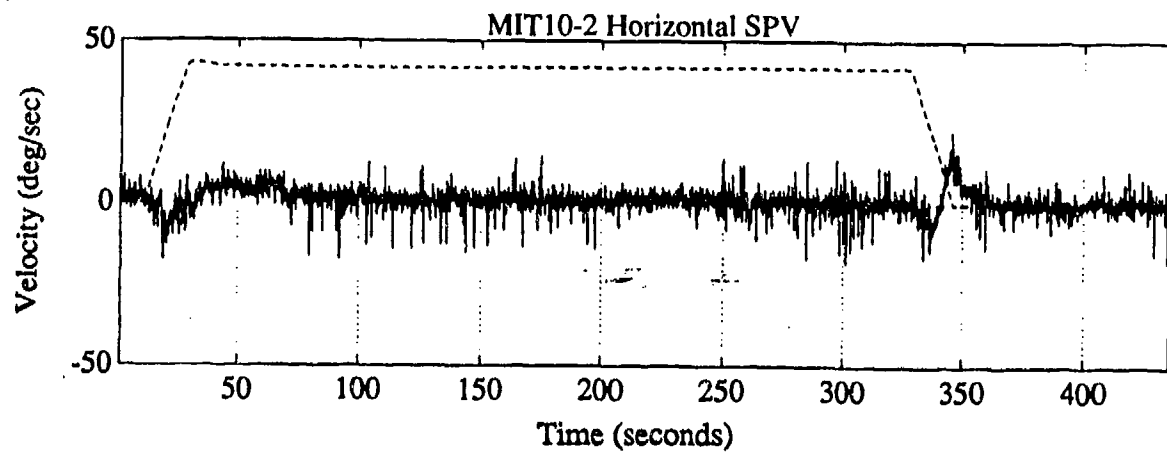
Figure 5.19: Horizontal SPV
Subject 10, CounterClockwise
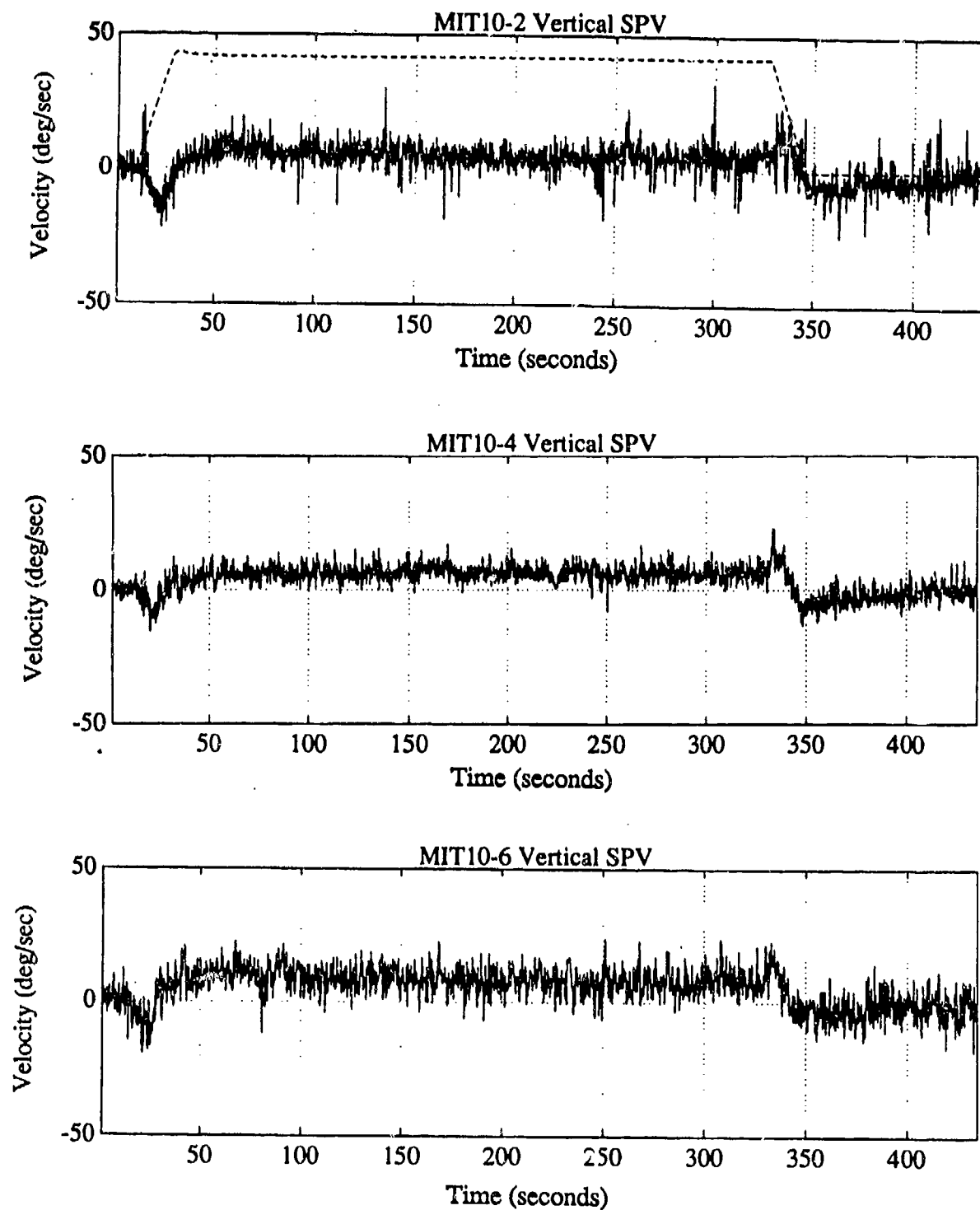
Figure 5.20: Vertical SPV
Subject 10, CounterClockwise

91
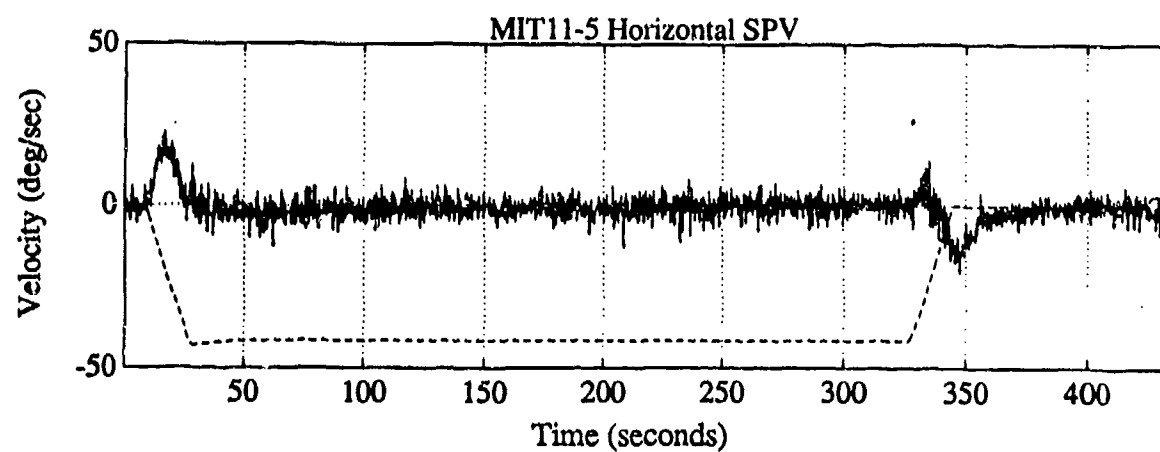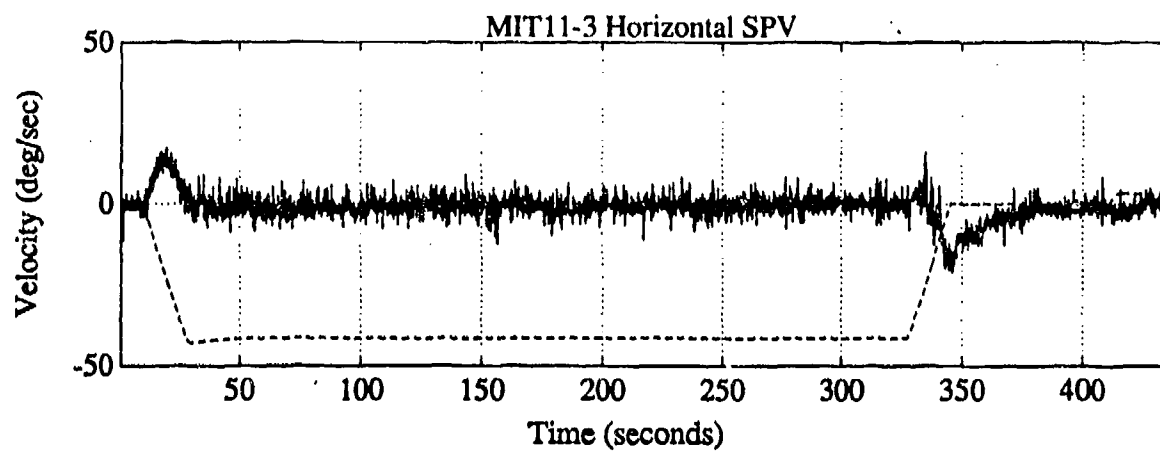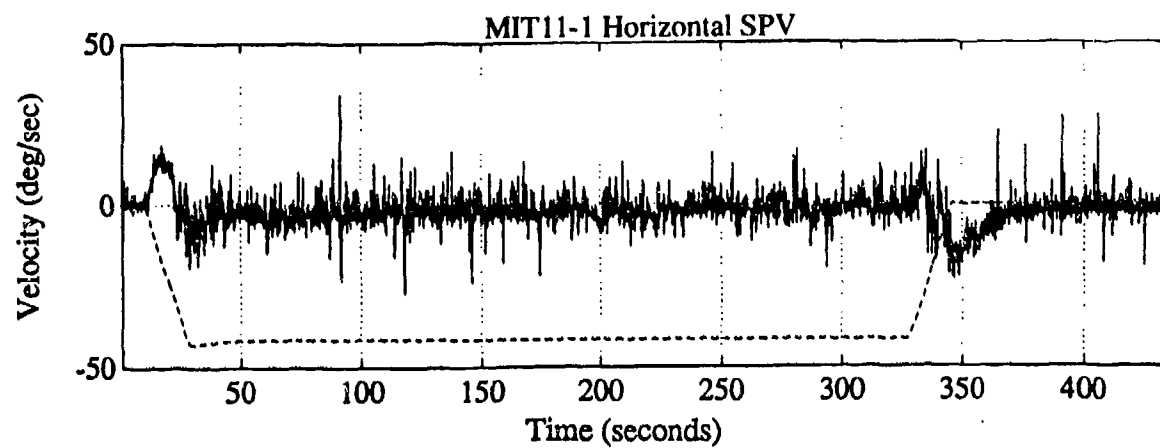
Figure 5.21: Horizontal SPV
Subject 11, Clockwise

92
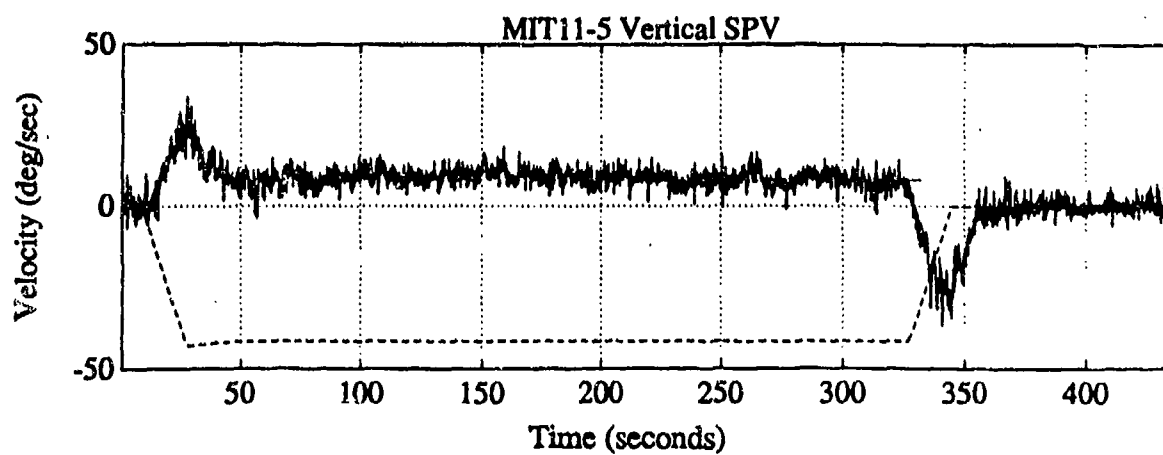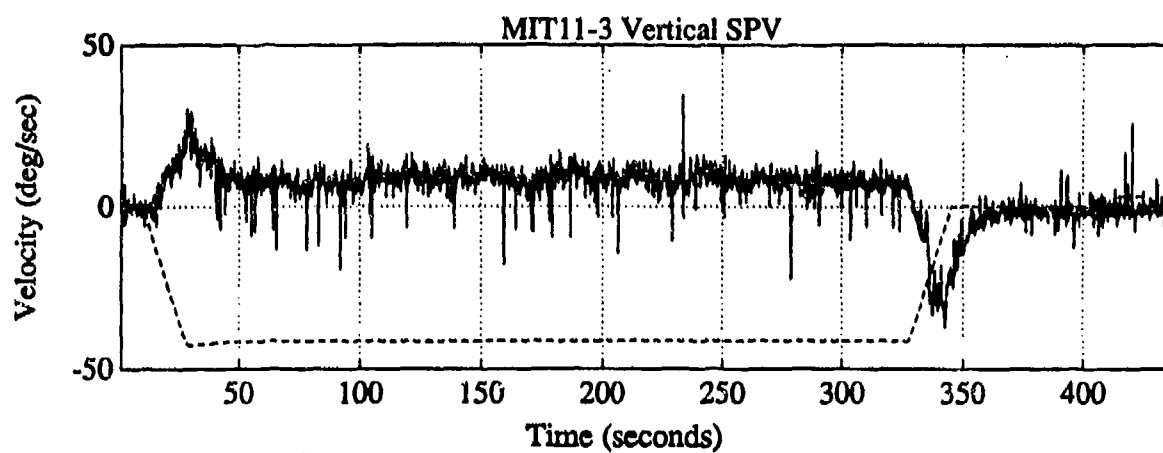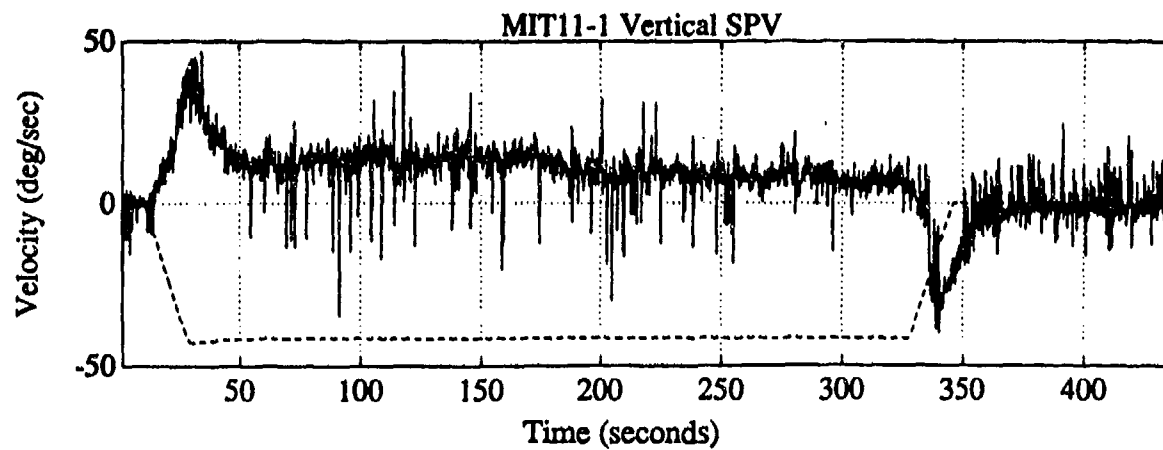
Figure 5.22: Vertical SPV
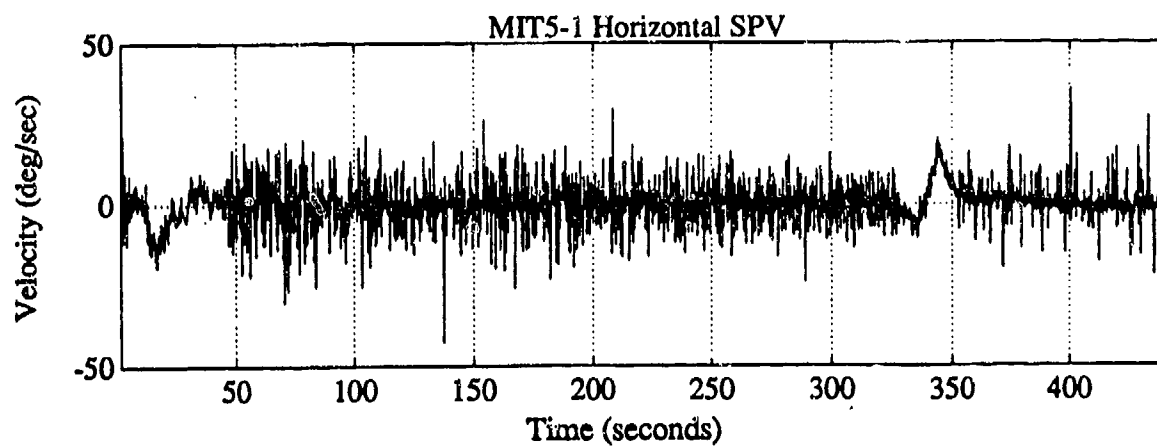Subject 11, Clockwise

93
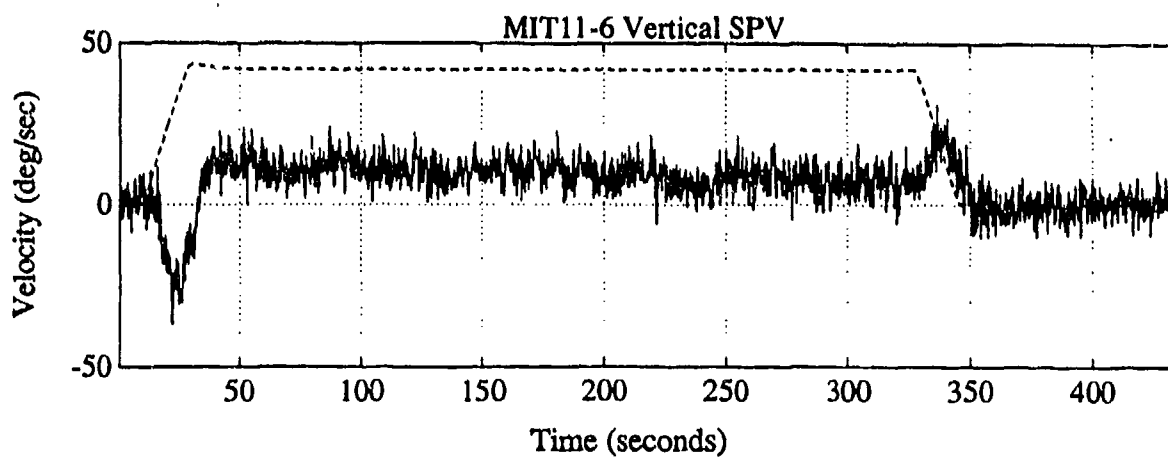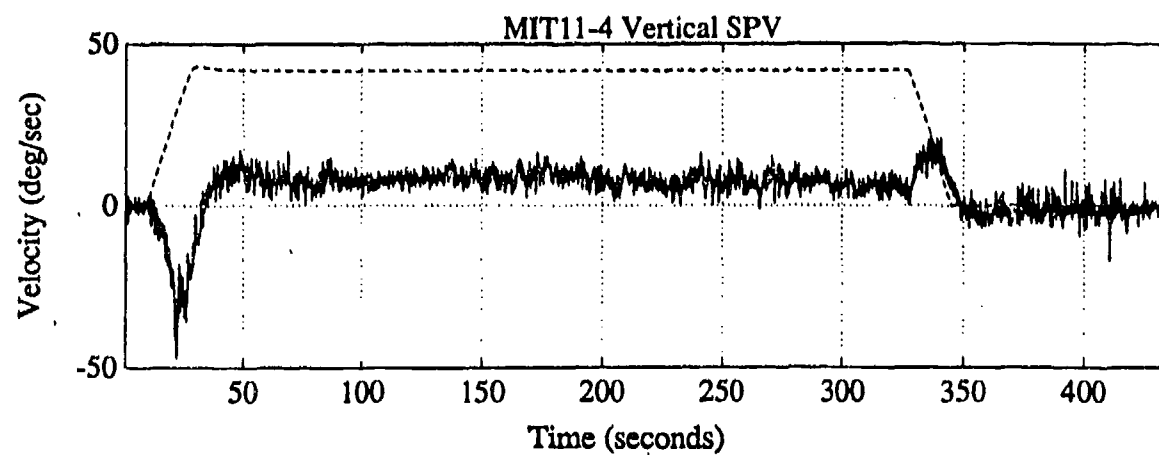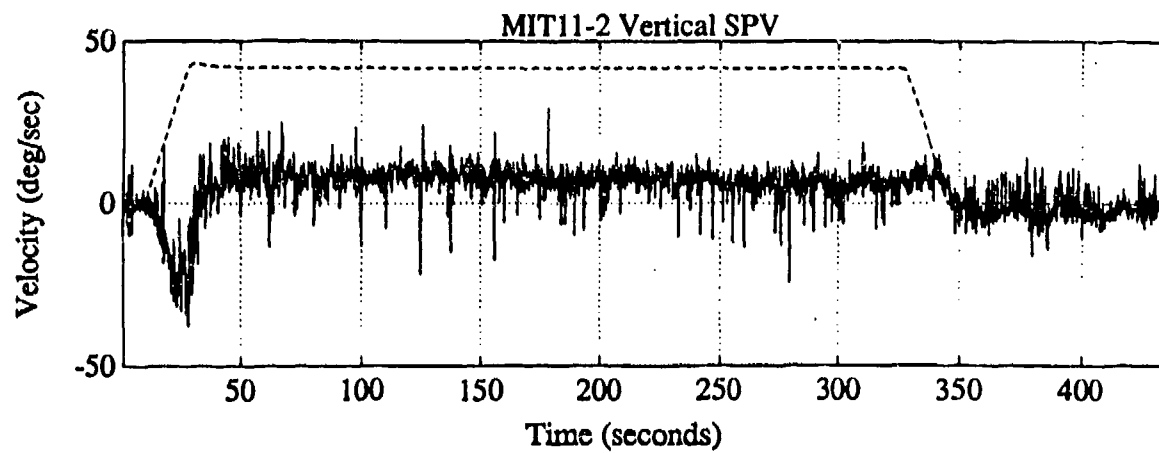
Figure 5.23: Horizontal SPV
Subject 11, CounterClockwise

94
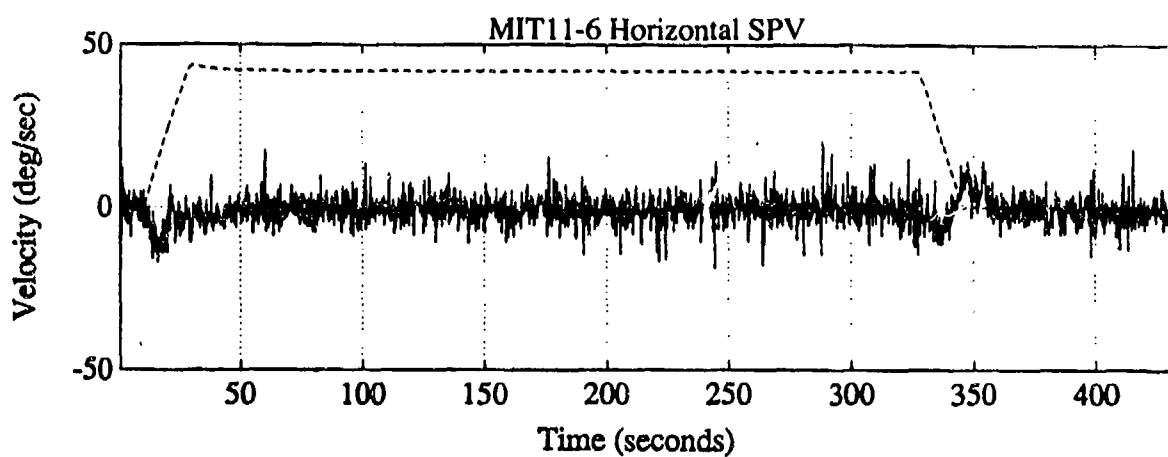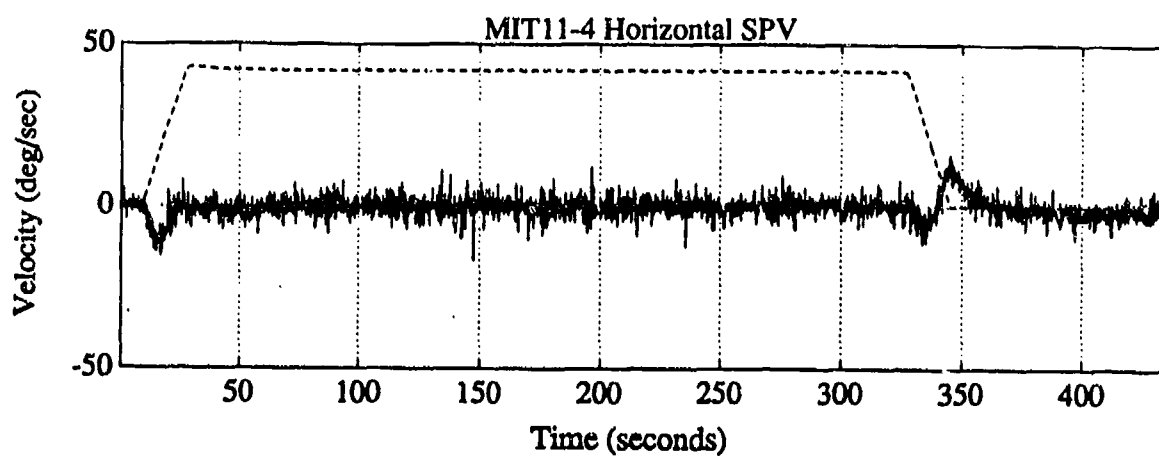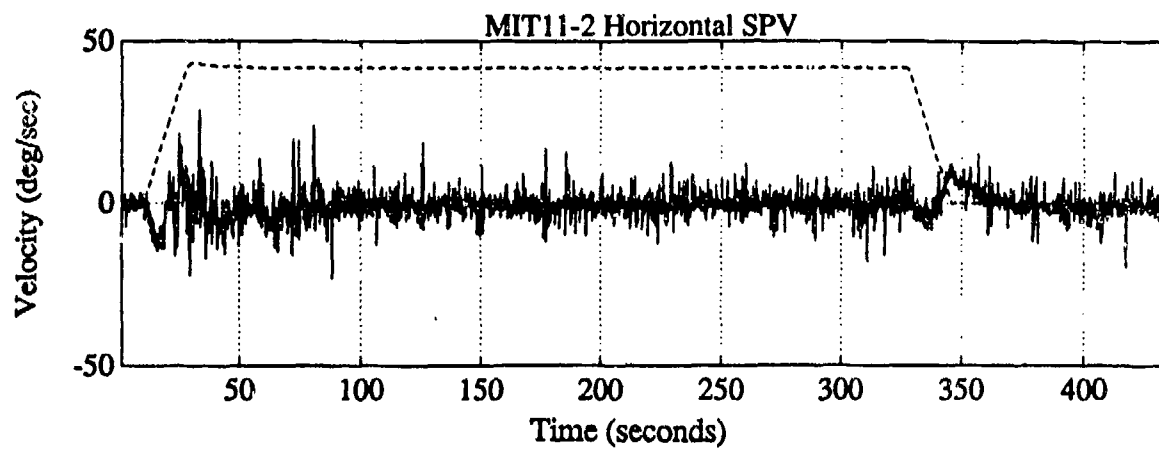
Figure 5.24: Vertical SPV
Subject 11, CounterClockwise
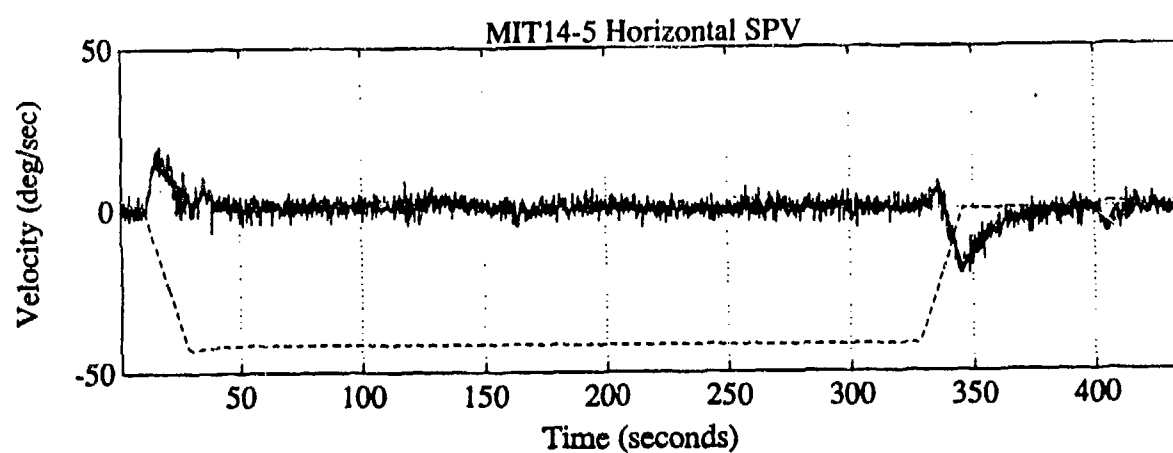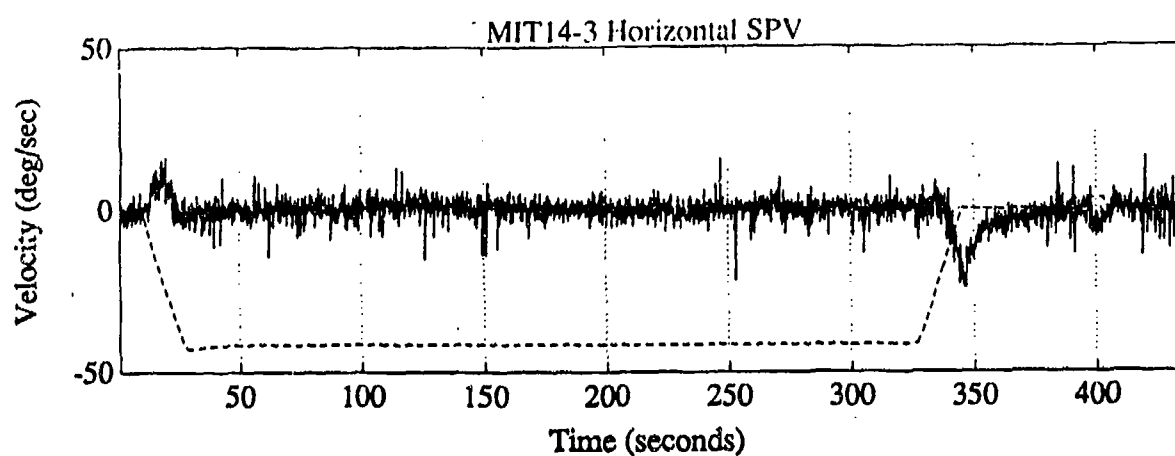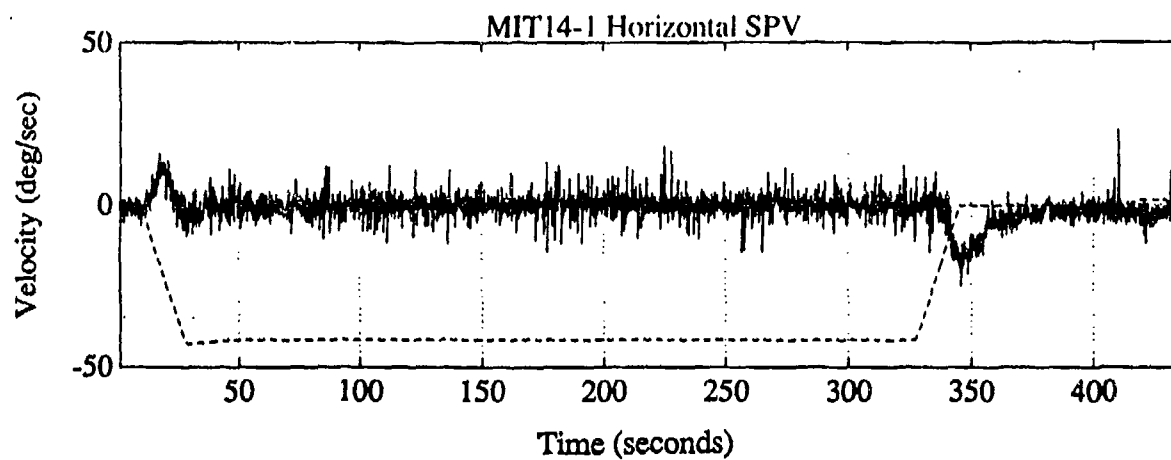
Figure 5.25: Horizontal SPV
Subject 14, Clockwise

96
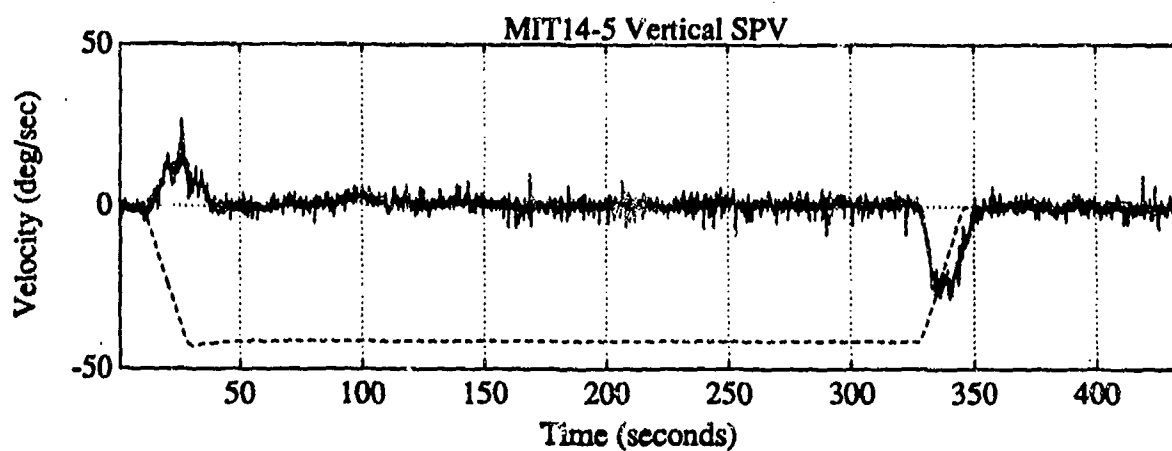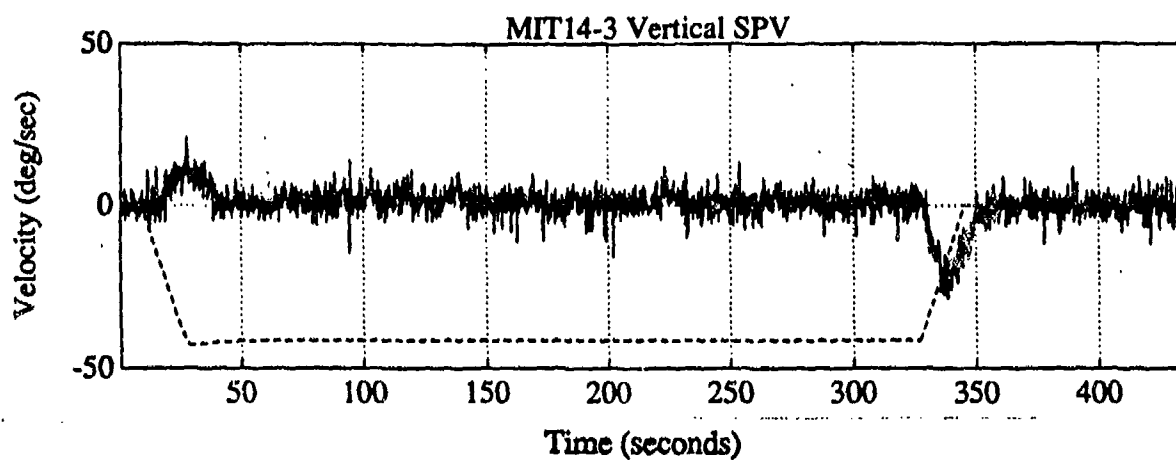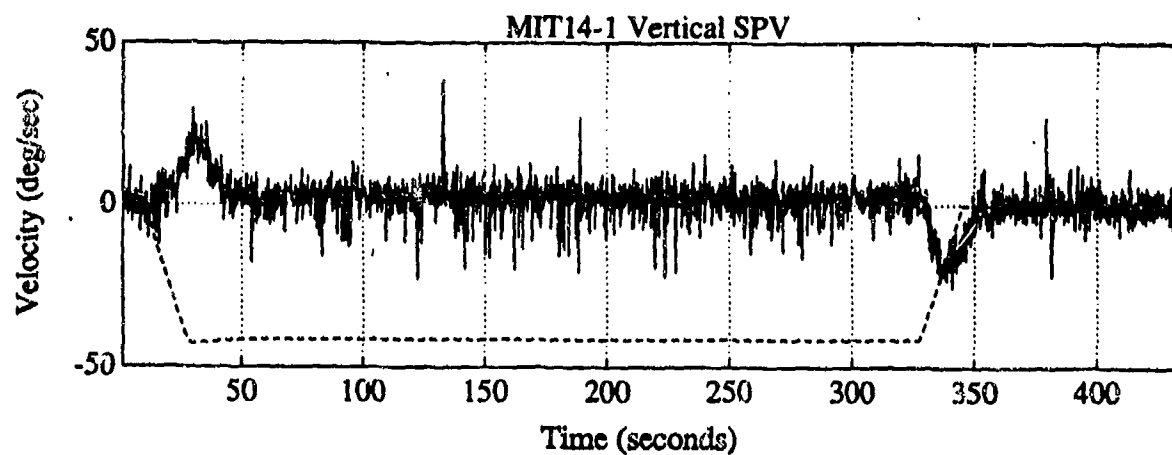
Figure 5.26: Vertical SPV
Subject 14, Clockwise

97
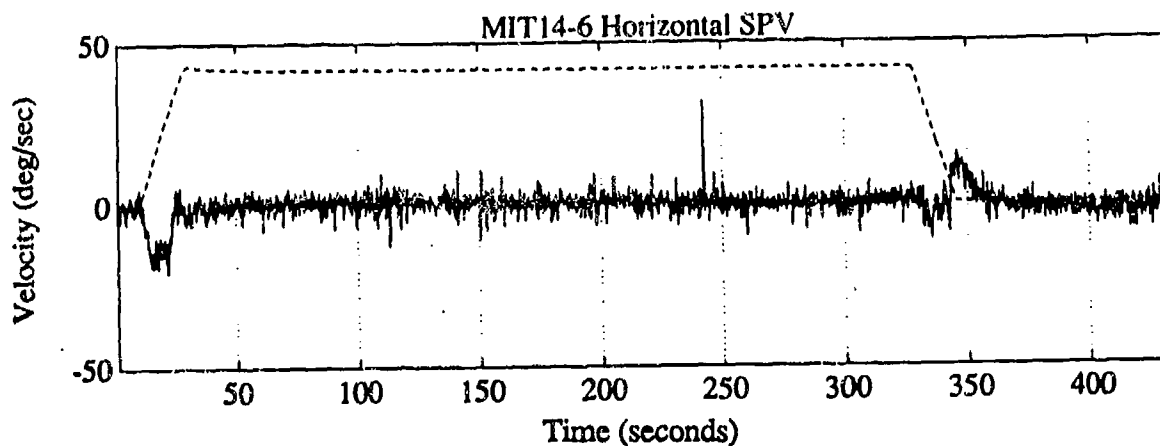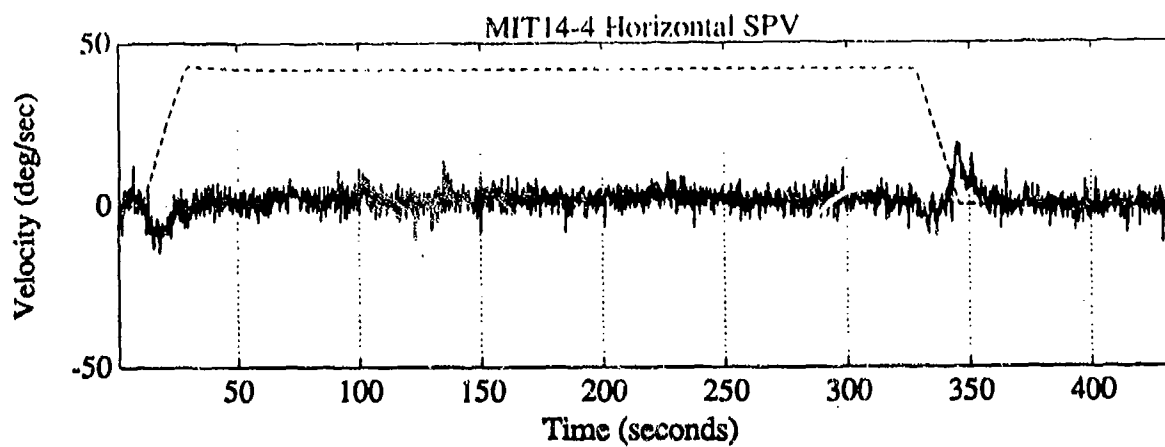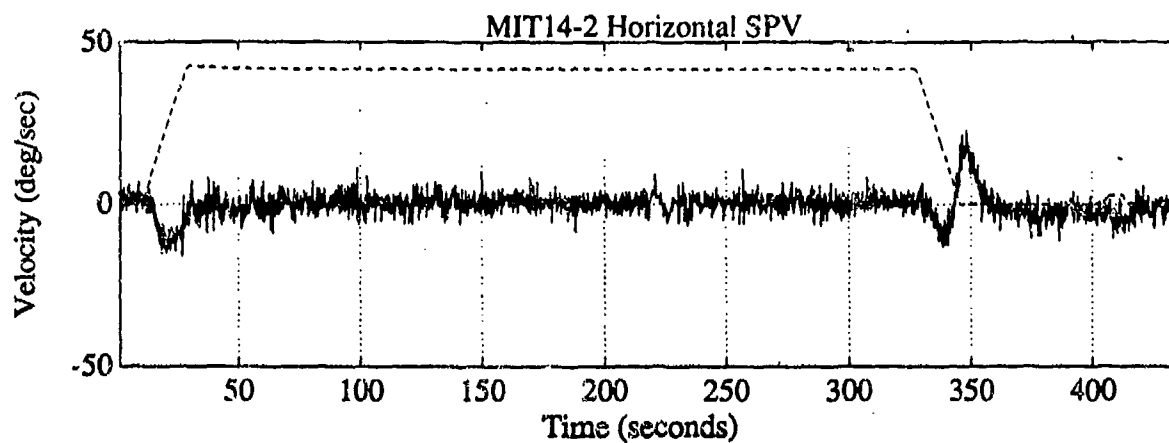
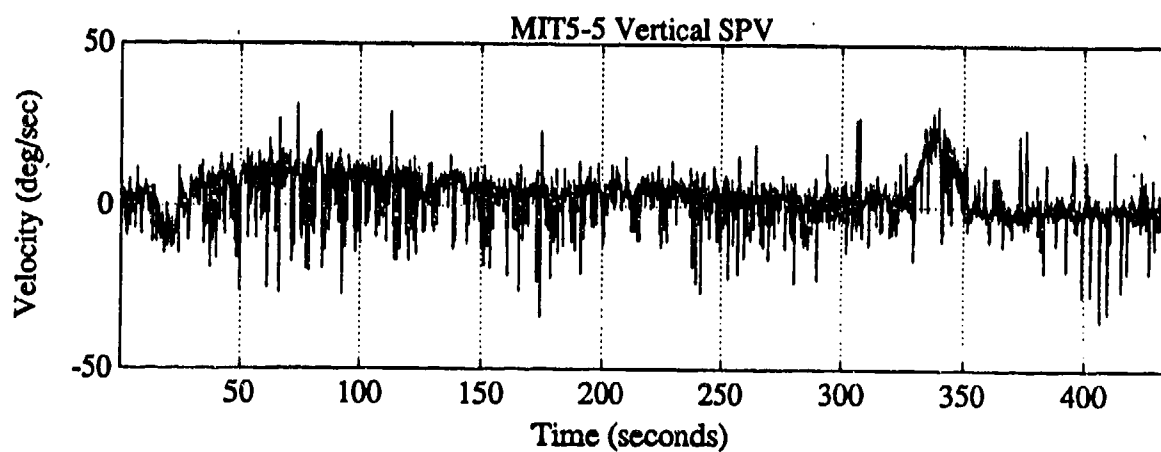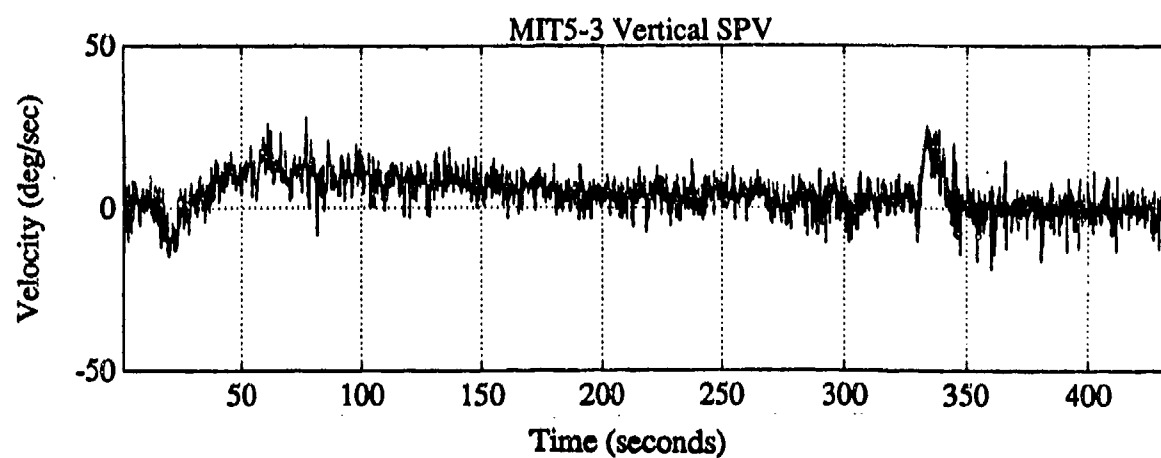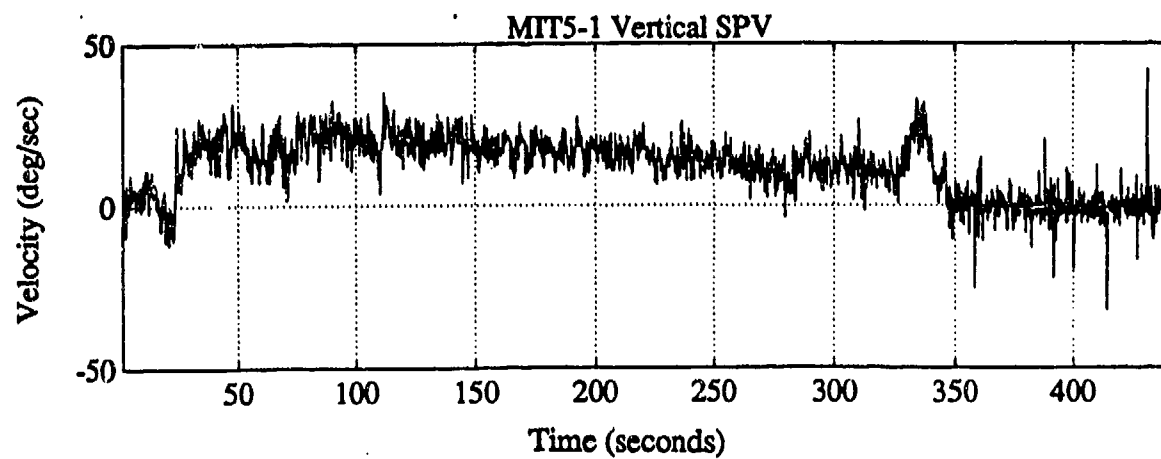Figure 5.27: Horizontal SPV
Subject 14, CounterClockwise

98
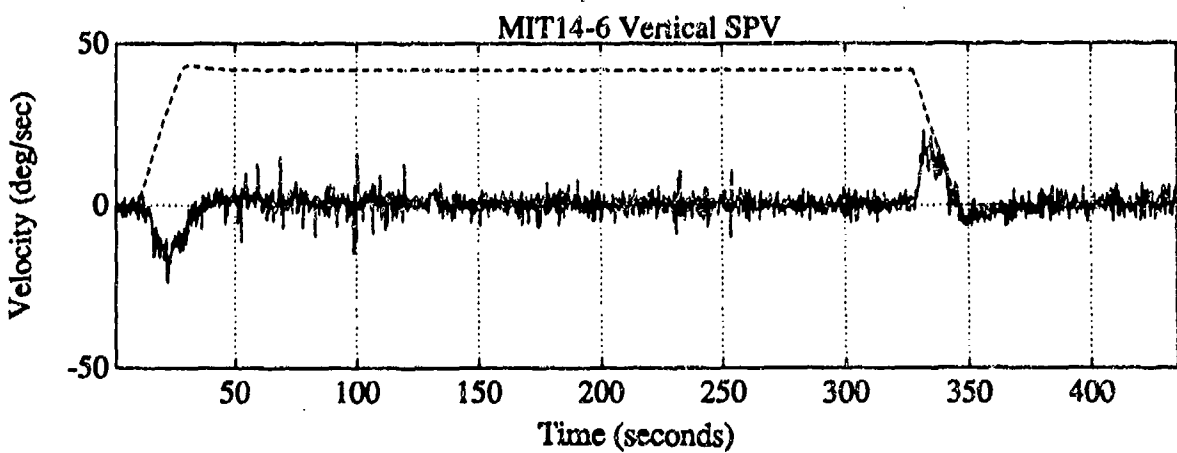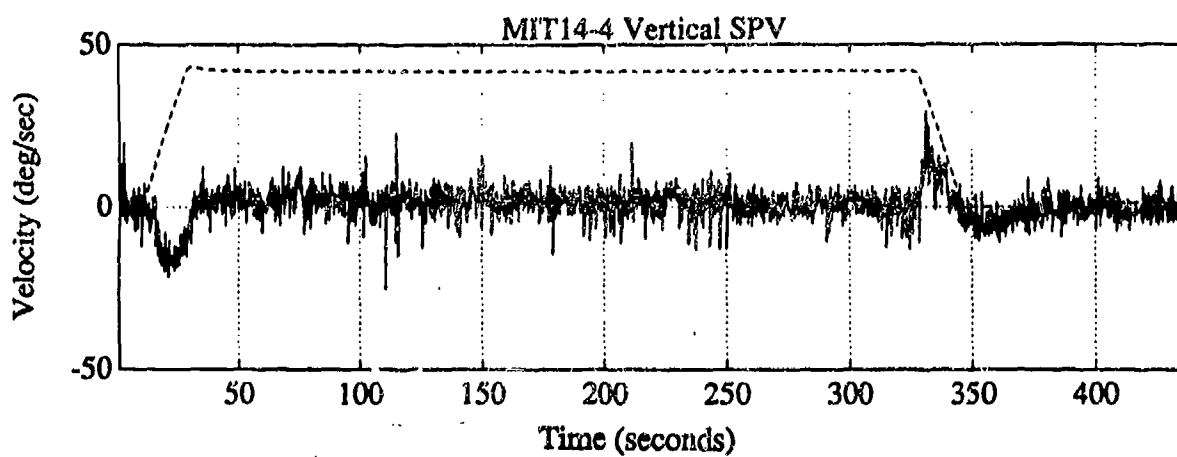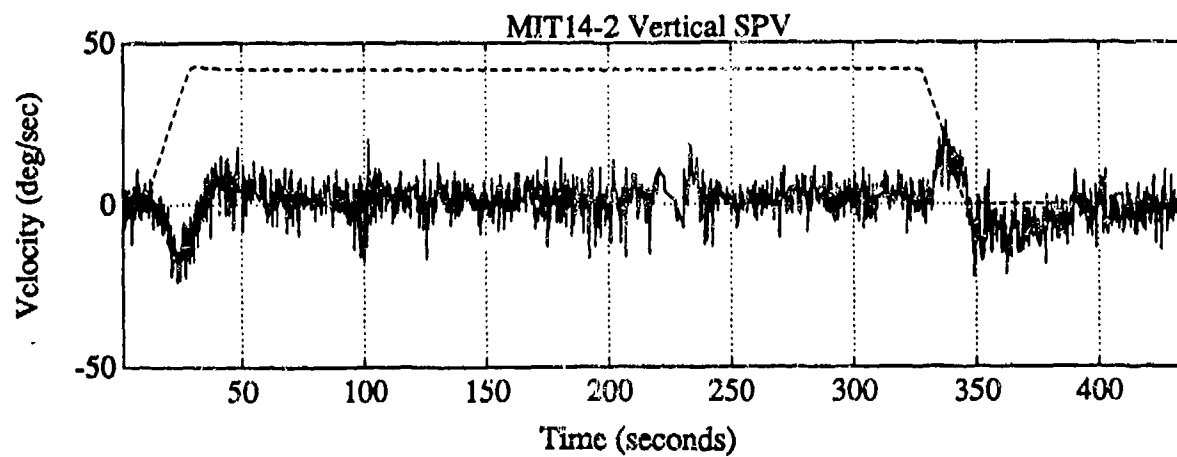
Figure 5.28: Vertical SPV
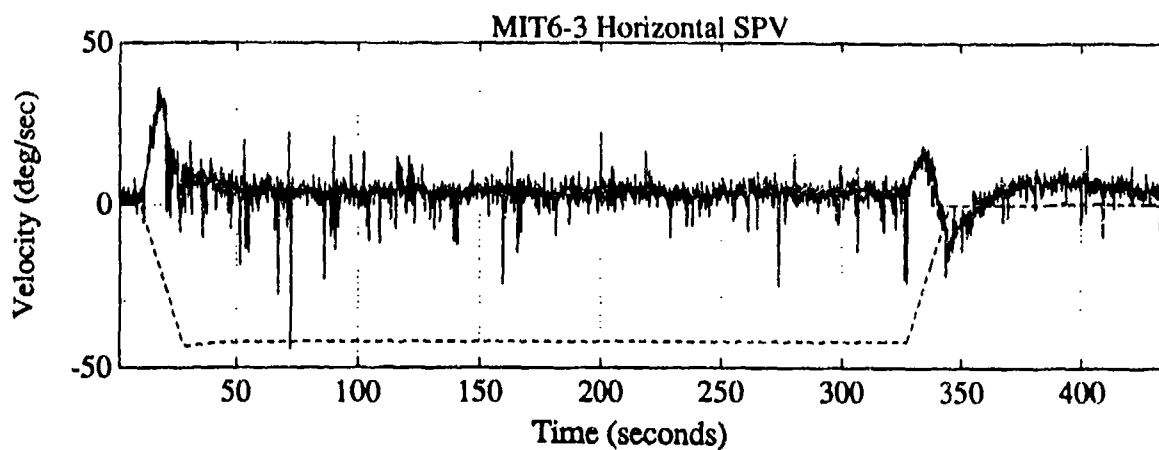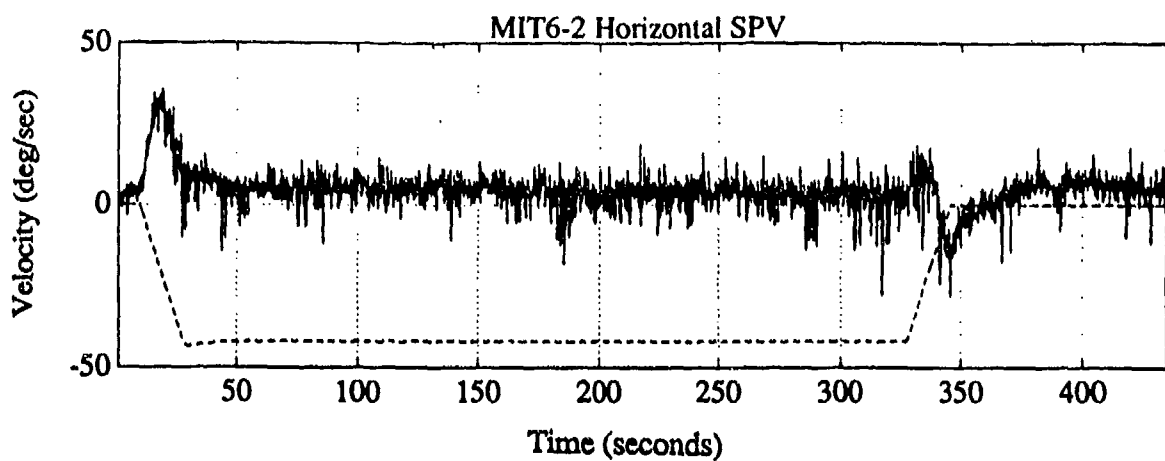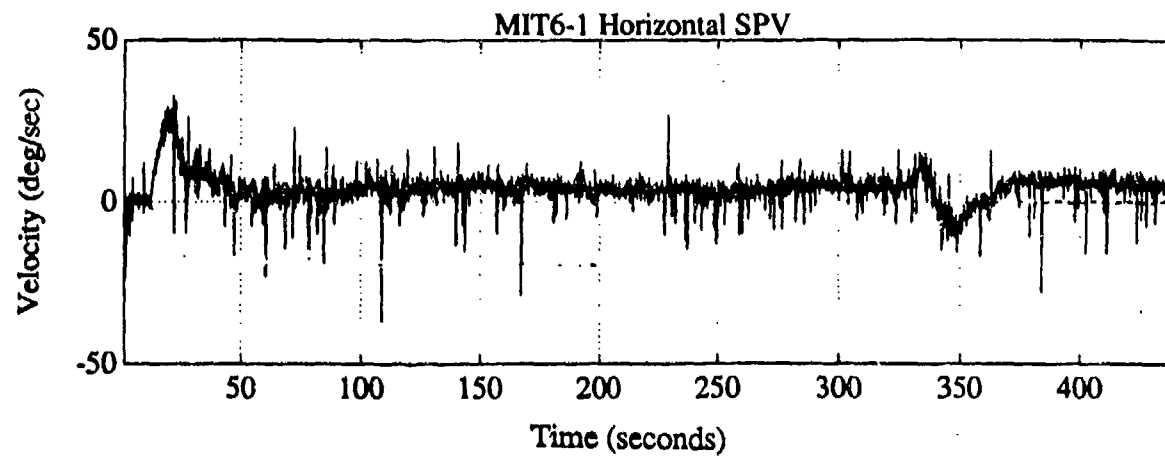Subject 14, CounterClockwise

99
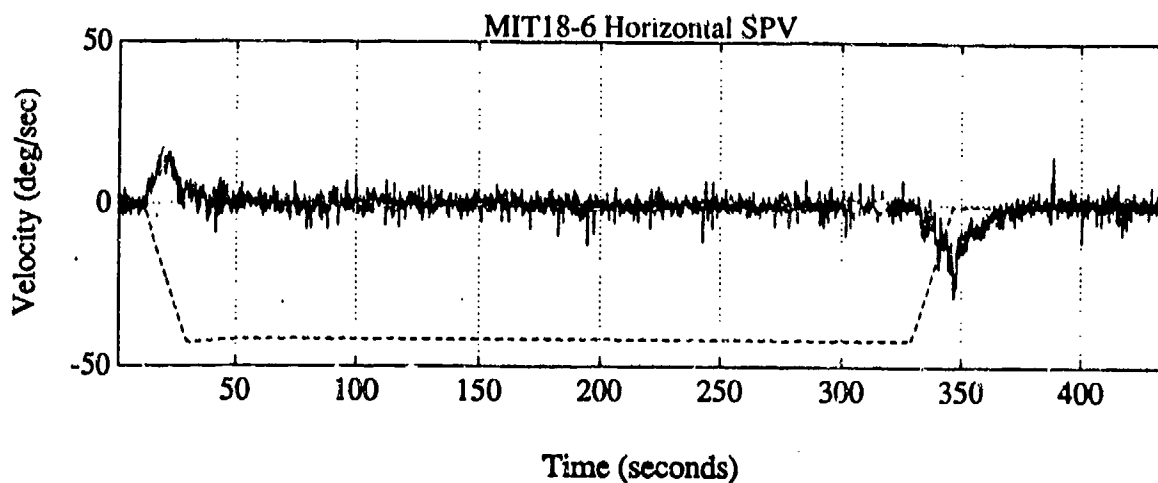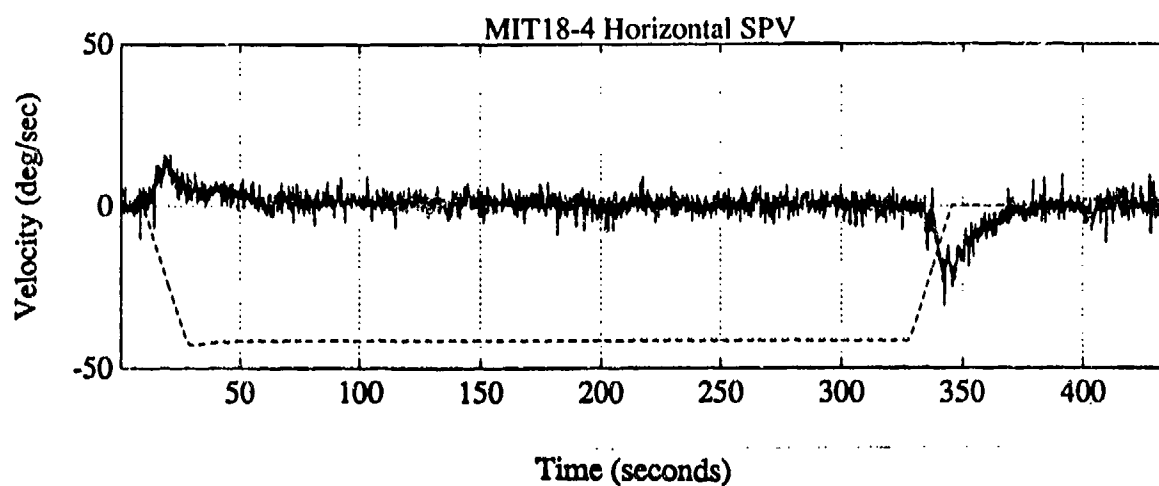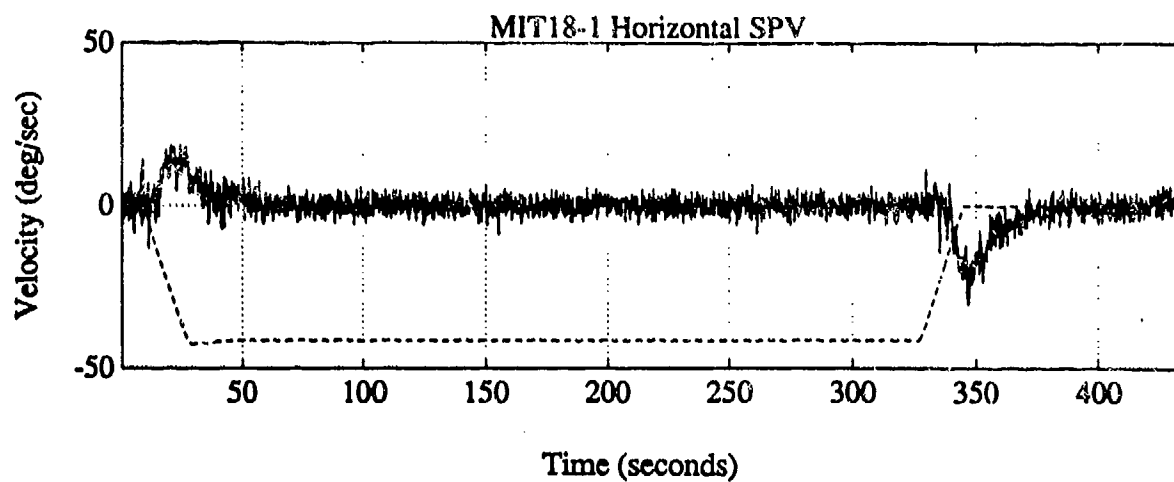
Figure 5.29: Horizontal SPV
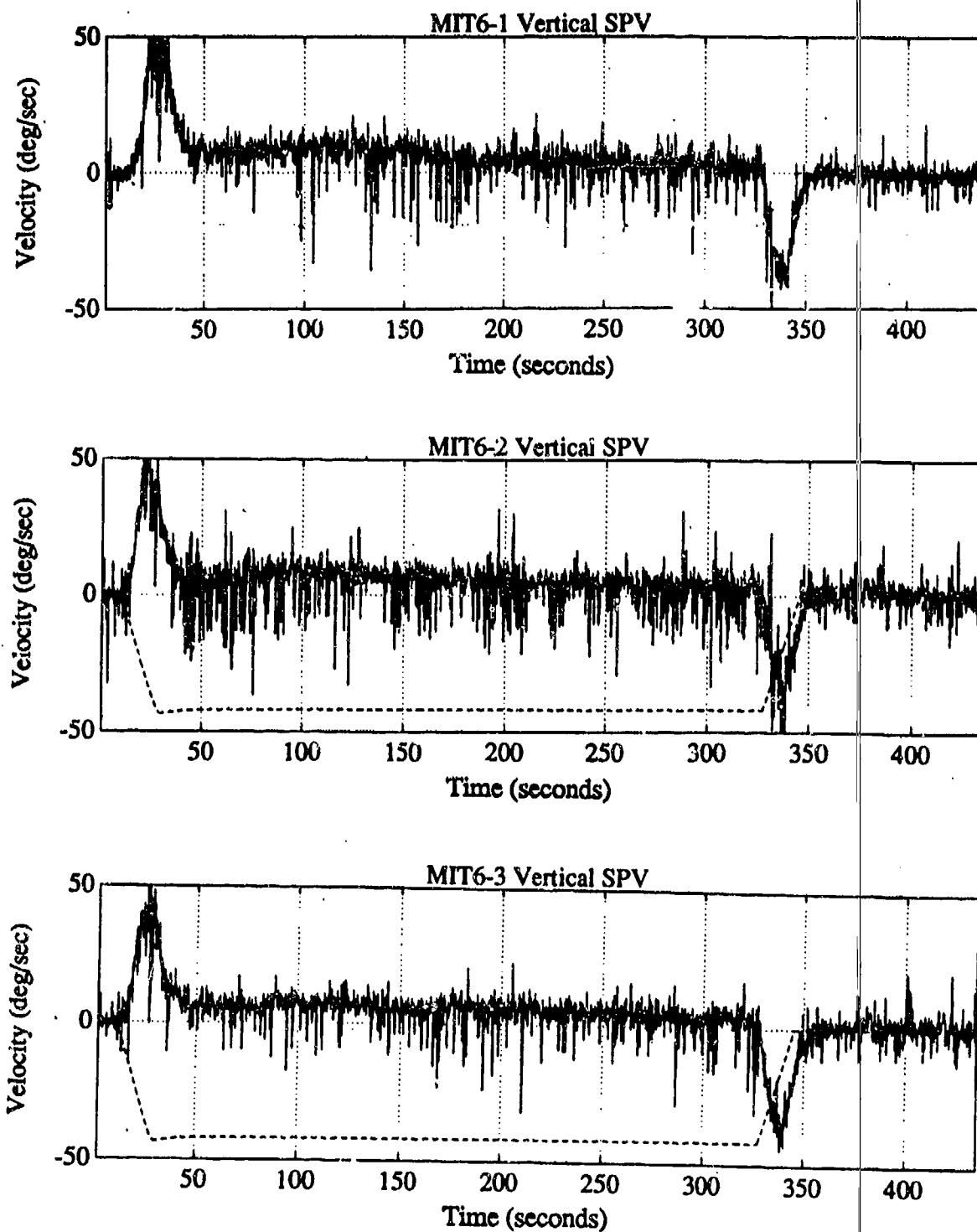Subject 18, Clockwise

100
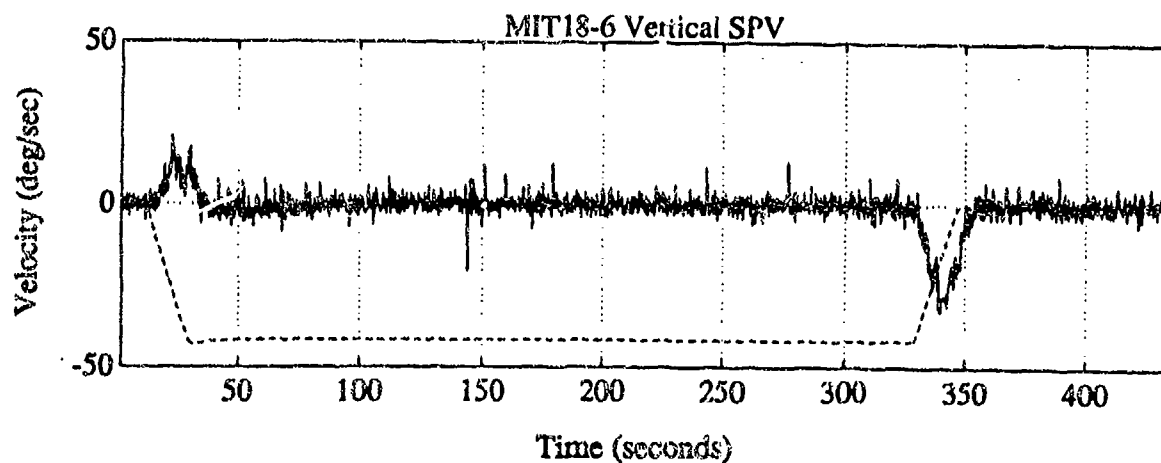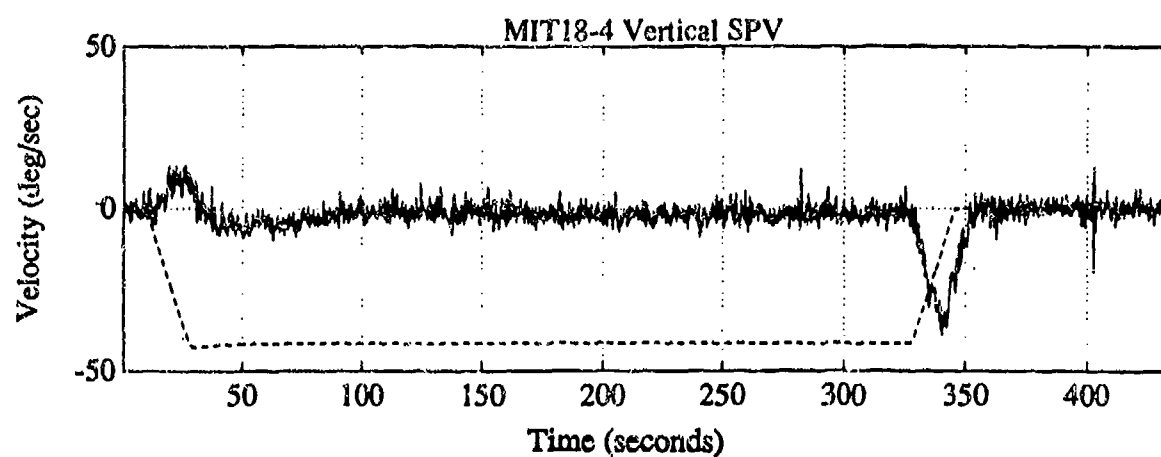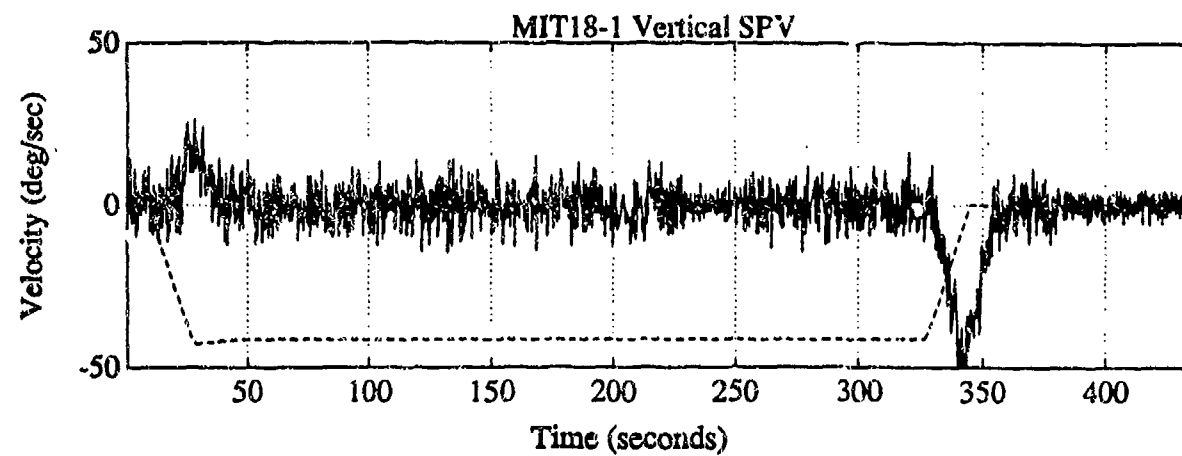
Figure 5.30: Vertical SPV
Subject 18, Clockwise

MIT18-2 Horizontal SPV
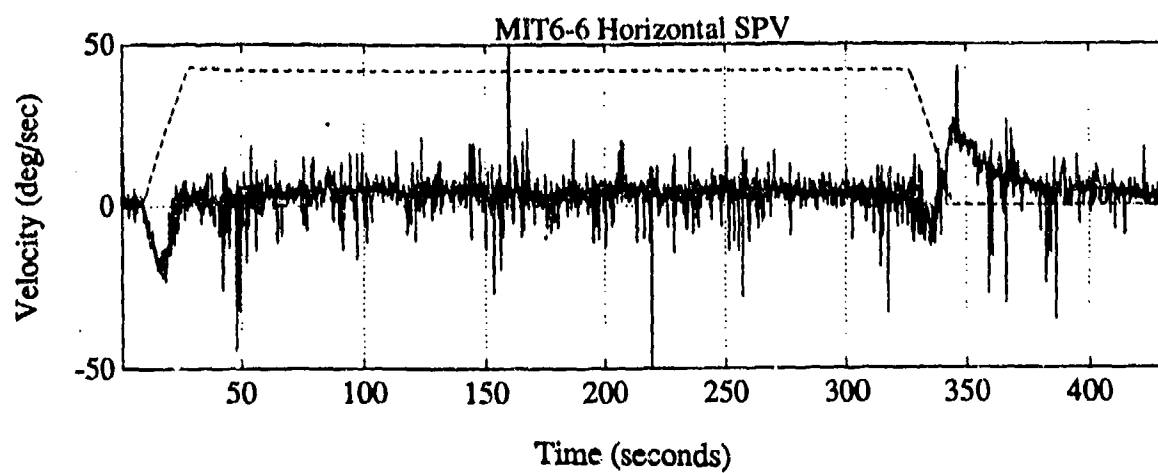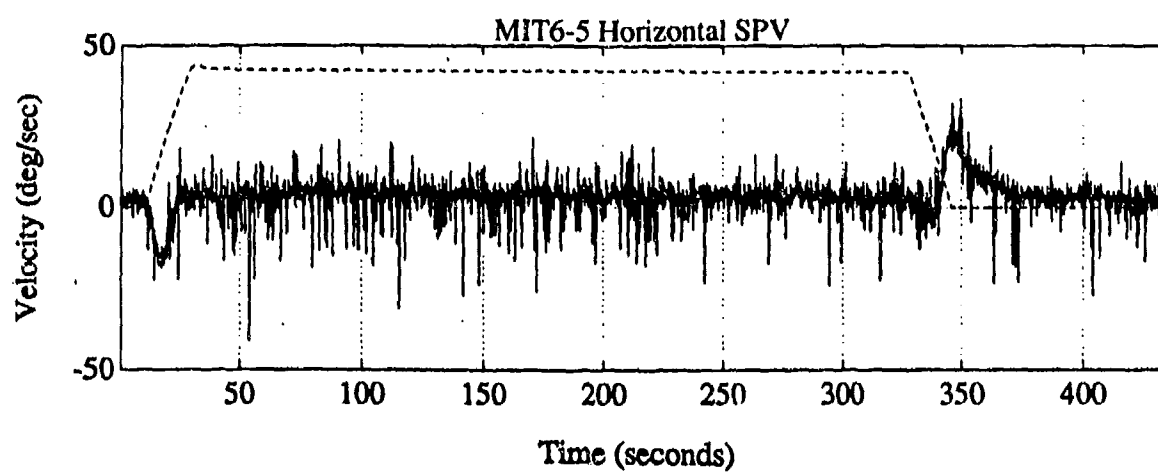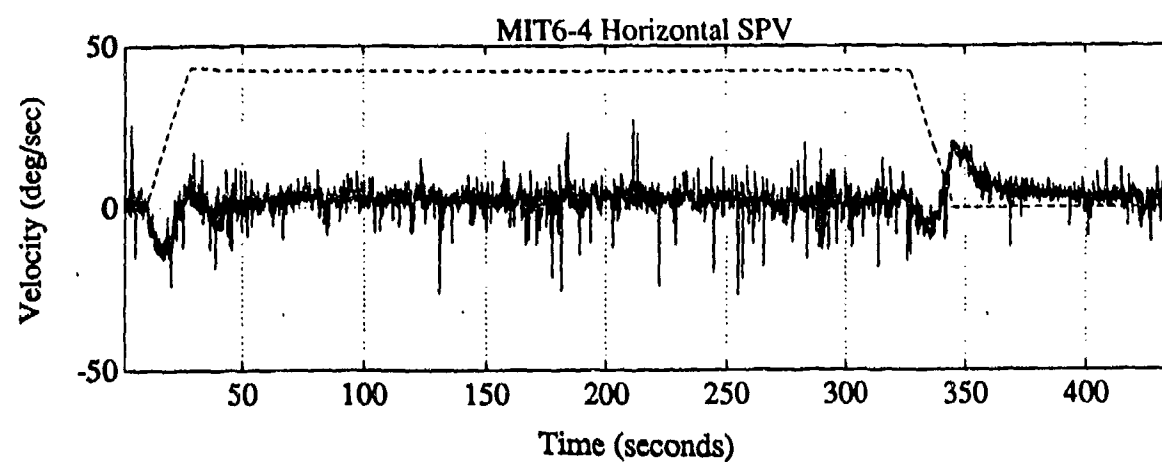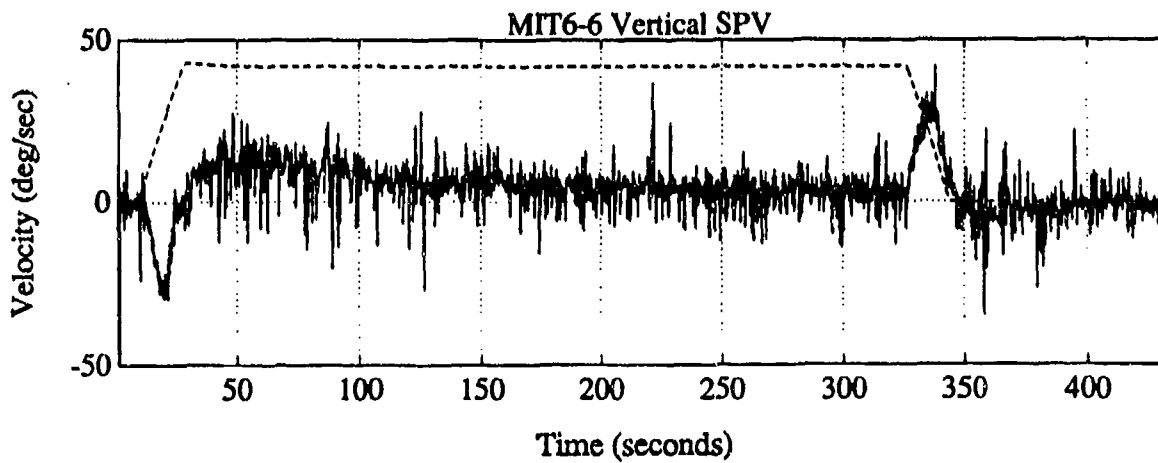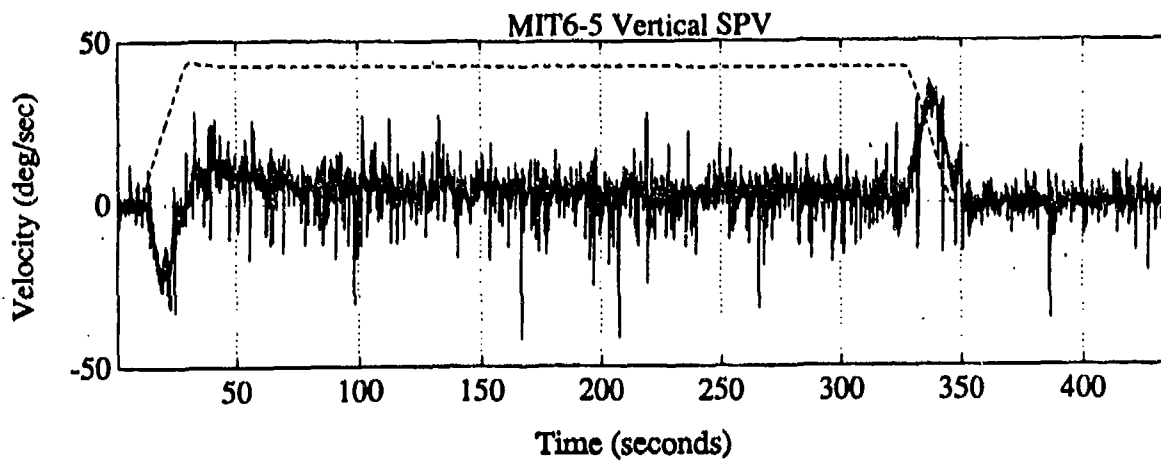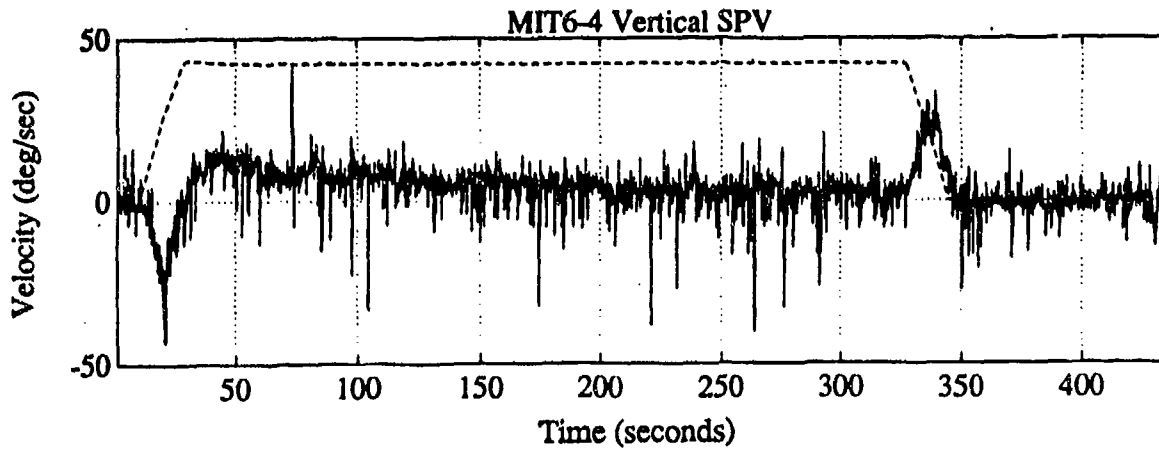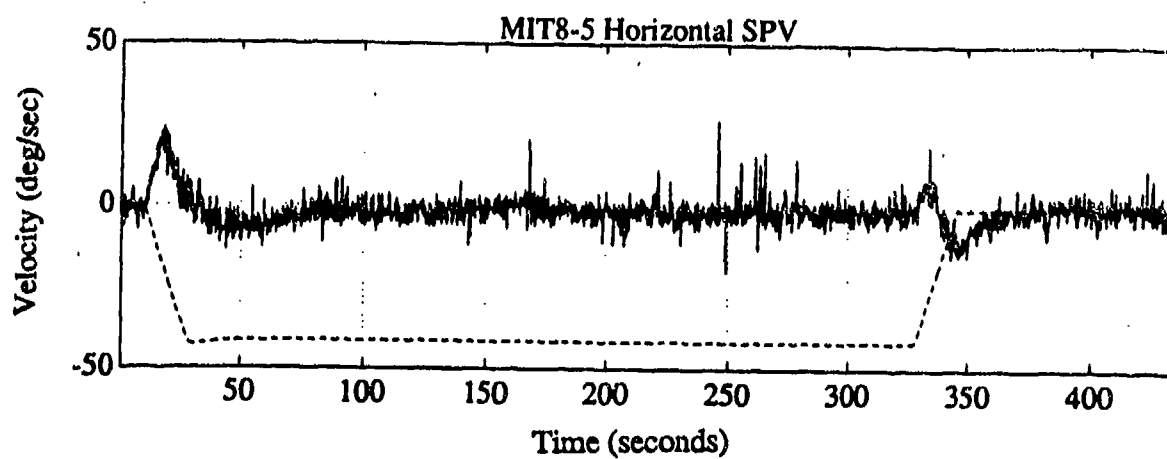
MIT18-3 Horizontal SPV

MIT18-5 Horizontal SPV
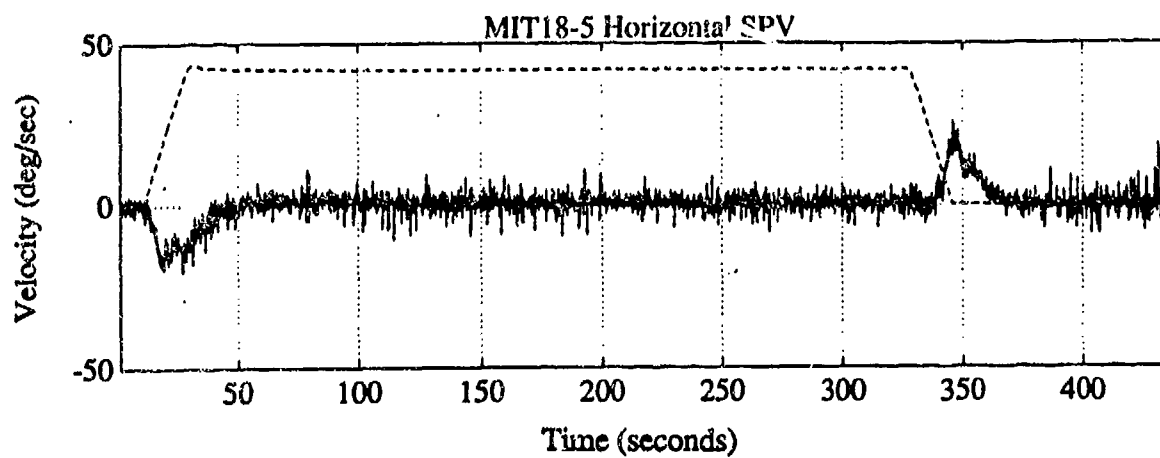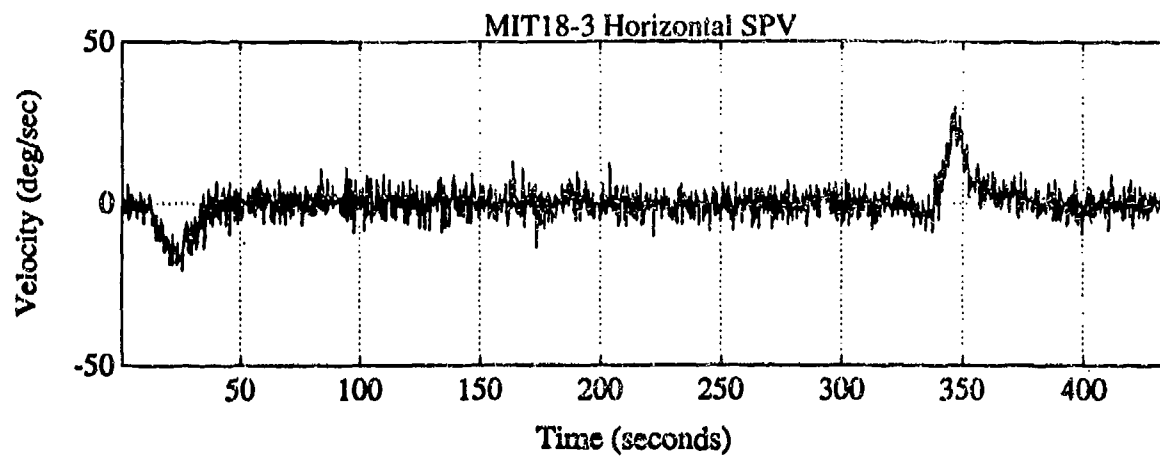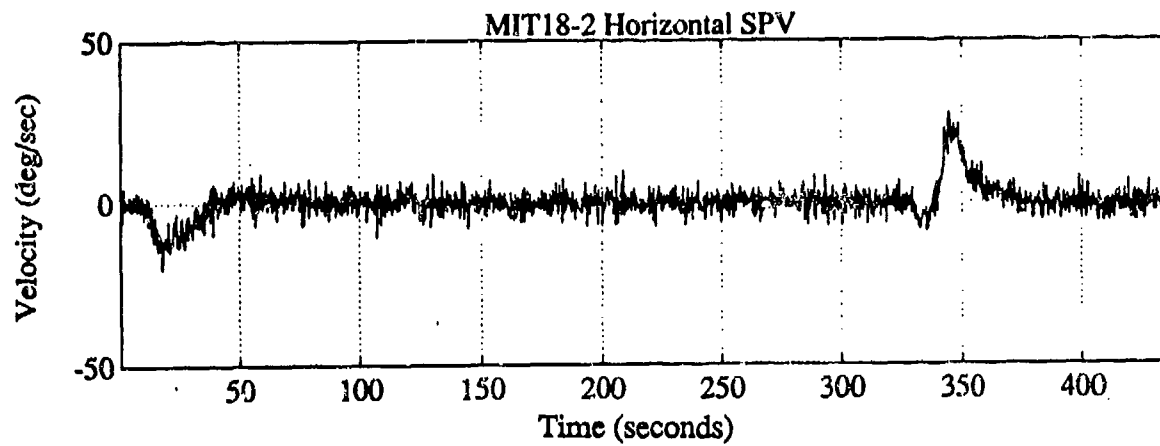
Figure 5.31: Horizontal SPV
Subject 18, CounterClockwise

102
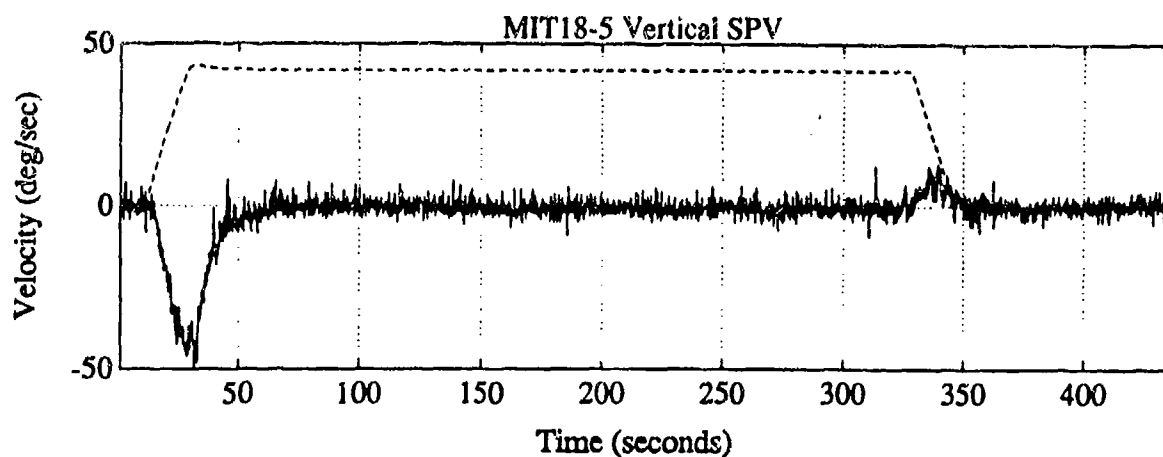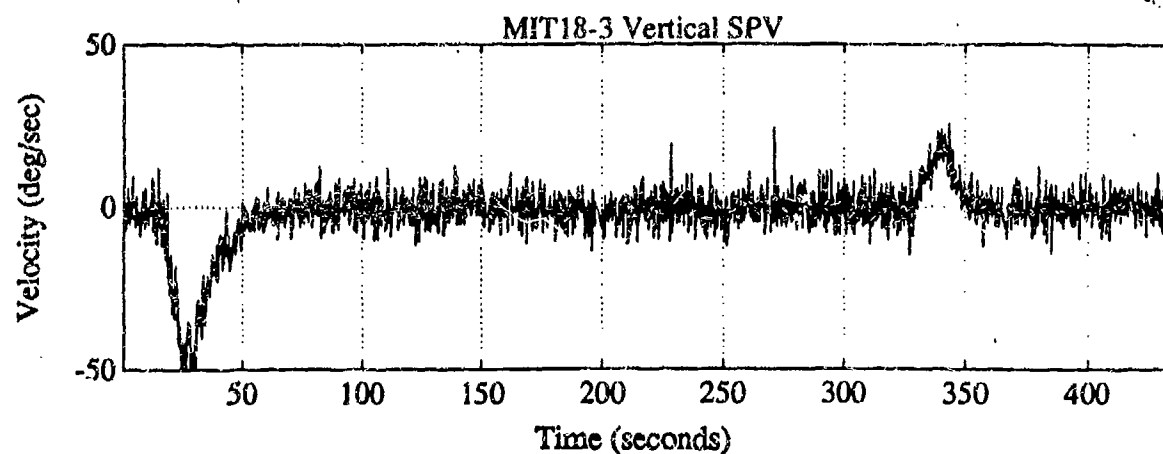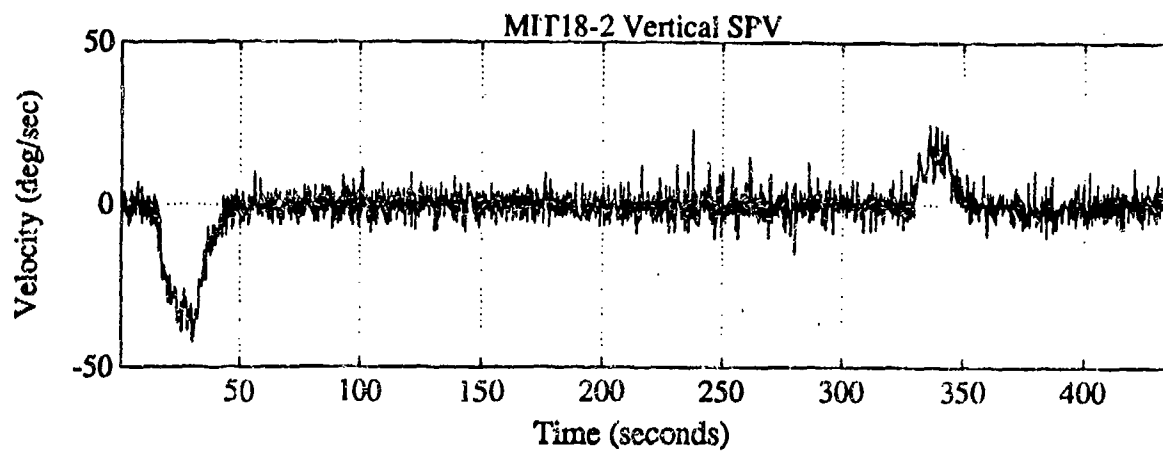
Figure 5.32: Vertical SPV
Subject 18, CounterClockwise

103

5.4. TYPICAL SLOW PHASE VELOCITY RESPONSE

Figures 5.33 and 5.34 show representative horizontal and vertical SPV responses for a human subject obtained during a clockwise (CW), and a counterclockwise (CCW) centrifuge run, respectively. The shapes of the SPV responses were similar for all runs in a given direction (CW/CCW). However, there were differences in the SPV magnitudes within subjects and between subjects. Estimates of the peak and L-nystagmus SPV magnitudes are provided in Table 5.2 (CW) and Table 5.3 (CCW). The variables in Tables 5.2 and 5.3 are defined below and are shown in Figures 5.33 and 5.34.

H_A - Peak Horizontal SPV during CAP acceleration
t_A - Time of Peak Horizontal SPV during CAP acceleration

H_B - Peak Horizontal SPV at the start of the CAP deceleration
t_B - Time of Peak Horizontal SPV at the start of the CAP deceleration

H_C - Peak Horizontal SPV during CAP deceleration
t_C - Time of Peak Horizontal SPV during CAP deceleration

V_A - Peak Vertical SPV during CAP acceleration
t_{VA} - Time of Peak Vertical SPV during CAP acceleration

V_B - Vertical SPV at 100 secs

V_C - Vertical SPV at 150 secs

V_D - Vertical SPV at 315 secs

V_E - Peak Horizontal SPV during CAP deceleration
t_{VE} - Time of Peak Vertical SPV during CAP deceleration

The times of peak SPV (t_A, t_B, t_C, t_{VA}, t_{VE}), peak SPV's estimates (H_A, H_B, H_C, V_A, V_E) and the vertical SPV's at set times (V_B, V_C, V_D) were obtained by the method described in section 3.4.2.4. Note that there is no data for 5-6, as this data was lost due to computer crashes, and 8-1 signal is lost during the run due to illuminator wire working its way loose.

Horizontal SPV
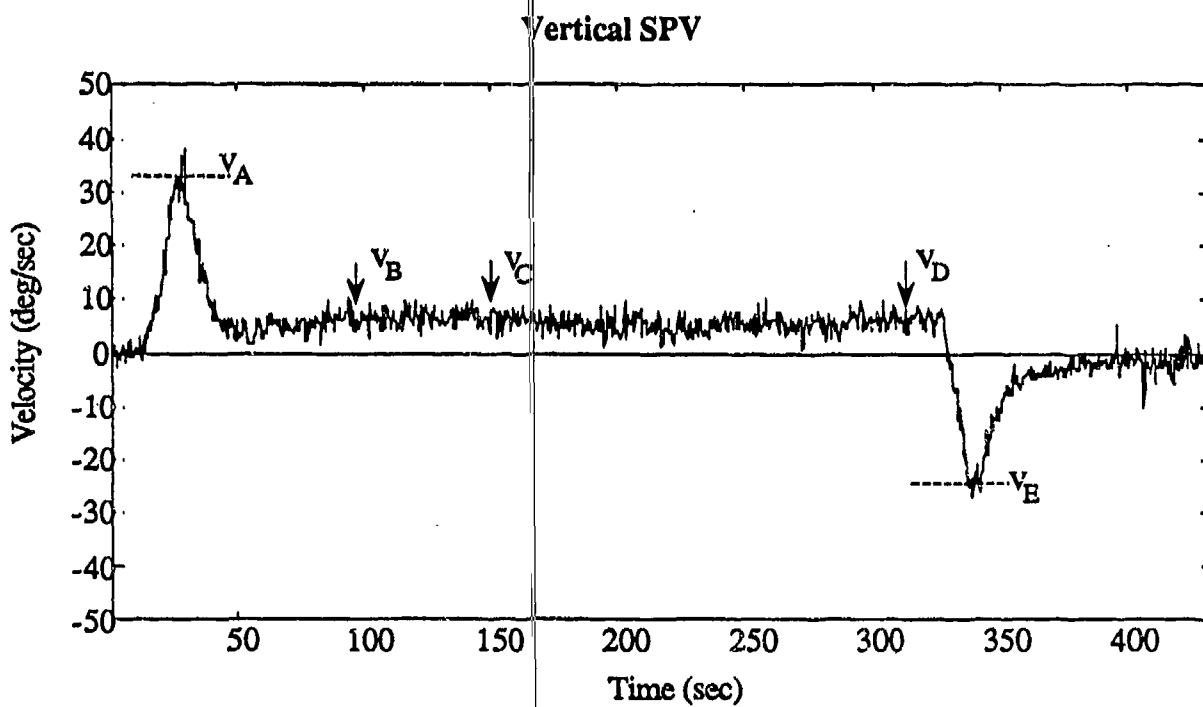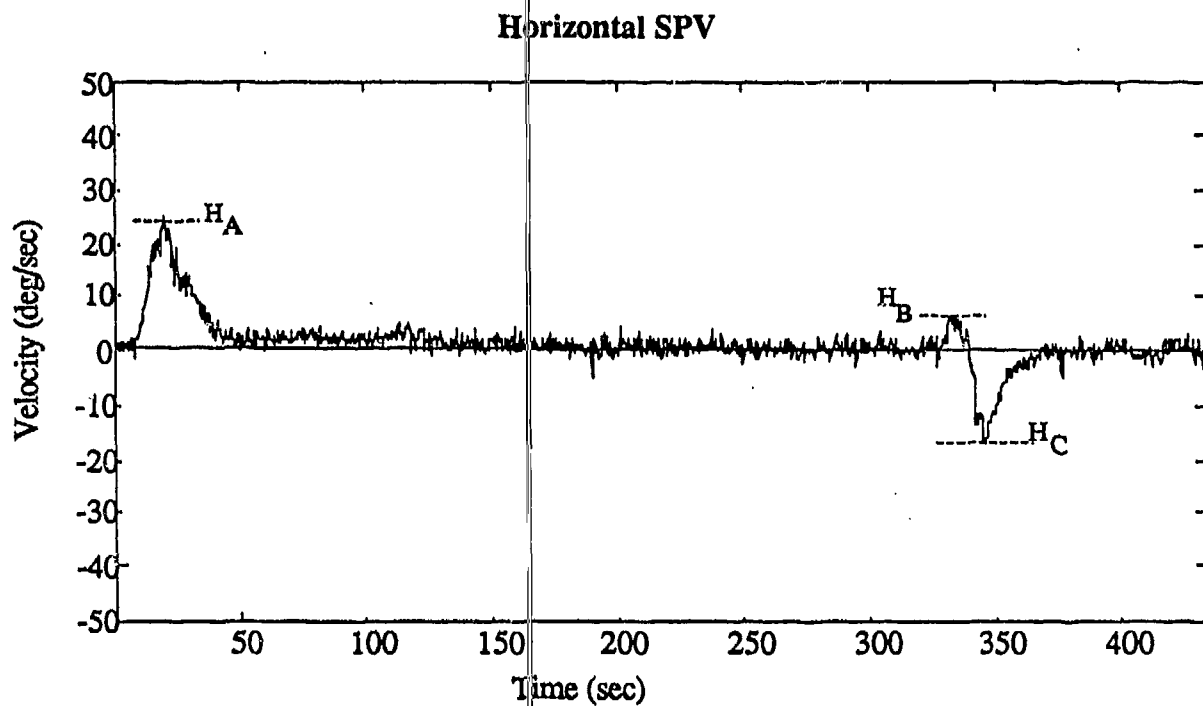
Vertical SPV

Figure 5.33: Typical Horizontal and Vertical SPV
during Clockwise Runs

Horizontal SPV
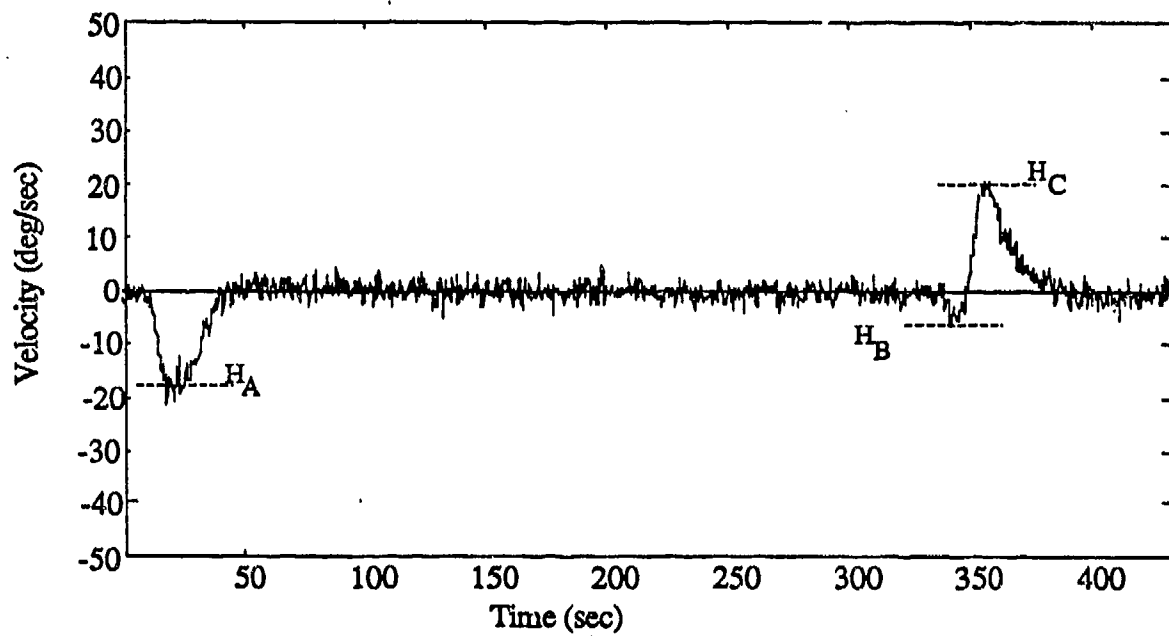
Vertical SPV
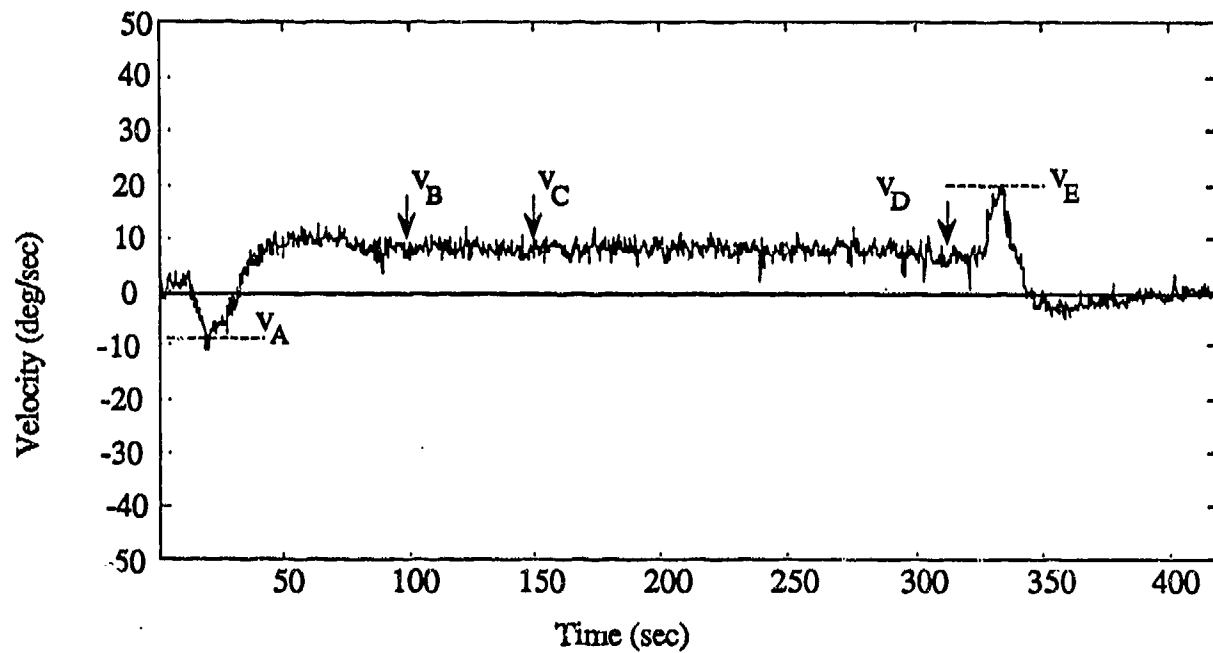
Figure 5.34: Typical Horizontal and Vertical SPV
during CounterClockwise Runs

	Horizontal						Vertical						
Subject & Run	t_A	H_A	t_B	H_B	t_C	H_C	t_{VA}	V_A	t_{VE}	V_E	V_B	V_C	V_D
5-2	18	31	333	4	344	-22	25	63	339	-23	10	9	6
5-4	18	22	332	3	344	-22	26	57	341	-30	8	6	4
5-6													
6-1	20	25	334	11	348	-9	30	51	338	-37	6	8	2
6-2	19	33	336	10	346	-16	25	45	337	-40	7	5	2
6-3	19	32	335	16	346	-13	26	40	339	-39	6	5	3
8-1	20	19					29	63					
8-3	19	21	336	11	345	-13	27	51	339	-30	14	12	11
8-5	18	20	334	7	345	-12	29	54	340	-32	8	8	7
9-1	19	18	333	5	344	-12	29	34	334	-35	15	12	12
9-3	19	21	334	5	345	-15	28	29	338	-25	12	12	8
9-6	20	17	335	3	345	-15	29	30	338	-16	10	10	9
10-1	21	24	336	4	346	-17	28	41	339	-26	6	6	5
10-3	21	22	335	6	346	-16	28	30	338	-23	5	5	5
10-5	21	26	333	8	345	-17	29	30	337	-29	7	8	8
11-1	18	14	335	8	347	-17	30	36	341	-28	13	13	8
11-3	19	13	335	9	346	-17	29	24	340	-30	8	9	7
11-5	18	18	334	5	346	-15	28	24	341	-27	9	9	8
14-1	19	12	335	3	345	-17	30	21	338	-19	3	2	2
14-3	19	11	335	3	345	-19	28	14	336	-25	2	1	1
14-5	17	16	336	6	346	-19	26	16	337	-25	3	1	1
18-1	22	16	334	3	347	-23	29	19	342	-49	0	0	0
18-4	19	13	333	0	346	-22	26	12	341	-36	-1	-2	-1
18-6	22	15	333	0	346	-31	29	14	340	-31	0	0	0
mean	19.3	19.9	334	5.9	346	-17.2	28	34.7	339	-29.8	6.9	6.3	4.9
s^2	1.3	6.3	1.2	3.8	1.0	4.75	1.6	16.0	1.9	7.5	4.5	4.4	3.7

Table 5.2: Clockwise Runs

Horizontal　　　　　　　　　　　　　　　　Vertical

Subject & Run	t_A	H_A	t_B	H_B	t_C	H_C	t_A	V_A	t_E	V_E	V_B	V_C	V_D
5-1	17	-14	333	-7	345	19	21	-7	337	27	21	19	11
5-3	17	-17	333	-6	346	16	20	-12	335	21	11	8	3
5-5	17	-16	337	-6	347	18	22	-10	338	24	10	7	3
6-4	17	-13	334	-6	345	19	20	-20	340	26	7	5	2
6-5	17	-16	335	-3	346	23	20	-24	337	33	4	4	2
6-6	16	-18	335	-7	345	25	20	-26	338	29	7	6	3
8-2	19	-12	336	-13	347	20	22	-17	338	42	14	12	12
8-4	20	-15	338	-11	346	13	23	-17	337	34	9	7	7
8-6	16	-18	333	-12	345	21	20	-16	338	35	7	7	6
9-2	16	-7	335	-5	346	18	22	-10	336	22	10	9	8
9-5	15	-4	334	-5	345	17	23	-8	334	17	10	10	9
9-7	16	-7	333	-8	346	18	22	-9	334	20	6	6	6
10-2	20	-7	336	-8	346	15	23	-15	338	16	7	5	5
10-4	20	-7	337	-5	346	16	21	-10	334	17	7	7	6
10-6	19	-8	336	-6	347	11	23	-10	334	17	9	9	9
11-2	16	-12	335	-3	346	10	24	-27	340	11	9	9	5
11-4	16	-12	334	-7	345	13	23	-30	338	16	7	8	6
11-6	17	-13	336	-8	347	11	25	-27	339	22	11	10	7
14-2	21	-13	339	-10	348	17	24	-18	338	19	1	2	2
14-4	18	-11	333	-6	345	17	23	-17	333	20	2	2	1
14-6	17	-15	335	-8	346	12	23	-18	335	17	1	1	1
18-2	19	-14	333	-8	345	23	29	-36	339	18	0	0	0
18-3	24	-16	333	-5	346	26	29	-49	342	18	0	0	0
18-5	22	-16	335	-2	347	20	30	-46	340	10	0	0	0
mean	18	-12.5	335	-6.9	346	17.4	23	-20	337	22.1	7.1	6.4	4.7
s^2	2.2	4.0	1.7	2.7	0.9	4.4	2.8	11.4	2.3	7.8	5.0	4.4	3.5

Table 5.3: Counter Clockwise Runs

108

5.4.1 Horizontal SPV Response

For CW runs (Figure 5.33), the horizontal SPV response during centrifuge acceleration increases to a peak (mean 19.9°/sec) at mean time 19.3 secs. The yaw stimulus angular velocity is 50.7°/sec at 21.3 secs. The peak SPV occurs before the end of centrifuge acceleration due to the reversal in yaw angular acceleration as shown in Figure 4.6a. Experimental results confirm this. At the start of centrifuge deceleration, the SPV response proceeds in the same direction as during acceleration, (mean 5.9°/sec) at mean time 334 secs. This "yaw reversal" at the start of centrifuge deceleration is predicted by consideration of the yaw angular velocity stimulus (Figure 4.7b), and is caused by the pendulous chair swinging through approximately 70°. The swinging chair causes the yaw angular acceleration stimulus to change sign as shown in Figure 4.6b. During centrifuge acceleration, this sign change in yaw angular acceleration is not of sufficient strength to change the sign of the yaw angular velocity, however it reduces the time of peak SPV as shown above. During centrifuge deceleration, the sign change in yaw angular acceleration produces a reversal in yaw angular velocity. The yaw reversal during centrifuge deceleration can be seen in the stimulus plot and the SPV response. After the yaw reversal, the horizontal SPV response changes sign to reach a peak (mean -17.2°/sec) at mean time 346 secs. The time of peak SPV occuring at centrifuge stop is predicted by the stimulus. The horizontal SPV response then decays to zero.

For horizontal SPV during CCW runs (Figure 5.34), we expect the mirror image of the CW response. For the overall general shape of the response this is appears to be true, however, a difference in the magnitudes of the peak SPV response is noted. The horizontal response during CCW centrifuge acceleration increases to peak SPV (mean -12.5°/sec) at mean time 18 secs. These values are lower than the corresponding CW values. At the start of centrifuge deceleration, the "yaw reversal" is evident (mean -6.9°/sec) at mean time 335

secs. After the yaw reversal, the horizontal SPV response changes sign to reach a peak (mean 17.4°/sec) at mean time 346 secs. The horizontal SPV response then decays to zero.

5.4.1.1 Horizontal Peak SPV Asymmetry

As noted above, during acceleration of the centrifuge the magnitude of the horizontal SPV appeared to be greater when the subject faced the motion (CW run) compared to when the subject had his back to the motion (CCW). To test this observation a one sided paired t-test was performed (Table 5.4).

Pairs	Subject 5		Subject 6		Subject 8		Subject 9		Subject 10		Subject 11		Subject 14		Subject 18	
	cw	ccw	cw	ccw	cw	ccw	cw	ccw	cw	ccw	cw	ccw	cw	ccw	cw	ccw
1	31	-14	25	-13	19	-12	18	-7	24	-7	14	-12	12	-13	16	-14
2	22	-17	33	-16	21	-15	21	-4	22	-7	13	-12	11	-11	13	-16
3		-16	32	-18	20	-18	16	-7	26	-8	18	-13	16	-15	15	-16
cw-ccw	11		14.33		5		12.33		16		2.67		0		-0.67*	
s	8.48		2.52		2.64		4.16		1		2.08		1		2.51	
t	1.83		9.83		3.28		5.12		27.7		2.22		0		0.46	
p	<0.2		<0.01		<0.05		<0.025		<0.005		<0.1				<0.25	

Table 5.4: Peak Horizontal SPV during Acceleration
Facing Motion (CW) vs Back to Motion (CCW)

Four of the 8 subjects (6, 8, 9 and 10) show a significant result. Subject 11 just missed significance at the $p < 0.05$ level and even though subject 5 did not show significance, the values indicate that CW (facing motion) peak SPV is greater than CCW (back to motion) peak SPV. Subject 5's insignificant result could be due to the missing data of run 5-6 thereby reducing analysis to a 1 degree of freedom problem. Hence for at least four and possibly six of the eight subjects, the horizontal SPV is greater when the subject faces the motion (CW run) as compared to when the subject has his back to the motion (CCW).

A similar effect was seen in monkeys by Merfeld (1990) in an experiment with a non-pendulous fixed chair, and was explained along the lines of the LVOR hypothesis suggested by Young (1967). As discussed by Merfeld, during combined linear and angular stimulation, the total VOR response may be composed of the summation of the LVOR and the angular VOR. During a centrifuge run where the chair is fixed, the subject experiences a horizontal linear stimulation from the centripetal force, and yaw angular stimulation from the centrifuge angular acceleration. When the subject is facing the motion, the angular VOR and the LVOR are additive, and when the subject has his back to the motion the angular VOR and the LVOR subtract. Therefore the peak horizontal SPV would be greater when the subject faced the motion as compared to when the subject had his back to the motion.

The above result thus raises the possibility that a horizontal linear force was present during acceleration of the centrifuge. Two possible origins of this horizontal linear force were considered. The first was that the pendulous chair did not pivot exactly so that the GIF during centrifuge acceleration was not aligned with the head fixed z axis, or secondly, the head was tilted with respect to the chair. Note that a head tilt of only 10° produces a horizontal linear force of 0.52G. Using a horizontal L-nystagmus sensitivity of 9°/sec/G (Young, 1967), this horizontal linear force corresponds to an approximate horizontal L-nystagmus of 5°/sec. However, if the head is tilted we would expect to see a constant horizontal L-nystagmus during the constant velocity phase of the centrifuge run. A constant horizontal L-nystagmus was observed only for Subject 6 (see Figures 5.5 and 5.7), but this was attributed to a subject dependent positional nystagmus, since it was observed before and after the centrifuge run. Therefore, a transient head tilt during centrifuge acceleration and deceleration is one possible explanation of the observed modification of horizontal SPV. This transient head tilt may be caused by vestibulocollic reflexes that may occur as a result of the chair rolling during centrifuge acceleration and

deceleration. As the chair rolls right, the vestibulocollic reflex would cause the head to roll slightly in the opposite direction. The direction of this reflex head tilt is in the correct direction to account for the observed SPV result. The addition of a head fixed accelerometer package in future experiments will be used to investigate this issue.

For the two subjects (Subjects 14 and 18) who did not record a significant result, it can be interpreted that these subjects have small or no horizontal LVOR. This observation is supported in the next section where the same two subjects are shown to have little or no vertical LVOR.

5.4.2 Vertical SPV Response

An up-beating nystagmus is evident in 7 of the 8 subjects during the constant velocity phase of the centrifuge run. Since the stimulus to the vestibular system during the constant velocity phase is the high G linear acceleration, it may be concluded that this response is an LVOR. Therefore this up-beating nystagmus can be called L-nystagmus as defined by Young (1967). Since this L-nystagmus is vertical, the term L_z-nystagmus will be used to avoid confusion with horizontal L-nystagmus. The observed L_z-nystagmus results from this thesis confirm the results obtained in two studies at the TNO Institute for Perception in Sosterberg, Holland (Marcus, 1989; Marcus and Van Holten, 1990). In these two separate studies a similar L_z-nystagmus response was obtained from human subjects when exposed to sustained 3 G_z in a centrifuge. The subjects were seated with head erect.

There appeared to be no effect of run direction on the magnitude of the L_z-nystagmus, thus supporting the linear acceleration origins of this response, since the linear stimulus is equivalent but the angular stimulus is reversed. To determine static sensitivity, consider the value V_B (from Tables 5.2 and 5.3) which is an estimate of the L_z-nystagmus at a time

112

(100 secs) where the response from the angular acceleration stimulus is considered to have decayed to approximately zero. Therefore, at this time the angular VOR is assumed to have no or little effect on the total VOR and the hence the measured VOR magnitude (V_B) represents the LVOR response only. Subjects displayed a range of V_B values from -1 to 21°/sec (Figure 5.35). Subject 18 recorded negative L_Z-nystagmus values for one run. However, these values are considered to be an artifact due to the accuracy of the analysis method. It is concluded that subject 18 probably had no significant L_Z-nystagmus. Excluding subject 18's data, the average static L_Z-nystagmus sensitivity to vertical linear acceleration is 8°/sec. Assuming a linear response to G, the average static L_Z-nystagmus sensitivity is approximately 3°/sec/G. This value is marginally lower than the 4°/sec/G estimated by Young (1967).

The L_Z-nystagmus response was noted to be an individual subject characteristic with two distinct features: a magnitude, and a time constant of decay. Some subjects displayed an L_Z-nystagmus response, whereas other subjects had no L_Z-nystagmus. Additionally, in some subjects the magnitude of the L_Z-nystagmus decayed substantially over the 5 minute run. A subject was defined to have an L_Z-nystagmus response if the magnitude of the SPV at time 100 secs (V_B) was greater than 2°/sec. Also, a subject was defined to have substantial L_Z-nystagmus decay if the ratio of L_Z-nystagmus at 100 secs to the L_Z-nystagmus at 315 secs (V_B/V_D) was greater than 2.0. Using this criteria, the overall L_Z-nystagmus response can be seen to fall into 3 categories:

-Subjects that displayed an L_Z-nystagmus that remained fairly constant over the 5 minute run (Subjects 8 9 10 11 14). ($V_B > 2°$/sec, $V_B/V_D < 2.0$)

-Subjects that displayed an L_Z-nystagmus that decayed over the 5 minute run (Subjects 5 6). ($V_B > 2°$/sec, $V_B/V_D > 2.0$)

-Subjects with no steady state L_Z-nystagmus (Subjects 18). ($V_B < 2°$/sec).

113
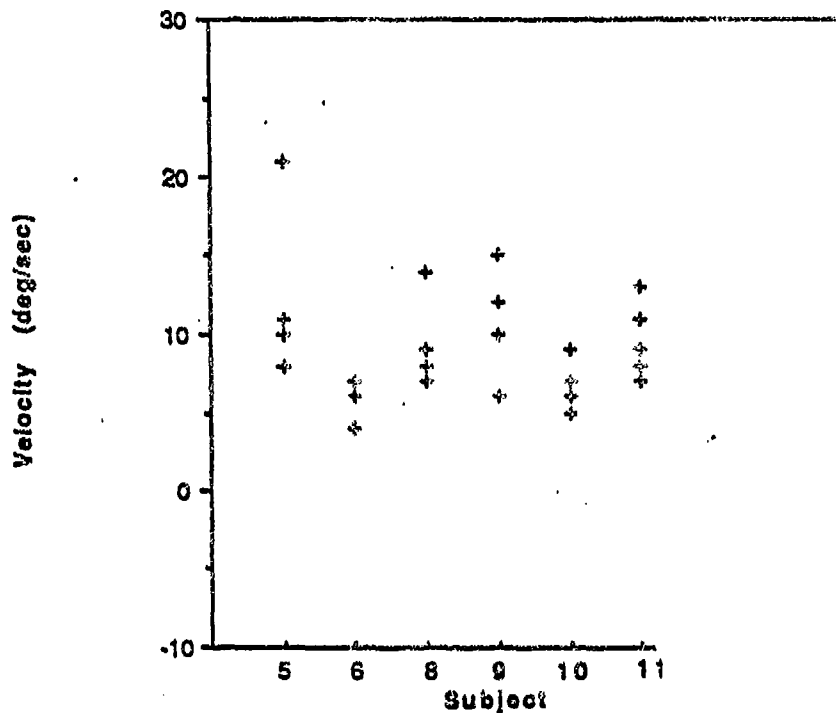
L Nystagmus

Figure 5.35 L_Z Nystagmus Magnitude at 100 secs (V_B) for
8 Subjects. 6 trials per subject

The L_Z-nystagmus appears to be a complex process that interacts with the angular VOR to give the total VOR during the cross-coupled stimulation. The build-up of L_Z-nystagmus occurs at the same time as the angular VOR, therefore the exact dynamics of the L_Z-nystagmus buildup, and the dynamics of the cross-coupled angular VOR are difficult to determine. However, insight into the nature of the interaction can be gained from consideration of the CW and CCW runs.

During centrifuge acceleration for a CW run (Figure 5.33) the mean time of vertical peak SPV (mean magnitude 34°/sec), is 28 secs which corresponds to the time predicted by the maximum pitch velocity stimulus. From angular stimulus considerations alone, the time

114

for vertical peak SPV during CCW centrifuge acceleration should be the same, just the magnitude of the SPV should be reversed. However, the mean time of vertical peak SPV (mean magnitude - 20°/sec) during CCW centrifuge acceleration is 23 secs. It appears that the onset of the upbeating L_z-nystagmus interacts with the angular nystagmus, decreasing the time and magnitude of peak SPV response during CCW acceleration (Figure 5.34). Further evidence that the L_z-nystagmus has modified the angular VOR comes from subject 18's data. This subject had no steady state L_z-nystagmus, and his mean times of peak vertical SPV for CW and CCW runs are similar (28 secs for CW, and 29 secs for CCW).

During deceleration of the centrifuge the influence of the L_z-nystagmus on the angular VOR response is not so clear. For the CW runs, the mean time of peak vertical SPV (magnitude -29.8°/sec) is 339 secs, and for CCW runs, the mean time of peak vertical SPV (magnitude 22.1°/sec) is 337 secs. Therefore the L_z-nystagmus has modified the angular VOR, however, the exact nature of the modification is unclear. As seen for centrifuge acceleration, Subject 18 who has no L_z-nystagmus has mean times of 341 secs for CW and 340 secs for CCW runs, which approximate the peak times as predicted by the angular stimulus.

The data is consistent with the view that the total VOR response is composed of two interacting components; a linear VOR and an angular VOR. It also provides evidence that LVOR can be elicited by a constant vertical linear acceleration. As to why a LVOR response is elicited in a constant 3 G environment, one possible explanation is to extend the following hypothesis reviewed by Merfeld (1990):

> "(results) indicate that gravito-inertial force is resolved into two components; one
>
> representing an internal estimate of linear acceleration and one representing an internal
>
> estimate of gravity"

Thus, the constant L_z-nystagmus result suggests that when subjected to a 3 G gravitio-inertial force, the otolith organs send a signal to the CNS that is interpreted as a 1 G gravitational field with an upward linear acceleration of approximate magnitude 2 G, thereby generating the observed upbeating L_z-nystagmus.

The times to peak SPV during acceleration (18 secs for CW, and 13 sec for CCW after start of stimulus) and the times to peak SPV during deceleration (10 for CW, and 8 secs for CCW after stimulus start) confirm the expected results from consideration of the pitch angular stimulus. During the initial phase of centrifuge acceleration there is a pitch ramp stimulus, and during the initial phase of centrifuge deceleration there is a pitch step stimulus (see Figure 4.6). Therefore, we would expect that the time constant of vertical SPV onset during centrifuge deceleration be faster than centrifuge acceleration. This result was obtained and may play a role in understanding the difference in pitch subjective sensations (Table 5.1).

5.4.2.1 Acceleration vs Deceleration

This section presents the results of the analysis to determine if there is a significant difference between the peak SPV response during acceleration and deceleration cf the centrifuge. Table 5.5 shows the ratio of the absolute magnitude of the estimate of the peak vertical SPV during CAP centrifuge acceleration versus centrifuge deceleration.

$$\text{Ratio (dec/acc)} = \frac{|V_E|}{|V_A|}$$

Subject Mean is the geometric mean of the individual ratios for each subject.

Figures 5.36 and 5.37 show the geometric means for the ratios of centrifuge deceleration vs acceleration for CW and CCW runs. As can be seen for CW runs, the subjects that showed a L_Z-nystagmus had a ratio less than one. This result was expected since the upbeating L_Z-nystagmus adds to the acceleration response and subtracts from the deceleration response. Conversely for CCW runs the ratio of deceleration/acceleration is greater than one for subjects who showed an L_Z-nystagmus except Subject 11. Subject 14 showed little L_Z-nystagmus and the deceleration/acceleration ratio is greater than one for CW runs, and approximately equal to one for CCW runs. Subject 18 who had essentially no steady state L_Z-nystagmus showed an asymmetry response in pitch. For this subject the pitch down response is consistently greater than pitch up response. Whether this is simply intrinsic to the subjects oculomotor system such that it would also be manifest in VOR responses to rotation about the earth vertical, or whether it involves interactions between angular responses and gravito-inertial force is unknown.

If peak vertical SPV magnitudes were an indication of the reported pitch sensation asymmetry, then we would expect that the deceleration/acceleration ratios shown in Figures 5.36 and 5.37 would be greater than 1 for both directions. From Figure 5.36 it can be seen that this is not the case. The peak vertical SPV deceleration/acceleration ratio can be explained along the lines of a subjects L_Z-nystagmus response. Therefore the peak vertical SPV magnitude does not correlate with pitch sensations. This result is not unexpected since only for simple stimuli (for example rotating chair) does the oculomotor response give an accurate indication of the sensations felt. For complicated stimulus such as this experiment, the combination of semicircular canal cues, otolith cues, proprioceptors and tactile cues combine to give sensations that are often not reflected in simple measures of the vestibular response, such as the magnitude of peak SPV.

Clockwise				Counter Clockwise		
Subject & Run	Ratio(Dec/Acc)	Subject Mean		Subject & Run	Ratio(Dec/Acc)	Subject Mean
5-2	0.36			5-1	3.85	
5-4	0.53			5-3	1.75	
5-6		0.44		5-5	2.4	2.53
6-1	0.72			6-4	1.30	
6-2	0.89			6-5	1.37	
6-3	0.97	0.85		6-6	1.11	1.25
8-1				8-2	2.47	
8-3	0.59			8-4	2.00	
8-5	0.59	0.59		8-6	2.19	2.21
9-1	1.03			9-2	2.20	
9-3	0.86			9-5	2.12	
9-5	0.53	0.78		9-7	2.22	2.17
10-1	0.63			10-2	1.07	
10-3	0.77			10-4	1.70	
10-5	0.97	0.78		10-6	1.70	1.46
11-1	0.78			11-2	0.41	
11-3	1.25			11-4	0.53	
11-5	1.12	1.03		11-6	0.81	0.56
14-1	0.90			14-2	1.06	
14-3	1.78			14-4	1.18	
14-5	1.56	1.36		14-6	0.94	1.05
18-1	2.58			18-2	0.50	
18-4	3.00			18-3	0.37	
18-6	2.21	2.57		18-5	0.22	0.34

Table 5.5: Ratio of Peak SPV during
Centrifuge Acceleration and Deceleration
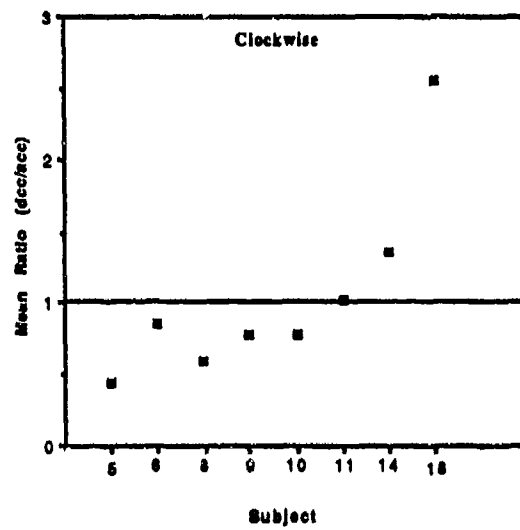
Figure 5.36: Geometric Means for the
Ratio of Centrifuge Deceleration vs Acceleration
Clockwise Runs.
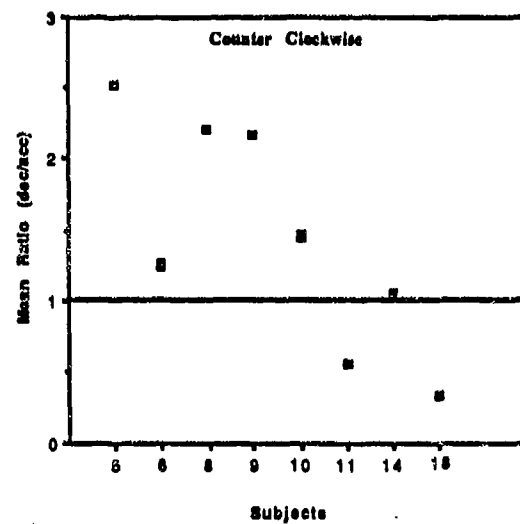
Figure 5.37: Geometric Means for the
Ratio of Centrifuge Deceleration vs Acceleration
Counter Clockwise Runs.

119

5.5 AVERAGE SLOW PHASE VELOCITY RESPONSE

As previously discussed in Chapter 2, one of the goals of this experiment was to obtain an average vestibular response whose parameters could be used to develop a vestibular model. The averaging of data obviously must be done across similar types of responses. From Table 5.2 it was noted that the magnitude of the peak SPV during centrifuge acceleration (V_A) for a subjects first run seemed different from subsequent runs. If true, this could be because stress and fear associated with the first run affects the vestibular response. That first run response therefore does not represent a "steady state" response, and we do not include it in an average. To calculate the average runs for each subject the following conservative approach was taken:

    1/ Exclude any subject that experienced GLOC.

    2/ Exclude response from run 1.

    3/ Exclude subjects from the first run in the opposite direction to that of run 1.

In Figures 5.42 through 5.49, the average horizontal and vertical slow phase velocity plots for each subject are presented. These responses characterize the consistent component of the VOR response for each subject. Comparison of results (Figures 5.42 through 5.49) show that the time course of the SPV response differed between subjects in the following manner:

    1/ Magnitudes of peak SPV response.

    2/ Steady state L_z nystagmus sensitivity.

    3/ Time constant of L_z nystagmus decay.

Since these appear to be important differences, it appears that the subjects do not represent a homogeneous population, so it is not appropriate simply to average their SPV responses to obtain an overall population SPV response curve.

The following sections detail the statistical analyses to determine whether the SPV response from a subjects first run 1 in a certain direction is different from subsequent runs in that same direction.

5.5.1 Response Modification for a Subjects First Run

This section presents the results of an analysis to determine if the SPV response from a subject's first run was different in subsequent runs in the same direction. Subjects 6, 8, 9, 10, 11, 14, 18 completed a CW run first, and Subject 5 completed a CCW run first. All other subjects with CCW runs first, happened to be excluded from the data set due to GLOC.

5.5.1.1 Peak Vertical SPV during CAP Acceleration and Deceleration - Clockwise

Figures 5.38 and 5.39 shows the difference in peak vertical SPV between runs 1 and 2, and runs 2 and 3. Figure 5.38 is for CW acceleration and Figure 5.39 is for CW deceleration. The data in these figures suggests that run 2 is similar to that of run 3, and the magnitude of run 1 is different.

To test the observation that the magnitude of SPV is different in run 1, an F-ratio test was developed based on the assumption that runs 2 and 3 are similar and that they represent a steady or typical value. The null hypothesis is that there is no difference in SPV magnitude among runs 1, 2 and 3. Two estimates of the variance of the individual x's (where x is the peak SPV magnitude during a run) are calculated that should be the same if the null hypothesis is correct. 9

121

The first statistic for estimating the variance of the individual x's is based on the difference from run 1 to the average of runs 2 and 3.

$$s_1^2 = \frac{2}{3}\left(x_1 - \frac{x_2+x_3}{2}\right)^2$$

The second such unbiased statistic is based on the difference between the values for runs 2 and 3.

$$s_2^2 = \frac{1}{2}(x_2 - x_3)^2$$

The individual variances were then summed over individuals to give an estimate of the variances for the group and an F ratio test performed. If the null hypothesis was sustained, there were no significant difference between the variances so estimated. Table 5.6 shows the values of the estimated peak SPV during CW acceleration and the variances s_1^2 and s_2^2. Table 5.7 shows the values of the estimated peak SPV during CW deceleration and the variances s_1^2 and s_2^2.

The difference in vertical SPV magnitude during CW acceleration between runs 1 and the average of runs 2 and 3 (F=16.74, 7 d.o.f., Table 5.6) was significant, and the null hypothesis was rejected at the $p < 0.01$ level. The difference in vertical SPV magnitude during CW deceleration between runs 1 and the average of 2 and 3 (F=4.32, 6 d.o.f., Table 5.7) was significant, and the null hypothesis was rejected at the $p < 0.05$ level.

Thus for subjects whose first runs were clockwise (facing the motion), the above results suggest that run 1 response is different from subsequent runs. For peak vertical SPV during acceleration a significant difference was recorded (Table 5.6) and all subjects demonstrated a larger response during run 1 than in subsequent runs (Figure 5.38). For peak SPV during deceleration the results were not quite so strong. As a group, a significant result was recorded. However two subjects (Subjects 9,18) displayed large differences (Figure 5.39) that contributed greatly in increasing the group variance s_1^2, such that a significant result occured. It was felt that fear or apprehension was a definite factor

122
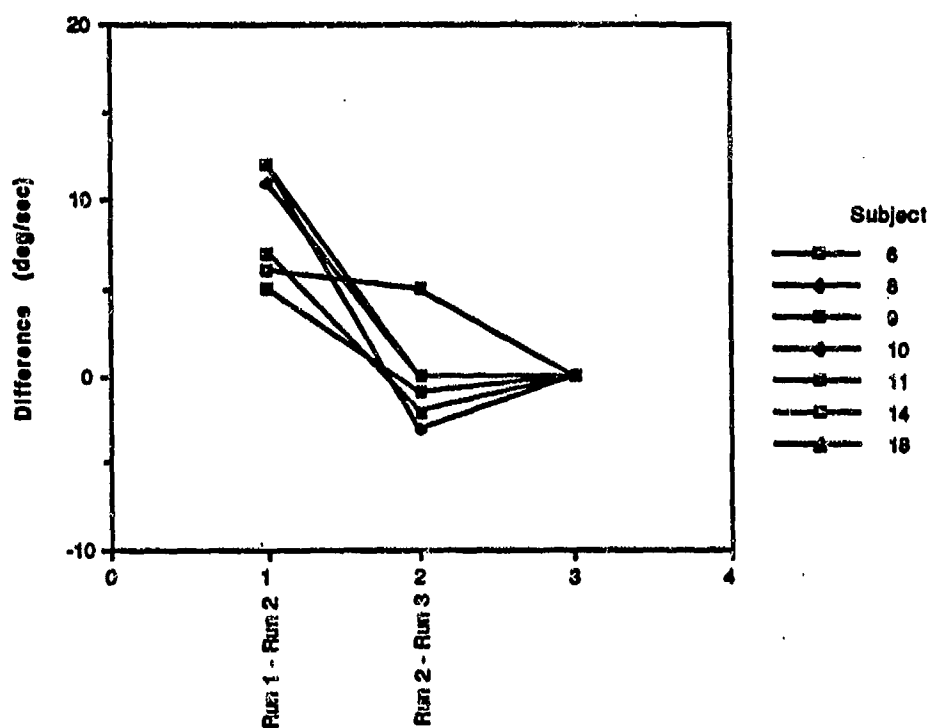
Figure 5.38: Vertical Peak SPV Difference between Runs
during Clockwise Acceleration

	Subject 6	Subject 8	Subject 9	Subject10	Subject11	Subject14	Subject18
Run #1	51	63	34	41	36	21	19
Run #2	45	51	29	30	24	14	12
Run #3	40	54	30	30	24	16	14
s_1^2	48.2	73.5	13.5	80.7	96	24	24
s_2^2	12.5	4.5	.5	0	0	2	2

$\Sigma s_1^2 = 359.87$

$\Sigma s_2^2 = 21.5$

F ratio = 16.74

Table 5.6: Peak SPV values during Acceleration
Clockwise

123
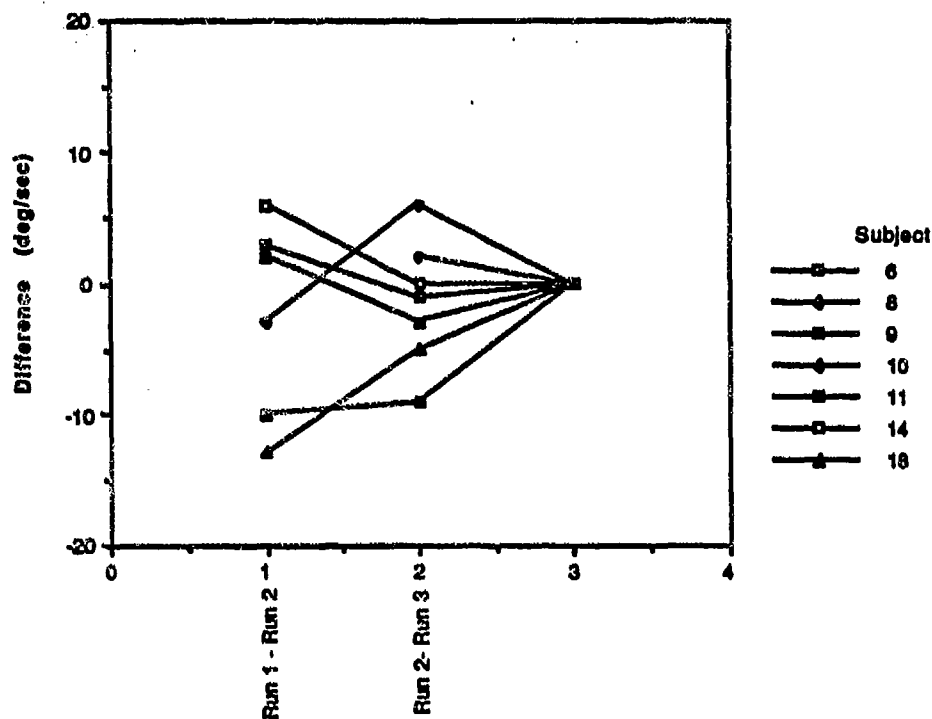
Figure 5.39:Vertical Peak SPV Difference between Runs
during Clockwise Deceleration

	Subject 6	Subject 8	Subject 9	Subject10	Subject11	Subject14	Subject18
Run #1	-37		-35	-26	-28	-19	-49
Run #2	-40	-30	-25	-23	-30	-25	-36
Run #3	-39	-32	-16	-29	-27	-25	-31
s_1^2	4.167		140.167	0	0.167	24	160.167
s_2^2	0.5		40.5	18	4.5	0	12.5

*N.B. Subject 8 not included in analysis due to only 2 data points.

$$\Sigma s_1^2 = 328.67$$

$$\Sigma s_2^2 = 76.0$$

$$F \text{ ratio} = 4.32$$

Table 5.7: Peak SPV values during Deceleration
Clockwise

124

in a subjects first run and the vestibular response was affected. Therefore, it was concluded that for subjects who completed a CW run first, run 1 is statistically significantly different from the average of runs 2 and 3. Thus the data from a subject's first run was not included in an average response for that subject.

5.5.1.2 Peak Vertical SPV during CAP Acceleration and Deceleration - Counter Clockwise

Subject 5 was the only subject who completed a CCW run first. Given the above result for CW runs, and looking at the plots of runs 5-1, 5-3 and 5-5 (Figures 5.3 and 5.4), the vertical SPV response appears to be different. From Table 5.3, the L_z-nystagmus value at 100 secs (V_B) has a value of 21°/sec for run 5-1, and 11°/sec and 10°/sec for runs 5-3 and 5-5 respectively. Therefore, it was concluded that data from run 1 is different from runs 2 and 3, and therefore was not included in an average response for subject 5.

5.5.2 Response Modification for a Subject's First Run in the Second Direction

The above result raises the following question: If a subject's first run is different from subsequent runs in the same direction, is a subjects first run in the other direction different from subsequent runs in that direction? Subjects 6, 8, 9, 10, 11, 14, 18 completed a CW run first, and this data was analyzed in the previous section. This section presents the results of the analysis to determine if the SPV response for Subjects 6, 8, 9, 10, 11, 14, 18 first CCW run was different from subsequent CCW runs.

5.5.2.1 Peak Vertical SPV during CAP Acceleration and Deceleration - Counter Clockwise

Figures 5.40 and 5.41 shows the difference in peak vertical SPV between runs 1 and 2, and runs 2 and 3. Figure 5.40 is for CCW acceleration and Figure 5.41 is for CCW deceleration. The data in these figures suggests that the response from run 2 is similar to run 3, and run 1 is different. To test the observation that the magnitude of SPV is different in run 1, the F-ratio test defined above was used with the results shown in Tables 5.8 and 5.9.

The difference in vertical SPV magnitude during CCW acceleration between runs 1 and the average of runs 2 and 3 (F=9.99, 7 d.o.f., Table 5.8) was significant, and the null hypothesis was rejected at the $p < 0.01$ level. The difference in vertical SPV magnitude during CCW deceleration between runs 1 and the average of runs 2 and 3 (F=1.57, 7 d.o.f., Table 5.9) was not significant at the $p = 0.1$ level.

For peak vertical SPV during acceleration a significant difference was recorded (Table 5.8) however, this significant result appears to be caused by the large difference in subject 18's response. (Figure 5.40). For peak SPV during deceleration the results show that the estimated variances calculated by both methods are large and thus the F-ratio was small and the null hypothesis was not rejected by the test.

However, given the significant result of the acceleration case and since fear and apprehension were possible causes in the CW first run case, it suggests that run 1 was sufficiently different from the average of runs 2 and 3. Therefore, each subject's first CCW run was not included in an average response.
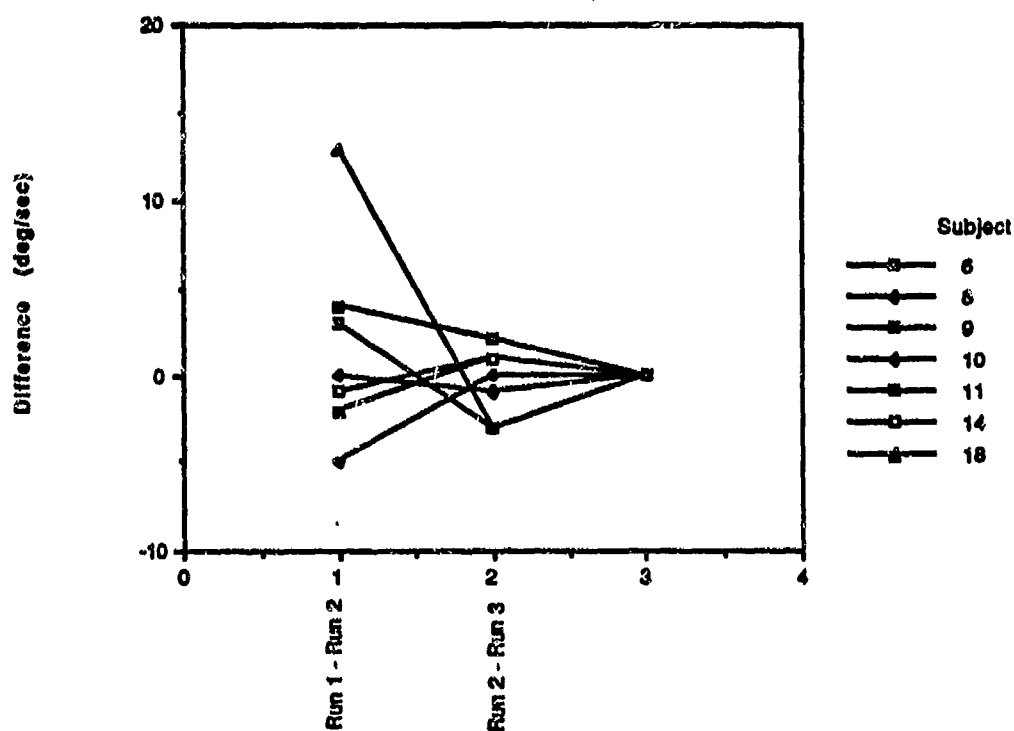
Figure 5.40: Vertical Peak SPV Difference between Runs
during Counter Clockwise Acceleration

	Subject 6	Subject 8	Subject 9	Subject10	Subject11	Subject14	Subject18
Run #1	-20	-17	-10	-15	-27	-18	-36
Run #2	-24	-17	-8	-10	-30	-17	-49
Run #3	-26	-16	-9	-10	-27	-18	-46
s_1^2	16.67	0.167	1.5	16.67	1.5	0.167	88.167
s_2^2	2	0.5	0.5	0	4.5	0.5	4.5

$\Sigma s_1^2 = 124.84$

$\Sigma s_2^2 = 12.5$

F ratio = 9.99

Table 5.8: Peak Vertical SPV values during Acceleration
Counter Clockwise

127
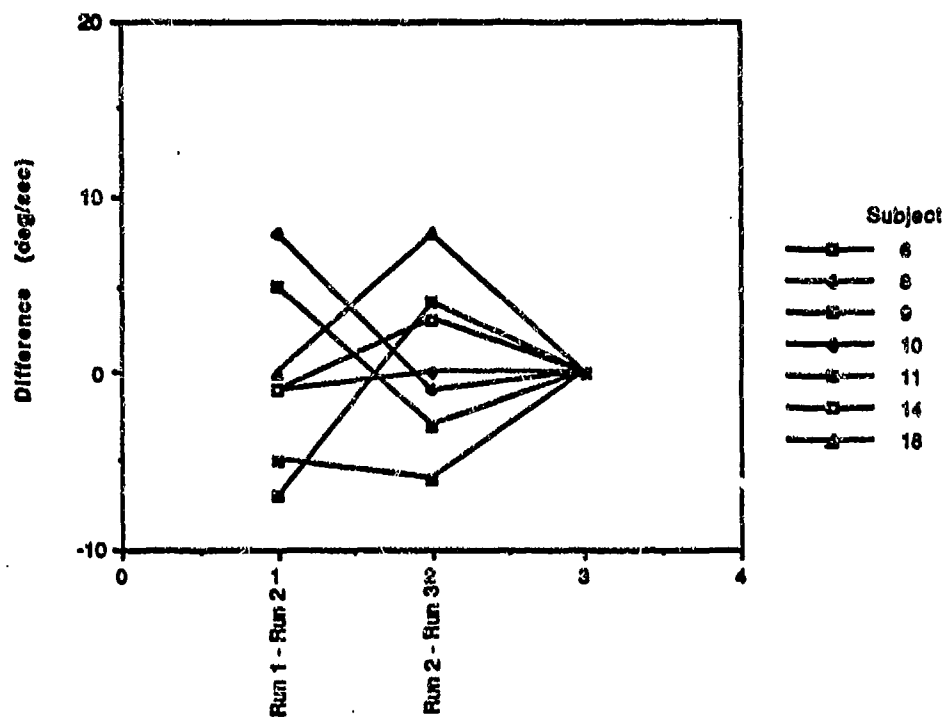
Figure 5.41: Vertical Peak SPV Difference between Runs
during Counter Clockwise Deceleration

	Subject 6	Subject 8	Subject 9	Subject10	Subject11	Subject14	Subject18
Run #1	26	42	22	16	11	19	18
Run #2	33	34	17	17	16	20	18
Run #3	29	35	20	17	22	17	10
s_1^2	16.67	37.5	8.167	0.67	42.667	0.167	0
s_2^2	8	0.5	4.5	0	18	4.5	32

$\Sigma s_1^2 = 105.84$

$\Sigma s_2^2 = 67.5$

F ratio = 1.57

Table 5.9: Peak Vertical SPV values during Deceleration
Counter Clockwise

128

5.5.2.2 Peak Vertical SPV during CAP Acceleration and Deceleration - Clockwise

For Subject 5 in the CW direction, to determine the difference between his first run (5-2) and subsequent runs (5-4 and 5-6) is difficult because of the loss of data from run 5-6. Comparing runs 5-2 and 5-4 (Figures 5.1 and 5.2 and Table 5.2) there appears to be no consistent differences in the SPV responses. However, to be consistent with the previous results run 5-2 will be excluded, leaving only 5-4 as the "average" CW run for subject 5.
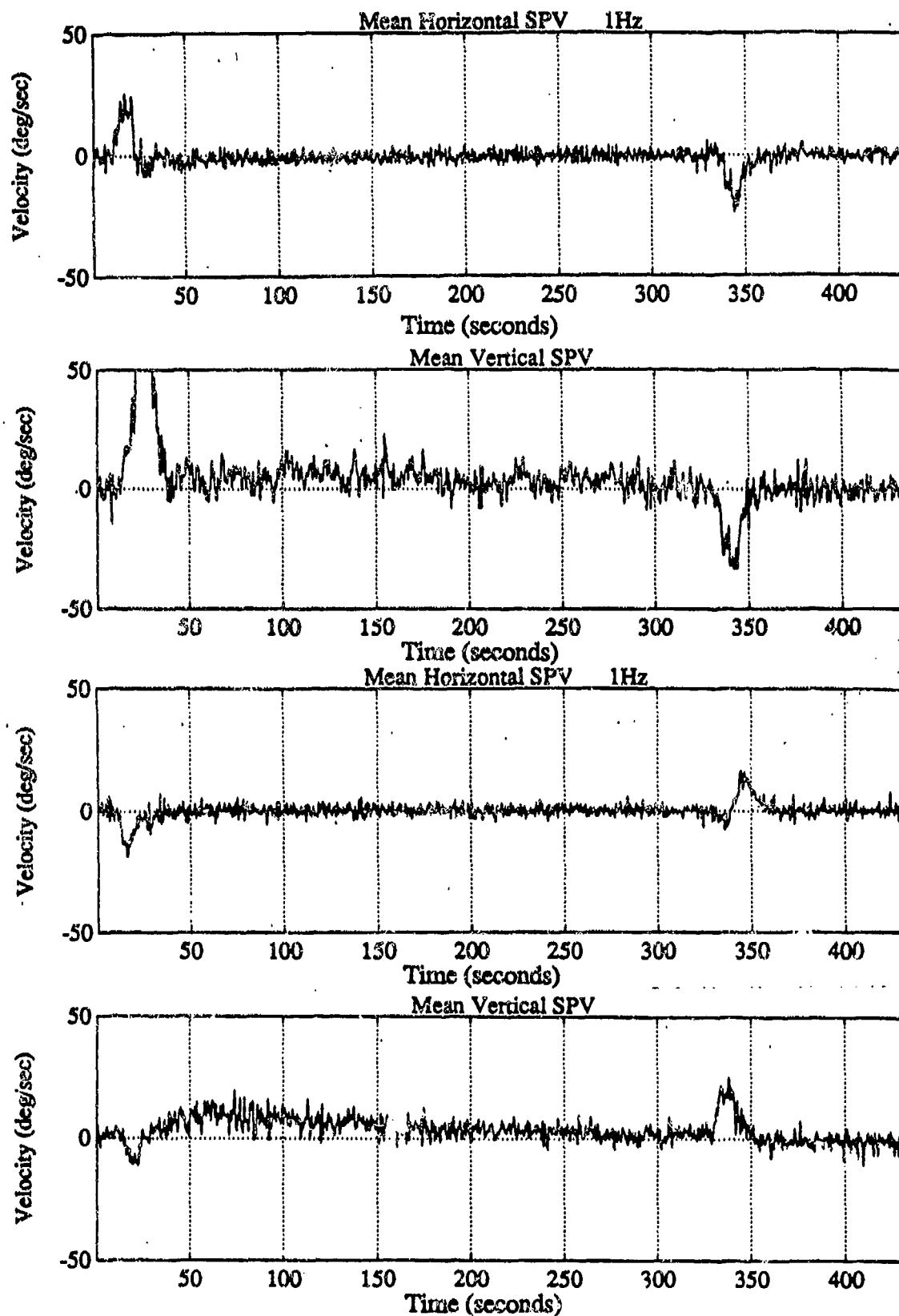
Figure 5.42: Subject 5 Average SPV
a. Clockwise
b. CounterClockwise

130
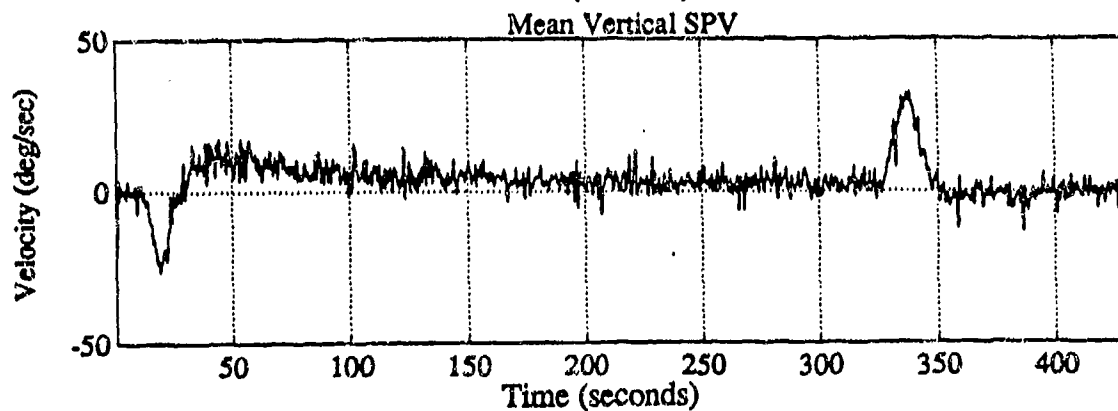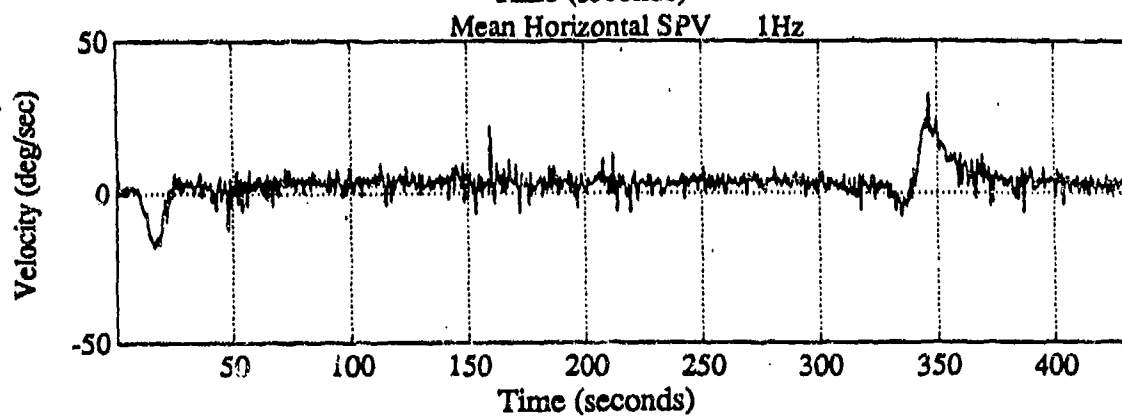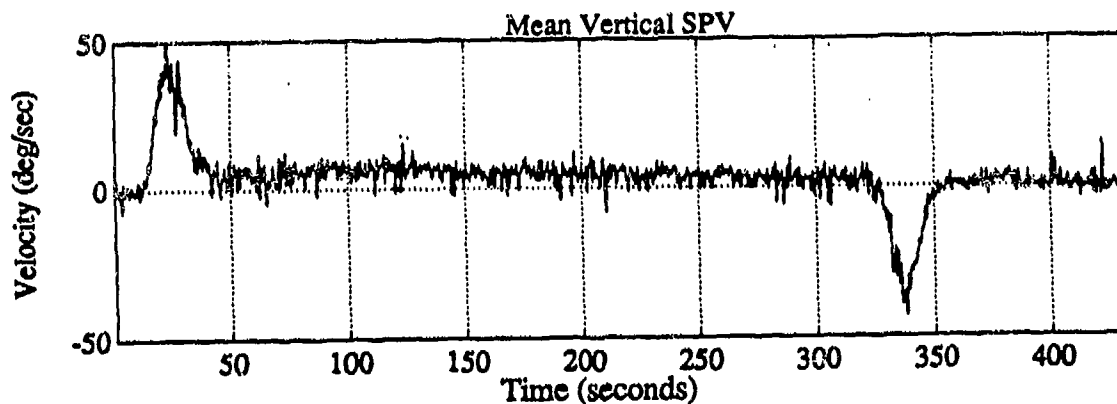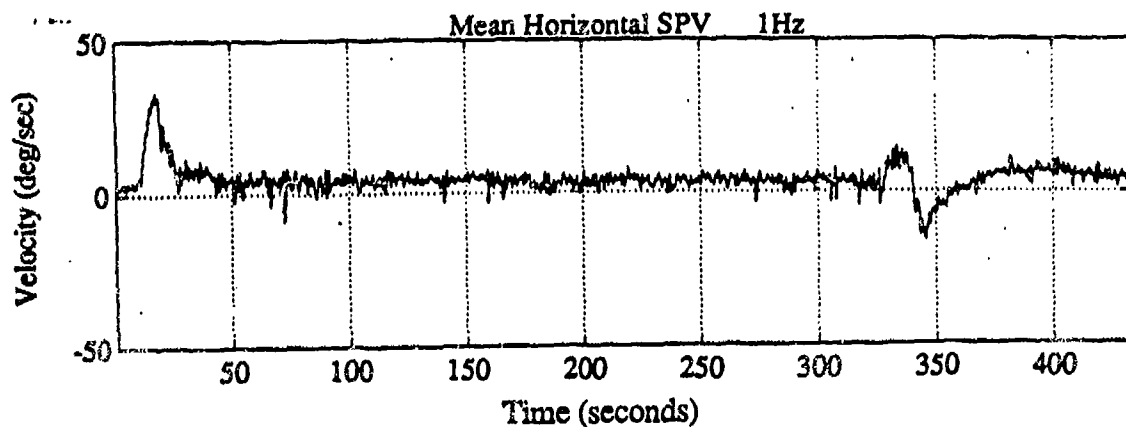
Figure 5.43: Subject 6 Average SPV
a. Clockwise
b. CounterClockwise

131
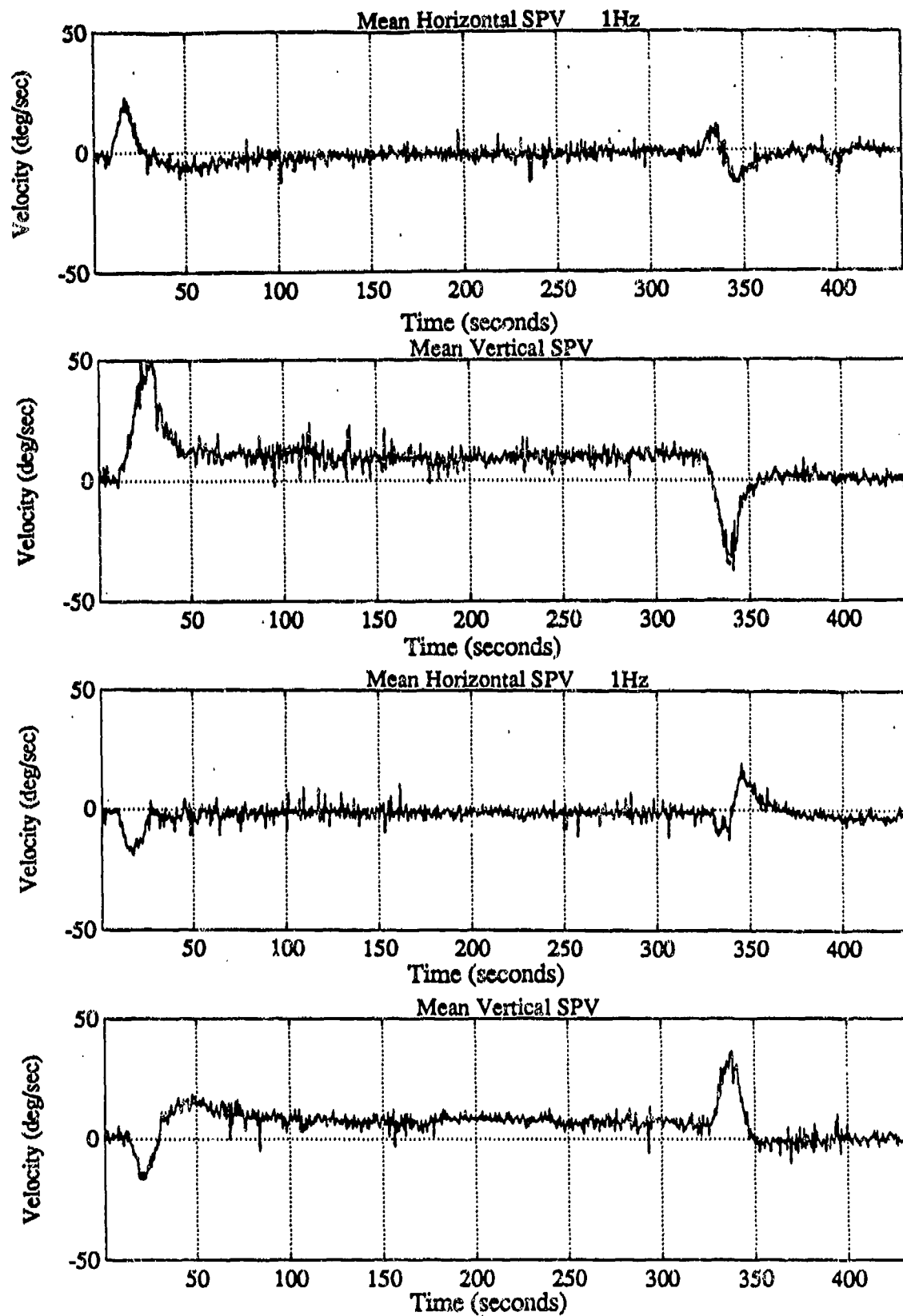
Figure 5.44: Subject 8 Average SPV
a. Clockwise
b. CounterClockwise
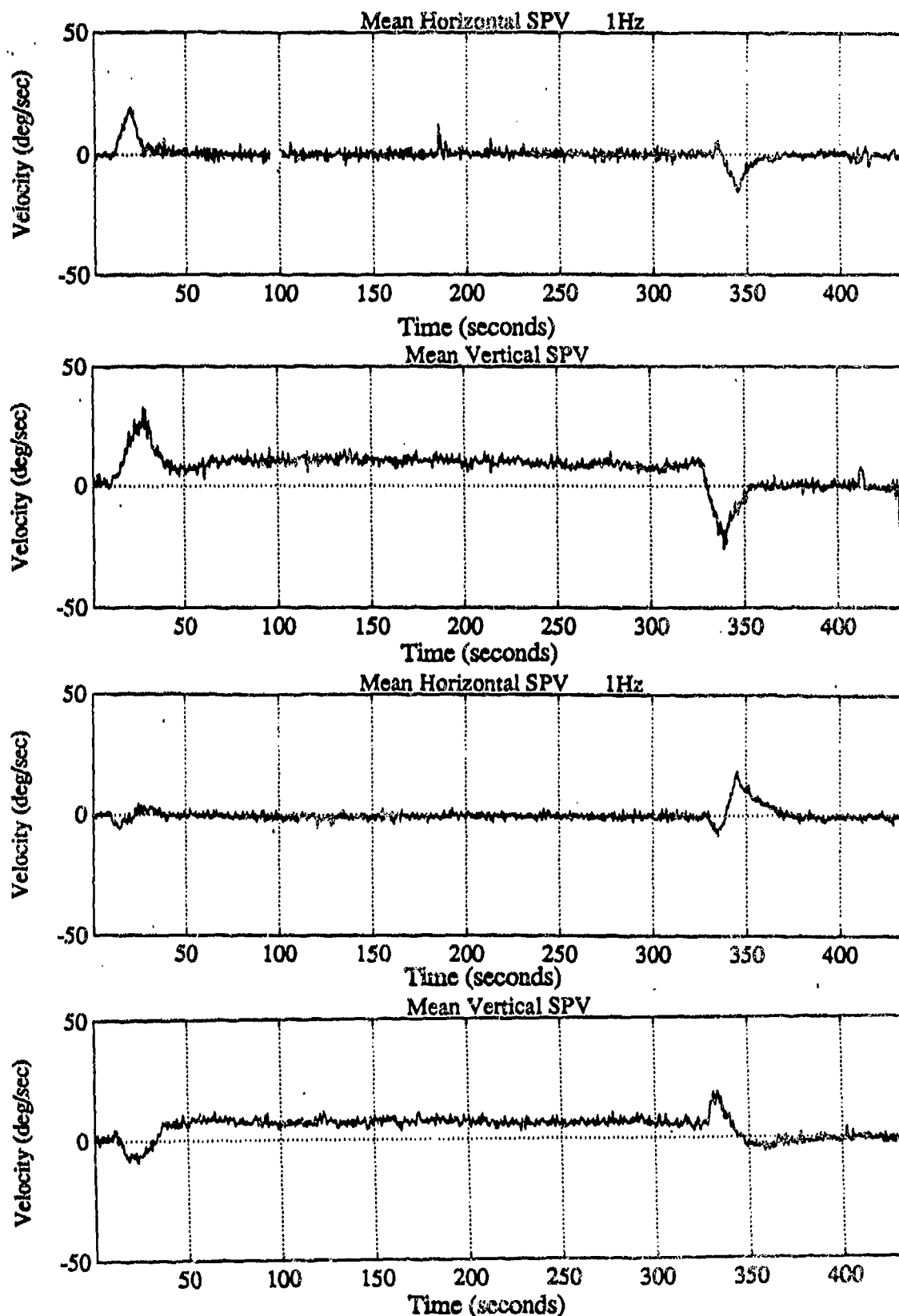
Figure 5.45: Subject 9 Average SPV
a. Clockwise
b. CounterClockwise
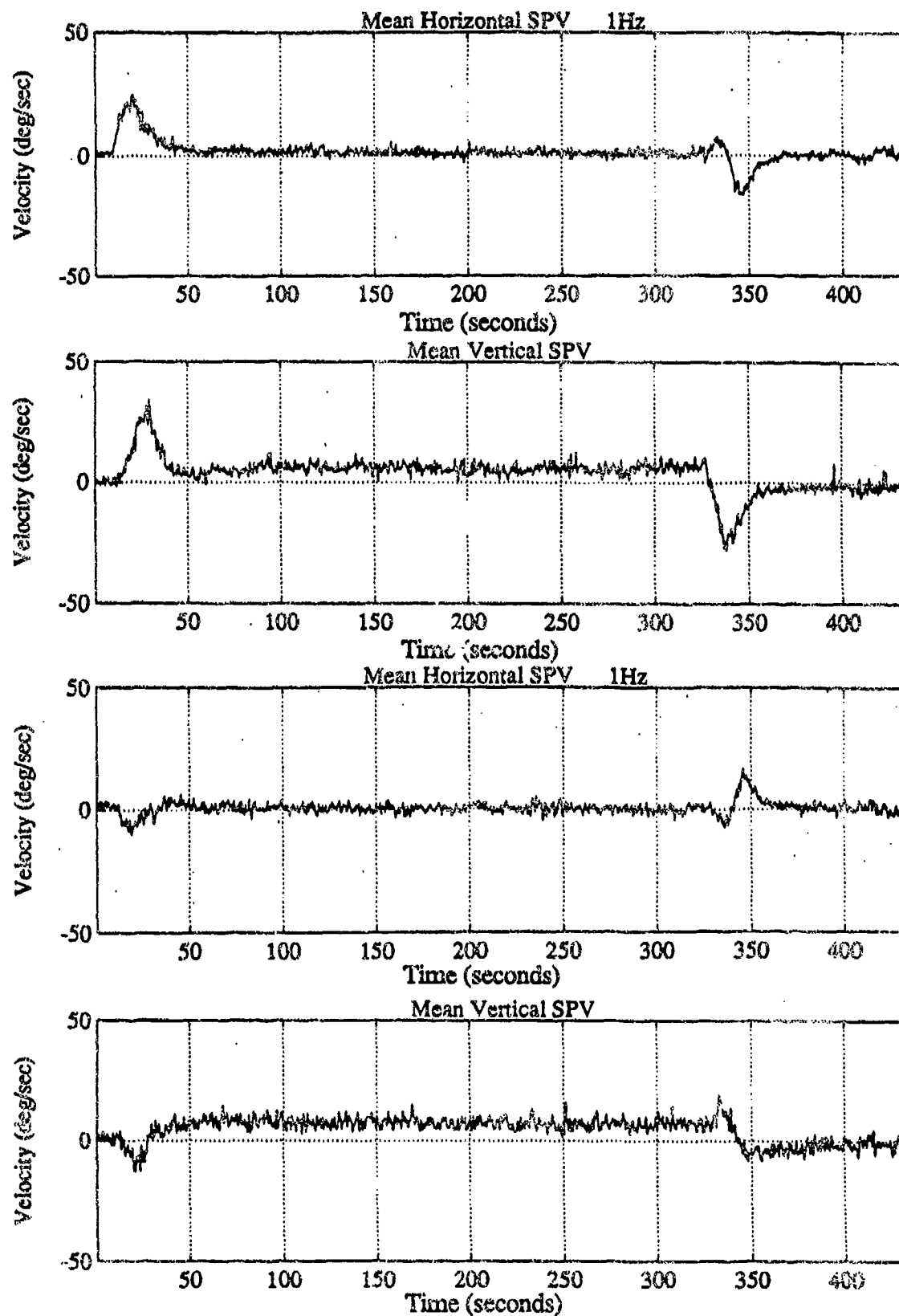
Figure 5.46: Subject 10 Average SPV
a. Clockwise
b. CounterClockwise
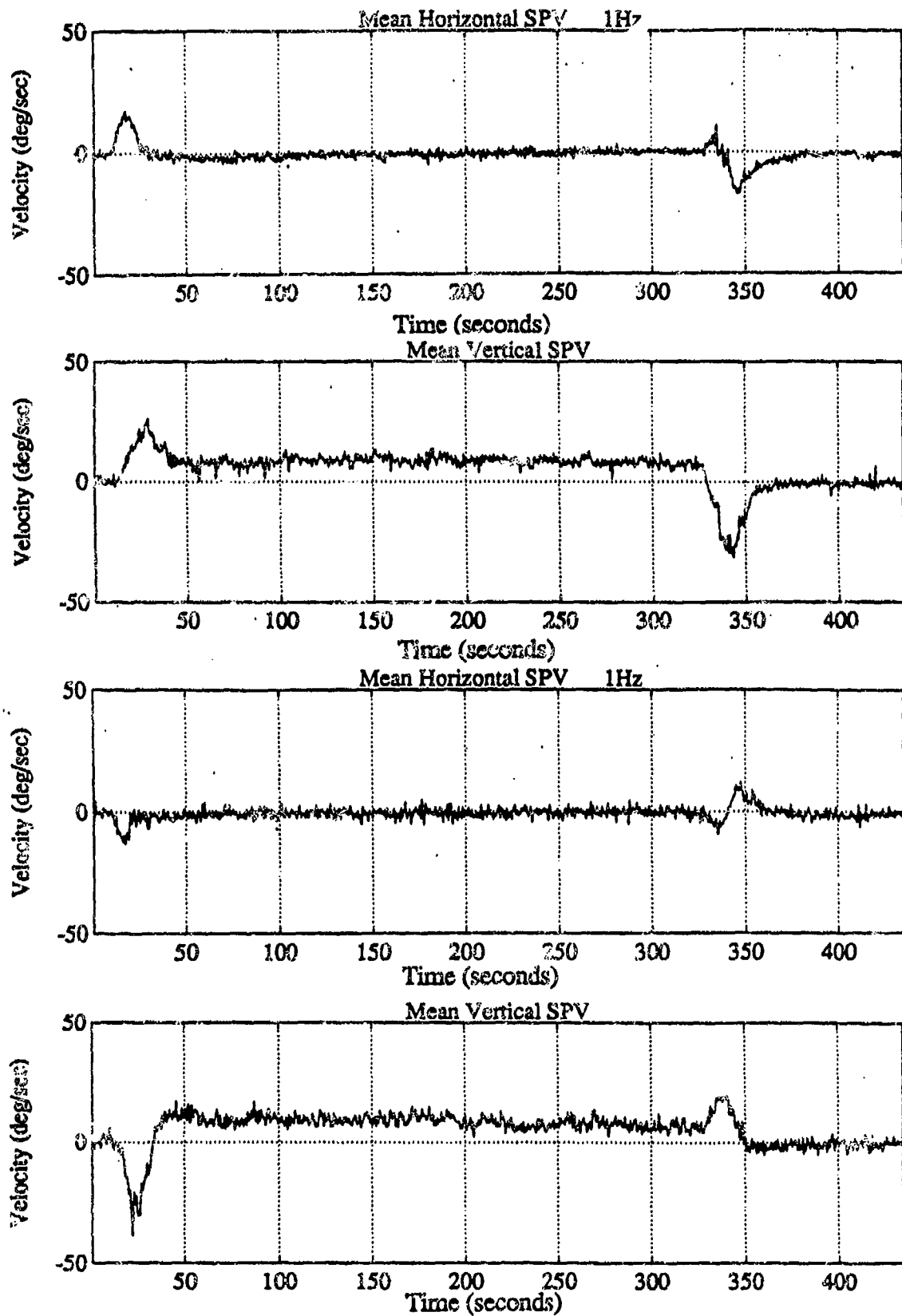
Figure 5.47: Subject 11 Average SPV
a. Clockwise
b. CounterClockwise

135
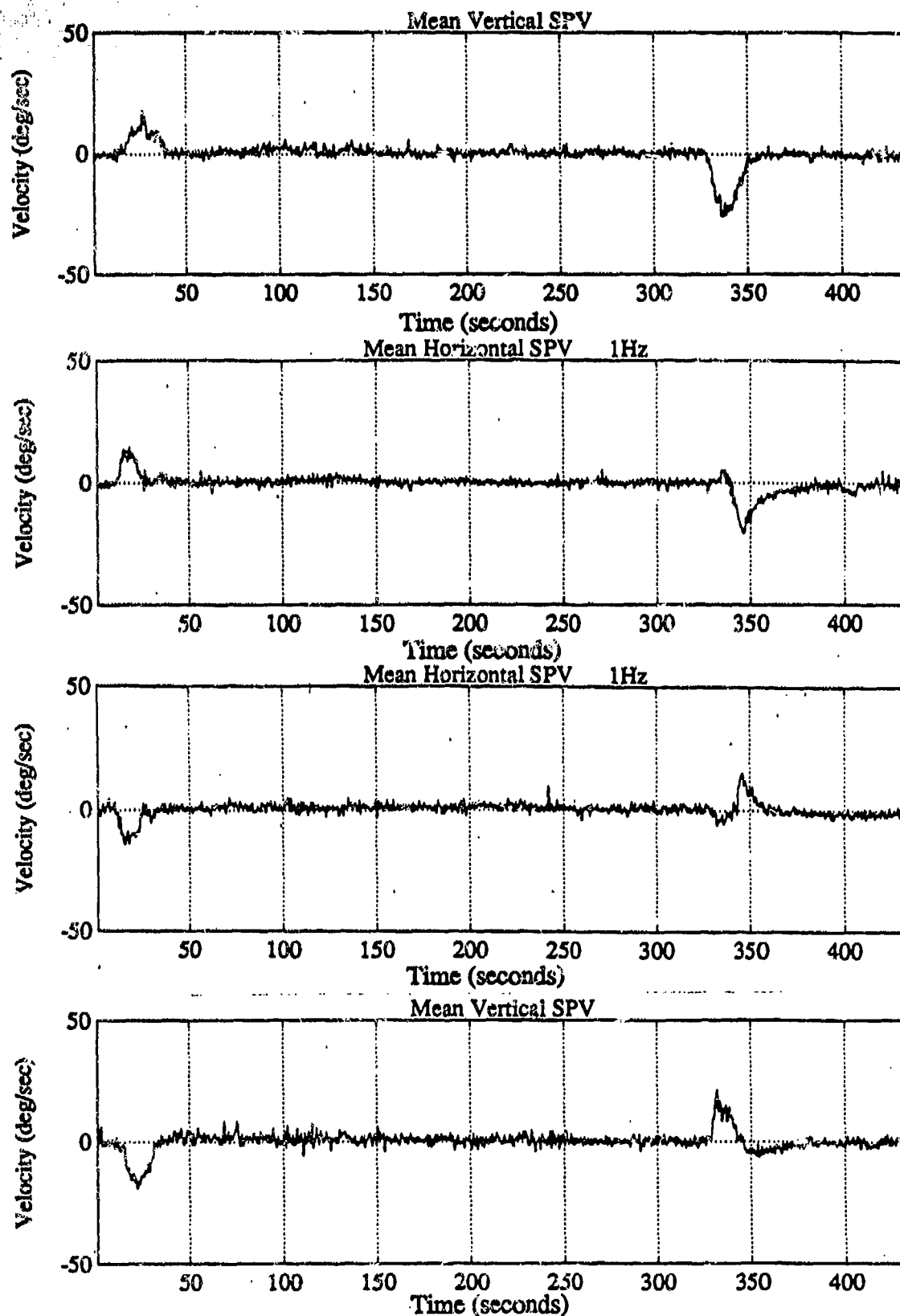
Figure 5.48: Subject 14 Average SPV
a. Clockwise
b. CounterClockwise
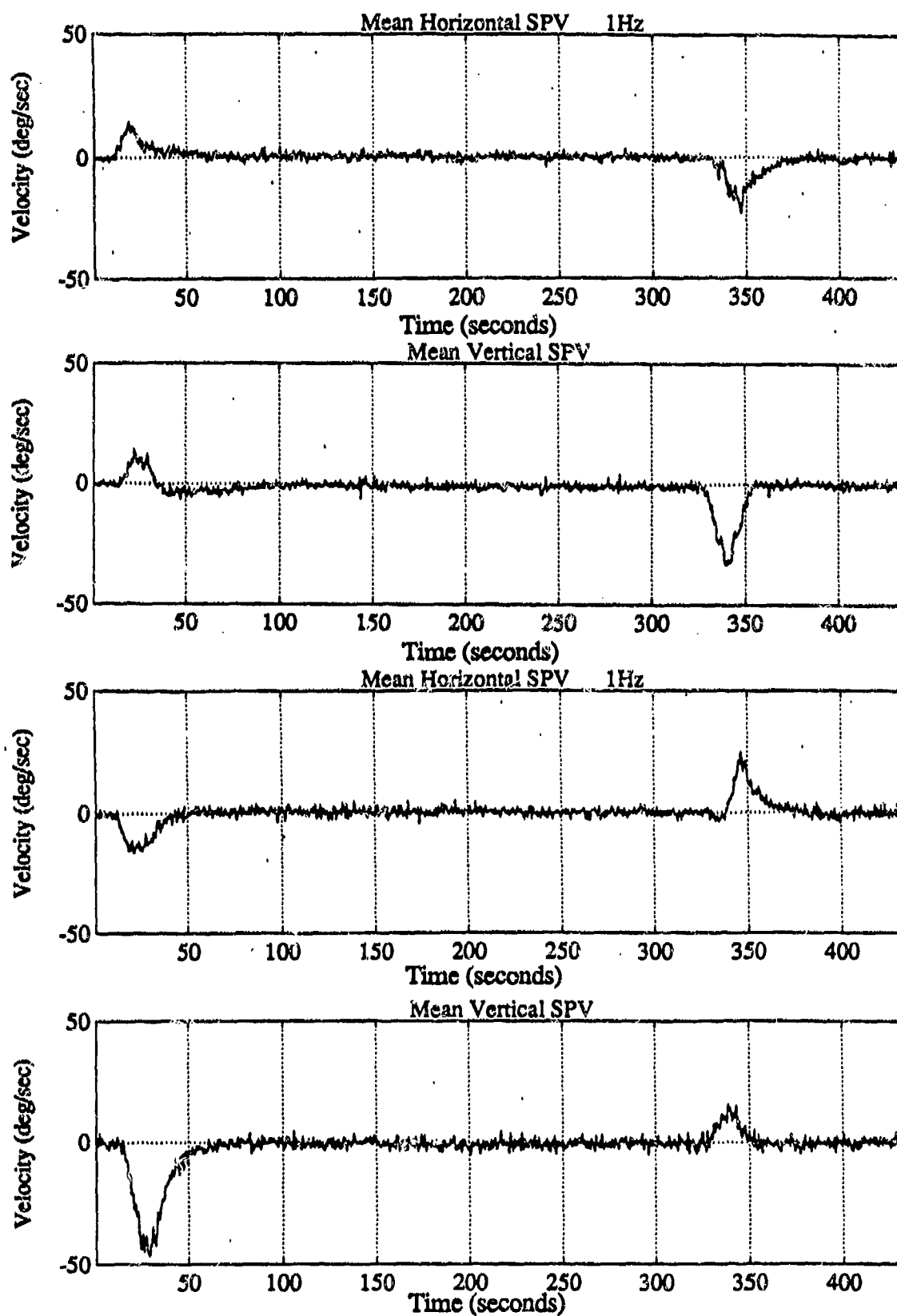
Figure 5.49: Subject 18 Average SPV
a. Clockwise
b. CounterClockwise

137

6. CONCLUSION

Today's high performance aircraft can generate large, prolonged G forces with rapid onset during dive pull outs and banked turns. Centrifuge training is used to expose pilots to large positive G forces to prepare them for their working environment. Vestibular research interest has recently focussed on human oculomotor and perceptual responses, both in centrifuges and maneuvering aircraft. During acceleration and deceleration of a centrifuge, the pendulous cab pivots so that the resultant gravito-inertial force is always directed down with respect to the body.

An experiment was conducted on human subjects to obtain horizontal and vertical eye movement data in the dark during a 3 G_z pendulous chair centrifuge run. During acceleration and deceleration of the centrifuge, the stimulus to the vestibular system is an off-axis, cross-coupled Coriolis stimulation. During the constant velocity stage of the centrifuge run, a constant sustained linear acceleration (G_z) is applied to the vestibular system.

The Coriolis Acceleration Platform (CAP) located at the Naval Aerospace Medical Research Laboratory (NAMRL) was used to generate the 3 G_z environment required. For this experiment, the CAP was configured with a swinging pendulous chair enclosed in a darkened cabin, located 20.5 ft from the center of rotation. Eye movement data was obtained using a commercially available video based technique (ISCAN). ISCAN is a real time, non invasive system that tracks movement of the pupil under infrared illumination. Fifteen US Navy and Marine Pilot candidates awaiting flight training served as subjects. Subjects sat head erect in a pendulous chair. Each subject participated in six $3G_z$ runs

138

unless disqualified due to GLOC or other problems: 3 runs were made facing the direction of motion (clockwise), and 3 runs were made with their back to the motion (counterclockwise). The CAP profile for each run consisted of a constant angular acceleration for 19 secs to a constant velocity of 120°/sec. This generated a 3 G_z force that was sustained for 5 minutes. A constant deceleration for 19 secs completed the run.

The separation of the nystagmus eye movements into slow and fast phase components and calculation of SPV was performed using a Macintosh based, semi-automated analysis package called NysA (Nystagmus Analysis Package). NysA uses the single axis, single pass, acceleration based algorithm (Massoumnia, 1983). Preprocessing of data (calculation of calibration scale factor, prefiltering), postprocessing (manual editing, filtering, decimation, hard copy), and statistical analysis (means, variances) were performed using the data analysis program MatLab for Macintosh (© MathWorks).

Eight subjects completed all six runs, 6 Subjects experienced GLOC, and 1 Subject withdrew due to unrelated illness. Eye movement data from the 8 subjects who completed all six runs without GLOC were analyzed for this study. The relatively high incidence of GLOC is possibly due to the following factors: fear and apprehension of the inexperienced subjects, no training in protective maneuvers, no G-suit, and in one case, fatigue.

Centrifuge acceleration and deceleration produced strong pitch, roll, and yaw sensations attributable to cross coupled vestibular Coriolis stimulation. Subjective pitch amplitude change was consistently greater during deceleration than acceleration, regardless of the direction of centrifuge rotation. Consideration of the stimulus to the vestibular system suggests possible causes of the asymmetry in pitch sensation. During the initial phases of the centrifuge acceleration and deceleration the onset of pitch velocity is greater during deceleration than acceleration. Similarly, the rate of G_z onset is much higher during

139

centrifuge deceleration then acceleration. So even though the cumulative angular velocity stimulus to the pitch canals during centrifuge acceleration or deceleration is equivalent, the temporal nature of the stimulus is different. This temporal difference in pitch canal stimulus may be a factor in the reported pitch amplitude sensation asymmetry. Another significant difference between centrifuge acceleration and deceleration that may explain the asymmetry in pitch sensation, is the magnitude of the linear acceleration in relation to the angular acceleration. At the end of centrifuge acceleration, the pitch angular acceleration stimulus and the linear acceleration stimulus are at a maximum. However, at the end of centrifuge deceleration, the pitch angular acceleration stimulus is a maximum whereas the linear acceleration stimulus is at a minimum. Cohen et al. (1973) in a study of the disorientating effects of aircraft catapult launchings using a centrifuge, demonstrated that large linear acceleration cues limit the perception of angular motion. In this experiment, the linear cues are at a maximum during centrifuge acceleration and may limit the sensation of the pitch angular cues. However, during centrifuge deceleration the linear cues are at a minimum, and the sensation of angular motion may not be attenuated by the linear acceleration, thus generating a greater pitching sensation.

Horizontal and vertical VOR results are consistent with the view that the total VOR response is composed of interacting angular VOR responses and linear VOR responses. An up-beating vertical nystagmus was recorded in 7 of the 8 subjects during the constant velocity phase of the centrifuge run. The magnitude and time course of this LVOR or L_z-nystagmus was subject dependent. At a time where angular VOR responses were expected to have little or no effect on the total VOR response (100 secs), the range of L_z-nystagmus magnitudes was 1 to 21°/sec with a mean of 8°/sec in these 7 subjects. The observed L_z-nystagmus provides evidence that LVOR can be elicited by a constant vertical linear acceleration.

The observed L_z-nystagmus results from this thesis confirm and extend the results obtained by the TNO Institute for Perception in Sosterberg, Holland (Marcus 1989; Marcus and Van Holten, 1990). There were several differences between the present NAMRL study and the TNO research. In the second TNO study, Marcus used EOG to measure vertical eye movements. However, there is some concern in the vestibulo-oculomotor research community about the calibration accuracy of vertical EOG measurements. Vertical EOG calibration characteristics have been shown to be very non-linear (Better et al. 1990), and EOG drift makes accurate measurement of position difficult. Eyelid artifacts are also a potential problem. In pilot studies for this experiment, ISCAN was shown to have linear calibration characteristics in the vertical direction. ISCAN is considered to give a more accurate indication of the eye position and hence the eye velocity. Also, the present NAMRL experiment involved multiple runs in each direction, while Marcus used one run in each direction. The present study demonstrated that L_z-nystagmus measures were a consistent characteristic for each subject. Analysis of horizontal and vertical SPV profiles showed that responses during the first run in a given direction were significantly different than the two subsequent runs in that direction. The present study also ran the subjects for a longer duration, showing that the L_z-nystagmus remained constant for some subjects and decayed for others.

Vertical SPV onset during centrifuge deceleration was faster than centrifuge acceleration. This result may play a role in the reported difference in pitch subjective sensations. The peak vertical SPV magnitude was found not to be an indicator of the asymmetry in pitch subjective sensations. Analysis of horizontal and vertical SPV profiles showed that responses during the first run in a given direction were significantly different than the two subsequent runs. Average SPV response profiles were computed for each of the 8 subjects for the 2nd and 3rd runs in each direction.

For at least four and possibly six of the eight subjects, the horizontal peak SPV magnitude during centrifuge acceleration was significantly greater when the subject faced the motion (CW run) as compared to when the subject had his back to the motion (CCW). Subjects with weak horizontal linear VOR also had weak vertical linear VOR. The addition of a transient linear VOR response is the most likely explanation for this result. The source of the horizontal linear force generating this horizontal LVOR is unknown, but plausibly may be due to small head motion. The addition of chair fixed accelerometers and securing the head in future experiments will provide insight into the nature of this phenomenon.

6.1 RECOMMENDATIONS

Further analysis of the current data set is recommended to improve our understanding of the vestibular response during high G centrifuge runs. Possible analyses include:

- ANOVA on L_z nystagmus data sets (V_B V_C V_D) to determine statistically whether L_z nystagmus is a personal, stable characteristic over 3 runs.

- For modelling purposes, calculate population mean for run 1 and population mean for runs 2 and 3. However, see Section 5.5 caveats.

- Analyze data from the subjects who experienced GLOC. Is there a correlation between GLOC and L_z nystagmus ?

- Add CW and CCW data to obtain estimate of "pure" L_z nystagmus. Compare with Marcus and Van Holten (1990) results. Results may show the problems associated with interpretations based on the linear approach.

142

Possible future experiments to increase the available data on the vestibular response during high G centrifuge runs include:

- Studies examining the effects of head position on L_z nystagmus.

- Single run screening of large population in order to find subjects who have large L_z nystagmus sensitivity. Follow up studies on these individuals to determine repeatability and origin of this characteristic. The rationale for this stems from the results of a pilot experiment where one subject displayed very high L_z nystagmus (>100°/secs). If some people have high L_z nystagmus sensitivity, potential operational problems arise. When experiencing high G's in the light, some aviators may have difficulty suppressing the L_z nystagmus, and hence may have impaired vision.

- Test L_z nystagmus sensitivity of very experienced fighter pilots.

- Effects of higher and lower G levels on total VOR response. How does L_z nystagmus scale with G ?

- Experiments conducted with the chair fixed. Either a repeat of Lansberg et al. (1965) experiments, or pre-tilting the pendulous chair to the angle required to align the subjects z-axis with the gravito-inertial force. Lansberg conducted experiments where the angular velocity of the body was maintained constant and the effect of linear acceleration was investigated. Subjects were placed in different orientations relative to the linear acceleration. The experiments involving pre-tilting of the chair will remove the cross-coupled Coriolis stimulus during centrifuge acceleration and deceleration. These experiments may provide further insight into the nature of the L_z nystagmus.

APPENDIX A

INFRARED (IR) LIGHT SOURCE
SAFETY STANDARDS

Prepared by: B.McGrath
and Ens. D. McKenna U.S.N.

ISCAN ILLUMINATOR SOURCE
-INFRARED SAFETY

To obtain the best results from ISCAN, it is desirable to operate the system with the brightest possible illumination sour·e. The illumination source is designed to provide good illumination, yet be entirely safe for subjects. Therefore, the establishment of safe levels of IR exposure to the human eye is essential. For the illuminators used in the ISCAN helmet, the IR band extended from 760-1400nm. The greatest safety concern of devices employing near IR radiation (700-1400 nm) are possible effects upon the lens of the eye (cataractogenesis) and the possibility of retinal injury. Hazard levels quoted below are from Sliney and Freasier (1973).

Occupational safety and health administration (OSHA) has established values that represent conditions to which it is believed individuals may be exposed to without adverse effects. These standards are for distant or collimated sources, where an important danger is that the image of the source might be focused on the retina. Because the IR source device is located close to the eye (approximately one cm) the illuminator image cannot be brought into focus on the retina; instead, it floods the retina with a diffuse beam.

The IR levels of the illuminator source were measured with a United Detector Technology Model 360 Autoranging Optometer and a Radiometric Filter Model 115-1. The maximum recorded level was approximately 0.3 mW/cm^2, and in the normal eye position the value never exceeded 0.1 mW/cm^2.

These theoretical and measured values are well below OSHA's figure for safe levels of near IR radiation of the lens (10 mW/cm^2). In regard to thermal injury, a retinal exposure of 1.2 mW/cm^2 of 940 nm light is the equivalent of .06 cd/cm^2 of white light . According to OSHA recommendations, white light of less than 1 cd/cm^2 may be regarded as safe and the hazard of IR light is less by an order of magnitude.

Appendix B

LABTECH NOTEBOOK
DATA ACQUISITION SET-UP

Ch.	Channel Name	Channel Type	Interface Device	Interface Channel	Schedule Name	Duration, sec.	Rate, Hz	File Name
1	Hori	DI	DT2211-PG	0	Iscan	1000	60	data1.prn
2	Vert	DI	DT2211-PG	1	Iscan	1000	60	data2.prn
3	Tach	AD	DT2211-PG	0	Iscan	1000	60	data3.prn
4	Button	AD	DT2211-PG	1	Iscan	1000	60	
5	Horiz_ca	AD	DT2211-PG	2	Iscan	1000	60	hori.prn
6	Vert_cal	AD	DT2211-PG	3	Iscan	1000	60	vert.prn

148

APPENDIX C

CONVERT

LabTech NoteBook Format
to
MatLab Format

Code by: D. Balkwill and B. McGrath

```c
#include <stdio.h>
#include <fcntl.h>
#include <unix.h>

#define BLOCKSIZE 16384

char in_buffer[BLOCKSIZE];
int in_handle;
char in_filename[81];
int num_bytes;

FILE *out_fptr;
char out_filename[81];
int out_handle;

typedef struct {
    long type;
    long mrows;
    long ncols;
    long imagf;
    long namlen;
    } Fmatrix;

main()
{
    int i,j,k;
    Fmatrix x;
    long mrows = 0;

    do {
        printf("Enter input file name:");
        gets(in_filename);
        in_handle = open(in_filename,O_BINARY|O_RDONLY);
        }
    while (in_handle <= 0);

    do {
        printf("Enter output file name:");
        gets(out_filename);
        out_fptr = fopen(out_filename,"wt+");
        }
    while (out_fptr == 0);

    num_bytes = read(in_handle,in_buffer,BLOCKSIZE);
    while (num_bytes > 0) {
        mrows += num_bytes;
        num_bytes = read(in_handle,in_buffer,BLOCKSIZE);
        }

    mrows /= 2;   /* two bytes per sample */
    close(in_handle);

    x.type = 1040;
```

```
x.mrows = mrows;
x.ncols = 1;
x.imagf = 0;
x.namlen = strlen(out_filename) + 1;
fwrite(&x,sizeof(Fmatrix),1,out_fptr);
fwrite(out_filename,sizeof(char),(int)x.namlen,out_fptr);
fclose(out_fptr);

out_handle = open(out_filename,O_BINARY|O_RDWR|O_APPEND);

in_handle = open(in_filename,O_BINARY|O_RDONLY);
num_bytes = read(in_handle,in_buffer,BLOCKSIZE);
while (num_bytes > 0) {
    write(out_handle,in_buffer,num_bytes);
    num_bytes = read(in_handle,in_buffer,BLOCKSIZE);
    }
close(in_handle);
close(out_handle);

printf("Conversion has finished");
}
```

APPENDIX D

MATLAB PREPROCESS
SCRIPTS

-Load Data
-Cal Hori
-Cal Vert
-Prepare

```
%LOAD_DATA: Load Eye Position and Tach Files

%B.McGrath  2 May 1990

su = input('ENTER SUBJECT NUMBER       ');
ru = input('ENTER RUN NUMBER        ');

cu = input('ENTER CALIBRATION DISTANCE        ');

eval(['load Hori',int2str(su),int2str(ru)])
eval(['load Vert',int2str(su),int2str(ru)])
eval (['hpos = Hori',int2str(su),int2str(ru),';'])
eval (['vpos = Vert',int2str(su),int2str(ru),';'])

eval (['clear Hori',int2str(su),int2str(ru)])
eval (['clear Vert',int2str(su),int2str(ru)])

eval(['load Tach',int2str(su),int2str(ru)])
eval (['tach = Tach',int2str(su),int2str(ru),';'])
eval (['clear Tach',int2str(su),int2str(ru),])
```

```
%CAL_HORI:   Calculates horizontal calibration factor for use
%in NysA. Calls script CAL which implements a 2pt calibration
%analysis that requires user input to define +/- target sets

%B.McGrath  2 May 1990

fu = 'Horizontal';
fus = 'h';
subplot(111)
axis([1 2 3 4]);axis;
plot (hpos), title(['MIT',int2str(su),int2str(ru),' ',fu,' Eye Position'])
fprintf('\nHORIZONTAL CALIBRATION\n')
cal

fprintf('\n\nHORIZONTAL CALIBRATION FACTOR = %4.4f\n',caln)
pause

clear caln fu fus
clear pos
```

154

```
%CAL_VERT:   Calculates vertical calibration factor for use
%in NysA. Calls MatLab script CAL which implements a 2pt calibration
%analysis that requires user input to define +/- target sets

%B.McGrath  2 May 1990

fu = 'Vertical';
fus = 'v';
subplot(111)
axis([1 2 3 4]);axis;
plot (vpos), title(['MIT',int2str(su),int2str(ru),' ',fu,' Eye Position'])
fprintf('\nVERTICAL CALIBRATION\n')

cal

fprintf('\n\nVERTICAL CALIBRATION FACTOR = %4.4f\n',caln)
pause
clear caln fu fus
```

```
%CAL:   2 pt Calibration Procedure for use with cal_hori and
%       cal_vert;
% CAL displays data file; user identifies segment where two
% point calibration was performed before and after the run.

% Then displays the before eye position data & crosshairs and
%       waits for user to identify time intervals where eye is stable
%       on positive target postion.
% Several such intervals can be identified.
% Eye position in these intervals is averaged
% Program expects and even number of mouse clicks.
% Script next asks user to similarly identify negative target data
% intervals.

%Repeat for calibartion after run

%Script then computes the Calibration Scale Factor (deg/unit) by averaging
%before and after results.

%B.McGrath  2 May 1990

fprintf('\nSelect Calibration Range Before Run\n')

[xcal,ycal] = ginput(2);
x1 = round(xcal(1));
x2 = round(xcal(2));

fprintf('\n\nSelect Calibration Range After Run\n')

[xc,yc] = ginput(2);
x3 = round(xc(1));
x4 = round(xc(2));

if fus == 'h'
        pos = hpos;
else
        pos = vpos;
end

bpos = pos(x1:x2);
apos = pos(x3:x4);
error = 5;

clear pos
bl = length(bpos);
axis_top = round(1.2*max(bpos));
axis_bottom = round(0.8*min(bpos));
axis_begin = [1,bl,axis_bottom,axis_top];

v1 = [1:bl];
clg
```

```
axis(axis_begin), plot(v1,bpos),grid,
title(['MIT ',int2str(su),int2str(ru),' Calibration Before Run'])

clear xcal ycal

fprintf('\nSelect Max Values of Calibration\n')
[xcal,ycal] = ginput;
x = round(xcal);
n = length (x);

clear y_max

for i = 1:2:n-1;
        trash = bpos(x(i):x(i+1));
        y_max = [y_max trash'];
end

upper_y_cal = mean(y_max);
cal_max = upper_y_cal*ones(1:bl);
clear xcal ycal

fprintf('\n\nSelect Min Values of Calibration\n')
[xcal,ycal] = ginput;
x_min = round(xcal);
m = length (x_min);

% if m = n continue else

clear y_min

for i = 1:2:m-1;
        y_min = [y_min bpos(x_min(i):x_min(i+1))'];
end

lower_y_cal = mean(y_min);
cal_min = lower_y_cal*ones(x1:x2);
plot (v1,cal_min,'--g',v1,cal_max,'--g',v1,bpos)
title(['MIT ',int2str(su),int2str(ru),' Calibration Before Run'])

pause
calibration_before = upper_y_cal - lower_y_cal;

clear x_min x_max upper_y_cal lower_y_cal
clear trash y_min y_max xcal ycal x axis_top axis_bottom bl

al = length(apos);
axis_top = round(1.2*max(apos));
axis_bottom = round(0.8*min(apos));
axis_after = [1,al,axis_bottom,axis_top];

v2 = [1:al];
clg

axis(axis_after), plot(v2,apos), grid,
```

```
title(['MIT ',int2str(su),int2str(ru),' Calibration After Run'])


clear xcal ycal xc yc

fprintf('\nSelect Max Values of Calibration\n')
[xcal,ycal] = ginput;
x = round(xcal);
n = length (x);

% if n is odd exit
clear y_max

for i = 1:2:n-1;
        trash = apos(x(i):x(i+1));
        y_max = [y_max trash'];
end

upper_y_cal = mean(y_max);
cal_max_after = upper_y_cal*ones(x3:x4);


clear xcal ycal
fprintf('\n\nSelect Min Values of Calibration\n')
[xcal,ycal] = ginput;
x_min = round(xcal);
m = length (x_min);

% if m = n continue else

clear y_min

for i = 1:2:m-1;
        y_min = [y_min apos(x_min(i):x_min(i+1))'];
end

lower_y_cal = mean(y_min);
cal_min_after = lower_y_cal*ones(x3:x4);
plot (v2,cal_min_after,'--g',v2,cal_max_after,'--g',v2,apos)
title(['MIT ',int2str(su),int2str(ru),' Calibration After Run'])

pause

subplot(211),axis(axis_begin)
plot (v1,cal_min,'--g',v1,cal_max,'--g',v1,bpos)
title(['MIT ',int2str(su),int2str(ru),' Calibration Before Run'])

subplot(212),axis(axis_after)
plot (v2,cal_min_after,'--g',v2,cal_max_after,'--g',v2,apos)
title(['MIT ',int2str(su),int2str(ru),' Calibration After Run'])

calibration_after = upper_y_cal - lower_y_cal;

fprintf('\ncalibration_before = %4.2f\n',calibration_before)
```

158

```
fprintf('calibration_after = %4.2f\n',calibration_after)

if (abs(calibration_before-calibration_after) > error)
        fprintf(' **WARNING, CALIBRATION DIFFERENCE IS LARGE** \n')
end

theta_rad = 2*(atan(11/cu));
theta_deg = theta_rad * (180/pi);
caln = theta_deg/((calibration_before + calibration_after)/2);

pause

clear  theta_rad theta_deg
clear x_min x_max cal_min_after cal_max_after cal_min cal_max
clear trash y_min y_max x xcal ycal calibration_before
clear calibration_after lower_y_cal upper_y_cal axis_after axis_before
clear x1 x2 v1 v2 o f axis_top axis_bottom al bl bpos apos
```

```
%PREPARE:   Prepare position data for analysis by NysA
%This script plots the tach and asks the user to identify the
%start of the acceleration and end of the decceleration.
%Script saves position and tach data 10secs before the start
%of acceleration to 90secs after deccelaration.

%B.McGrath  2 May 1990

axis([1 2 3 4]);axis;
subplot(111);

plot(tach), title(['MIT-',int2str(su),int2str(ru),' Tach'])
grid

fprintf('\n\nSelect Beginning and End of Acceleration \n')
[x,y] = ginput(2);
z = round(x);
z(1) = z(1) - 600;
z(2) = z(2) + 5400;

tach = tach(z(1):z(2));
hpos = -1*hpos(z(1):z(2));
vpos = vpos(z(1):z(2));

plot(tach), title(['MIT-',int2str(su),int2str(ru),' Tach'])
grid

eval(['save  MIT-',int2str(su),int2str(ru),'TACH tach'])
clear tach

l = length(hpos);
fprintf('\nlength of data file = %4.2f \n',l)

eval (['save horiposition',int2str(su),int2str(ru),' hpos'])
eval (['save vertposition',int2str(su),int2str(ru),' vpos'])
clear vpos x y hpos z x3 x4 i l m n axis_begin
```

APPENDIX E

MATLAB POSTPROCESS
SCRIPTS

-XSpike
-XMistake
-XReSpike
-Decimate10
-Decimate3
-SubjectMean

```
%XSPIKE:   Manual Editing of NysA SPV Plot
%This script loads NysA SlowPhaseVelocity, NysA RawVelocity
%and Position Files for removal of spikes from SPV data.
%SPV is stripped using a straight line interpolation method.

%B.McGrath  2 May 1990

clg
clear

su = input ('ENTER SUBJECT NUMBER      ');
ru = input('ENTER RUN NUMBER       ');
fu = input('ENTER AXIS        ','s');

%Load position file "vertposition(subject nos.)(run nos.)"
if fu == 'v'
        fu = 'Vertical';
        eval(['load vertposition',int2str(su),int2str(ru)])
        pos = vpos-60;
        clear vpos

%Load position file "horiposition(subject nos.)(run nos.)"
else
        fu = 'Horizontal';
        eval(['load horiposition',int2str(su),int2str(ru)])
        pos = hpos+180;
        clear hpos
end

%Load SPV file  "SlowPhaseVelocity" (note: Default NysA name)
eval (['load SlowPhaseVelocity'])
spv = DATA;
clear DATA

%Load eye velocity file  "EyeVelocity" (note: Default NysA name)
eval (['load EyeVelocity'])
vel = DATA;
clear DATA

spv_1 = spv;

%Plot SPV data and zoom to region of interest
q= 'p';
while q == 'p'

        axis([1 2 3 4]);axis;
        plot (spv_1)
        grid

        fprintf('\n\nSelect Section of Data To Be Edited\n')

        [xplot,yplot] = ginput(2);
```

162

```
                x1 = round(xplot(1));
                x2 = round(xplot(2));


            · q='s';
                while q == 's'

                        clg

                        top = round(1.2*max(spv_1(x1:x2)));
                        bottom = round(1.2*min(spv_1(x1:x2)));
                        a = [x1,x2,bottom,top];
                        axis(a)
                        v = [x1:x2];
                        plot   (v,spv_1(x1:x2),'w.') ·

                        fprintf('\n\nSelect Range of Data Spike(s) To Be Removed\n')
                        [xpl,ypl] = ginput(2);
                        x5 = round(xpl(1));
                        x6 = round(xpl(2));

                        clg
                        a1 = [x5,x6,-100,100];
                        axis(a1)
                        v1 = [x5:x6];

%Plot SPV, raw eye velocity and position, to allow user to identify artifacts.
                        plot   (v1,spv_1(x5:x6),'w',v1,vel(x5:x6),'r',v1,pos(x5:x6),'g-')

                        q = 'e';
                        while q == 'e'
                                fprintf('\n\nSelect Data Points To Be Connected\n')
                                [x,y_coord] = ginput;
                                x = round(x);
                                n = length (x);

%Replace selected SPV data with a linear line
                                for i = 1:2:n

                                        diff = x(i+1) - x(i);
                                        y = spv_1(x(i+1))-spv_1(x(i));
                                        m = y / diff;
                                        for j = 1:diff-1
                                                spv_1(x(i) + j) = spv_1(x(i)) + (j*m);
                                        end
                                clear diff y m
                                end
                                plot   (v1,spv_1(x5:x6),'w.')


                                q = input ('Complete Plot, Section or Edit      ','s');
                        end
                end
end
```

```
clear v1 v xplot yplot xpl ypl m n o q x1 x2 x3 x4 x5 x6

%Save data and plot results if required

save_data
```

```matlab
%XMISTAKE: This script is used to restart XSPIKE if an error
%is made whilst editing SPV data.

%B.McGrath  2 May 1990

q= 'p';
while q == 'p'

        axis([1 2 3 4]);axis;
        plot (spv_1)
        grid

        fprintf('\n\nSelect Section of Data To Be Edited\n')

        [xplot,yplot] = ginput(2);
        x1 = round(xplot(1));
        x2 = round(xplot(2));

        q='s';
        while q == 's'

                clg

                top = round(1.2*max(spv_1(x1:x2)));
                bottom = round(1.2*min(spv_1(x1:x2)));
                a = [x1,x2,bottom,top];
                axis(a)
                v = [x1:x2];
                plot  (v,spv_1(x1:x2),'w.')

                fprintf('\n\nSelect Range of Data Spike(s) To Be Removed\n')
                [xpl,ypl] = ginput(2);
                x5 = round(xpl(1));
                x6 = round(xpl(2));

                clg
                a1 = [x5,x6,-100,100];
                axis(a1)
                v1 = [x5:x6];
                plot  (v1,spv_1(x5:x6),'w',v1,vel(x5:x6),'r',v1,pos(x5:x6),'g-')

                q = 'e';
                while q == 'e'
                        fprintf('\n\nSelect Data Points To Be Connected\n')
                        [x,y_coord] = ginput;
                        x = round(x);
                        n = length (x);

                        for i = 1:2:n

                                diff = x(i+1) - x(i);
                                y = spv_1(x(i+1))-spv_1(x(i));
```

165

```
                        m = y / diff;
                        for j = 1:diff-1
                                spv_1(x(i) + j) = spv_1(x(i)) + (j*m);
                        end
                clear diff y m
                end
                plot   (v1,spv_1(x5:x6),'w')


                q = input ('Complete Plot, Section or Edit      ','s');
        end
    end
end

%Save data and plot results if required
save_data
```

```
%SAVE_DATA:  Saves Eye Velocity, SPV NysA and SPV Edit data
%in Matlab Files. Also plots SPV NysA and SPV Edit data if required.

%B.McGrath  2 May 1990

u = length(spv_1);

time = [1:u];
time = time/60;
w = u/60;
vel = vel(1:u);
clg

eval(['save MIT-',int2str(su),int2str(ru),fu,'VEL vel'])
clear vel
eval(['save  MIT-',int2str(su),int2str(ru),fu,'SPV_M spv'])
eval(['save  MIT-',int2str(su),int2str(ru),fu,'SPV_F spv_1'])

zxs = input('DO YOU WANT TO SEE SPV PLOTS      ','s');

if zxs =='y'
        axis ([1 w -50 50])
        subplot(211),  grid, plot (time,spv)
        title(['MIT-',int2str(su),int2str(ru),' ',fu,' SPV-NysA'])
        xlabel('Time (sec)'),ylabel('Velocity (deg/sec)')

        clear spv

        axis ([1 w -50 50])
        subplot(212),  grid, plot (time,spv_1)
        title(['MIT-',int2str(su),int2str(ru),' ',fu,' Slow Phase Velocity'])
        ylabel('Velocity (deg/sec)')

end
clear
```

```
%XRESPIKE:    Manual Editing of SPV Plot.
% This program removes spikes from SPV plots that have already
%been analysed using XSPIKE. It functions in the same manner as
%XSPIKE.

%B.McGrath  2 May 1990

clear
clg

su = input ('ENTER SUBJECT NUMBER        ');
ru = input('ENTER RUN NUMBER         ');
fu = input('ENTER AXIS        ','s');

if fu == 'v'
        fu = 'Vertical';
        eval(['load vertposition',int2str(su),int2str(ru)])

        %Rescale position data to approx velocity
        pos = vpos-60;
        clear vpos
else
        fu = 'Horizontal';
        eval(['load horiposition',int2str(su),int2str(ru)])

        %Rescale position data to approx velocity
        pos = hpos+180;
        clear hpos
end

eval(['load MIT-',int2str(su),int2str(ru),fu,'VEL'])
eval(['load MIT-',int2str(su),int2str(ru),fu,'SPV_F'])

q= 'p';
while q == 'p'

        axis([1 2 3 4]);axis;
        plot (spv_1)
        grid

        fprintf('\n\nSelect Section of Data To Be Edited\n')

        [xplot,yplot] = ginput(2);
        x1 = round(xplot(1));
        x2 = round(xplot(2));

        q='s';
        while q == 's'

                clg

                top = round(1.2*max(spv_1(x1:x2)));
                bottom = round(1.2*min(spv_1(x1:x2)));
```

168

```
a = [x1,x2,bottom,top];
axis(a)
v = [x1:x2];
plot  (v,spv_1(x1:x2),'w.')

fprintf('\n\nSelect Range of Data Spike(s) To Be Removed\n')
[xpl,ypl] = ginput(2);
x5 = round(xpl(1));
x6 = round(xpl(2));

clg
a1 = [x5,x6,-100,100];
axis(a1)
v1 = [x5:x6];


plot  (v1,spv_1(x5:x6),'w',v1,vel(x5:x6),'r',v1,pos(x5:x6),'g-')

q = 'e';
while q == 'e'
        fprintf('\n\nSelect Data Points To Be Connected\n')
        [x,y_coord] = ginput;
        x = round(x);
        n = length (x);
```

%Replace selected SPV data with a linear line

```
        for i = 1:2:n

                diff = x(i+1) - x(i);
                y = spv_1(x(i+1))-spv_1(x(i));
                m = y / diff;
                for j = 1:diff-1
                        spv_1(x(i) + j) = spv_1(x(i)) + (j*m);
                end
        clear diff y m
        end
        plot  (v1,spv_1(x5:x6),'w.')


        q = input ('Complete Plot, Section or Edit     ','s');
    end
  end
end

eval(['save  MIT-',int2str(su),int2str(ru),fu,'SPV_F spv_1'])
clear
```

```
%DECIMATE10:  Decrease the sampling rate of the SPV file
%from 60Hz to 10Hz
%Decimate10 uses the MatLab function DECIMATE to lower sampling rate
%then saves data then plots results.

%MatLab function DECIMATE resamples data at a lower rate
%after lowpass filtering.
%yhori = DECIMATE(xhori,6,12) resamples the sequence in vector
%xhori at 1/6 times the original sample rate.
%The resulting resampled vector yhori is 6 times shorter,
%LENGTH(yhori) = LENGTH(xhori)/6.
%DECIMATE filters the data with an 12th order Chebyshev
%type I lowpass filter with cutoff frequency .8*(60/2)/6,
%before resampling.


%       References:
%         "Programs for Digital Signal Processing", IEEE Press
%         John Wiley & Sons, 1979, Chap. 8.3.


%B.McGrath  2 May 1990


clear
clg
su = input ('ENTER SUBJECT NUMBER        ');
ru = input('ENTER RUN NUMBER        ');

eval(['load   MIT-',int2str(su),int2str(ru),'HorizontalSPV_F'])
xhori = spv_1;
clear spv_1

eval(['load   MIT-',int2str(su),int2str(ru),'VerticalSPV_F'])
xvert = spv_1;
clear spv_1

eval(['load   MIT-',int2str(su),int2str(ru),'TACH'])

tachone = tach(1);
xtach= -1*((tach-tachone)/80);

clear tach

yhori = decimate(xhori,6,12);
yvert = decimate(xvert,6,12);
ytach = decimate(xtach,6,12);
hlen = length(yhori);
vlen = length(yvert);

h = min([hlen vlen]);

time = [1:h];
time = time/10;
w = h/10;
yhori = yhori(1:h);
```

```
ytach = ytach(1:h);
yvert = yvert(1:h);
clg

zx = input('DO YOU WANT TO PLOT TACH      ','s');

if zx == 'y'
        axis ([1 w -50 50])
        subplot(211), grid,
        plot (time,yhori,time,ytach)
        title(['MIT',int2str(su),'-',int2str(ru),' Horizontal SPV '])
        ylabel('Velocity (deg/sec)')

        axis ([1 w -50 50]);
        subplot(212), grid,
        plot (time,yvert,time,ytach)
        title(['MIT',int2str(su),'-',int2str(ru),' Vertical SPV '])
        xlabel('Time (sec)'),ylabel('Velocity (deg/sec)')

else
        axis ([1 w -50 50])
        subplot(211), grid,
        plot (time,yhori)
        title(['MIT',int2str(su),'-',int2str(ru),' Horizontal SPV '])
        ylabel('Velocity (deg/sec)')

        axis ([1 w -50 50]);
        subplot(212), grid,
        plot (time,yvert)
        title(['MIT',int2str(su),'-',int2str(ru),' Vertical SPV '])
        xlabel('Time (sec)'),ylabel('Velocity (deg/sec)')
end

eval(['save  MIT-',int2str(su),int2str(ru),'HorizontalSPV_D yhori'])
eval(['save  MIT-',int2str(su),int2str(ru),'VerticalSPV_D yvert'])
```

```
%DECIMATE3: Reduce Sampling Rate for Statistical analysis

%B McGrath May 1990

nucw = input ('NUMBER OF CW RUNS
                    ');

for i = 1:nucw,
      eval(['su',int2str(i),' = input("ENTER SUBJECT NUMBER     ");'])
      eval(['ru',int2str(i),' = input("ENTER RUN NUMBER        ");'])
end

nuccw = input ('NUMBER OF CCW RUNS
                       ');

for i = nucw+1:nucw+nuccw,
      eval(['su',int2str(i),' = input("ENTER SUBJECT NUMBER     ");'])
      eval(['ru',int2str(i),' = input("ENTER RUN NUMBER        ");'])
end

for i = 1:nucw+nuccw,

      eval(['su = su',int2str(i),';'])
      eval(['ru = ru',int2str(i),';'])

      eval(['load  MIT-',int2str(su),int2str(ru),'HorizontalSPV_F'])
      eval(['yhori',int2str(i),' = decimate(spv_1,20);'])
      clear spv_1

      eval(['load  MIT-',int2str(su),int2str(ru),'VerticalSPV_F'])
      eval(['yvert',int2str(i),' = decimate(spv_1,20);'])
      clear spv_1

      eval(['load  MIT-',int2str(su),int2str(ru),'TACH'])
      eval(['ytach',int2str(i),' = decimate(tach,20);'])
      clear tach
      clear ru su

      eval(['yh',int2str(i),' = length(yhori',int2str(i),');'])
      eval(['yv',int2str(i),' = length(yvert',int2str(i),');'])
      eval(['yt',int2str(i),' = length(ytach',int2str(i),');'])

end
lengthvector = [yh1 yv1];
for i = 2:nucw+nuccw,
      eval(['lengthvector = [lengthvector yh',int2str(i),' yv',int2str(i),'];'])
end

h = min(lengthvector);
time = [1:h];
time = time/3;
w = h/3;
```

172

```
for i=1:nucw+nuccw,
        eval(['su = su',int2str(i),';'])
        eval(['ru = ru',int2str(i),';'])

        eval(['yhori',int2str(i),'= yhori',int2str(i),'(1:h);'])
        eval(['yvert',int2str(i),'= yvert',int2str(i),'(1:h);'])
        eval(['ytach',int2str(i),'= ytach',int2str(i),'(1:h);'])

        eval(['spv = yhori',int2str(i),';'])
        eval(['clear yhori',int2str(i)])
        eval(['save  MIT',int2str(su),int2str(ru),'HoriSPV spv'])
        clear spv

        eval(['spv = yvert',int2str(i),';'])
        eval(['clear yvert',int2str(i)])
        eval(['save  MIT',int2str(su),int2str(ru),'VertSPV spv'])
        clear spv

        eval(['tach = ytach',int2str(i),';'])
        eval(['clear ytach',int2str(i)])
        eval(['save  MIT',int2str(su),int2str(ru),'Tach tach'])
        clear tach

end
```

```
%SUBJECTMEAN:

%B.McGrath
%June 1990

clg
nucw = input ('NUMBER OF RUNS
             ');

for i = 1:nucw,
        eval(['su',int2str(i),' = input("ENTER SUBJECT AND RUN     ");'])
end

for i = 1:nucw,

        eval(['su = su',int2str(i),';'])

        eval(['load  MIT-',int2str(su),'HorizontalSPV_F'])
        spv = decimate(spv_1,6,12);
        eval(['yhori',int2str(i),' = spv;'])
        clear spv spv_1

        eval(['load  MIT-',int2str(su),'VerticalSPV_F'])
        spv = decimate(spv_1,6,12);
        eval(['yvert',int2str(i),' = spv;'])
        clear spv spv_1

        clear su

        eval(['yh',int2str(i),' = length(yhori',int2str(i),');'])
        eval(['yv',int2str(i),' = length(yvert',int2str(i),');'])
end
lengthvector = [yh1 yv1];

for i = 2:nucw,
        eval(['lengthvector = [lengthvector yh',int2str(i),' yv',int2str(i),'];'])
end


h = min(lengthvector);
time = [1:h];
time = time/10;
w = h/10;

hori = zeros(h,nucw);
vert = zeros(h,nucw);


for i=1:nucw,

        eval(['yhori',int2str(i),'= yhori',int2str(i),'(1:h);'])
        eval(['yvert',int2str(i),'= yvert',int2str(i),'(1:h);'])
```

174

```
        eval(['hori(1:h,i) = yhori',int2str(i),';'])
        eval(['clear yhori',int2str(i)])

        eval(['vert(1:h,i) = yvert',int2str(i),';'])
        eval(['clear yvert',int2str(i)])


    end

    hori = hori';
    vert = vert';
    meanhspv = mean(hori);
    meanvspv = mean(vert);

    [b,a]=cheby1(12,.05,0.2);
    new_meanhspv = filtfilt(b,a,meanhspv);
    new_meanvspv = filtfilt(b,a,meanvspv);

    hold off
    axis ([1 w -50 50])
    subplot(211),  grid,
    plot (time,new_meanhspv)
    title([' Mean Horizontal SPV      1Hz'])
    ylabel('Velocity (deg/sec)')

    axis ([1 w -50 50]);
    subplot(212),  grid,
    plot (time,new_meanvspv)
    title([' Mean Vertical SPV '])
    xlabel('Time (sec)'),ylabel('Velocity (deg/sec)')

    xpure = input ('ENTER TITLE   ','s');
    gtext (xpure)
    pause

    std_cw_hspv = std(hori);
    std_cw_vspv = std(vert);
    var_hspv = std_cw_hspv.^2;
    var_vspv = std_cw_vspv.^2;
    clg
    code = input ('INPUT ANALYSIS CODE
                   ');
    clear i
    eval(['save  MIT',int2str(code),'SubjMean'])
    clear
```

175

APPENDIX F

EXPERIMENT INSTRUCTIONS

-Instructions To Subjects
-Subject PreBrief
-Subject DeBrief

NAVAL AEROSPACE MEDICAL RESEARCH LABORATORY
PENSACOLA, FLORIDA 32508-5700

INFORMATION FOR SUBJECTS PARTICIPATING IN
THE RESEARCH PROJECT ENTITLED:

"Quantitative Experiments on the Vestibular Response
during Off-Axis Cross-Coupled Stimulation"

The purpose of this study is to increase the knowledge of man's perceptions and reactions to motion involving linear and angular acceleration stimuli. Prolonged acceleration, such as experienced in aircraft turns and pull-outs and in space-craft launches and reentries, can cause a degradation in performance, disorientation, motion sickness, and in extreme cases, loss of consciousness. Virtually all research and acceleration adaption training is conducted in human centrifuges, which provide the only suitable means of achieving prolonged acceleration in a controlled environment.

Your privacy is very important and it will be safeguarded. You will be given a unique control number by the test operator which will document your participation. The test results will contain this control number rather than your full name. The principal investigator will maintain a record that matches your name with your control number. This record will be kept in a secure place. Decoding will not be done except to provide you access to your data or unless the research team finds some aspect of the data that they believe you should know about, or if the value of the research data could be enhanced by more testing or further inquiry into your medical record. In no case will results be openly reported such that someone could determine that the data came from you.

The remainder of this information contains a brief description of the test. As you read this material, you may want to underline items of special interest to you or make notes for questions you will want to ask. Ask the test operator all the questions you want until you are satisfied. If you do not want to participate in the test, simply tell the operator that you prefer not to take the test. You do not have to give an explanation.

The test involves the use of the rotational capabilities of the Coriolis Acceleration Platform (CAP), a large man-rated motion research device. The test involves being seated in a gondala-type chair, located outboard on the CAP. CAP will be programmed to rotate for 5 mins with a rpm such that the maximum resultant gravio-inertial force is 3g. The head will be supported upright by a headrest. You will run clockwise on one day and counterclockwise the next.

Test conditions require you to wear an adjustable helmet; this helmet supports a camera and associated equipment that is used to record eye movements. A custom bitebar is employed to stabilize the helmet. Eye motions will also be recorded using conventional surface mounted electrodes temporarily attached to the skin to either side and above and below your eyes. During each run you will asked to keep your eyes open, look straight ahead and keep your head still. Tasks involving key presses will be requested to maintain alertness.

Immediately following each run your task will be to report your perceptions, reactions, and/or sensations of the motion during a debrief session. Before your first run, a prebrief will be conducted to familiarize you with the expected responses.

177

Alcohol can cause large detrimental effects on the test results, therefore we ask the subject to refrain from alcohol for at least 12hrs before the experiment. The best results would be obtained if you abstained from alcohol during the course of the experiments.

For some individuals, the test may produce symptoms of motion sickness (for example, pallor, sweating, drowsiness, and occasionally vomiting). You may stop the test at anytime you desire. We have had rare cases of brief fainting (approximately 1 in 500 individuals) and our personnel are trained to handle such situationss.

The experimenter will explain the details of each test condition and you are urged to ask questions or express any concern that you may have relative to these procedures and your participation in them.

Your participation in these tests is voluntary. You are free to withdraw at anytime without prejudice to you or your military or civilian career.

There is no specific benefit to you as a result of your participation in this experiment. However, the resulting research data may advance scientific knowledge so that future benefits to individuals or the Navy mission may ultimately arise.

The procedure will take about 75 minutes to complete.

PREBRIEF

PROTOCOL 1:
CAP, 3g, 5mins, CW & CCW.
July 1989.

Vestibular Sensations
-Define pitch, roll and yaw

-Does subject move in a linear or curvilinear motion

-On vs off axis

-Teach subject to differentiate between a sensation of velocity (i.e. position fixed , but motion continues) and a sensation of change in position

-Ask subject to try and remember magnitude, direction and duration of sensation and the approx time of the sensation

G Sensations
-Describe g environment and its effects (heaviness, tingling in the extremities etc)
-No need for breathing manoeuvres
-G-LOC

ISCAN
-Describe Iscan system
-Bitebar
-Need for no head motion
-Non invasive, IR low power, below acceptable standards

General Safety
-Blood pressure monitor
-Iscan eye image
-Subject camera
-Button

Background
-Physical parameters
    20 rpm.
    3g.
    5 min.
    Swinging chair ~70degs
    Upright head position.

Subject Responsibilities
-No Alcohol   (at least 12 hrs, however if one does drink to report it)
-No Head motion
-Relax, enjoy the ride, keep the eyes open, look straight ahead, stay alert

DEBRIEF

A) Subject describes in own words
   - Resist temptation to interupt and question
   - Make list of questions to ask at the end
   - Watch what he does with model and his own body (may be more accurate)

B) SPECIFIC
   - Pitch / Roll / Yaw
      - Extent
      - Duration
      - Velocity
      - Axis-- Between ears, hips, torso, or outside body
   - Which stimulus is stronger ? (Velocity and/or Position)-- Acceleration/ Deceleration
      and Forward/ Backward
   - Floating ?
   - Time Change ?
   - Coordination (Could you walk ? What could you do ?)
   - Did you make-- Head movements ?
                       -- Antistrain ?
   - Experience-- Motion sickness or Dizziness ?
   - Overall Pleasant or Not ?
   - ANY LIGHT LEAKS ?

C) After effects-- End of day or next day
   - Fatigue or disorientation ?
   - Sleep changes ?
   - Day to day or intra/inter day ?

APPENDIX G

EXTEND PROGRAM LISTING

Icon of block CAP

Omega[ ] ──────── [ ] Rates

[ ] Forces

G.I.F

[ ] G.I.F

CAP   NAMRL
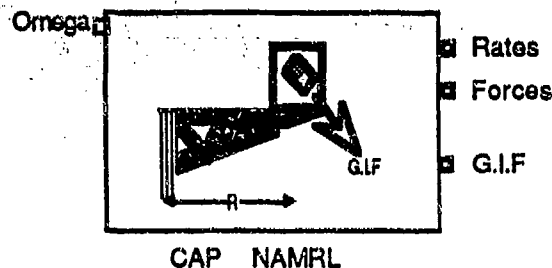
Connectors of block CAP

OmegaIn
ForcesOut
RatesOut
GOut

Dialog of block CAP

```
┌──────────────────────────────────────────────┐
│   ( 1 )      ( C 2 el )      ( 3 )            │
│                                               │
│                                               │
│   Centrifuge 7 dius (m)      │    6    │      │
│                                               │
│                                               │
│   Con 5 nts                                   │
│   │           4           │                   │
└──────────────────────────────────────────────┘
```

User messages of block CAP

<1>   OK
<2>   Cancel
<3>   Help
<4>   Comments
<5>
<6>   Radius
<7>

Script of block CAP

```
real Omega,Theta,Centrip,Alpha,Tangent;
real NewOmega,PsiDot,Psi,Psi_initial;
real ThetaDot;
real NewPhi,PhiDot,Phi,TotalPsiDot;
real a[4],Fx,Fy,Fz;

real dirncos[],bodyrates[],bodyforces[];

on simulate
{


**Angular Velocity of CAP

NewOmega=OmegaIn/57.3;


**Angular Acceleration of CAP

Alpha = (NewOmega-Omega)/deltaTime;
Omega = NewOmega;

**Forces w.r.t Capsule

Centrip=(Radius*Omega^2)/9.8;
Tangent=(Radius*Alpha)/9.8;
GOut=Sqrt(1+(Centrip^2) + (Tangent^2));

**Euler Rates and Angles w.r.t Capsule

PsiDot = 0;
Psi = 0;

ThetaDot = 0;
Theta = 0;

NewPhi = atan(Centrip);
PhiDot = (NewPhi-Phi)/deltaTime;
Phi = NewPhi;

**Direction Cosine

dirncos[0] = cos(Theta)*cos(Psi);
dirncos[1] = cos(Theta)*sin(Psi);
dirncos[2] = -sin(Theta);

dirncos[3] = sin(Phi)*sin(Theta)*cos(Psi) - cos(Phi)*sin(Psi);
dirncos[4] = sin(Phi)*sin(Theta)*sin(Psi) + cos(Phi)*cos(Psi);
dirncos[5] = sin(Phi)*cos(Theta);

dirncos[6] = cos(Phi)*sin(Theta)*cos(Psi) + sin(Phi)*sin(Psi);
dirncos[7] = cos(Phi)*sin(Theta)*sin(Psi) - sin(Phi)*cos(Psi);
dirncos[8] = cos(Phi)*cos(Theta);

**Total Stimulus to Capsule Reference Frame

TotalPsiDot = PsiDot + Omega;
```

Body Rates

```
bodyrates[0] = (-ThetaDot*sin(Phi) + TotalPsiDot*cos(Theta)*cos(Phi))*57.3;
bodyrates[1] = (ThetaDot*cos(Phi) + TotalPsiDot*cos(Theta)*sin(Phi))*57.3;
bodyrates[2] = (PhiDot - TotalPsiDot*sin(Theta))*57.3;
```

Inertial Force Vector Relative to Capsule

```
Fx = Tangent;
Fy = Centrip;
Fz = -1;
```

Body Forces

```
bodyforces[0] = dirncos[0]*Fx + dirncos[1]*Fy + dirncos[2]*Fz;
bodyforces[1] = dirncos[3]*Fx + dirncos[4]*Fy + dirncos[5]*Fz;
bodyforces[2] = dirncos[6]*Fx + dirncos[7]*Fy + dirncos[8]*Fz;
```

Output Arrays

```
RatesOut = passarray(bodyrates);
ForcesOut = passArray(bodyforces);
}
```

```
** If the dialog data is inconsistent for simulation, abort.
on checkdata
{
}
```

```
** Initialize any simulation variables.
on initsim
{
makearray(bodyforces,3);
makearray(bodyrates,3);
makearray(dirncos,9);

Omega = 0;
Phi = 0;


}
```

```
** User clicked the dialog HELP button.
on help
{
showHelp();
}
```

Help Text of block CRP

This block computes the angular velocities, angular accelerations and inertial forces in body axes during a pendulous centrifuge cab moving at angular velocity Omega about an earth vertical axis in a 1 g field. Radius of cab from centrifuge rotation axis is assumed constant.

All inputs and outputs are in degrees/sec
Omega is centrifuge angular velocity (deg/sec)
Centrifuge Radius is in metres.
g is assumed 9.8 ft/sec^2

REFERENCES

Benson AJ. Perceptual illusions. In: Aviation Medicine, ed. G Dhenin. London: Tri-Med Books, 1978.

Benson AJ, Bodin MA. Interaction of linear and angular accelerations on vestibular receptors in man. Aerospace Med. 37:144-154, 1966a

Benson AJ, Bodin MA. Effect of orientation to the gravitational vertical on nystagmus following rotation about a horizontal axis. Acta Oto. 61:517-526, 1966b .

Better HS, Marino LA, Paloski WH, Reschke MF. Electro-oculographic potential as a function of range of eye position. Abstract 363. Aerospace Med. 61:507, 1990

Bornschein H, Schubert G. Vestibular coriolis reaction stimulation parameters. Zeitschrift fur Biologie (Journal of Biology) 10:269-275, 1958.

Clark B, Stewart JD. Vestibular and nonvestibular information in judgements of attitude and coriolis motion in a piloted flight simulator. Aerospace Med. 38: 936-940, 1967.

Cohen MM, Crosbie RJ, Blackburn LH. Disorientating effects of aircraft catapult launchings. Aerospace Med. 44 (1):37-39, 1973

Correia MJ, Guedry FE. Modification of vestibular responses as a function of rate of rotation about an earth-horizontal axis. Report No. 957. Pensacola, FL Nav. Aerospace Med. Inst., 1966 .

Correia MJ, Money KE. The effect of blockage of all six semicircular canal ducts on nystagmus produced by dynamic linear acceleration in cat. Acta Oto. 69:7-16, 1970.

Crampton GH. Does linear acceleration modify cupular deflection? 2nd Symposium of the Role of the Vestibular System in Space Exploration NASA SP-115:169-184, 1966.

DiZio P, Lackner JR, Evanoff JN. The influence of gravitoinertial force level on oculomotor and perceptual responses to Coriolis, cross-coupling stimulation. Aviat. Space and Env. Med. 58(9,suppl.):A218-23, 1987.

Gentles W, Barber HO. Computer and human variation in the measurement of post caloric nystagmus. Equilibrium Res. Bul., 1973.

Gillingham KK, Fosdick JP. High-G training for fighter aircrew. Aviat. Space and Env. Med. 12-19, 1988.

Gillingham KK, Wolfe JW. Spatial orientation in flight. USAF Technical Report USAFSAM-TR-85-31, 1986.

Graybiel A, Miller EF, Homick JL. Experiment M131. Human Vestibular Function. In: Johnston RS & Dietlein LF, ed. Biomedical Results from Skylab. NASA SP-377, 1977.

Guedry FE Jr., Benson AJ. Coriolis cross-coupling effects: Disorientating and nauseogenic or not? Aviat Space Environ Med 49(1):29-35, 1978.

Guedry FE, Jr., Montague EK. Quantitative evaluation of the vestibular coriolis reaction. Aerospace Med. 32: 487-500, 1961.

Harris LR. Vestibular and optokinetic eye movements evoked in the cat by rotation about a tilted axis. Exp. Brain Res. 66:522-532, 1987.

Hixson WC, Anderson JJ. The coriolis acceleration platform: A unique vestibular research device. NAMI-980. NASA R-93. Pensacola, Fla. Naval Aerospace Medical Institute, 1966.

Hixson WC, Niven JI, Correia MJ. Kinematics nomenclature for physiological accelerations: with special reference to vestibular applications. Monograph 14. Naval Aerospace Medical Institute, Pensacola, Fla., 1966.

Janeke JB. On nystagmus and otoliths. A vestibular study of responses as provoked by a cephalo-caudal horizontal axis rotation; Thesis Clueden M(vedigh, Amsterdam, 1968.

Jongkees LBW. On the otoliths: Their function and the way to test them. 3rd Symposium of the Role of the Vestibular Organs in Space Exploration NASA SP-152, 1967.

Jongkees LBW Philpszoon AJ. Nystagmus provoked by linear acceleration. Acta physiol. pharmacol. neerl. 10:239-247, 1962.

Lackner JR, Graybiel A. Influence of gravitoinertial force level on apparent magnitude of coriolis, cross-coupled angular accelerations and motion sickness. AGARD Conference Proceedings No. 372, 1984.

Lackner JR, Graybiel A. The effective intensity of coriolis, cross-coupled stimulation is gravitoinertial force dependent: implications for space motion sickness. Aviat. Space and Env. Med. 57:229-35 1986.

Lansberg MP. A primer of space medicine. Amsterdam/New York: Elsevier 1960.

Lansberg MP, Guedry FE, Graybiel A. Effect of changing resultant linear acceleration relative to the subject on nystagmus generated by angular acceleration. Aerospace Medicine Vol. 36 No. 5 pp 456-460, 1965 .

Marcus JT. Influence of gravito-inertial force on vestibular nystagmus in man. TNO Institute for Perception. Report No. IZF 1989-24, 1989.

Marcus JT, Van Holten MD. Vestibulo-ocular response in man to +Gz hypergravity. Aviat. Space and Env. Med. 61:631-5, 1990.

Massoumnia MA. Detection of fast phase of nystagmus using digital filtering. SM Thesis Cambridge Mass. Massachusetts Institute of Technology, 1983.

McCabe BF. Nystagmus response of the otolith organs. Laryngoscope 74:372-381, 1964.

Merfeld DM. Spatial orientation in the squirrel monkey: An experimental and theoretical investigation. PhD Thesis Cambridge Mass. Massachusetts Institute of Technology, 1990.

Niven JI, Hixson WC, Correia MJ. Elicitation of Horizontal Nystagmus by Periodic Linear Acceleration. Acta Oto. 62:429-441 1965.

Oman CM, Shubentsov I, McGrath BJ. NysA: Nystagmus eye movement analysis program. Man Vehicle Laboratory, Massachusetts Institute of Technology, 1990.

Peters RA. Dynamics of the vestibular system and their relation to motion perception, spatial disorientation, and illusions. NASA CR 1309, 1969.

Raphan T, Cohen B, Henn V. Effects of gravity on rotatory nystagmus in monkeys. Ann NY Acad. Sci. 374:44-55, 1981.

Raphan T, Matsuo V, Cohen B. A velocity storage mechanism responsible for optokinetic nystagmus (OKN), optokinetic after-nystagmus (OKAN) and vestibular nystagmus. In: Control of Gaze by Brain Stem Neurons. Elsevier/North Holland Biomedical Press pp 37-47, 1977.

Raphan T, Matsuo V, Cohen B. Velocity storage in the vestibulo-ocular reflex arc (VOR). Exp. Brain Res. 35:229-248, 1979.

Robinson DA. Vestibular and optokinetic symbiosis: An example of explaining by modelling. In: Control of Gaze by Brain Stem Neurons, Developments in Neuroscience, Vol. 1. Elsevier/North-Holland Biomedical Press pp. 49-58, 1977.

Rolfe JM, Staples KJ. Flight simulation. Cambridge University Press Cambridge, 1986.

Schubert G. Die physiologischen auswirkungen der Coriolisbeschleunigungen bei flugzeugsteuerung. Arch. Ohr.-,Nas.-,u. Kehlk.-Heilk. 30, 595-604, 1932.

Sliney DH, Freasier BC. Evaluation of optical radiation hazards. Applied Optics. Vol 12, No. 1, 1-24, 1973.

Valentinuzzi M. An analysis of the mechanical forces in each semicircular canal of the cat under single and combined rotations. Bul. of Math. Biophysics, Vol 29, 1967.

Van Egmond AAJ, Groen JJ, Jongkees LBW. The mechanics of the semicircular canals. J Physiol Lond. 110:1-17. 1949

Wilson VJ, Melvill Jones G. Mammalian vestibular physiology, New York: Plenum Press, 1979.

Young LR. Effects of linear acceleration on vestibular nystagmus. 3rd Symposium of the Role of the Vestibular Organs in Space Exploration NASA SP-152 1967 .

Young LR, Meiry JL. A revised dynamic otolith model. 3rd Symposium of the Role of the Vestibular Organs in Space Exploration NASA SP-152 1967 .

REPORT DOCUMENTATION PAGE

1. AGENCY USE ONLY (Leave blank)	2. REPORT DATE	3. REPORT TYPE AND DATES COVERED
	April 1993	Final

4. TITLE AND SUBTITLE

HUMAN VESTIBULAR RESPONSE DURING 3 Gz CENTRIFUGE STIMULATION

5. FUNDING NUMBERS

61153.MR04101.00B-7008

6. AUTHOR(S)

Braden J. McGrath

7. PERFORMING ORGANIZATION NAME(S) AND ADDRESS(ES)

Naval Aerospace Medical Research Laboratory
51 Hovey Road
Pensacola, FL 32508-1046

8. PERFORMING ORGANIZATION REPORT NUMBER

NAMRL Monograph 46

9. SPONSORING / MONITORING AGENCY NAME(S) AND ADDRESS(ES)

Naval Medical Research and Development Command
National Naval Medical Center, Bldg. 1
Bethesda, MD 20889-5606

10. SPONSORING / MONITORING AGENCY REPORT NUMBER

11. SUPPLEMENTARY NOTES

Submitted in partial fulfillment of the requirements for the degree of Master of Science in Aeronautics and Astronautics at the Massachusetts Institute of Technology, Cambridge, MA, Sept 90.

12a. DISTRIBUTION / AVAILABILITY STATEMENT

Approved for public release; distribution is unlimited.

12b. DISTRIBUTION CODE

13. ABSTRACT (Maximum 200 words)

The use of centrifuges in training aircrew to avoid GLOC is increasing. The purpose of this study was to record the vestibulo-ocular reflex (VOR) and subjective sensations to gain insight into reports of asymmetrical disorientation and disturbance during acceleration and deceleration of GLOC training centrifuges. Horizontal and vertical eye movements and post run sensations were recorded from 15 naive male human subjects seated head erect in a 20.5-ft radius pendulous chair centrifuge. Centrifuge profile was acceleration from 1 to 3 Gz in 19 s, 5 min of sustained 3 Gz, and deceleration to 1 Gz in 19 s. Tests were repeated up to three times with the subject facing the motion, and three times with the subject's back to the motion. Eye position was recorded in the dark using an ISCAN infrared video system. Six subjects experienced GLOC, and 1 withdrew due to unrelated sickness. Slow phase velocity (SPV) and sensations from the 8 subjects who completed all 6 runs were analyzed. Roll of the chair during acceleration and deceleration produced strong pitch, roll, and yaw sensations and eye movements attributable to vestibular Coriolis stimulation. Subjective pitch amplitude change was consistently greater during deceleration than acceleration, regardless of rotation direction. The SPV magnitude during the first run in a given direction was significantly different than the two subsequent runs. A sustained upbeating ("Lz") nystagmus (1-21°/s, mean 8°/s at 100 s; 1-12°/s at 315 s) was observed in 7 of 8 subjects. VOR during centrifugation is composed of interacting transient angular and sustained linear VOR components. Sensation asymmetries are not observed in the VOR. Lz nystagmus magnitude is an individual subject characteristic.

14. SUBJECT TERMS

Centrifuge, Vestibulo-ocular, Lz nystagmus, Spatial Orientation

15. NUMBER OF PAGES

191

16. PRICE CODE

17. SECURITY CLASSIFICATION OF REPORT	18. SECURITY CLASSIFICATION OF THIS PAGE	19. SECURITY CLASSIFICATION OF ABSTRACT	20. LIMITATION OF ABSTRACT
Unclassified	Unclassified	Unclassified	SAR